DOCTOR OF PHILOSOPHY

Behaviour of ultra-low density foamed concrete

Ozlutas, Kezban

Award date:
2015

BEHAVIOUR OF ULTRA-LOW DENSITY FOAMED CONCRETE

KEZBAN OZLUTAS

A thesis presented in application for the Degree of Doctor of Philosophy
Division of Civil Engineering
University of Dundee
April 2015

DECLARATION

I hereby declare that I am the author of this thesis, that the work recorded has been composed by me, all references cited have been consulted, and that it was not been previously used for a higher degree.

Kezban Ozlutas

CERTIFICATE

This is to certify that **Kezban Ozlutas** has carried out her research under my supervision and that she has fulfilled the conditions of Ordinance 14 of the University of Dundee, so that she is qualified to submit the following Thesis in application for the Degree of Doctor of Philosophy.

Prof. M R Jones CEng, MICE

Director of Concrete Technology Unit

University of Dundee

PUBLICATIONS

- Jones, M R, Ozlutas, K, Ouzounidou, A. and Rathbone, R F (2013). "Behaviour of PC/CSA/FA blends in foamed concrete". World of Coal Ash Conference, 22-25 April 2013, Lexington, KY, USA.

- Jones, M R, Ozlutas, K and Zheng, L. "Stability and instability of foamed concrete". Magazine of Concrete Research. (Accepted for publishing, April 2015).

ACKNOWLEDGEMENTS

I would like to express my gratitudes to all people who helped and supported me throughout my PhD. First of all, I would like to thank to my supervisor Prof. Rod Jones whose supervision and vast knowledge greatly contributed to successful completion of this thesis. Knowing and working with him for the past 5 years was very inspiring and enjoyable.

Constant assistance of all CTU staff and the technicians on various aspects of this project is highly appreciated. I would like to extend my gratitudes to Alan Tough and Aikaterini McCarthy for their support especially at the final stages of my studies. Furthermore, I would like to acknowledge Propump Engineering Ltd for their technical and financial support throughout the project. I also want to thank to all of my friends and colleagues, especially Noushin, for being there and supporting me all the time.

Finally, I would like to express my gratitude to my family, especially to my parents. Their endless love, support, encouragement and trust were invaluable. It is to my parents and grandparents that this thesis is dedicated.

ABSTRACT

Increased demand for lightweight materials to reduce the dead loads of structures has stimulated the need for even lighter foamed concrete (FC). However, ultra-lightweight FCs (ULFCs) (plastic density < 600 kg/m^3) were reported to often result in unstable mixes, with some of them (plastic densities below 400 kg/m^3) even leading to failures due to segregation. There is, in fact, insufficient information available on ultra-lightweight FCs. Therefore, this study aimed to examine ULFCs focusing on stability, microstructure, contribution to sustainable construction, insulation performance as well as fresh and hardened properties.

The study provided an empirical insight into the stability mechanism of FC by considering a series of hypotheses leading to a proposed solution for stability issues. Accordingly, the study described use of calcium sulfoaluminate (CSA) cement, in combination with Portland cement (PC), in order to reduce the setting times of the mixes to achieve stable ULFCs. Plastic densities ranging from 150 to 300 kg/m^3 with combinations of PC with 5% and 10% CSA by mass and w/c ratio of 0.50 were utilised. To support the hypotheses and the proposed solution, stability, initial setting and collapse time as well as bubble and microstructure analyses were carried out on the mixes under consideration. The data suggested that FCs with densities down to 150 kg/m^3 can be produced successfully, provided that the initial setting time of the base mix does not exceed 20-25 minutes. Furthermore, the data proved the linkage between the setting time, bubble size and stability such that shorter setting times resulted in smaller bubble sizes hence stable mixes, while SEM images provided a comparison of microstructure for a range of FCs.

In the next phase of the study, fine fly ash (FA) was incorporated in the mixes at levels from 30% to 70% by mass forming PC/CSA/FA combinations to enhance the sustainability of ULFCs. Mixes with FA contents up to 40%, 50% and 70% by mass were found to yield stable ULFCs at 150, 200 and 300 kg/m^3 densities respectively. However, given the low-strength of ULFCs accompanied by delayed hydration in fly ash mixes, 40% FA was chosen as the optimum FA content for ULFCs. Moreover, embodied carbon dioxide (eCO_2) of a range of FCs with and without fly ash were calculated. Compared to higher densities, FCs below 500 kg/m^3 showed reduced eCO_2 with further reductions provided by FA mixes. Furthermore, microstructure (SEM) images showed that FA mixes were found to enhance and densify the microstructure of ULFCs in the long-term.

To assess the performance of and identify the possible application areas for ULFCs some of the key properties (in particular thermo-acoustic insulation) were evaluated. Thermal conductivities of ULFCs were found to decrease significantly, with values down to 0.078 W/mK for D200 (200 kg/m^3) FCs. FA was found to further decrease the thermal conductivities, but these values were found to increase in the long-term as the microstructure of FA mixes get denser. Sound insulation performance of ULFC suggested that it also has a potential to be used as an alternative to the sound insulation products on the market.

It was found that the flow of ULFC is reduced as well as the peak temperatures developed due to heat of hydration, with further reductions in the peak temperatures provided by the inclusion of 40% fly ash as a cement replacement. Compressive strength and E-value were found to be lower in ULFC compared to low/high density FCs. Poisson's ratio of FCs with densities from 300 to 1000 kg/m^3 ranged from 0.08 to 0.19 (with no definite trend) which is lower than normal weight concrete (which is typically 0.15-0.22). Drying shrinkage strains and coefficient of thermal expansion (CTE) of ULFC were found to be lower than high/low densities whilst CTE values were mostly higher than the values reported for cellular concrete apart from the D300 90%PC/10%CSA mix (which exhibited 8.1 microstrains per °C). For D200 to D600, sorption increased with decreasing density, whilst FA seemed to yield higher sorption overall.

Overall, the data suggested that ULFC can be used in various applications. Excellent thermal insulation accompanied by good sound insulation potential can be combined in a multi-layer, composite wall system to provide lightweight, durable thermo-acoustic insulation. Low Poisson's ratio and lightweight are advantageous for using ULFC for the rehabilitation of historic structures (such as bridges), while ULFCs containing fly ash with reduced peak temperatures developed due to heat of hydration can be used as a low eCO_2 fill material. On the other hand, reduced flow and fast initial setting times of ULFC may restrict its production in-situ, giving rise to its manufacture as lightweight blocks or elements. Finally, a matrix schedule of a range of FCs and properties was developed to identify the most suitable FC for a specified application. Additionally, recommendations for future research were proposed as well as the practical implications.

ABBREVIATIONS

CSA	calcium sulfoaluminate
PC	Portland cement
FA	fly ash
SF	silica fume
CNT	carbon nano-tube
FC	foamed concrete
ULFC	ultra-lightweight foamed concrete (plastic density < 600 kg/m^3), ultra-low density foamed concrete
D300	300 kg/m^3 density
w/c ratio	water/cement ratio

Table of Contents

List of Figures

List of Tables

CHAPTER 1

1. INTRODUCTION

1.1 BACKGROUND

Foamed concrete, a cementitious material comprising mechanically introduced air-voids, is a lightweight, relatively durable and multifunctional construction material which has been used world-wide. Its unique characteristics which of being free-flowing, self-compacting and having excellent thermal insulation, makes foamed concrete an attractive material for various applications, including large void fills, mine backfills, floor screeds, thermally insulating foundations, bridge strengthening and pre-cast blocks. Moreover, the ability of producing foamed concrete at a range of plastic densities (typically 375 to 1600 kg/m^3) helps to the specifications of the most suitable mix to satisfy the design needs. Figure 1.1 shows a range of applications of foamed concrete produced with various densities.

Figure 1.1 Typical foamed concrete applications

The growing pressure for more sustainable construction technologies such as reducing the self-weight of structures and embodied carbon dioxide (eCO_2), minimising use of primary resources, and energy conservation as well as environmental noise control, have also stimulated the need for lighter foamed concretes. Typically, foamed concrete densities used in industry range from 400 to 1400 kg/m^3 which can be classified as ultra-low, low and high density foamed concretes. Therefore, plastic densities above 1000 kg/m^3 are high, from 600 to 1000 kg/m^3 are low and below 600 kg/m^3 are ultra-low density foamed concretes. Research carried out and industry use suggest that foamed concrete with reduced densities, self-weight and cement content would potentially provide further advantages in contributing to sustainable construction, mainly through the reduction of eCO_2, use of primary resources and thermal conductivity.

Furthermore, the viability of incorporating secondary materials, such as, fly ash in foamed concrete, as well as its potential to be re-used itself at the end of its service life, increases its sustainability potential (Jones and McCarthy, 2005b, 2006; Jones and Zheng, 2012; Jones et. al, 2009). However, given the typical use of foamed concrete as a large volume fill material, it is vital to monitor its impact on sustainable construction, as potentially high PC contents can lead to high eCO_2 contents. In order to avoid this, design needs must be specified clearly and the lowest possible cement content and foamed concrete density must be employed as well as incorporating secondary materials (e.g fly ash) in the mix.

In one case study, foamed concrete was used to stabilise approximately 40 acres of historic stone mines that put nearly 350 properties under risk of subsidence in the village of Combe Down, England. Given the pour volume of 600,000 m^3, this is thought to be the world's largest single use of foamed concrete, where a lightweight 600 kg/m^3 mix was used (Propump Ltd, 2014). However, 375 kg/m^3 of cement content used in this particular mix (Ansell, 2010) had a negative impact on sustainable construction in terms of material use and embodied carbon dioxide (eCO_2).

As there was no structural function for the foamed concrete mix used in this case, a lighter mix could have been employed for infilling and stabilising the mines. Accordingly, Table1.1 shows the material and eCO_2 savings if a 300kg/m^3 mix was employed instead of a 600 kg/m^3 one. The table also shows the reductions that would be obtained, if a 300 kg/m^3 mix comprising 30% fly ash addition had been used.

Table 1.1 Comparison of material consumption and eCO_2 of 600 and 300 kg/m^3 foamed concretes for the Combe Down case study

Foamed concrete density, kg/m^3	**600**	**300**	**300 (30% FA)**
Portland cement, kg/m^3	375	200	140
Water, kg/m^3	225	120	120
Portland cement, kt/ 600,000 m^3	225	120	84
Water, kt/ 600,000 m^3	135	72	72
eCO_2, kt eCO_2/ 600,000 m^3	209.4	105	73.8
Reduction in eCO_2, kt	-	**104.4**	**135.6**

Notes: eCO_2 of the foam was not considered and an example calculation is shown in Appendix B. w/c ratio of 0.60 was assumed.

As seen in the Table, compared to a low density foamed concrete mix, an ultra-low density mix leads to significant savings on material use and up to 65% reduction in eCO_2 while fulfilling the same function as higher densities. Therefore, ultra-low density foamed concrete is a good alternative to be looked at as fill and insulation material for various applications, especially for the restoration of historic structures where minimising self-weight is required.

However, as the users of foamed concretes will be aware the instability, i.e segregation of the fresh mix due to the separation of solids and air phases of the mix prior to initial setting, can be problematic at ultra-low plastic densities. More specifically, experience of its applications in industry and the research conducted at the University of Dundee have shown that foamed concretes with plastic densities below 400 kg/m^3 are highly susceptible to failures due to instability. Figure 1.2 illustrates an example of in-situ failure where a foamed concrete mix with plastic density of 350 kg/m^3 was utilised.

There is no clear understanding of underlying mechanism of foamed concrete instability or why ultra-low densities are more prone to becoming unstable. Therefore, even though there has been an increasing demand from the industry, stability issues have led to an inability to deploy foamed concretes with densities below 400 kg/m^3. Previously, at the University of Dundee, Mohammad (2011), attempted to produce 300 kg/m^3 foamed concrete, however the attempts failed. Consequently, the current research has been built

on the key outcomes of Mohammad's research. Therefore, the main focus of this research has been to develop a mechanism to produce stable ultra-low density foamed concretes and characterising their behaviour while maximising the sustainability of foamed concrete in every aspect, including environmental, economic and social, while maintaining the mechanical stability and durability.

Figure 1.2 An example of in-situ failure of ultra-low density foamed concrete

1.2 OVERALL AIM AND OBJECTIVES

The overall aim of this research is to characterise ultra-low density foamed concrete focusing on stability issues, microstructure, insulation performance, properties (fresh, early age and hardened) as well as its contribution to sustainable construction. In order to achieve this, several objectives were adopted as follows:

i) To understand the mechanism of instability in foamed concrete and provide a solution to produce stable, ultra-lightweight foamed concretes below 400 kg/m^3.

ii) To test the proposed solution with a range of materials and, if successful, utilise fly ash in ultra-lightweight foamed concretes in order to evaluate the efficiency of fly ash in producing stable ultra-lightweight foamed concretes as well as reducing the eCO_2 of the mixes.

iii) To carry out bubble size analysis and visual microstructure analysis of microscopic images of a range of foamed concretes with various densities and material combinations.

iv) To assess the thermo-acoustic insulation performance and key fresh, early age and hardened state properties of ultra-lightweight foamed concretes, in order to identify the potential as a sustainable insulation and fill material for wider applications in areas which require minimal self-weight.

1.3 SCOPE OF RESEARCH

The research was carried out in three phases. In ***Phase 1***, the study focused on understanding the stability and instability mechanism of foamed concrete. In ***Phase 2,*** attempts to resolve the issues of stability to enable the production of stable ultra-low density mixes were made as well as characterising the microstructural properties of ultra-low density mixes. Moreover, the contribution of ultra-low density foamed concrete to sustainable construction was also assessed in the second phase. In ***Phase 3***, performance of ultra-low density foamed concrete in respect to insulation, fresh, early age and hardened properties was evaluated.

Given the non-Newtonian nature of foamed concrete, which acts similar to a Bingham fluid (McCarthy, 2004; Mohammad, 2011), it was not suitable to use the models for Newtonian fluids through a numerical or computational approach in order to analyse its behaviour. On the other hand, there is a lack of information on the behaviour of foams in paste/mortar and at this stage it was not practical to quantify the parameters affecting the foam stability, such as drainage rate and surface tension in these mediums. Therefore, an empirical approach based on hypotheses on the stability and instability was chosen in order to carry out this research study. The hypotheses on stability and instability mechanism of foamed

concrete were discussed with the industry who had experienced stability issues in ultra-low density foamed concretes. Consequently, the first phase of the current study was carried out based on hypotheses that were built on the observations made in previous cases both in the laboratory and on site in order to propose a solution to resolve the issues of instability.

In the second phase which included experimental investigations, foamed concrete densities ranging from 100 to 1000 kg/m^3 were considered with a greater focus on densities ranging from 150 to 600 kg/m^3. For the investigation focusing on stability, the plastic density range was limited to 100 to 500 kg/m^3. On the other hand, for the microstructural properties range of densities from 100 to 1000 kg/m^3 were analysed to observe the changes in the microstructure while shifting from a higher density class to an ultra-low density class.

The highest cement content used was 333 kg/m^3 for 500 kg/m^3 density foamed concretes whilst the cement contents used for lower densities were below 300 kg/m^3. A constant water/cement ratio of 0.50 was used throughout the study to minimise the number of variables, for resolving the stability issues while providing sufficient consistency to obtain a homogeneous and self-flowing mix. However, w/c ratio of 0.45 and 0.60 were also applied where recommended or when the effect of w/c ratio was of interest. Protein surfactants were used throughout the study as they were likely to yield more stable and closed cell foam compared to synthetic surfactants (Dransfield, 2000; McGovern, 2000).

Different cement types were examined either solely or in a binary cement combination in order to evaluate their effect in resolving the stability issues. These cements consisted of high early strength PC, specialist type of PC which is referred to as PC2, microfine cement (MF) and two types of CSA (calcium sulfoaluminate) cements, referred to as CSA and CSA_P. CSA and CSA_P were utilised in combination with PC. Besides these materials, two types of fine fly ashes, FA1 and FA2, were also considered in order to provide reductions in the eCO_2.

Initially, trial mixes were produced to evaluate the proposed hypotheses. Then, bubble size and microstructural analyses were carried out on the ultra-low density foamed concretes. Bubble analysis was carried on 2D images using image analysis software, whilst

SEM (Scanning Electron Microscopy) images were visually observed for microstructural analysis. At a later stage, influence of fly ash on stability and microstructural properties were evaluated as well as its influence on reducing the eCO_2. Therefore, calculations for determining the eCO_2 (due to production) of a range of foamed concrete mixes were carried out to evaluate the effect of ultra-low density levels and fly ash on the eCO_2.

In the final phase, the properties of ultra-low density foamed concretes in comparison with low density ones were evaluated. The properties evaluated included insulation, fresh, early age and hardened properties. Evaluation of insulation performance covered thermal conductivity and sound absorption and transmission loss. Additional mixes, comprising silica fume and carbon nano-tubes (CNTs), were also tested for thermal conductivity and sound absorption as these materials are reported to produce closed-cell bubbles which affect the insulation performance.

Considering one of the most common applications of foamed concrete, i.e as a large scale fill material, flow behaviour and heat of hydration are of importance. Therefore, flow behaviour of ultra-low density foamed concrete was characterised as a fresh state property as well as monitoring the heat development upon hydration as an early age property. Finally, compressive strength, modulus of elasticity, Poisson's ratio, drying shrinkage, coefficient of thermal expansion and sorptivity were evaluated in the hardened state.

Finally, based on the findings of the experimental study, recommendations on the use of ultra-low density foamed concretes were made and a matrix schedule was developed summarising the typical behaviour to aid users adopting the most suitable mix for the required application. Moreover, recommendations for future research were also investigated.

1.4 OUTLINE OF THE THESIS

Chapter 2 critically reviews the recent literature related to the aim and objectives of this study. These mainly include the stability of foamed concrete as well as some of the key characteristics and properties of foamed concrete under consideration. Additionally, the key regulations regarding sustainable construction are covered in terms of energy efficiency, sound insulation as well as CO_2 emissions.

Chapter 3 provides the research programme, methodology and experimental details of the study. Materials, test methods, mix proportions, and production and preparation of the specimens used to meet the aim and objectives are discussed.

Chapter 4 presents the observed behaviour and developed hypotheses on foamed concrete stability supported by schematics to provide a better understanding of the stability mechanism of foamed concrete. Additionally, a solution to overcome the issues of stability was developed and proposed.

Chapter 5 explains how the issues of stability are evaluated and resolved. This Chapter provides the data obtained using various material combinations to support the proposed solution for overcoming the issues of stability. In addition, bubble size and microstructural (SEM images) analyses of the foamed concretes considered are presented.

Chapter 6 covers the influence of fly ash on stability, bubble size and microstructural properties. Additionally, embodied carbon dioxide (eCO_2) levels of a range of foamed concretes produced with and without fly ash are presented.

Chapter 7 investigates the potential of ultra-low density foamed concrete as an insulating material. More specifically, thermal conductivity, sound absorption and transmission loss of ultra-low density foamed concretes are covered in comparison to higher density ones. Discussion of the results in relation to plastic density, constituents and microstructural properties are provided as well as the discussions on test methods.

Chapter 8 evaluates the performance of ultra-low density foamed concretes in relation to a number of fresh, early age and hardened properties including consistency, heat development upon hydration, compressive strength, modulus of elasticity, Poisson's ratio, drying shrinkage, thermal expansion and sorptivity. Discussion of the results in relation to plastic density, constituents and microstructural properties are detailed as well as the discussions on the test methods, where applicable. Similar to Chapters 5, 6 and 7, conclusions are summarised at the end of the Chapter.

Chapter 9, reviews the overall outcomes of the study and discusses the potential applications and associated practical implications of ultra-low density foamed concretes as well as proposing recommendations for further research.

CHAPTER 2

2. LITERATURE REVIEW

2.1 INTRODUCTION

The Chapter provides a brief review on the key regulations and strategies regarding sustainable construction in order to emphasize the need for lighter foamed concretes. The review is then extended to the literature on foamed concrete. Mainly, the focus was given to background of foamed concrete, fresh, early age and hardened properties as well as insulation and microstructural properties, with an intention to show the knowledge gaps in ultra-low density foamed concretes. Finally, a summary of the literature review is provided to clarify the need for studying ultra-low density foamed concretes. The resources used were mainly accessed through the library, ICE (Institution of Civil Engineers) and web as well as private communications.

2.2 SUSTAINABLE CONSTRUCTION: REGULATIONS AND STRATEGIES

Concrete is the most widely used construction material (MPA, 2012b), therefore, it is vital to monitor its performance on contributing sustainability, lowering embodied carbon dioxide (eCO_2), enhancing resource and energy efficiency. As a result, the UK concrete industry agreed on a Concrete Industry Sustainable Construction Strategy in 2008, setting targets for sustainability and monitoring the performance (MPA, 2012a).

Since the launch of the Concrete Industry Sustainable Construction Strategy, industry showed increasing improvements on eCO_2 reduction, waste consumption, responsible sourcing and actions towards zero carbon. In 2012, the reduction in eCO_2 (cradle to gate) of a standardised concrete mix was reported as 23% (6% higher than the 2012 target) compared to 1990 baseline values (Figure 2.1), whilst the use of waste and recovered materials was reported as 62% more than the amount sent to landfill (MPA, 2013).

Furthermore, use of additional cementitious materials with lower embodied CO_2 such as fly ash and ground granulated blastfurnace slag was promoted. Although the values for the amount of additional cementitious materials used are consistently around 30%, the target of 33% set for 2012 was not reached (Figure 2.2). Therefore, the target value for 2020 has been set to 35% (MPA, 2013). Although the focus was given to cradle to gate eCO_2 contents in this literature review, it is not purely the measure of sustainability while it is directly related to the climate change.

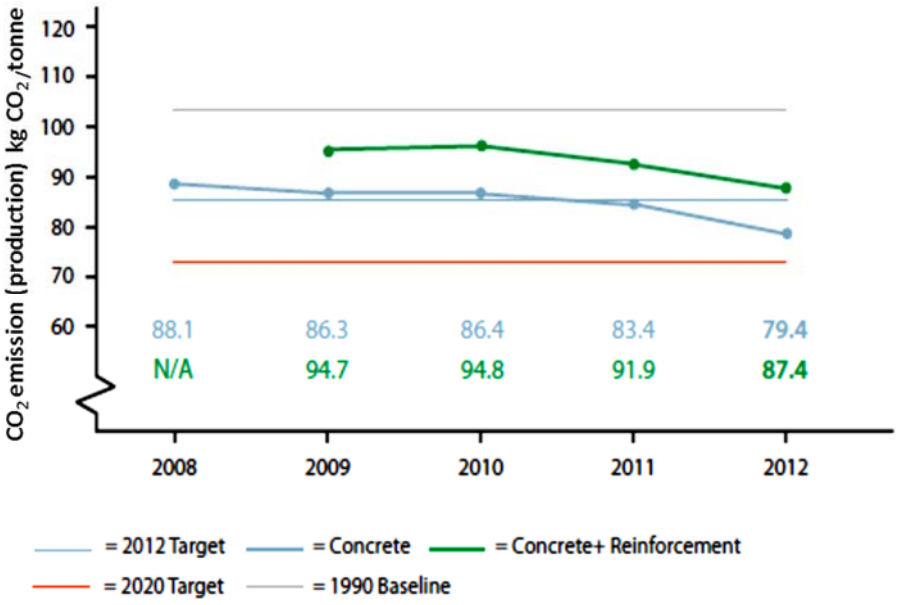

Figure 2.1 CO_2 emissions due to production of a standardised mix (MPA, 2013)

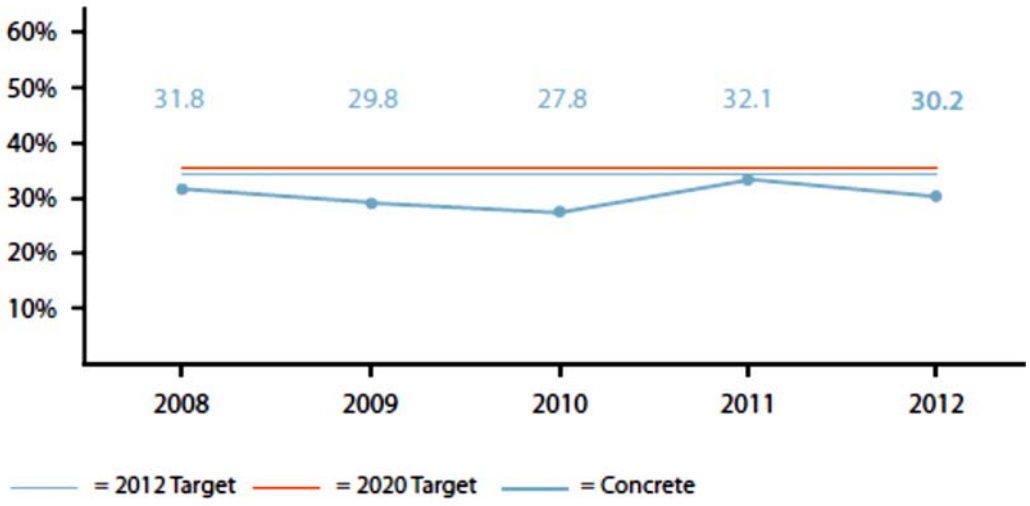

Figure 2.2 Amount of additional cementitious materials as a proportion of total cementitious materials (MPA, 2013)

Regulations supporting the sustainable construction have also been stimulated in the EU, such that the Construction Products Regulation (CPR) came into force in July 2013. CPR requires all construction materials to meet 7 basics for construction works. The basic requirements cover:

(i) mechanical resistance and stability,
(ii) safety in case of fire,
(iii) hygiene, health and environment,
(iv) safety and accessibility in use,
(v) protection against noise,
(vi) energy economy and heat retention and
(vii) sustainable use of natural resources. (EC, 2011a).

Of particular relevance to Basic Works Requirement 7: Sustainable use of natural resources, 3 key demands are set for designers and specifiers; (i) recyclability of the construction works, their materials and parts after demolition, (ii) durability of the construction works, (iii) use of environmentally compatible raw and secondary materials in the construction works (European Commission, 2011a). Apparently, designers have also been contributing to the sustainable design and construction by embracing the key requirements in their design criteria (see Table 2.1) (Fordham, 2010).

As one of the most important parameters regarding sustainable construction, requirements are set for energy conservation of dwellings in Building Regulations Part L (2013). Therefore, designing and building a thermally efficient environment is of great importance in order to minimise the energy usage. Building Regulations Part L (2013) targeted for the reduction of U-values (i.e thermal transmittance which is a measure of ability to conduct heat out of the building and can be calculated using the thermal conductivity of the material used) of buildings to increase the energy efficiency.

Table 2.1 Sustainability matrix towards 'Zero Carbon' (Fordham, 2010)

Sustainability Criteria		Minimum Standard	Best Practice	Innovative	Pioneering
Building & Operational Targets	Proposed Building Regulations	2010 Part L	2013 Part L	2016 Part L	2019 Part L 'Zero Carbon'
	CO_2 emission target (kg $CO_2/m^2/yr$)	30	21	8	'Carbon neutral'
	Energy Consumption -Heating & hot water load (kWh/ m^2/yr)	61	46	30	15
	U-values -Wall (W/m^2K)	0.35	0.2	0.15	0.1
Construction Materials	Embodied carbon in fabric	Embodied carbon not assessed	Minimise material mass	LCA of embodied carbon	Use of all low eEnergy materials
	Recycled and reclaimed content (%)	15	30	45	60
	Material toxicity	Avoidance of high VOC contents & all ozone depleting materials	Non petro-chemical based insulation materials	VOC free paints and timber, natural materials where possible	Use only natural materials where products exist
Waste	Construction waste minimisation	Produce SWWP & identify waste streams for segregation or post	Divert 75% of non-hazardous waste from landfill	Implement modern methods of construction, account for site conditions	Zero net waste

On the other hand, environmental noise is a significant problem affecting people's comfort, health and well-being. Noise pollution caused mainly by means of transportation, construction and industrial activities is considered as one most important environmental problems. It has significant health effects on people such as annoyance, sleep disturbance, physiological stress reactions, stress-related increased blood pressure and even deaf at high exposure conditions. World Health Organization (WHO) proposed several threshold levels, ranging from 32 (L_{Amax} ; max sound pressure level inside) to 42 (L_{night}, outside) dB addressing these negative health effects of noise. Table 2.2 summarises the noise mapping data collected in Member States of the EU as required in the EU Noise Directive (EC, 2002) in order to assess the environmental noise exposure of the population (EC, 2011b).

In consequence of increasing level of disturbance due to noise, Part E of Building Regulations (2013) specifies the performance requirements to increase the resistance against passage of sound within dwelling-houses, from other parts of the building or adjoining buildings. Example values (a single-number quantity characterising the sound insulation between two rooms) for the specified performance requirements are given in Table 2.3.

Table 2.2 Summary of the noise mapping data in the EU (EC, 2011b)

Scope	No. of people exposed to noise above L_{den} > 55 dB (million)	No. of people exposed to noise above L_{night} > 50 dB (million)
Within agglomerations (163 agglomerations in EU > 250 000 inhabitants)		
All roads	55.8	40.1
All railways	6.3	4.5
All airports	3.3	1.8
Industrial sites	0.8	0.5
Major infrastructures, outside agglomerations		
Major roads	34	25.4
Major railways	5.4	4.5
Major airports	1	0.3

L_{den} – day-evening-night noise indicator

Table 2.3 Dwelling houses and flats-performance standards for separating floors, stairs and walls that have a separating function (Building Regulations Part E, 2013)

	Airborne and sound insulation **DnT,w + Ctr dB (Minimum Values)**
Purpose built dwelling-houses or flats	
Floors and Stairs	45
Walls	45
Dwelling-houses or flats formed by material change of use	
Floors and Stairs	43
Walls	43

2.3 FOAMED CONCRETE

2.3.1 Background of foamed concrete

Foamed concrete is an innovative construction material which is widely used in countries like UK, China, Malaysia, India and South Africa. Although there are no internationally standardised test methods for testing foamed concrete, properties and behaviour of conventional foamed concretes are well-established and documented. Foamed concrete, also known as cellular concrete, is a lightweight construction material which comprises mechanically introduced air-voids (by means of pre-foamed foam) into a base mix of either a cement paste or mortar (Ramamurthy et. al, 2009). A more widely cited definition for foamed concrete is "a cementitious material having a minimum of 20% by volume of mechanically entrained foam in the plastic mortar or grout" (Concrete Society, 2009).

Foamed concrete has become an increasingly popular material for non- and semi-structural applications in the past 20 years, given its unique properties of lightweight, free flow (Figure 2.3-a), self-compaction, ease for pumping/excavation and excellent thermal

insulation (Concrete Society, 2009; Ramamurthy et. al, 2009). Accordingly, amount of foamed concrete used in the United Kingdom was reported to be 1 million m^3 per annum by 2005 (Aldridge, 2005). Some of the application areas of foamed concrete are listed as trench infills, thermally insulating foundations, pre-cast panels, mine infills, blocks, load/lateral load reduction, flat roofs and road sub-base (Figure 2.3-b) with the order of decreasing density from 1400 to 300 kg/m^3 (Concrete Society, 2009).

There are no standards for foamed concrete in the UK or any known world-wide available apart from a record for a Japanese standard covering the testing methods for volume change of cellular concrete (JIS A 1162:1973) which has the most updated version from 1973. In spite of the lack of standards, there are specifications for foamed concrete published in the UK which are listed in Table 2.4. Specifications of BCA (1991) and BCA (1994) are the first specifications on foamed concrete, in the UK, providing guideline on its properties, advantages, and potential applications. The focus of these publications as well as UKWIR (1995) and HAUC (2010) was the use of foamed concrete for trench reinstatements, as foamed concrete was mostly known and used for void fillings and ground works.

The defining and design criterion of foamed concrete is mostly by its dry density otherwise plastic density is taken as the criterion. Accordingly, foamed concretes generally range from 1600 kg/m^3 down to 300 kg/m^3 dry density (Concrete Society, 2009), in some cases even lower. Having reviewed the classification of studies on the properties of foamed concrete (Ramamurthy et. al, 2009; Concrete Society, 2009), it is clear that minimum foamed concrete density (dry) considered is 300 kg/m^3.

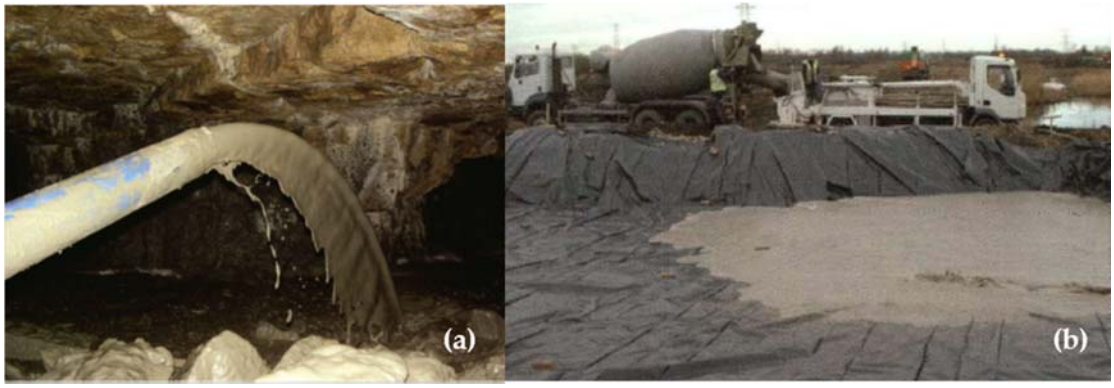

Figure 2.3 (a) Free flowing characteristics of foamed concrete used for mine infill and (b) application as road foundation (Concrete Society, 2009)

Table 2.4 Specifications for foamed concrete (United Kingdom)

Publishing body	Title of the specification	Contents
BCA (1991)	Foamed concrete - a Dutch view	Definition, properties, advantages, and potential applications
BCA (1994)	Foamed concrete- composition and properties	
UKWIR (1995)	Specification of foamed concrete	Use as a reinstatement material
HAUC(2010) 1st & 2nd publications in 1992 and 2002	Specification for the reinstatement of openings in highways	General requirements for foamed concrete as an alternative reinstatement material
TRL- Brady et. al (2001) with contributions of University of Dundee	TRL Report AG39 – Specification for foamed concrete	Constituents, production, properties, uses, guideline for specifications, uses and quality control
Jones et. al (2004), CTU, University of Dundee	Development of foamed concrete insulating foundations for buildings and pilot demonstration project	Specification and quality control test framework for use in thermally insulating foundations and ground slabs
WRAP (2005)	Recycled and secondary aggregates in foamed concrete	Specification on the use of recycled and secondary aggregates in production
WRAP (2007)	Specification and quality control of foamed concrete incorporating RSA	Constituent materials, requirements, production control, transport, formwork pressure and end of-life and recycling of RSA foamed concrete
Concrete Society (2009)	Good Concrete Guide 7-Foamed concrete: application & specification	Case studies, practicalities, properties, quality control

In recent years, as a result of increasing need for lighter materials (to reduce the self-weight of structures), the focus on lighter foamed concretes has started to increase. While there was very limited information on ULFCs, Mohammad (2011) considered foamed concretes at plastic density of 300 kg/m^3 in an attempt to resolve the stability issues and could not be successful. On the other hand, Wei et. al (2013) reported characterization and simulation of microstructure and thermal properties of 300kg/m^3 foamed concretes, however the mix proportions and amount of admixtures used was not reported.

2.3.2 Foamed concrete in relation to sustainable construction

Foamed concrete is an inorganic, low self-weight construction material that can contain up to 80-90% air at low densities, which in turn greatly reduces the amount of constituents used and waste produced. Its self-flowing ability eliminates the need for compaction (Jones and McCarthy, 2005a) saving from the energy used during placement and also reducing noise during construction. Moreover, due to its low strength, foamed concrete can be easily excavated and removed from applications (Concrete Society, 2009)

Lack of coarse aggregates in foamed concrete mixes and elimination of fine aggregates at densities below 600 kg/m^3 (BCA, 1994) adds on to its contribution to sustainable construction through reducing the use of non-renewable primary sources. On the other hand, recycled (e.g. demolition fines, which are mostly sent to landfills) and secondary materials (e.g. crumb rubber, coarse fly ash) can be used in foamed concrete as filler (Jones et. al, 2012). Furthermore, foamed concrete can be crushed and re-used in the production of other foamed concrete mixes with the benefit of increasing the compressive strength due to the hydration of unhydrated cement particles present in the crushed foamed concrete (Jones et. al, 2009).

On the other hand, fine fly ash (up to 75% by mass) is effectively used in foamed concrete mixes replacing Portland cement in order to reduce the embodied CO_2 and promote certain behaviours such as lower thermal conductivity and drying shrinkage strains and reduced heat of hydration (Kearsley and Wainwright 2001b; Giannakou and Jones, 2002; Jones et. al, 2003; Jones and McCarthy, 2006).

Given its porous nature, foamed concrete has good thermal insulation and sound absorption properties (Ramamurthy et. al, 2009), therefore it can increase the energy efficiency of the buildings as well as the comfort (against noise). Excellent thermal insulation behaviour of foamed concrete which improves with decreasing plastic density was reported by (Giannakou and Jones, 2002; Jones et. al, 2003; Kearsley and Mostert, 2005; Jones and McCarthy, 2005a, 2005b; Concrete Society, 2009; Othuman and Wang, 2011; Wei et. al, 2013). Furthermore, foamed concrete was reported to have good fire resistance (Jones and McCarthy, 2005a, Ramamurthy et. al, 2009) as well as sulfate and freeze-thaw resistance (Ramamurth et. al, 2009).

Table 2.5 Summary of the key developments in foamed concrete at the University of Dundee

Researcher	Key Developments
McCarthy (2004)	✓ Development of thermally insulating foundations and ground slabs as well as evaluating number of fresh, engineering and permeation properties of foamed concretes with plastic densities ranging from 1000 to 1400 kg/m³.
Rao (2008)	✓ Examined the effect of replacing primary aggregates with air, demolition fines and fly ash at densities of 600 to 1400 kg/m³ by assessing fresh, engineering and permeation properties. ✓ Characterising 1000 and 1400 kg/m³ foamed concretes produced with wider range of recycled secondary aggregates (RSA) than fly ash and demolition fines. ✓ Developed foamed concrete with no/minimal primary aggregates with plastic density of 500 kg/m³.
Yerramala (2008)	✓ Designed and assessed performance of RSA foamed concrete with densities ranging from 600 to 1400 kg/m³. ✓ Explored the recycling potential of RSA foamed concrete for utilising it as fine aggregate in new foamed concrete. ✓ Evaluated the energy absorption potential of foamed concrete.
Mohammad (2011)	✓ Studied the effect of mix constituents and proportions on rheological and microstructural properties of foamed concretes (densities ranging from 600 to 1400 kg/m³) in relation to instability. ✓ Attempted to solve the issues of stability in 300 kg/m³ foamed concrete and gained further understanding on instability.

Foamed concrete, by its nature, has a great potential to contribute sustainable construction providing significant advantages on load, waste and embodied CO_2 reductions, thermal insulation as well as the consumption of secondary/recycled materials. To improve these advantages and promote the increase in the number of its application areas, more must be known about its behaviour at ultra-low densities. However, firstly, stability issues arising during the production of ultra-low density foamed concretes needs to be solved. Table 2.5 shows the summary of the key developments in foamed concrete at the University of Dundee with the focus of enhancing its contribution to sustainable construction. As seen in the Table, there is still a lack of understanding on stability and instability of foamed concrete which leads to inability of producing stable mixes.

2.3.3 Constituent materials and mix design

Foamed concrete basically consists of cement mortar/paste (base mix) comprising cement, water and sand (or filler) or cement and water which then mixed with pre-formed foam. Usually, at plastic densities 600 kg/m^3 and above base mix contains sand while at densities below no sand is used (BCA, 1994), but fillers may be utilised instead.

Cement

Portland cement (PC)

In most cases, CEM I Portland cement is the main cementitious constituent of foamed concrete (BCA, 1994; Brady et. al, 2001; Concrete Society, 2009). Total cement contents of around 300-400 kg/m^3 are usually employed, however these can increase depending on the strength requirements (Jones, 2000) or decrease depending on the design density of the mix. In addition to CEM I PC, utilisation of rapid hardening PC to obtain higher strengths and faster strength gain was also reported (BCA, 1994).

Fine fly ash (FA)

Fine fly ash (Category S fine fly ash conforming to BS EN 450-1:2012) is commonly used in foamed concrete, mostly in combination with PC in order to reduce the cost, enhance the long-term strength, mix stability and sustainability. Kearsley and Wainwright (2001b;

2002b) reported successful utilisation of fly ash in foamed concrete up to 75% by weight (replacing PC) without affecting the strength significantly. Furthermore, Jones et. al (2003) reported the advantages of fine fly ash (as 30% by mass cement replacement) on reducing the heat of hydration, drying shrinkage, thermal conductivity.

Regarding the practical considerations of utilisation of fly ash in foamed concrete, McGovern (2000) emphasized the need for taking measures when concreting at low temperatures as the rate of strength gain would be reduced due to slower reaction rate of fly ash. Moreover, due to the greater surface area of fly ash particles, water demand of the mix increases with the incorporation of fly ash in order to maintain the required consistency. On the other hand, fly ash was reported to cause foam instability in the mix (i.e leading to foam collapse) resulting in addition of higher amount of foam than calculated in order to reach the target density (Jones and McCarthy, 2006). This behaviour is attributed to the surface charges and residual active carbon in fly ash, however the critical carbon level causing this is not known.

Calcium sulfoaluminate cement (CSA)

McCarthy (2004) reported the use of calcium sulfoaluminate cement in foamed concrete by Turner (2001) for reducing the setting times. CSA cements are not readily available in the UK and they are imported from China where they are originated and have been manufactured and used in large scale for both structural and non-structural applications including office blocks and flyovers. As CSA cements can be manufactured at lower temperatures than PC, less energy is used leading to reduced carbon dioxide (CO_2) emissions. CSA cements vary considerably by their chemical compositions and behaviour mainly depending on the phases present and the presence and/or amount of gypsum and anhydrite (BRE, 2007).

CSA cements contain ye'elimite, naturally occurring calcium sulfoaluminate ($Ca_4(AlO_2)6SO_4$), as a major constituent (30–70%). CSA clinker is inter-ground with calcium sulfate of varying levels to obtain rapid-hardening, high strength, expansive, or self-stressing cements (Juenger et. al, 2011). The primary hydration product of CSA cement is ettringite (Ioannou et. al, 2014). Compared to Portland cement, CSA cements hydrate faster, and most of the heat evolution due to hydration occurs between 2 and 24 hours of

hydration. The setting times of CSA cements depends on the ye'elimite content, type and content of minor phases as well as the amount and reactivity of the added calcium sulfate source. As high water/cement ratio is required for the complete hydration of CSA cement (Ioannou et. al, 2014), which is typically around 0.60, CSA cements tend to undergo self-desiccation, if low w/c ratios of 0.30–0.45 are used (Juenger et. al, 2011).

Durability of building materials produced using CSA cements were reported to be at least comparable to PC whereas they can exhibit high freeze-thaw and chemical attack resistance. On the other hand, concretes with CSA cements carbonate faster than the ones with PC depending on the w/c ratio leading to decomposition of ettringite that result in strength loss (Juenger et. al, 2011).

While there is no literature available on the ternary blends of PC/CSA/FA, the most similar case reported is the ternary blends of CSA/calcium sulfate/FA. Ioannou et. al (2014) reported the use of FA in CSA/anhydrite combinations promoted an earlier formation of a strong ettringite-rich matrix. FA particles and the hydrated phases contributed to a dense microstructure whilst early strengths reached higher values compared to CSA/calcium sulfate combination. Furthermore, addition of fly ash was reported to delay the final setting times whilst exhibiting no effect on the initial setting times (Ioannou et. al, 2014).

Silica fume (SF)

Silica fume has been used in foamed concrete at a rate of up to 10% by mass of cement improving the compressive strength (Kearsley, 1996). Silica fume was also reported to decrease the thermal conductivity of lightweight aggregate concrete (Demirboğa and Gül, 2003) which may further improve the excellent thermal insulation performance of foamed concrete.

Fine aggregates/fillers

Sand

Utilising sand with maximum size of 2 mm is common practice which yields higher foamed concrete strengths than 5 mm sand. Coarse aggregates cannot be used in foamed concrete as the fine air bubble structure cannot support them resulting in segregation

(BCA, 1994). It is suggested to use fine sand in mixes with dry densities down to 600 kg/m^3 and replace it with fillers like coarse fly ash at lower foamed concrete densities (BCA, 1994; Dransfield, 2000). For foamed concretes with plastic densities 300 kg/m^3 and below, sand is not of concern.

Carbon nanotubes (CNTs)

There are records of incorporating carbon nano-tubes into foamed concrete mixes as fillers for reinforcement. Yakovlev et. al (2006) reported that the carbon nanotubes used as high strength dispersed reinforcement have a cylindric form, with diameter ranging up to 100 nm and length up to 20 μm. It was reported that utilising 0.05% (by mass) CNTs in foamed concretes (on the basis of Portland cement) with densities around 310-330 kg/m^3 decreased the thermal conductivity up to 12 – 20% and increased the compressive strength up to 70%.

Furthermore, as shown in Figure 2.4, CNTs were found to yield more homogeneous cell structure with closed cell bubbles rather than open-cell bubbles (Yakovlev et. al, 2006). However, as CNTs particles have extremely high surface area accompanied by high aspect ratios and flexibilities, CNTs are likely to entangle and closely pack forming clumps with low disperseability, therefore, surfactants are used to disperse the CNTs (Vaisman et.al, 2006). However, regarding the high sensitivity of foamed concretes to chemical admixtures causing foam instability, CNTs need to be dispersed in water which may not be the most efficient method.

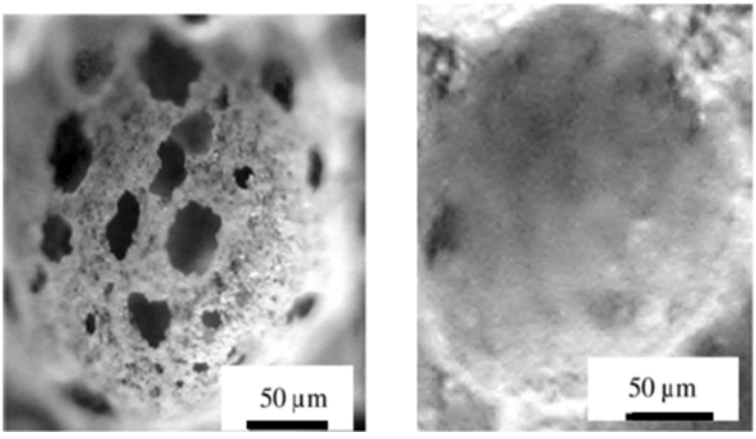

Figure 2.4 Influence of CNTs on the bubble structure of 300 kg/m^3 foamed concrete; without CNTs (left), with 0.05% CNTs (right) (Yakovlev, 2006)

Water

Potable water as specified by BS EN 1008 should be used in foamed concrete, especially in when protein-based foaming agents are used to produce the foam. This is because organic contamination may have an adverse effect on the quality of the foam, hence the concrete produced (Brady et. al, 2001). Similarly, Mohammad (2011) emphasized that, it is vital for foamed concrete stability to use mixing water that is not acidic or hot (60 °C) as these conditions exhibit higher drop out level of pre-formed foam.

The role of water in foamed concrete is well-documented and differs from normal weight concrete from some aspects such that strength increased with increasing water/cement (w/c) ratio (Dransfield, 2000). As w/c ratio plays a vital role on the quality and stability of foamed concrete, w/c ratio must be chosen considering the type of constituents used and their characteristics in order to provide the required workability of the base mix as well as maintain the mix stability (Brady et al., 2001; Ramamurthy et. al, 2009). Accordingly, Kearsley (1996) reported higher water requirement at greater fly ash contents due to the high specific surface area of fly ash particles.

W/c ratio used in foamed concrete typically ranges from 0.40 to 1.25 (Ramamurthy et. al, 2009). Insufficient water in the mix tends to cause extraction of water from the foam leading to disintegration of the foam, hence potential collapse of the mix. In contrast, excess water in the mix favours segregation that may also lead to collapses and increased drying shrinkage (Kearsley, 1999b; Brady et al., 2001; Kearsley and Mostert, 2005; Nambiar and Ramurthy et al., 2006).

Foam

Pre-formed foam consists of a foaming agent diluted in water and compressed air which are forced through a restriction to produce foam (BCA, 1994). Pre-formed foam incorporated into the base mix has the ability to control the plastic density of the foamed concrete mix when added in calculated amounts (Wee et. al, 2006). In order produce concrete with reasonable strength, foam should contain homogeneous bubbles of regular shape, preferably small and spherical bubbles, and thick walls which do not coalescence

much (Brady, et. al, 2001). Similarly, Ramamurthy et. al (2009), noted that the foam should be stable enough to resist the pressure of the base mix until the time of initial set and formation of a strong skeleton of concrete surrounding the air bubbles.

As foam determines the stability state of the mix (if the foam is not stable it collapses leaving a dense base mix) and final properties of foamed concrete, the quality of the foam is of great importance. BCA (1991) noted that, the quality of the foam is determined by its density, the dilution factor of the agent, the foam-making process and the incorporation and blending process with the base mix. On the other hand, Aldridge (2005) noted that the role of pre-formed foam in the mix is more critical when the foam comprises more than 50% of the mix. Therefore, as density of the foamed concrete mix decreases, the quality of the foam gains more importance in maintaining the stability of the mix.

Preformed foam is categorised as either wet foam or dry foam. Wet foam, which is produced by spraying a foaming agent solution and water over a fine mesh, has larger bubble size ranging from 2-5 mm in diameter. As wet foam is loose, it is not recommended for foamed concretes with densities below 1000 kg/m^3. On the other hand, dry foam, which is produced by forcing the foaming solution, water and compressed air through high-density restrictions, has smaller bubbles of even size with diameters of less than 1mm. As dry foam is very stable and thick, it is specifically preferred for low density foamed concretes where state of mix stability is critical (Concrete Society, 2009).

Foaming agents

Foaming agents (surfactants) are required to reduce the high surface tension of water and create foam (Myers, 1992). Table 2.6 gives the surfactant types and properties used in foamed concrete. Prior to foam production, the surfactant is usually diluted with a ratio of one part surfactant to between 5 to 40 parts water (BCA, 1994)

Due to their nature, protein surfactants are variable and can be unstable, especially in the presence of contaminants (McGovern, 2000). Furthermore, they can also be quite sensitive to the chemistry of the mix, such as alkalinity (Dransfield, 2000). On the other hand, synthetic surfactants are categorised depending on the type of charge that the head carries.

Therefore, they can be categorised as anionic (negatively charged), cationic (positively charged), non-ionic and zwitterionic (two oppositely charged heads). Anionic, non-ionic and cationic surfactants forms the 70%, 25% and less than 5% of the surfactants used for foamed concrete respectively while zwitterionic surfactants are rarely used in foamed concrete (Myers, 1992).

Foam stability

Almost similar to all other systems comprising two or more immiscible phases, foams also involve thermodynamic conditions in which the primary driving force is to reduce the total interfacial area between the phases (i.e these systems are thermodynamically unstable. Inspite of their tendency to contract, foams can be prepared to have a persistence life time up to months (Myers, 1992). However, on some time-scale all foams collapse and this usually occur from the surface inwards as the films are thinnest at the upper surface (Weaire and Hutzler, 1999), given the higher buoyancy of the bubbles at the surface.

Table 2.6 Surfactant types and properties (BCA, 1991; Dransfield, 2000; McGovern, 2000; McCarthy, 2004)

Surfactant type	Example composition	Properties	Characteristics of foam produced	Application areas in foamed concrete
Protein	Hydrolysed animal proteins & keratin	Variable, highly refined & stabilised	Stable, relatively low drainage, strong & firm texture, closed cell bubbles	In low density FCs and when high strength or waterproofing is required
Synthetic	Alkyl sulfates	Stable, easy to formulate & consistent	Larger & more open cells due to higher expansion, lower strength	In higher density FCs, good for large, fast placing

Fundamentally, upon the formation of foam and where two or more bubbles are in contact, pressure (P) and surface tension (γ) differentials occur at the two distinct areas of the bubbles. This is caused due to the presence of greater curvature at the Plateau borders (which have low surface tension) and surface tension at the lamellar film (with greater surface tension) (see Figure 2.5) exceeding the equilibrium value respectively. Laplace law applies on these phenomena at the gas-liquid interface (Myers, 1992; Weaire and Hutzler, 1999; Stevenson, 2011). Therefore, the balance of pressure differentials across the gas-liquid interface and the surface tension acting upon an element of the surface is expressed by the Laplace law, given by Equation 2.1.

$$\Delta P = \frac{\gamma}{r1} + \frac{\gamma}{r2} \qquad \text{Equation 2.1}$$

where,

ΔP = pressure difference across a curved interface due to the surface tension of the solution

γ = surface tension of the solution

r_1, r_2 = principal radii of curvature of the surface

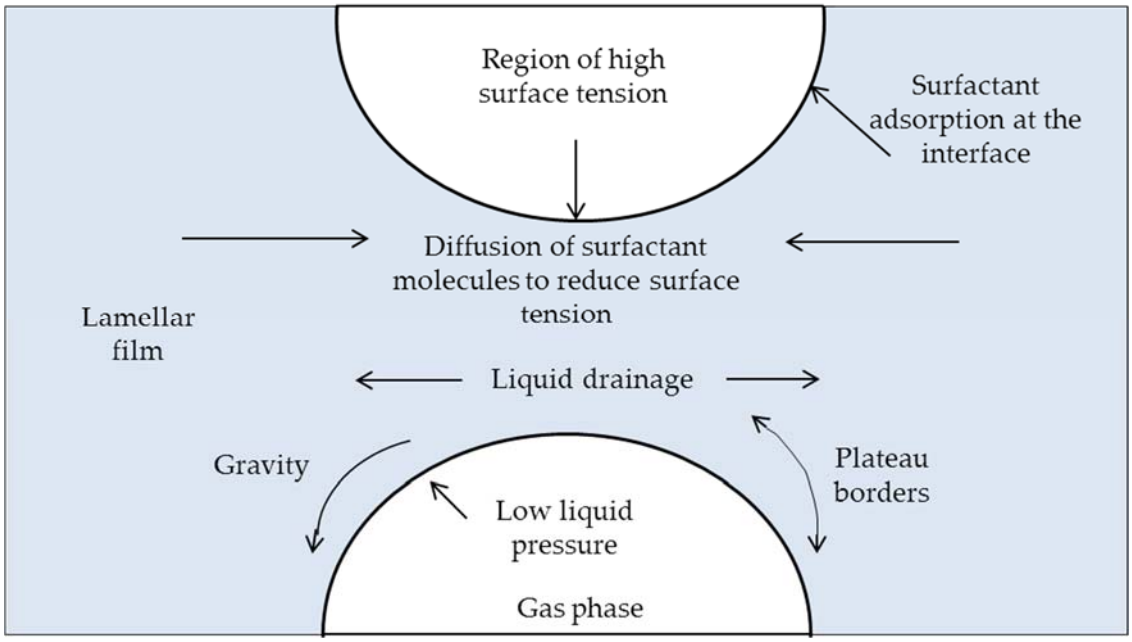

Figure 2.5 Schematic representation of the effect of dynamic equilibrium state (Gibbs-Marangoni effect) of foams (Myers, 1992)

The radii differences in curvature cause fluid drainage from the lamellar regions to the Plateau borders in order to restore the imbalance in liquid pressure (Gibbs effect). In addition, gravitational forces also results in liquid drainage from the lamellae leading to thinning of the film which separates the adjacent bubbles. On the other hand, surfactant molecules diffuse from the Plateau borders to the lamellar film to oppose film thinning due to drainage and restore surface tension to equilibrium values (Marangoni effect). These two mechanisms occur until the critical bubble film thickness is reached (Myers, 1992).

Once the critical thickness is reached, the film can't withstand the exerted pressures and ruptures resulting in foam collapse hence transformation of foam back into surfactant solution (Stevenson, 2011). Moreover, in the case of thick bubble films (in high density foams) gravity has a significant contribution to liquid drainage in opposed to the cases in which, the film thickness is below the critical thickness where interfacial dynamic interactions have more control over the drainage (Myers, 1992; Weaire and Hutzler, 1999).

Mix design

There is no standard method to calculate the mix proportions of foamed concrete (Brady et. al, 2001) and an approach on volumetric basis, followed at the University of Dundee to do the mix design is commonly used (Brady et. al, 2001; Jones and McCarthy, 2005a, Jones et. al. 2012; Wei et. al, 2014). Unlike normal concrete mix design, the design criterion is the target plastic density as it is difficult to design for target dry density, given 50 to 200 kg/m^3 desorption values of foamed concrete (Jones and McCarthy, 2005a). In contrast, Kearsley and Mostert (2005), Tarasov et. al (2010) followed the same design method by specifying a target dry density.

The mix design approach adopted at the University of Dundee (shown in Section 3.4) and described in Jones and McCarthy (2005a) was used as the basis for most researchers. Accordingly, amount of foam required to achieve the target density (plastic/dry) is calculated by using the cement and fine aggregate contents, w/c ratio and specific density values of all corresponding constituents (including the foam). Additionally, when different cement/aggregate types are used such as fine/coarse fly ash respectively, the mix design

needs to be tailored considering the higher water requirement of fly ash (Giannakou and Jones, 2002; Jones and McCarthy, 2005a; Kearsley and Mostert, 2005).

Density has a strong influence on the properties of foamed concrete whether it is dry or plastic density. Therefore, a tolerance of ±50 kg/m^3 on the target plastic density is usually acceptable which is also applied in industry practice for foamed concrete production (Jones and McCarthy, 2005a). In addition, instabilities due to foam collapse leads to increased target density that may result in alterations in the properties of the resultant concrete (Mohammad, 2011). Therefore, it is vital to maintain the mix stability hence the design density within the tolerance limits in order to obtain the properties from the specified foamed concrete.

2.3.4 Mixing process and curing

The most successful mixing process for the production of foamed concrete has a folding action where paddles rotate on a horizontal shaft or a screw action in a trough (Dransfield, 2000 and Jones, 2000). On the other hand, the rotating mixers, used for some of the mixes in this study, were reported to not provide enough shear forces to produce sufficient base-mix consistency (Jones, 2000).

Regarding the curing regime, as it provides the highest strengths with the most cost-effective way sealed curing at 65±5% RH and 20±2°C was used by many researchers (Jones and McCarthy 2005a, 2005b; Kearsley and Wainwright, 2001a, 2001b; Wee et al., 2006). Other types of curing regimes could be applied if specified in the standard test method.

2.4 PROPERTIES OF FOAMED CONCRETE

2.4.1 Fresh state properties

Fresh state properties of foamed concrete are evaluated mainly in terms of mix stability (in terms of volumetric stability) and consistency (in terms of flow behaviour). Although there are research studies conducted on the mix stability and consistency, most of these considered foamed concrete densities of 600 kg/m^3 and above, apart from Mohammad

(2011) who studied the stability issues at ultra-low densities (mainly at 300 kg/m^3). On the other hand, there is limited information (Jones and McCarthy, 2005b; Mohammad, 2011) on the rheology of foamed concrete which is related to the consistency. In general, fresh state properties of foamed concrete are described as free-flowing, self-levelling and self-compacting (Dransfield, 2000; Jones et al., 2003; Jones and McCarthy, 2005a, 2005b, 2006; Concrete Society, 2009). On the other hand, foamed concrete is quite thixotropic (BCA, 1994) and while this not always the case, it can be quite difficult to restart the flow once the concrete has been static for several minutes (Concrete Society, 2009).

Generally, the workability of foamed concrete containing relatively high volume of air is excellent such that it is easily pourable and does not need further consolidation during placing (Basiurski, 2000). However, at very low densities foamed concrete exhibits reduced self-levelling, possibly due to the reduced self-weight and increased cohesion of the mix resulting from increased volume of air (Nambiar and Ramamurthy, 2006).

In an agreement with this statement made by Nambiar and Ramamurthy (2006), Jones and McCarthy (2005b) reported that foamed concrete with lowest density (densities ranging from 1000-1400 kg/m^3) exhibited highest apparent yield stress (which is the minimum stress required to initiate the flow) and attributed this behaviour to reduced self-weight and increased air volume. Furthermore, Jones and McCarthy (2005b) reported the decrease in yield stress when sand is replaced with coarse fly ash due to rounded particle morphology of fly ash compared to larger and angular shaped sand particles.

Contrarily, Mohammad (2011) reported an increase in yield stress values with increasing density on density range of 600-1400 kg/m^3 and attributed this behaviour to the increased cohesion of the mix due to the increased foam content. Furthermore, it was reported that replacing 30% (by mass) of PC with fine fly ash reduced the yield stress (Mohammad, 2011).

Mix stability

Definition

Neville (2011) defined stability of normal weight concrete as its ability to resist segregation by referring to the cohesion state of the mix. Another definition made by Khayat and Assaad (2002) was cited as; stability is required to ensure presence of an adequate air void system and maintain it stable until the time of hardening in self-consolidating concrete (SCC). More specifically, Nambiar and Ramamurthy (2007a, 2007b) defined the state of stability in foamed concrete as the unity of design and measured density (i.e measured density is within the acceptance limits of ±50 kg/m^3). Given the similarities of high flowability and relatively low cement contents (Khayat and Assaad, 2002), definition of stability for SCC may potentially be used to describe stability of foamed concrete.

Factors affecting the mix stability

The main factors affecting the mix stability mainly includes environmental conditions, materials used and the quality of the production as well as time dependent factors. Brady et. al (2001) listed the external environmental factors influencing the foam concrete stability as vibration, wind, evaporation and temperature. On the other hand, many others considered the most dominant cause of instability as foam (its quality and volume) (McGovern, 2000; Aldridge, 2005; Jones and McCarthy, 2005b, 2006; Nambiar and Ramamurthy, 2007a, 2007b, 2008; Mohammad, 2011).

Although foams are very stable, easy to blend with the base mix and possess low drainage forming closed cell bubbles in a good system, chemistry of the constituents (e.g alkalinity) in the mix can adversely affect the foam stability leading to foam collapse (Dransfield, 2000; McGovern, 2000; Brady et. al 2001). It was also reported that the performance of synthetic surfactants in foamed concrete is not as good as protein surfactants as synthetic surfactants tend to yield open cell bubbles with larger bubble size unlike protein surfactants. On the other hand, McGovern (2000) and Brady et. al (2001) suggested that protein based surfactants can be unstable given their variable nature and tend to break down by time. However, it was suggested to use protein surfactants at low densities and in applications where strength is an important factor (McGovern, 2000; Ansell, 2010). Supporting the

statements made for synthetic surfactants, Mohammad (2011) observed higher degree of instability in foamed concrete mixes with densities ranging from 300 to 1400 kg/m^3 when synthetic surfactant is utilised.

Aldridge (2005) emphasized the importance of foam quality on maintaining a stable mix throughout the mixing, placing and placing process (by means of stable bubbles) and the increasing risk of instability when the foam content comprises more than 50% of the mix. In an agreement with Aldridge (2005), Jones and McCarthy (2006) and Mohammad (2011) reported that for a given type of constituents, mixes become more prone to instability as density of foamed concrete decreases. More specifically, Mohammad (2011) found that it was impossible to produce stable foamed concretes with plastic densities below 400 kg/m^3 using PC. Given some reported failures in industry applications, colleagues from the industry also support the fact that foamed concretes with densities below 400 kg/m^3 have stability issues (Ansell, 2010). In addition, Mohammad (2011) found that the severity and speed of collapses due to instability increased both in the case of decreased density (1400 to 600 kg/m^3) and increased w/c ratio as the yield stress of the mix reduces in both cases.

Moreover, Nambiar and Ramamurthy (2008) also stated that stability is dependent on the base mix consistency (which is function of w/c ratio, foam volume and the filler type) that reduces with the addition of foam. Similarly, it was reported that stiff base mixes cause bubble break down due to extraction of water from the foam whilst high water content slurries lead to segregation (Kearsley, 1999b; Nambiar and Ramamurthy, 2006). Apparently, w/c ratio of the base mix, that directly affects the consistency, has a governing role on the stability of foamed concrete, especially at low w/c ratios.

Jones and McCarthy (2005b and 2006) reported further causes of instability as; use of chemical admixtures (e.g water-reducing chemical admixtures) that interact with the chemistry of the surfactant and surface charges of the constituents used. More specifically, they reported the influence of fly ash on the stability of foam, hence foamed concrete. Accordingly, it was found that, utilisation of fly ash (coarse/fine) causes foam collapse (releasing 'free' water as a result of foam collapse during mixing) due to surface charges and the residual active carbon content of fly ash that possibly adsorbs on the surfactant like in the case of air-entrained concrete (RILEM, 1991; Joshi and Lohtia, 1997) requiring

utilisation of higher volume of foam than calculated to achieve the design density. Similarly, utilisation of GGBS in foamed concrete was observed to cause foam collapse and segregation, possibly as a result of chemical interaction (Jones and McCarthy, 2005c). Jones and McCarthy (2005b and 2006) suggested that comparison of calculated and actual foam contents required to achieve the design density as well as visual observation can be used for assessing stability in fresh state. Additionally, it was suggested to compare the actual and specified w/c ratios of the mixes, as the actual w/c ratio would increase in case of foam collapse. Segregation (determined on hardened concrete) is also considered as the measure of instability (Dransfield, 2000; Jones and McCarthy, 2005b; 2006).

In spite of the literature covering the potential and causes of foamed concrete instability, there were evidences that foamed concrete was assumed to be stable in the absence of extreme conditions. Baisurski (2000) stated that if foamed concrete is made correctly, it does not collapse after placing, as it sets. However, severe collapses of foamed concretes at ultra-low densities (below 500 kg/m^3) were visually observed in industry applications, questioning the validity of these assumptions. Obviously, there was a lack of detailed research on the stability of foamed concrete, especially with wider range of densities being considered.

Previously, many researchers (McGovern, 2000; Aldridge, 2005; Jones and McCarthy, 2005b, 2006; Nambiar and Ramamurthy, 2007a, 2007b, 2008; Mohammad, 2011) mostly attributed the instability of foamed concrete to the quality of foam as well as the type constituents used. However, in case of instability at ultra-low densities, the scenario is different since instability tends to occur regardless of foam quality and the type of constituents. Moreover, most of the studies on instability reported in the literature are in the range of low/high densities (600 kg/m^3 and above). Only Mohammad (2011) studied the instability of foamed concrete down to 300 kg/m^3 density as well as covering various factors that affect stability such as, external relative humidity and temperature, different surfactants, cement and filler types, chemical additions, bubble sizes and types, production methods as well as rheology.

Mohammad (2011) attempted to describe the occurrence of instability with a schematic illustrating the behaviour of foam on a timeline vs surface tension basis (Figure 2.6).

Accordingly, bubble sizes increase by time due to coalescence which is caused by liquid drainage. As time passes, bubbles continue to increase in size hence the rate of drainage leading to collapse of the foam. Meanwhile, the strength of bubbles decreases and can't support the exerted pressures leading to collapse of the foam. Therefore, beyond a critical bubble size, strength of the bubbles is not enough to withstand the surrounding pressures leading to foam, hence foamed concrete mix failure.

Apart from one recent study by Mohammad (2011), assessment methods for stability covered in the literature are applied either in the fresh state (during mixing) or hardened state. Mohammad (2011) suggested assessing the stability as an early age property by visual observation. Therefore, it was proposed to cast foamed concretes in cylinders and measure the drop in level after 24 hours as a measure of stability. This method is an indication of post-mixing interactions within the mix that lead to instability, hence collapse of the mix.

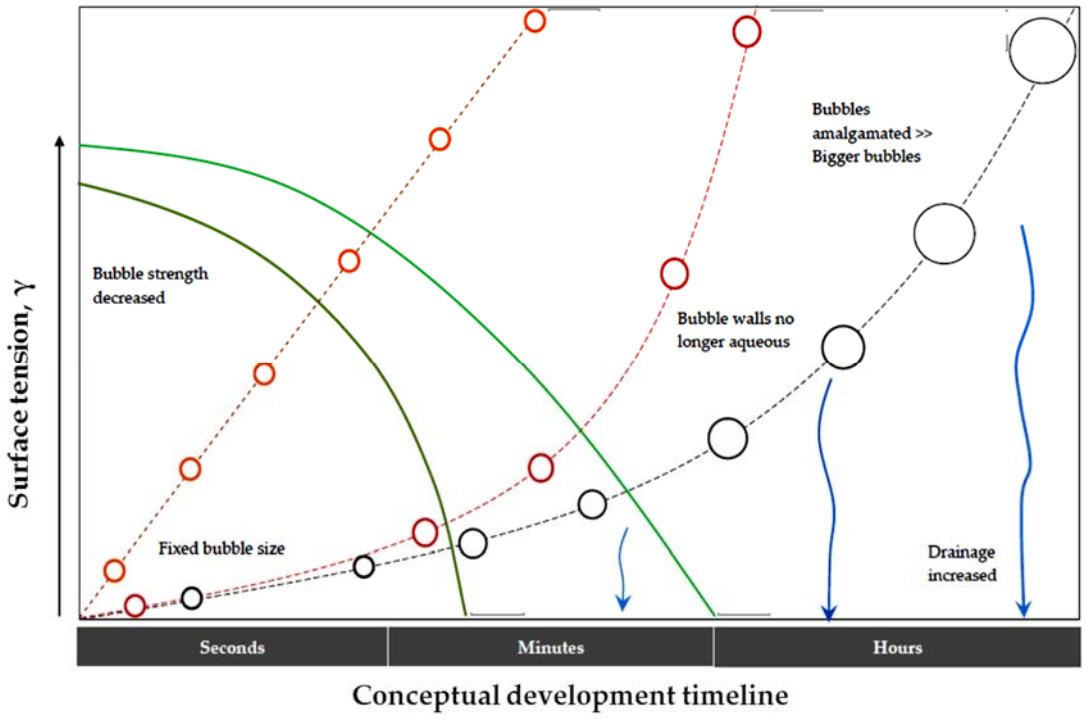

Figure 2.6 Conceptual development timeline for instability (Mohammad, 2011)

Consistency

Consistency of foamed concrete that characterizes its flow behaviour is well established for densities 600 kg/m^3 and above (Dhir et. al, 1999; Jones and McCarthy, 2005b; Nambiar and Ramamurthy, 2006; Mohammad, 2011). However, there is no information available to public on the consistency of ultra-low density foamed concretes (mainly 300kg/m^3 and below) with/without sand.

Nambiar and Ramamurthy (2006) reported that the flow of foamed concrete reduces with decreasing density (increase in foam volume), which is more significant at lower densities (where the amount of foam is larger in comparison to solids). This was attributed to the adhesion between the bubbles and the solid particles which increases the stiffness of the mix at lower densities. Furthermore, similar to Jones and McCarthy (2006) they reported an increase in the flow when sand is replaced with coarse fly ash.

On the other hand, Mohammad (2011) reported similar results that 600 kg/m^3 density exhibited longer flow times than 1000 kg/m^3 (which implied reduced flow at lower densities). Furthermore, incorporation of 30% (by mass) fly ash improved the flow and resulted in shorter flow times for 600 kg/m^3 mixes compared to 1000 kg/m^3 mixes. On the other hand, fly ash is reported to improve the workability of concrete given its spherical shape and glassy surface provided its carbon content is low (around 1% to provide low water absorption) (RILEM, 1991; Joshi and Lohita, 1997; Neville, 2011).

2.4.2 Early age properties

Temperature development upon hydration

Given its cellular structure, foamed concrete has good thermal insulation properties hence it is expected to have higher heat of hydration that lasts for longer compared to normal weight concrete. The parameters influencing the heat of hydration in foamed concrete were listed as the volume of the pour, the cement content, the density of the concrete and the amount, type and characteristics of the cement/filler/aggregate used (Brady et. al, 2001; Jones and McCarthy, 2006; Tarasov et. al, 2010). Tarasov et. al (2010) then extended the internal parameters as, w/c ratio, initial temperature of the mix, pore size, distribution and

connectivity and added the insulation and environmental conditions (such as humidity, pressure, air temperature) as external parameters. In contrast, Brady et. al (2001) reported that w/c ratio as well as the surfactant type does not have an effect on heat of hydration in foamed concrete.

Brady et. al (2001) cited temperatures of up to 100°C occurring up on cement hydration in foamed concrete and these temperatures could be sustained up to 3 days that potentially result in thermal strains and cracks. On the other hand, the risk of delayed ettringite formation (DEF) was also reported where the temperatures are above 65°C. However, given the cellular characteristics of foamed concrete, ettringite formed due to DEF fills the pores showing no evidence of expansion (Brady et. al, 2001), especially at lower density foamed concretes which are more porous.

Temperature development of foamed concrete due to heat of hydration in was assessed under semi-adiabatic conditions with an insulated box in which the foamed concrete is placed and a Type K thermocouple is used to measure the core temperatures. Consequently, the general outcome reported was decreased foamed concrete densities lead to higher temperature rise due to heat of hydration (Brady et. al, 2001; Jones and McCarthy, 2006; Tarasov et. al, 2010) due to the higher insulating capacity of lower density foamed concretes that would maintain the temperature developed during hydration.

Despite Jones and McCarthy (2006) showed that for a given cement content and materials combination foamed concrete mixes with 600 kg/m^3 density exhibited higher temperature peaks in comparison to 1000 kg/m^3 mixes, 800 kg/m^3 mixes which yielded the highest peaks was not found to be in line with this trend. Similarly, comparison of 1000 and 1200 kg/m^3 mixes was not found to yield the expected trend as 1200 kg/m^3 mixes reached to higher peaks.

Jones and McCarthy (2006) reported that, effect of plastic density on temperature peaks due to heat of hydration of foamed concrete is combination of factors, such as thermal insulating capacity, specific heat of individual constituents and microstructure. On the other hand, Tarasov et. al (2010), reported the inverse relationship between plastic density

and peak temperatures for a given cement content and type under semi-adiabatic conditions such that lower densities exhibited higher peak temperatures due to their higher insulating capacity. Furthermore, the pour volume was reported to play a dominant role on the peak temperatures especially at lower foamed concrete densities.

More specifically, Jones and McCarthy (2006) reported a decrease of 40% in the peak temperature developed upon heat of hydration when the cement content is decreased from 600 to 300 kg/m³. Similarly, Tarasov et. al (2010) concluded that decrease in cement content decreases the peak temperature regardless of the volume of the pour (Figure 2.7).

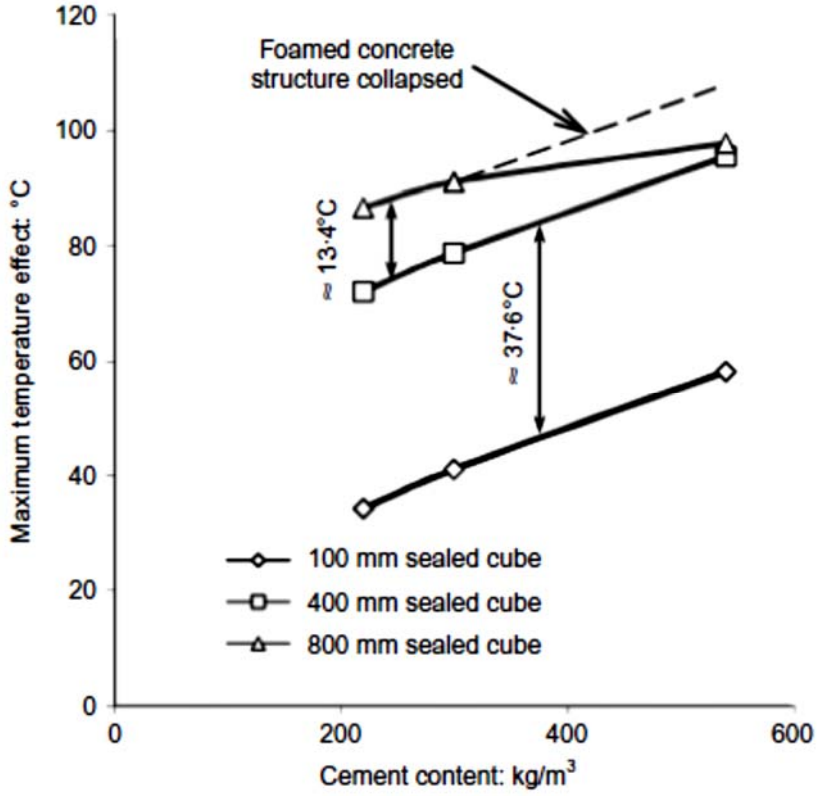

Figure 2.7 Effect of cement content on maximum temperature rise (Tarasov et. al, 2010)

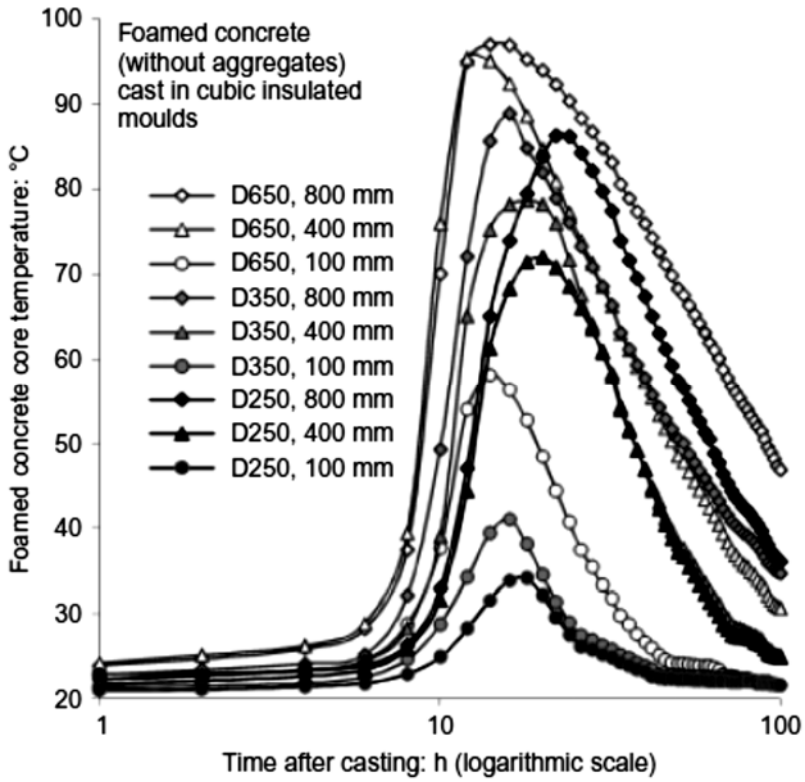

Figure 2.8 Temperature profiles of foamed concretes with different cement contents and no aggregates (Tarasov et. al, 2010)

While the data reported by Jones and McCarthy (2006) considered foamed concretes with plastic densities down to 600 kg/m^3, Tarasov et. al (2010) studied the heat of hydration of foamed concretes down to dry densities of 250 kg/m^3 with no aggregates. Given the density range, absence of aggregates and the cement content used, D250 mix (tested in 100mm cube) reported by Tarasov et. al (2010), which exhibited the peak temperature of around 33°C, is the closest reference to the ultra-low density foamed concretes considered in this study. Figure 2.8 illustrates the temperature profiles of foamed concretes with varying cement contents and no aggregate.

Furthermore, it was reported that using fine fly ash as a cement replacement aided to reduce the heat of hydration (Jones and McCarthy, 2006; Tarasov et. al, 2010). Figure 2.9 shows the influence of replacing 30% (by mass) of PC with fine fly ash on heat of hydration.

Jones and McCarthy (2006) reported that it is not suitable to use prediction models with foamed concrete as there is high number of parameters involved. On the other hand, Tarasov et. al (2010) presented a prediction equation as a function of cement content and volume of pour obtaining 89.3% correlation with the measured data. However, both emphasized the need for further work for developing a prediction model for foamed concrete that considers all the influencing parameters.

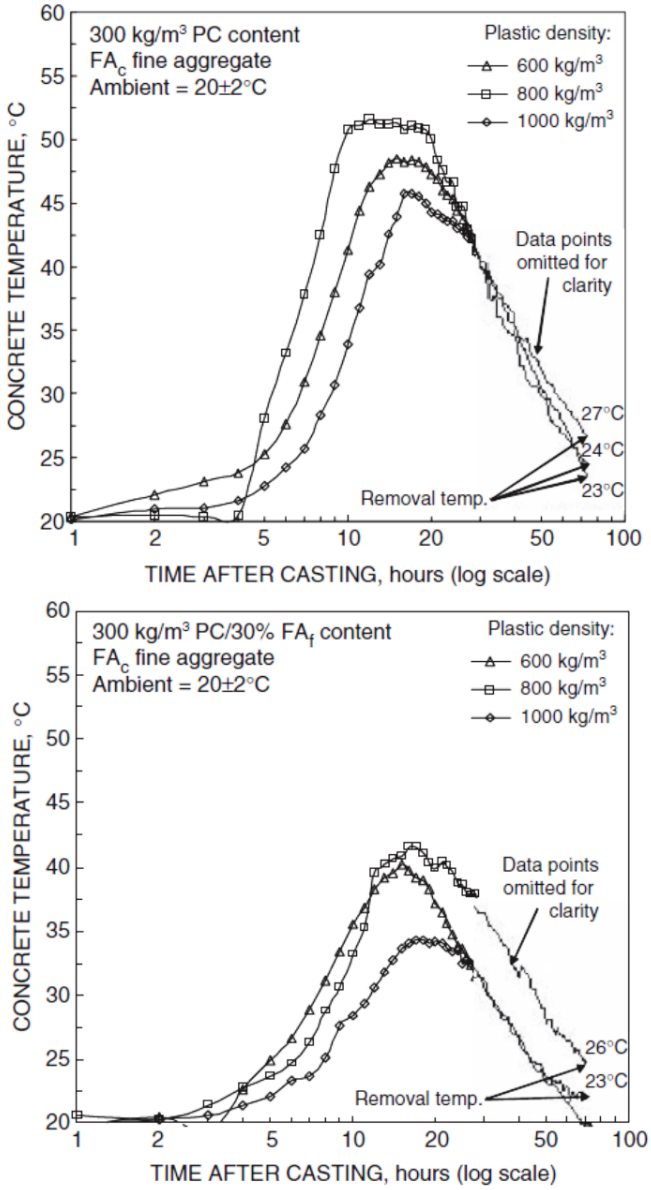

Figure 2.9 Influence of plastic density and fly ash as a cement replacing material on heat of hydration of foamed concrete (Jones and McCarthy, 2006)

Setting time

There is no standard method for determination of foamed concrete setting times, instead standard test methods for testing cements provided the basis for testing foamed concrete (Brady et. al, 2001). Dhir et. al (1999) and Jones (2000) reported that setting of foamed concrete does not occur until 5 hours after casting at 20°C. Similarly, in a recent study covering a wider range of foamed concrete densities (from 300 kg/m³ to 1000 kg/m³) it was reported that initial setting of foamed concrete does not occur until after 5 hours (Wei et. al, 2014). On the other hand, in this particular study, setting times were reported to shorten when the temperature is higher.

In case of high densities, it was reported that using sand or coarse fly ash did not make a significant change on the setting times (Dhir et. al, 1999; Jones, 2000). In contrast, Wei et. al (2014) concluded that addition of fine fly ash as a cementitious material at levels from 20% to 60% (by mass) increased the setting times for 1000 kg/m³ foamed concrete mixes produced with no aggregates. Overall, it was agreed that setting time of foamed concrete increases as plastic density decreases as it is presumed that foam chemistry has a retarding effect (Figure 2.10 and 2.11) (Dhir et. al, 1999; Jones, 2000; Wei et. al, 2014).

As illustrated in Figure 2.10 the focus on setting time of foamed concrete was regarding the strength gain such that the specified strength in the standard was achieved in 9 to 10 hours (Dhir et. al, 1999; Jones, 2000). On the other hand, Brady et. al (2001) cites the setting time of foamed concrete as 12 to 24 hours.

Dhir et. al (1999) assessed setting time of foamed concrete was by measuring the resistance of the concrete to a standard plunger (in accordance to (BS 5075-Part 1:1982). Both Dhir et. al (1999) and Wei et. al (2014) stored the freshly made foamed concrete mixes undisturbed in a temperature and humidity controlled environment prior to Vicat needle test, whilst latter specified the duration of storage as 2 hours in a moist cabinet.

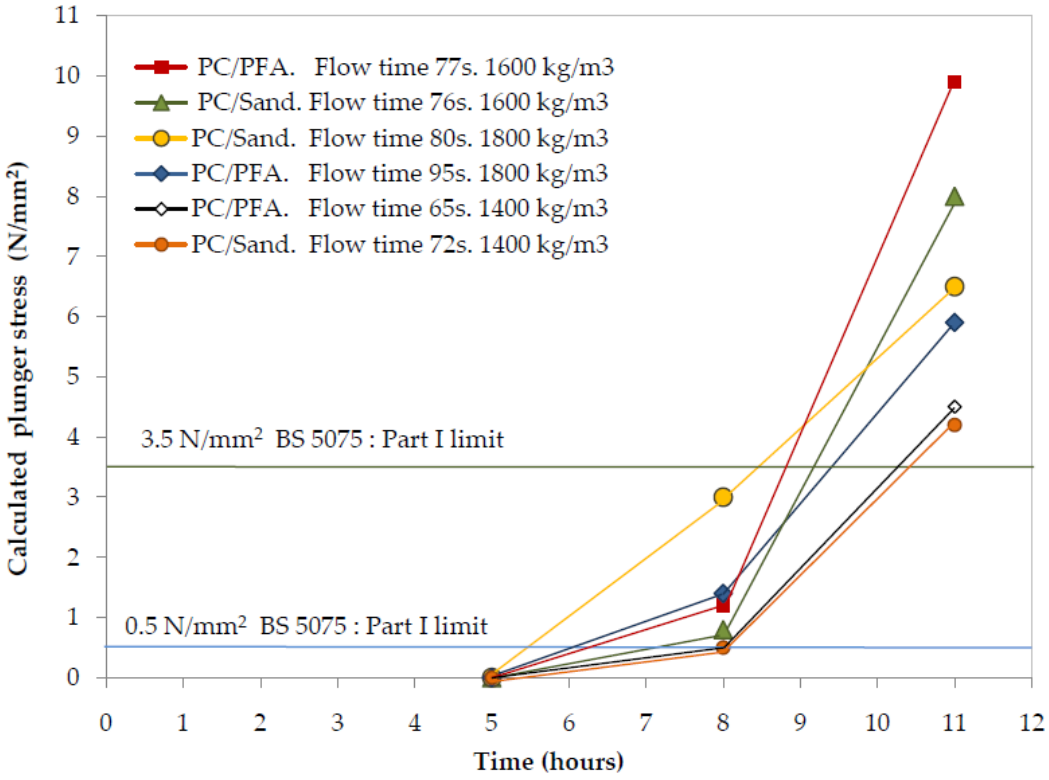

Figure 2.10 Comparison of setting time for various foamed concretes (Dhir et. al, 1999; Jones, 2000)

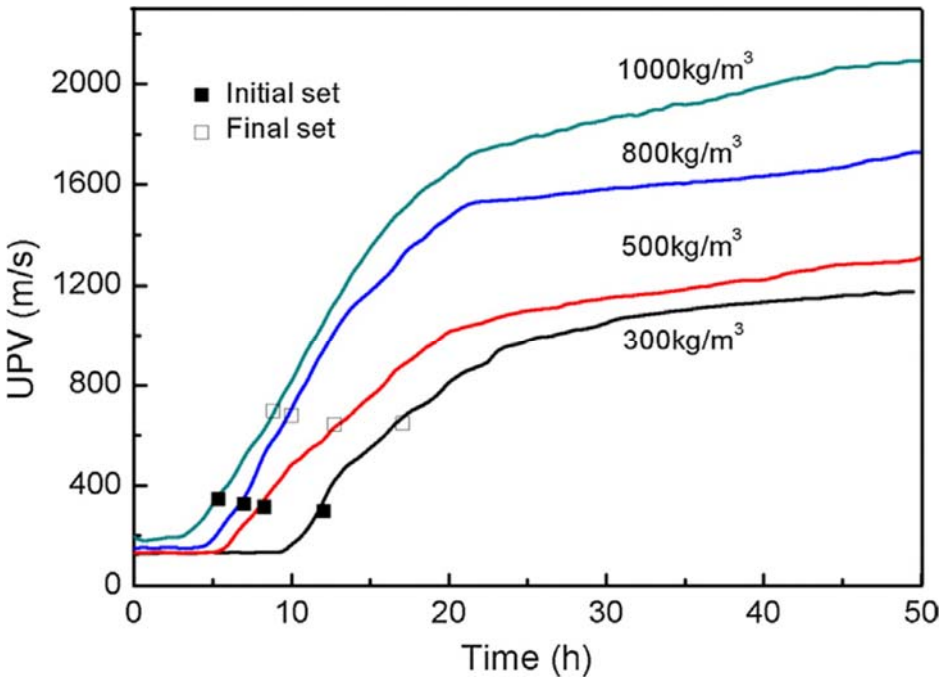

Figure 2.11 Setting behaviour of foamed concretes - determined by ultrasonic wave transmission method (Wei et. al, 2014)

In contrast, Wei et. al (2014) used ultrasonic wave transmission method to determine the setting time of foamed concrete as it is non-destructive and continuous method unlike Vicat needle test, scanning electron microscopy and infrared radiation test. In this particular study, foamed concrete mixes with densities ranging from 300 to 1000 kg/m^3 were tested for setting time. More specifically, effect of utilisation of various fly ash levels as well as different curing temperatures on setting time was studied.

In parallel, Vicat needle test was also utilised and the trends obtained for different conditions tested were the same. Given the nature of the Vicat needle test and ultrasonic wave transmission method they cannot be compared as former exhibits chosen stages of setting (initial and final setting time) in practice whilst latter provides a more continuous picture on the setting process. Furthermore, ultrasonic wave transmission method was also reported to give good reproducibility. Figure 2.11 illustrates the results obtained from ultrasonic wave transmission method for varying foamed concrete densities (Wei et. al, 2014).

2.4.3 Hardened state properties

Compressive strength

Compressive strength of foamed concrete was reported to decrease with decreasing density (BCA, 1994; Kearsley and Wainwright, 2002a, 2002b; Jones and McCarthy, 2005a; Concrete Society, 2009). Typical compressive strength values for foamed concretes with dry densities down to 400 kg/m^3 are shown in Table 2.7. Main parameters affecting the compressive strength of foamed concrete are the size and shape of the specimens, direction of loading, type of constituents, water content, age and method of curing. Moreover, cement/sand and water/cement ratios, type of foaming agent and sand as well as the size distribution of sand (Ramamurthy et. al, 2009).

Moreover, increase in void diameter was found to reduce the strength (Kearsley and Wainwright, 2002a; Nambiar and Ramamurthy, 2007a; Ramamurthy et. al, 2009). On the other hand, small changes in w/c ratio were not found to affect the strength of foamed concrete (Jones and McCarthy, 2006). Furthermore Jones et. al (2003) reported that

replacing 30% of PC with fly ash did not cause significant decrease in strength in long-term up to 180 days. Similarly, Kearsley and Wainwright (2001b) reported that up to 75% fine fly ash can be used to replace PC without causing significant reduction in strength.

While the compressive strength values reported are only down to foamed concrete (dry) density of 400 kg/m^3 which range from 0.5 to 1 N/mm^2, there is no compressive strength value reported for foamed concretes with plastic density of 300 kg/m^3 or below. Only Yakovlev et. al (2006) reported the compressive strength for 330 kg/m^3 which is 0.18N/mm^2, however it was not specified whether the density is plastic or dry.

Static modulus of elasticity (E-value)

Modulus of elasticity of foamed concrete is reported to be lower than normal weight concrete (Jones, 2000) and ranges from 0.8 to 6.0 kN/mm^2 for dry densities ranging from 400 to 1400 kg/m^3 as shown in Table 2.7 (BCA, 1994; Brady et. al, 2001; Concrete Society, 2009). Brady et. al (2001) attributes the lower E-values of foamed concrete to the lack of coarse aggregates, while further attributing the lower E-values of mixes with coarse fly ash (Brady et. al, 2001; Jones and McCarthy, 2005a; Ramamurthy et. al, 2009) to the lack of interlocking effect of sand.

Figure 2.12 illustrates the relationship between 28-day sealed cured cube compressive strength and E-value in comparison to normal weight and lightweight aggregate concretes. On the other hand, there are prediction equations reported in Table 2.8 for estimating the E-value of foamed concrete (Jones and McCarthy, 2005a; Ramamurthy et. al, 2009), however the suitability of these are questionable as the constituents and state of density (dry/plastic) assumed may differ from the ULFC mixes under consideration which do not comprise any fine aggregates.

Table 2.7 Typical properties of foamed concrete (BCA, 1994; Concrete Society, 2009)

Dry density, kg/m^3	Compressive strength N/mm^2	Modulus of elasticity, kN/mm^2	Drying shrinkage, %	Thermal conductivity, W/mK
400	0.5-1.0	0.8-1.0	0.3-0.35	0.10
600	1.0-1.5	1.0-1.5	0.22-0.25	0.11
800	1.5-2.0	2.0-2.5	0.2-0.22	0.17-0.23
1000	2.5-3.0	2.5-3.0	0.18-0.15	0.23-0.30
1400	6.0-8.0	5.0-6.0	0.09-0.07	0.50-0.55

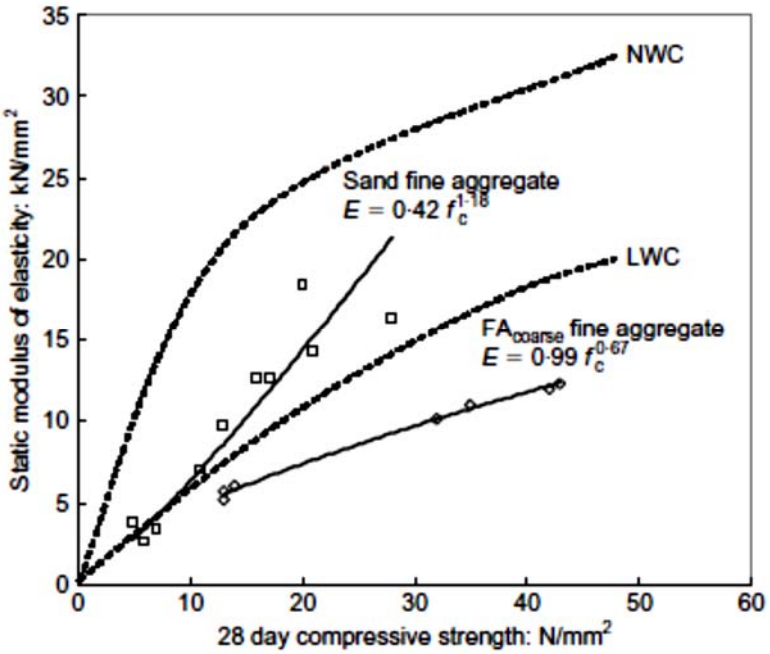

Figure 2.12 Relationship between E-value and 28-day sealed cured cube compressive strength of foamed concrete (Jones and McCarthy, 2005a)

Table 2.8 Relations for E-value of foamed concrete ([†]Ramamurthy et. al, 2009; [‡]Jones and McCarthy, 2005a)

Relationship	**Remarks**
[†]E= 5.31 * W-853	Density from 200 to 800kg/m^3 (Autoclaved aerated concrete)
[†]E= 33 * $W^{1.5}$ $\sqrt{f_c}$	Pauw's equation
[‡]E= 0.42 * $f_c^{1.18}$	Sand as fine aggregate

W: density of concrete (kg/m^3), f_c: compressive strength (N/mm^2), E: E-value (kN/mm^2)

Poisson's ratio

Poisson's ratio is the ratio of lateral strain to the longitudinal strain under a uniaxial load. Poisson's ratio of normal weight concrete ranges from 0.15 to 0.22 and lightweight aggregate concrete has Poisson's ratio at the lower end of the range (Neville, 2011). However, there is no information published regarding the Poisson's ratio of foamed concrete apart from the data reported by Lee et al. (2004). Therefore, Poisson's ratio of foamed concretes with densities 1000kg/m^3 and 1400kg/m^3 was reported to range from 0.13 to 0.16 and 0.18 and 0.19 respectively. As a result, it can be expected to have lower Poisson's ratio in lower density foamed concretes.

Drying shrinkage

Foamed concrete exhibits drying shrinkage of up to 10 times greater than normal weight concrete due to the lack/less amount of aggregates in foamed concrete (Ramamurthy et. al, 2009). Ramamurthy et. al (2009) noted that drying shrinkage of foamed concrete reduces with decreasing density due to the decreasing amount of shrinking cement paste. Contrarily, De Rose and Morris (1999), Dransfield (2000), McCarthy (2004) and Concrete Society (2009) reported an increase in drying shrinkage with decreasing density. Drying shrinkage values for corresponding densities are given as a guide in Table 2.7 and it can be seen that there is no data considering densities below 400 kg/m^3.

More specifically, McCarthy (2004) reported increased shrinkage strains with decreasing plastic density (foamed concrete densities ranging from 1000 to 1400 kg/m^3) on the mixes produced with sand as fine aggregate. However, it must be noted that the mixes reported had the same cement and water contents with varying aggregate and foam contents. Therefore, it was the aggregate content determining the drying shrinkage behaviour of foamed concretes considered.

Furthermore, De Rose and Morris (1999), McCarthy (2004) reported that replacing PC with fine fly ash reduced the drying shrinkage strains up to 64% (Figure 2.13). Similarly, Jones et. al (2003) reported the influence of 30% fine fly ash (by mass) as a cement replacement on reducing the drying shrinkage strains by 1.6 times. This behaviour was attributed to the shrinkage restraining effect of unreacted fly ash particles that act as filler.

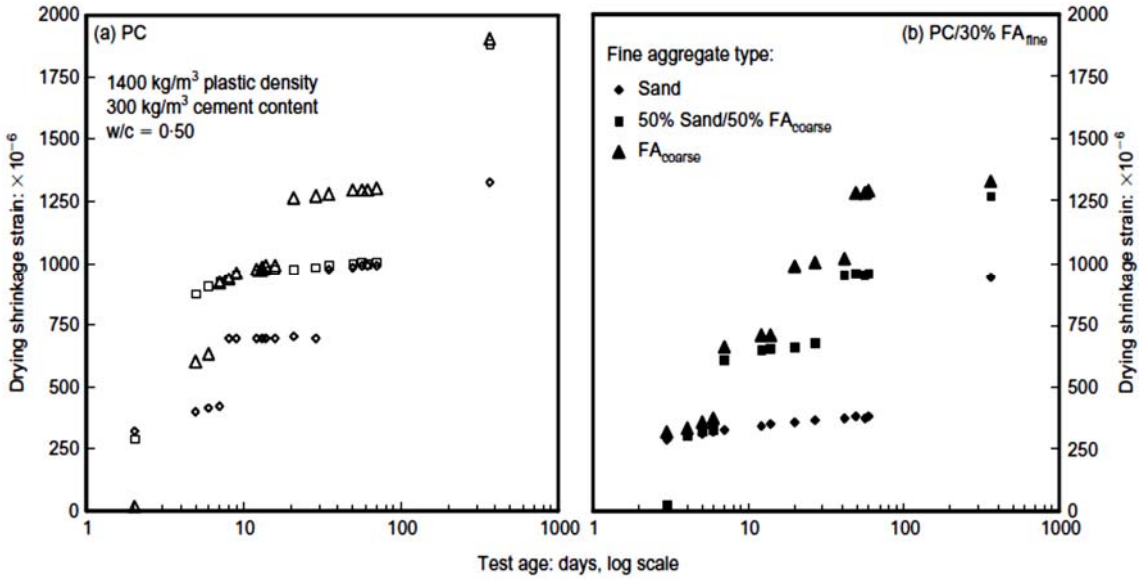

Figure 2.13 Influence of coarse and fine fly ash on drying shrinkage strains of 1400kg/m^3 foamed concrete (Jones and McCarthy, 2005a)

Coefficient of thermal expansion

There is limited information on the thermal expansion of foamed concrete and the data available is for either aerated or cellular concrete which can be related to the behaviour of foamed concrete. Neville (2011) stated that the coefficient of thermal expansion of concrete is the resultant of the individual values for hydrated cement paste and aggregates, as they have dissimilar thermal expansion values. It was reported that the coefficient of thermal expansion of hydrated cement paste ranges between 11x10^{-6} and 20x10^{-6} per °C and neat cement has a much higher coefficient of thermal expansion (CTE) than concrete containing sand, with the thermal expansion coefficient decreasing as the sand content increases (Neville, 2011).

On the other hand, the CTE values stated for autoclaved aerated and cellular concrete are reported as 8x10^{-6} per °C (Valore, 1961; Hebel, 2009; Tanaçan et. al, 2009), however the specimens tested were reported to be commercial provided from the manufacturers. Moreover, for 500 kg/m^3 autoclaved aerated concrete containing fly ash, Qian and Zheng (1990) reported the CTE as 9.4×10^{-6} per °C. While there was no information available about the influence of PC/CSA or PC/CSA/FA cement combinations on thermal expansion, Joshi

and Lohtia (1997) stated that fly ash does not really affect the coefficient of thermal expansion. Consequently, it can be concluded that, the lower the aggregate content (to restrain the expansive strains) the higher the coefficient of thermal expansion value. As there is lower amount of aggregates (or no aggregates) in foamed concretes than normal weight concrete, thermal expansion is expected to be higher in foamed concrete.

Sorptivity

Liquid transport and permeation mechanism in porous media which has variable, evolving microstructure and pore structure (resulting from different constituents, specifically fly ash used for production as cement/sand replacement) is complex (Jones and McCarthy, 2005b). Similarly, Nambiar and Ramamurthy (2007b) stated that water movement into concrete is not simply the function of porosity but also depends on the pore diameter, distribution, continuity and tortuosity suggesting that the water movement in foamed concrete becomes more complex. Sorptivity of foamed concrete (measured by the method described by Hall (1989)) was reported to reduce with decreasing density (Giannakou and Jones, 2002; Jones and McCarthy, 2005b, Nambiar and Ramamurthy, 2007b; Ramamurthy et. al, 2009). Sorptivity indices of foamed concretes with plastic densities ranging from 1000 to 1400kg/m^3 and the influence of fine fly ash as cement replacement (which increases sorptivity) are shown in Table 2.9.

Similar to fine fly ash as cement replacement, coarse fly ash utilised as fine aggregates replacing sand was reported to increase the sorptivity indices (Giannakou and Jones, 2002; Jones and McCarthy, 2005b; Nambiar and Ramamurthy, 2007b). Higher sorptivity indices of foamed concretes containing fly ash was attributed to the (i) formation of finer flow channels and pores in fly ash mixes (Giannakou and Jones, 2002), (ii) slower hydration of fly ash hence more 'open' microstructure which may increase the number of flow channels, (iii) increased water requirement of mixes containing fly ash which results in a more pervious matrix (Nambiar and Ramamurthy, 2007b). Although the effect of fly ash on sorptivity was considered, long-term effect of fly ash which results in evolving microstructure was not studied.

Table 2.9 Sorptivity indices of foamed concretes (Giannakou and Jones, 2002)

Plastic density, kg/m^3	Cement type	Sorptivity, mm/min$^{1/2}$
1000	PC	0.101
	70%PC/30%FA$_f$	0.102
1200	PC	0.075
	70%PC/30%FA$_f$	0.09
1400	PC	0.079
	70%PC/30%FA$_f$	0.077

FA$_f$: fine fly ash; sand as fine aggregate

2.5 INSULATION PROPERTIES

2.5.1 Thermal insulation

Thermal conductivity

Foamed concrete is reported to have an excellent thermal insulation with low thermal conductivity values (Giannakou and Jones, 2002; Jones et. al, 2003; Aldridge, 2005; Kearsley and Mostert, 2005; Jones and McCarthy, 2005a, 2005b; Concrete Society, 2009; Othuman and Wang, 2011). Kearsley and Mostert (2005) stated that thermal insulation property of foamed concrete is function of its density. Accordingly, thermal conductivity of foamed concrete was reported to range from 0.1 to 0.55 W/mK for dry densities from 400 to 1400kg/m^3 as shown in Table 2.7 (BCA, 1994; Concrete Society, 2009).

McCarthy (2004) reported that, although thermal conductivity of normal weight concrete and mortars are independent of testing age, there are some cases reporting changes in thermal conductivity at early ages (like 2 days; Kim et. al, 2003), possibly due to different thermal conductivity of water and hydration products. Furthermore, it was reported that foamed concretes containing fly ash potentially show variations in thermal conductivity when tested in long-term. In the literature, fly ash was reported to decrease the thermal conductivity when tested in 28 days. Table 2.10 shows the influence of utilising 30% (by mass) fine fly ash addition on the thermal conductivity of foamed concrete. Although it

was expressed that there is a need for testing in long-term, there is still lack of data on long-term effect of fly ash on thermal conductivity.

Moreover, closed cell foams are thought to have better thermal insulation and resistance to moisture in comparison to open cell foams (Lyons, 2010). Yakovlev et. al (2006) reported the influence of incorporating 0.05% (by mass) carbon nanotubes (CNTs) into foamed concrete on thermal conductivity. At 300 kg/m^3 density, up to 20% reduction (down to 0.056 W/mK) in thermal conductivity was reported caused by the reinforcing effect of CNTs forming more closed bubbles.

Table 2.10 Influence of fly ash on thermal conductivity (Giannakou and Jones, 2002)

Plastic density, kg/m^3	Thermal conductivity, W/mK	
	100%PC/sand	70%PC/30%FA/sand
1000	0.402	0.280
1200	0.533	0.434
1400	0.481	0.590

Table 2.11 Thermal conductivity values of foamed concretes tested at 0 (downstream) and 40°C (upstream) temperature gradient (Wei et. al, 2013)

Plastic density, kg/m^3	Dry density, kg/m^3	Thermal conductivity, W/mK
300	252	0.065
400	374	0.08
500	453	0.091
600	570	0.124
800	757	0.165
1000	948	0.217

Furthermore, temperatures (upstream and downstream) used during testing were reported have an effect on indicative thermal conductivity such that at different temperatures thermal conductivity was observed to vary. More specifically, Kim et. al (2003) reported that increased temperature of the concrete results in lower thermal conductivity. Giannakou and Jones (2002) and McCarthy (2004) reported that 30°C and 5°C were representative for the potential foamed concrete applications as a thermally insulating material and these temperatures yielded the thermal conductivity values quoted for aircrete blocks. On the other hand, supporting the statement made by Kim et. al (2003), Wei et. al (2013) who used 40 and 0 °C during testing reported lower thermal conductivity values for plastic densities ranging from 300 to 1000 kg/m^3 (shown in Table 2.11). Similarly, Othuman and Wang (2011) who tested thermal properties of foamed concrete at elevated temperatures (up to 250 °C), reported decreasing thermal conductivity with increasing temperatures up to a certain temperature (170°C), beyond this temperature thermal conductivity started to increase.

Besides constituent materials, moisture content also have an effect on thermal conductivity (Narayanan and Ramamurthy, 2000; Kim et. al, 2003). Given the high thermal conductivity of water (0.61 W/mK as noted by McCarthy, 2004) concretes with higher moisture contents exhibit higher thermal conductivities (Kim et. al, 2003) such that 1% (by mass) of increase in the moisture increases the thermal conductivity by 42% (Narayanan and Ramamurthy, 2000). Like porosity and air volume, bubble characteristics such as size, shape and distribution were also reported to influence thermal conductivity (Narayanan and Ramamurthy, 2000).

2.5.2 Sound insulation

Generally, foamed concrete is reported to have good sound insulation potential due to its porous structure (BCA, 1994; Kearsley, 1999b; Jones and McCarthy, 2005c; Othuman and Wang, 2011). On the other hand, Ramamurthy et al. (2009) noted that cellular concrete does not show significant or unique sound insulation characteristics. However, this statement was made considering the transmission loss which is dependent on mass law (NRCC, 1990), whilst others considered the sound insulation properties in terms of sound absorption which is more of a function of porosity and microstructure (Crocker, 1998;

Kutruff, 2000). However, there is no detailed data available on the sound absorption or transmission loss performance of foamed concrete apart from the literature available on cellular/aerated autoclaved concrete which can be related.

There are numerous parameters that affect the sound absorption capacity of a material. The most common parameters are summarised as porosity (pore size, characteristic, orientation and closed/open pores), tortuosity, air flow resistance, viscous thermal characteristic length and thermal characteristic length (Mosanenzadeh et. al, 2013) as well as the thickness of the material (Arenas and Crocker, 2010). Additionally, Dong et. al (2009) emphasized the influence of stiffness (in term of E-value) on the acoustic response of the material (Table 2.12), whereas Kutruff (2000) and Arenas and Crocker (2010) noted the higher efficiency of open-cell pores on the sound absorption.

Furthermore, Kutruff (2000) noted the influence of materials surface on the sound absorption performance. Therefore, when sound waves impinge on smooth surfaces, there are inevitable reflection losses occurring due to viscous and thermal processes within a boundary layer next to the surface. However, losses due to these effects are negligible compared to rough and porous surfaces. Rough surfaces increase the surface area hence the boundary layer of which these processes take place increasing the absorption. Porous materials with pores and channels connected to outside further increases the efficiency in absorbing the sound as sound waves penetrate inside the material. Figure 2.14 shows different surface textures affecting the boundary layers in which sound energy is lost.

Two sound absorption mechanisms that are believed to occur in sound absorbing materials are shown in Figure 2.15; (i) viscous dissipation of energy by the sound waves as they travel in the open air channels of a porous or fibrous material and (ii) the loss of sound energy through the friction of fibres under the vibrating effect of sound waves. Both mechanisms lead to conversion of sound energy into heat and the sound absorption coefficient of most acoustic materials tend to increase with increasing frequency (Crocker, 1998).

Transmission loss of cellular concrete was reported to be 2-3% higher than normal weight concrete, over the most audible frequencies, as the mass law (increase in the sound

transmission loss of around 5 dB, when the mass of the material for a given unit area is doubled), rigidity and internal resistance of the material determine its transmission loss capacity. Similar to Ramamurthy et. al (2009), Laukaitis and Fiks (2006) reported that lightweight aerated concrete (250–500 kg/m^3) possess high porosity (82.1–91.5%) and the walls of the pores of such materials are very thin and well enough transmits sound waves (i.e. possess lower transmission loss).

Table 2.12 Influence of elasticity and porosity on the acoustic response of a material (Dong et. al, 2009)

E-value	Porosity	Example	Reflection	Transmission	Absorption
↑	↑	Concrete	**High**	Low	None
↑	↓	Steel	**High**	None	None
↓	↓	Water	Low	**High**	Low
↓	↑	Snow	Low	Low	**High**

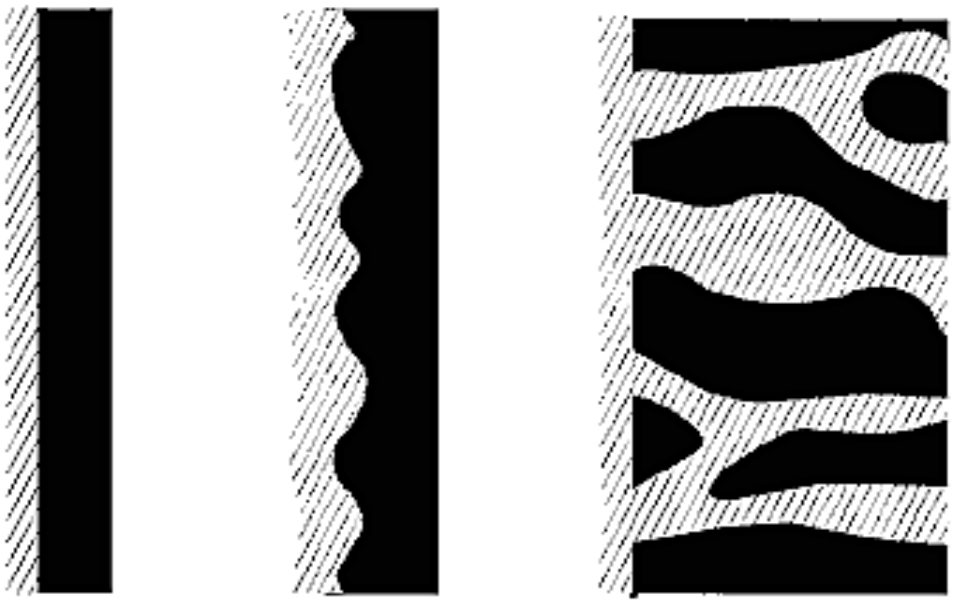

Figure 2.14 Different surface textures affecting the sound energy is loss; smooth, rough and porous (from left to right) (Kuttruff, 2000)

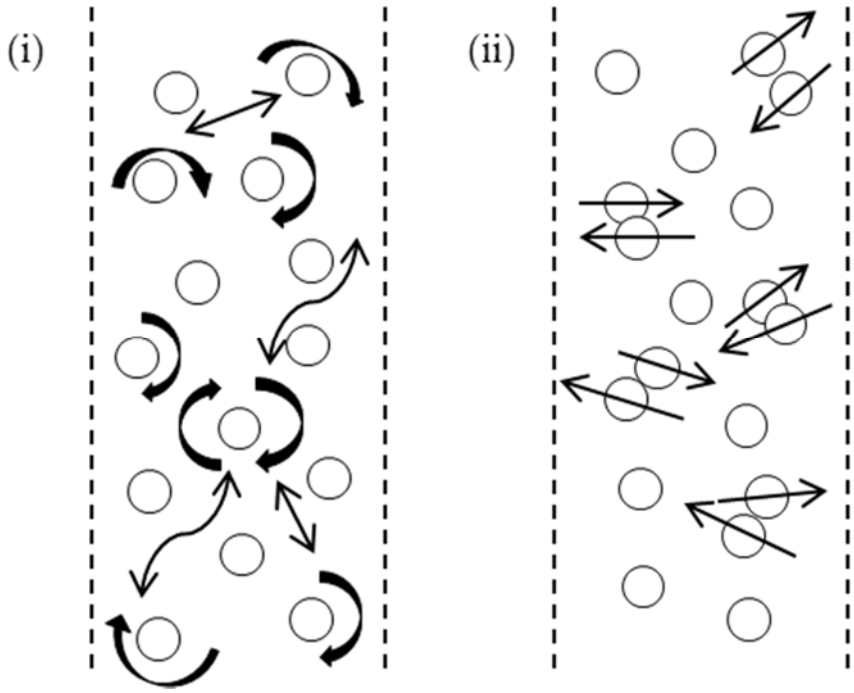

Figure 2.15 Mechanisms in sound absorbing materials: (i) viscous losses in the air channels and (ii) mechanical friction caused by fibers rubbing together (Crocker, 1998)

2.6 MICROSTRUCTURE OF AIR VOIDS

Owing to high porosity, mechanical, physical and durability properties of foamed concrete are largely controlled by its pore network (Ramamurthy et. al, 2009). More specifically, porosity, permeability and pore size distribution influences strength and durability while the mechanical properties are mainly influenced by the distribution of the pores within the hardened paste (Visagie and Kearsley, 1999). Additionally, Narayanan and Ramamurthy (2000) reported the influence of bubble size, shape and distribution on the thermal insulation properties whilst Han et. al (2003) and Lee et. al (2011) noted the effect of bubble size on sound absorption capacity.

The main parameters of the air voids are shape, size distribution, spacing factor (Nambiar and Ramamurthy, 2007a). In general, air void sizes of foamed concrete range from 0.1 mm to 2 mm (Brady et. al, 2001, Aldridge, 2005; Nambiar and Ramamurthy, 2007a; Mohammad et. al, 2011, Wei et. al, 2014). Density, w/c ratio, constituent materials and additives are the

main parameters affecting the size and distribution of the air voids (Wee et. al, 2006; Nambiar and Ramamurthy, 2007a, Mohammad, 2011). More specifically, increasing void diameter with decreasing density (shown in Table 2.13 and Figure 2.16, 2.17, 2.18) was reported by Visagie and Kearsley (1999), Nambiar and Ramamurthy (2007a), Mohammad (2011) and Wei et. al (2014). Moreover, increase in foam volume (decrease in density) results in increase in the number of bigger sized air voids as well as less uniform air void distribution (Nambiar and Ramamurthy, 2007a). Figure 2.16 illustrates the air void size distribution in terms of D50 and D90, which represent the air void sizes that 50% and 90% (respectively) of the bubbles have sizes smaller than these.

Mohammad (2011) reported a decrease in the air void diameters when fly ash is used as a cement and/or sand replacement. Similarly, Nambiar and Ramamurthy (2007a) reported the influence of replacing sand with fly ash on reducing the air void sizes and obtaining a more uniform distribution (shown in Figure 2.18). They attributed this to the ability of finer materials to coat the bubbles preventing them from merging and increasing in diameter. In another study, Yakovlev et. al (2006) reported the pore diameter range of 300kg/m^3 foamed concrete as 40-600 μm and a reduction in the diameters of bigger pores with the utilisation of CNTs into the mix (Figure 2.19).

Table 2.13 Porosity and bubble size of foamed concretes measured by 3D X-ray computerised tomography imaging (Wei et. al, 2014)

Plastic density, kg/m^3	Porosity, %	Median diameter, mm	Min. diameter, mm	Max. diameter, mm
300	84.2	0.956	0.01	2.12
500	75.5	0.700	0.02	1.70
800	59.0	0.263	0.04	1.20
1000	50.6	0.173	0.08	1.00
*1000FA	48.6	0.186	0.06	1.92

* 40% fly as h was used to replace PC

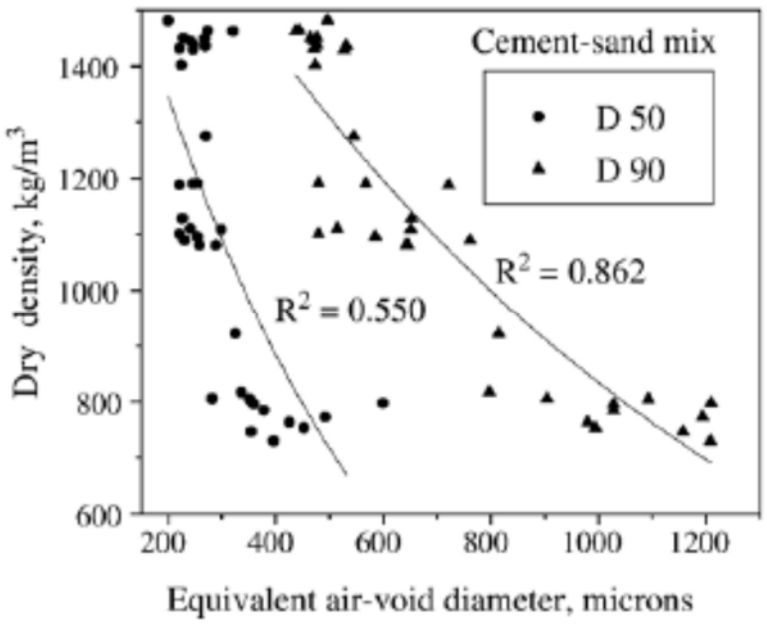

Figure 2.16 Relationship between density and air-void size distribution parameters (Nambiar and Ramamurthy, 2007a)

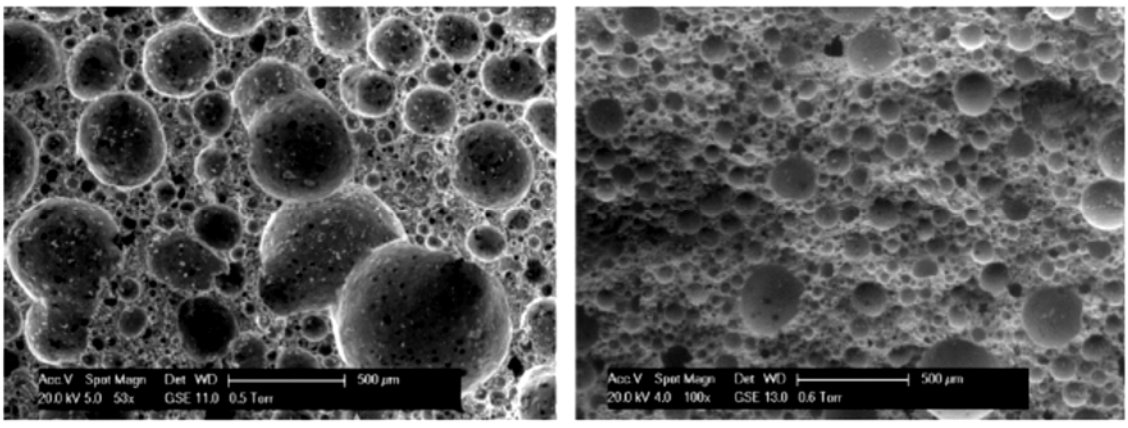

Figure 2.17 SEM images of 500 kg/m^3 (left) and 1000 kg/m^3 (right) foamed concretes (Wei et. al, 2013)

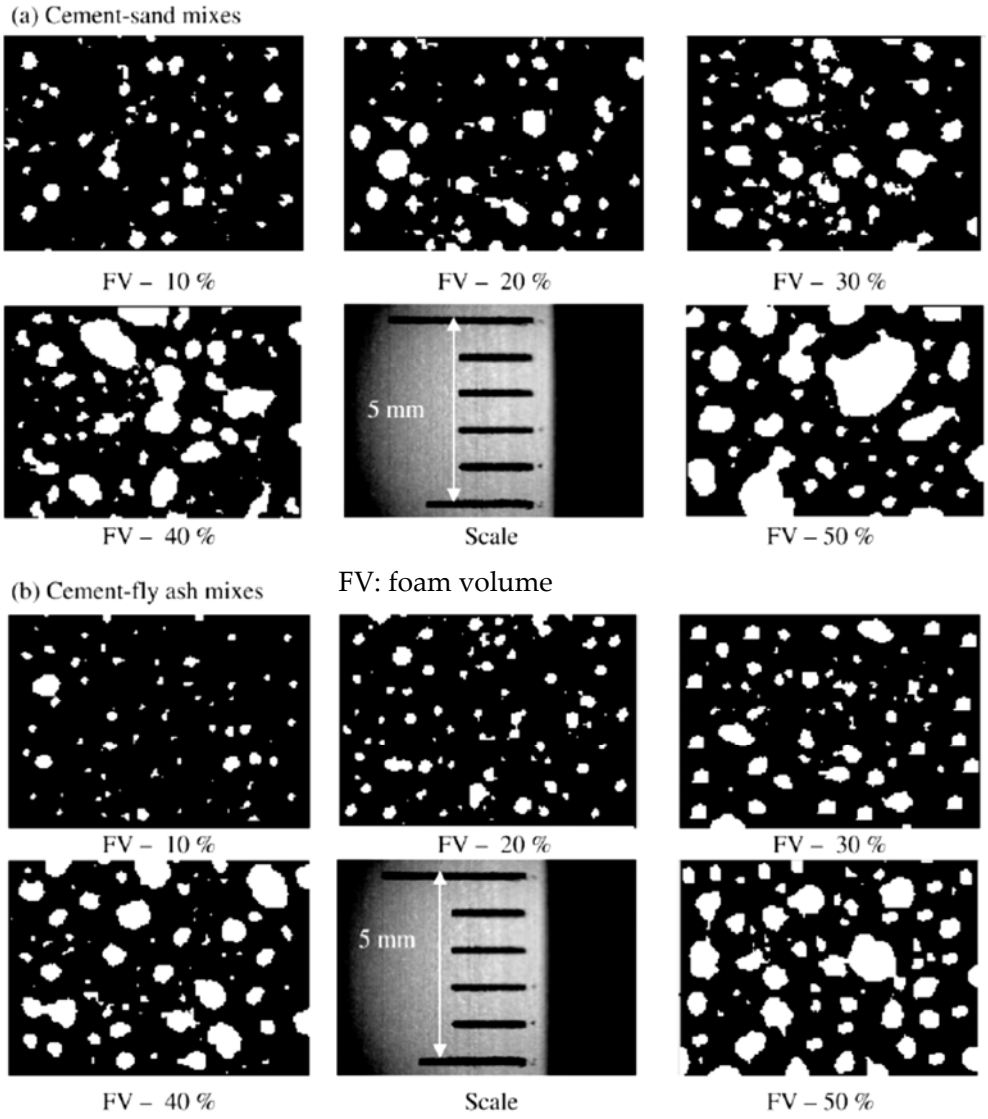

Figure 2.18 Typical binary images of varying foamed concretes densities and material combinations (Nambiar and Ramamurthy, 2007a)

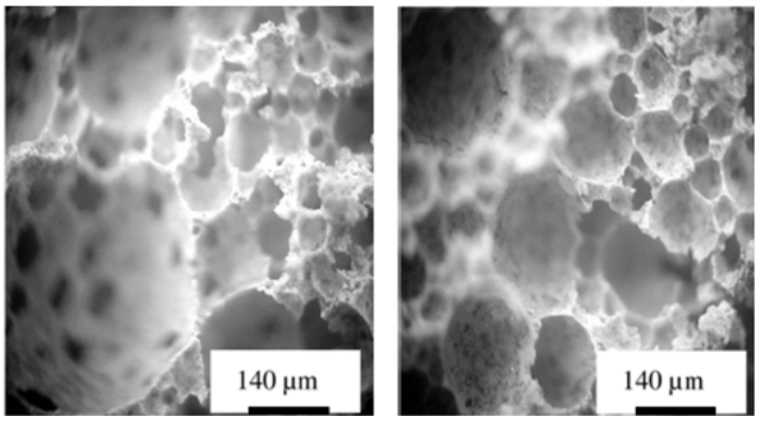

Figure 2.19 Influence of CNTs on the pore diameter of 300 kg/m^3 foamed concrete; without CNTs (left), with 0.05% CNTs (right) (Yakovlev et. al, 2006)

Having reviewed the microstructure of foamed concretes, it is beneficial to highlight the differing bubble microstructure of liquid foams. Soap bubbles try to minimise their surface area for enclosing a given volume of air and spherical shape is the optimal shape for his in the case of a single bubble. However, as the number of bubbles increases the science behind becomes more challenging and the foams with many bubbles feature more complex shapes (Taylor, 2011). The search aiming to find the most suitable arrangement of bubbles, of equal volume, efficiently packing bubbles into foam as well as minimising the surface area of the walls among the bubbles is known as the 'Kelvin problem' which was posed by Lord Kelvin (Freiberger, 2009).

To solve his problem, Kelvin suggested that a structure made up of slightly curved copies of a truncated octahedron (which is a shape with 6 square and 8 hexagonal faces; Figure 2.20 (a)). On the other hand, Phelan and Weaire proposed an improved structure resulting in 0.3% less surface area (Freiberger, 2009). However, structure of bubbles in foamed concrete differ from liquid foams and look spherical, possibly due to the transformation of the shape caused by solid particles surrounding them once the foam is mixed with the base mix. Therefore in this study bubbles assumed to be spherical.

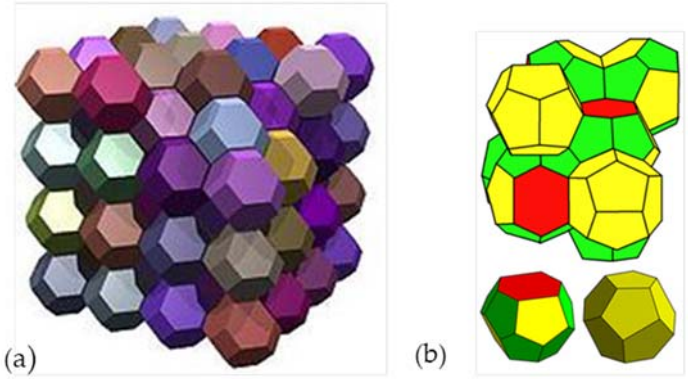

Figure 2.20 Foam bubble structure (a) the Kelvin structure; (b) the Weaire-Phelan structure (Freiberger, 2009)

2.7 OUTCOME OF THE LITERATURE

Increasing number of requirements and targets set for achieving sustainable construction through its activities and materials have stimulated the need for responsible design, sourcing and production. Therefore, it is vital to specify and design for durable

construction materials/structures in a way to promote reductions in the dead loads, embodied CO_2, waste generation and use of primary materials as well as increase in the energy efficiency and use of recycled/secondary materials. The literature shows that foamed concrete contributes to satisfying these requirements and lighter foamed concrete has a greater potential for contributing to these.

Due to their higher air contents, hence less volume of constituents, foamed concretes with lower plastic densities possess lower environmental impact. Moreover, increased air content improves the thermal insulation capacity of foamed concrete while providing a reduced self-weight. Although there is some information available on ultra-low density foamed concretes with dry densities down to 250 kg/m^3 (i.e plastic densities of approximately 300 kg/m^3 and above) it is very limited and does not provide a full coverage on the characteristic, behaviour and implications.

On the other hand, issues with producing stable ultra-low density (plastic density below 600 kg/m^3) foamed concretes were reported by the researchers at the University of Dundee and industrial bodies. Although there is information available in the literature regarding the instability and its causes, very limited information is provided on the stability and instability mechanism of foamed concretes. Therefore, in order to proceed with assessing the behaviour and properties of ultra-low density foamed concretes, it is compulsory to resolve the stability issues and produce stable mixes.

Besides the knowledge gap on ultra-low density foamed concretes, there is also lack of information on some engineering properties of conventional foamed concretes (plastic densities 600 kg/m^3 and above). Therefore, to widen its application areas, contribute to the design of its application and respond to the enquiries from the industrial bodies, Poisson's ratio and coefficient of thermal expansion of foamed concrete need to be evaluated.

Consequently, as a primary aim, an attempt will be made to resolve the issues of stability in ultra-low density foamed concretes focusing on the underlying mechanisms and factors. Upon satisfying this primary aim successfully, characteristics and performance behaviour of ultra-low density foamed concretes will be evaluated to provide information for the potential application areas.

CHAPTER 3

3. RESEARCH PROGRAMME, MATERIALS, TEST METHODOLOGIES AND PRACTICAL OBSERVATIONS

3.1 INTRODUCTION

Unlike ultra-low density (plastic densities below 600 kg/m^3) foamed concretes, properties and behaviour of 'conventional' foamed concretes have been widely explored. From the potential use as a structural material (Jones and McCarthy, 2005a) to thermal insulation properties (McCarthy, 2004) as well as basic fresh and engineering properties such as consistency, temperature development due to heat of hydration, compressive strength, drying shrinkage and permeation properties have been explored (Kearsley and Wainwright, 2001a, 2001b; McCarthy, 2004; Jones and McCarthy, 2006; Concrete Society, 2009; Ramamurthy et. al, 2009). More exceptionally, energy absorption properties (Jones and Zheng, 2013) and recycling potential (Jones et. al, 2012) of foamed concrete were also studied.

In addition to these, Mohammad (2011) presented an attempt to transform from high/low to ultra-low density foamed concretes (ULFCs) trying to resolve stability issues at ultra-low densities as well as carrying out bubble size analysis on foamed concretes with various densities. Therefore, building up on the previous studies, experimental work of the current study mainly focused on understanding the mechanism of stability and producing stable ULFCs as well as exploring the key properties and behaviour.

3.2 RESEARCH PROGRAMME

Research programme comprised hypothetical analysis of instability in foamed concrete followed by laboratory investigations as shown in Figure 3.1. Initially, in Phase 1, a hypothetical approach was followed based on the fundamentals and observations to evaluate the causes of instability in foamed concrete and propose a solution for producing stable ULFC.

In Phase 2, preliminary trials were carried out with a range of materials to test the developed hypotheses for achieving stable ULFCs. The preliminary studies comprised visual assessment of mix stability of ULFC mixes produced with the range of materials considered. Following the preliminary trials, effect of the materials on mix stability, initial setting times, bubble and microstructural properties (bubble analysis and visual microscopic image analysis) was evaluated in order to choose the materials for the main study. Moreover the availability and cost were also considered while choosing these materials for further investigation. At a further stage in Phase 2, the effect of utilisation of fly ash (as a cement addition) at rates of 30% (by mass) and beyond on stability, microstructure and embodied carbon dioxide (eCO_2) of ULFC was evaluated.

In the last phase (Phase 3) of the research, insulation performance, fresh, early age and hardened state properties of ULFCs were evaluated. With the expectation of obtaining improved insulation performance from ultra-low density materials, thermal conductivity and sound absorption of ULFCs were evaluated as well as sound transmission loss. Fresh and early age properties consisted of flow behaviour and temperature development respectively, while hardened state properties considered were compressive strength, static modulus of elasticity, Poissons's ratio, drying shrinkage, thermal expansion and sorptivity. The hardened state tests were carried out at 28 days age or at a later age where required.

Mainly, the plastic densities ranging from 150 to 600 kg/m^3 and w/c ratio of 0.50 were considered for the laboratory investigation. Additionally, 100 and 1000 kg/m^3 densities were considered where appropriate. Cement contents of minimum 67 kg/m^3 and maximum 333 kg/m^3 were used as well as different cement combinations (PC, PC/CSA, PC/CSA/FA, PC/CSA/SF). Given the nature of some test methods, 'open' microstructure and ultra-low strength characteristics of some ULFCs, it was not practical to evaluate the whole range of plastic densities for all the properties considered. Plastic densities and cement combinations considered for each property examined will be mentioned in the relevant sections.

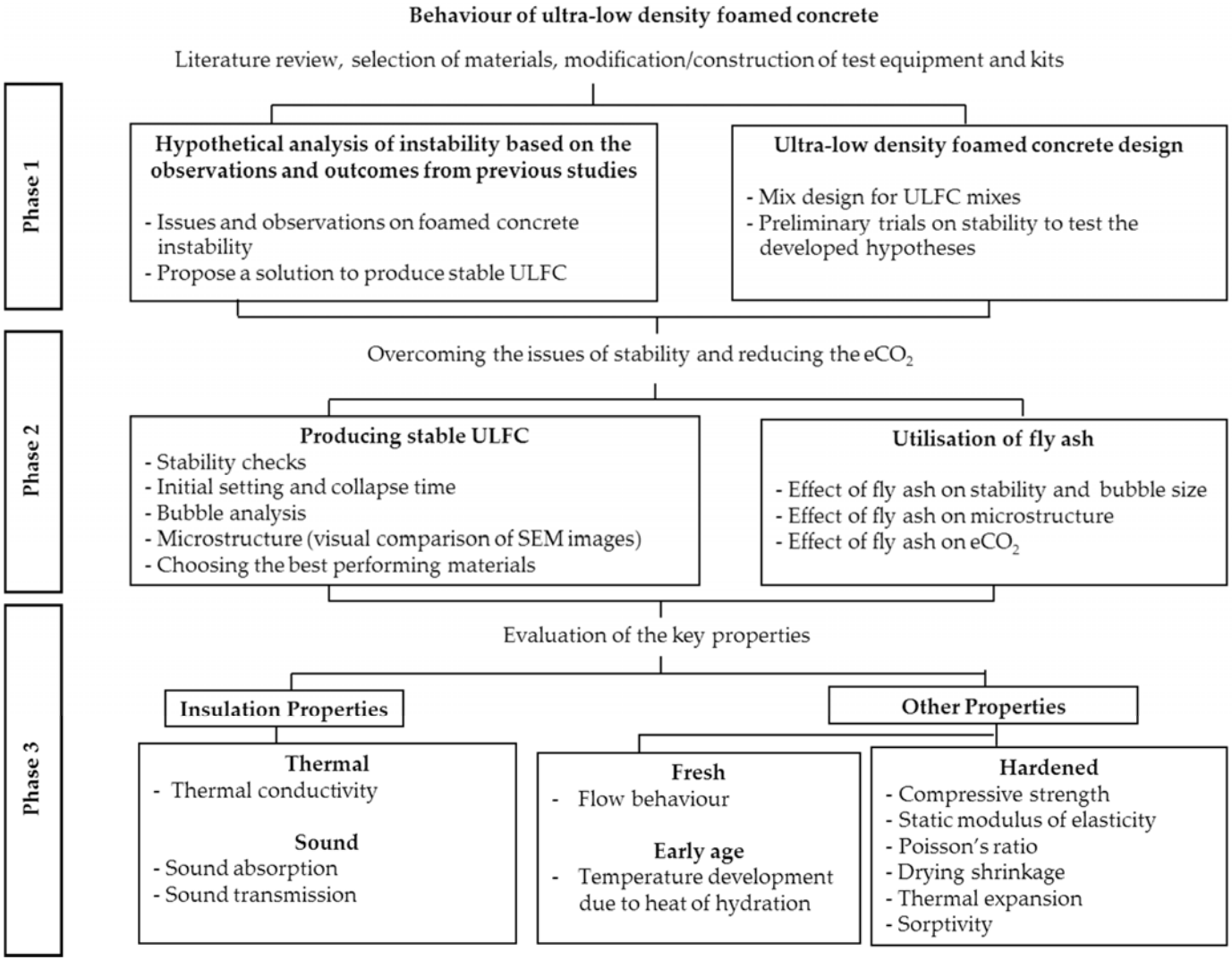

Figure 3.1 Flowchart of the research programme

3.3 MATERIALS

3.3.1 Cements

The *Portland cement (PC)* used in this study was CEM I 52.5N conforming to BS EN 197-1:2011. Portland cement was the main cementitious material used to produce foamed concrete specimens. In this study, Portland cement was used in combination with other cementitious and/or pozzolanic materials. Properties of cements used for the main study were shown in Table 3.1.

Commercially available *Calcium sulfoaluminate (CSA) cement* was used to benefit from its fast setting properties. As there are many different CSA cements with varying chemical properties available on the market, CSA cement compatible with PC was chosen. It must be noted that, the CSA cement under consideration is, in fact, a slow reacting cement. However, in the presence of lime and calcium sulfate it reacts rapidly forming ettringite crystals. CSA cement employed in the main study was used in combination with PC.

Two types of category S *fine fly ashes* conforming to BS EN 450-1:2012 were used in this study. Fly ashes were labelled as FA 1 and FA 2, where they were used as additions.

The *silica fume (SF)* used in this study (in slurry form) was conforming to BS EN 13263:2005 + (A1:2009) and possessing specific surface area of 20000 m^2/kg and a water content of 50%. Silica fume was utilised for assessing its effect on thermal conductivity and sound absorption of foamed concrete.

As *alternative materials*, another CSA from a different source (CSA_p) which was combined with PC was utilised as well as *buxton lime (PC2)* and *microfine cement (MF)*. Alternative materials were used to test the proposed solution for producing stable ultra-low density foamed concretes with a range of materials. CSA_p was chosen given its higher fineness and varying chemical composition than the *CSA*. *PC2* was chosen as it was reported to produce stable foamed concretes down to 200 kg/m^3 plastic density (Ansell, 2010). *MF* which is not available commercially was chosen given its high fineness and fast setting times. Properties of alternative materials are also included in Table 3.1.

Table 3.1 Properties of cements used in the main study and as alternative materials

Main oxides, % by mass	Main study				Alternative Materials		
	PC	**CSA**	**FA 1**	**FA 2**	**PC2**	**MF**	**CSA_p**
CaO	66.7	36.9	3.9	5.1	67.1	65.7	47.6
SiO_2	19.9	4.6	50.1	58.7	18.7	20.4	8.8
Al_2O_3	4.8	47.2	23.4	21.2	5.1	5.5	24.3
SO_3	2.7	5.4	2.4	0.5	5.5	2.5	14.6
Fe_2O_3	3.1	1.5	11.4	6.8	3.9	3.1	3.10
MgO	1.1	1.1	1.4	1.7	1.0	1.6	0.90
K_2O	0.7	0.5	3.3	2.2	0.7	0.7	0.5
Na_2O	0.3	0.1	2.3	1.6	0.2	0.7	0.1
LOI	-	-	4.0	2.2	-	-	-
Phase composition, % by mass							
C_3S	54.1	-	-	-	38.1	58.3	-
C_2S	16.6	19.3	-	-	25.6	33.3	14.6
C_3A	10.8	6.7	-	-	4.8	-	4.53
C_4AF	9.1	-	-	-	14.7	43.6	-
Ye'elimite	-	52.9	-	-	-	-	34.6
C_2AS	-	17.5	-	-	-	-	-
Quartz	-	-	11.1	15.3	-	-	-
Mullite	-	-	11.0	7.2	-	-	-
Hematite	-	-	2.29	5.7	-	-	-
Calcite	-	-	-	0.7	-	-	-
Magnetite	-	-	0.2	0.1	-	-	-
45 μm sieve retention, %	-	-	13.2	7.5	-	-	-
Sp. surface area (Blaine test), m^2/kg	456	502	485	526	433	758	700
Particle size distribution, mm							
D10	3.0	2.6	2.7	1.6	3.0	1.2	1.9
D50	11.9	12.0	14.1	10.5	15.1	5.9	10.3
D90	33.9	48.4	65.1	36.4	42.8	15.2	42.4
Particle density, g/cm^3	3.1†	3.0†	2.3	2.2	n.a	n.a	n.a
Initial setting time, hh:mm	03:25	04:00	n.a	n.a	04:30*	00:20	04:20

* w/c ratio of 0.45 was used; n.a: not available; † manufacturer's data, otherwise tested

3.3.2 Fillers

Fine aggregates

For plastic densities 600 kg/m^3 and above, natural siliceous sand conforming to BS EN 12620 (2013) Category G_F85, further sieved to remove particles greater than 2.36 mm was used. At ultra-low densities (≤ 500 kg/m^3), fine aggregates were eliminated as they cannot be supported by the highly foamed, reduced self-weight foamed concrete mixes. Sand was air dried in the laboratory conditions in order to maintain the laboratory dry condition prior to use.

Carbon nanotubes (CNTs)

Industrial grade multi-walled carbon nanotubes (MWCNTs) were used as filler in order to investigate the effect of CNTs on producing closed cell bubbles and reinforcing the bubble walls of low density foamed concretes. The diameter, length and specific surface area of the CNTs used were 30-70 nm, 5-15 μm and bigger than 200m^2/g respectively (Arry Nano, 2014). Clearly, CNTs have extremely high specific surface area when compared with the specific surface area of CEM I (≈ 0.456 m^2/g) and silica fume (≈ 15-25 m^2/g). Scanning Electron Microscopy (SEM) image and structure of MWCNTs were illustrated in Figure 3.2.

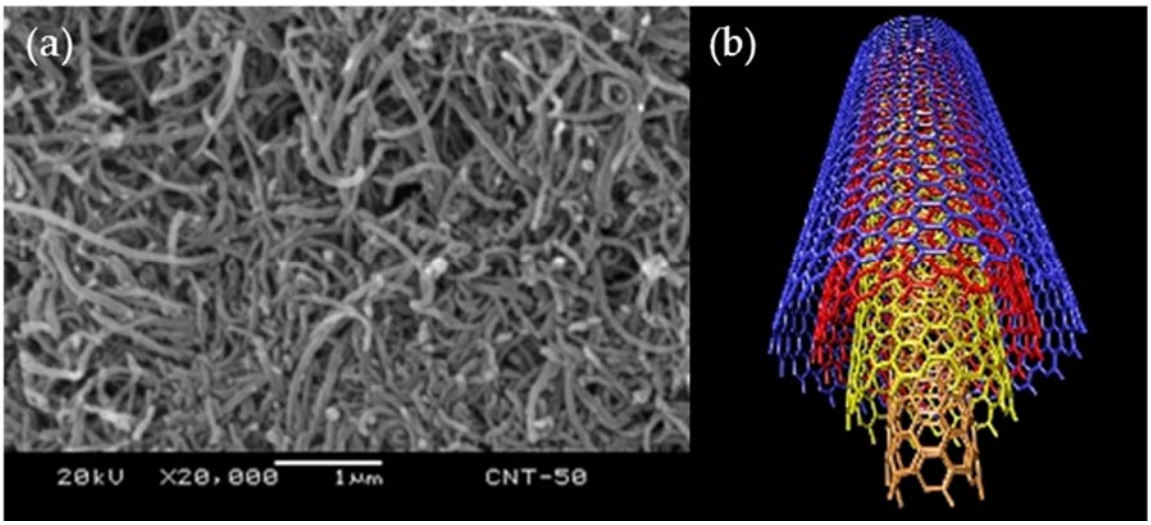

Figure 3.2 (a) Multi-walled CNTs at micro level (Arry, 2014) and (b) structure of MWCNTs (Nanotech Now, 2014)

Dispersion of CNTs

Given the extremely high surface area of the particles accompanied by high aspect ratios and flexibilities, CNTs are likely to entangle and closely pack forming clumps with low disperseability (Vaisman et.al, 2006). For the utilisation of the properties and maintaining the even distribution of CNTs within foamed concrete mixes, CNTs were dispersed in water using sonicator prior to use. As foamed concrete is not compatible with the addition of most chemicals, CNTs were dispersed in water rather than any other surfactant suggested by Vaisman et. al (2006) and Yakovlev et al (2006).

For dispersion, CNTs provided in powder form were diluted in the mix water as shown in Figure 3.3. Following dilution, CNTs were dispersed with a sonicator that applies ultrasound energy for a minimum of 3 hours. Based on the preliminary trials and visual observations, 3 hours of sonication was found to be the optimum for even distribution of the CNTs. After 3 hours of dispersion the sample turns into a jet black, opaque solution (Figure 3.4). It must be noted that, dispersed CNTs should be added into the foamed concrete mix immediately after dispersion in order to prevent the re-agglomeration and settlement of CNTs. It must be noted that, it was not monitored in hardened foamed concrete whether the CNTs were dispersed as this was out of the scope of this study.

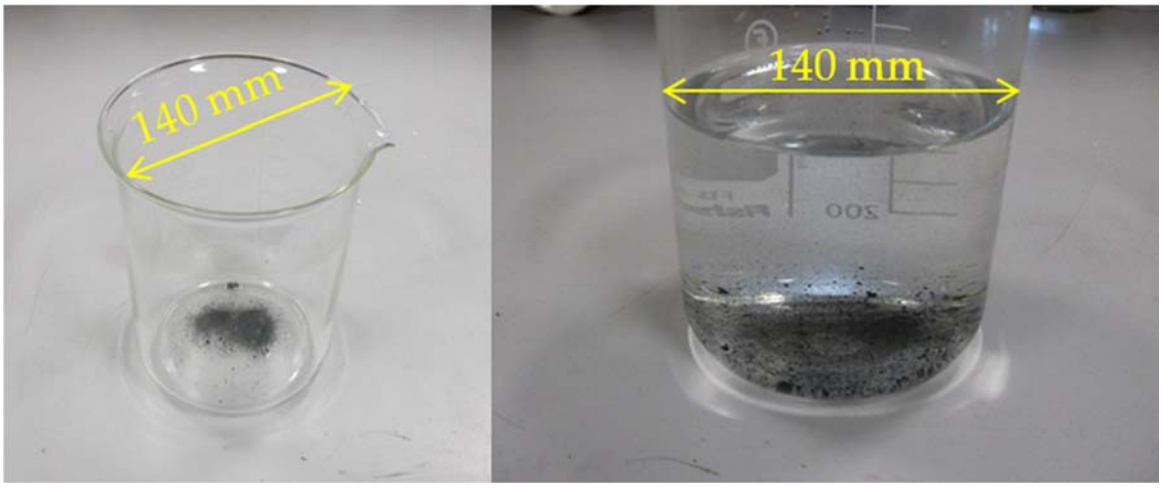

Figure 3.3 Dilution of CNTs in the mix water

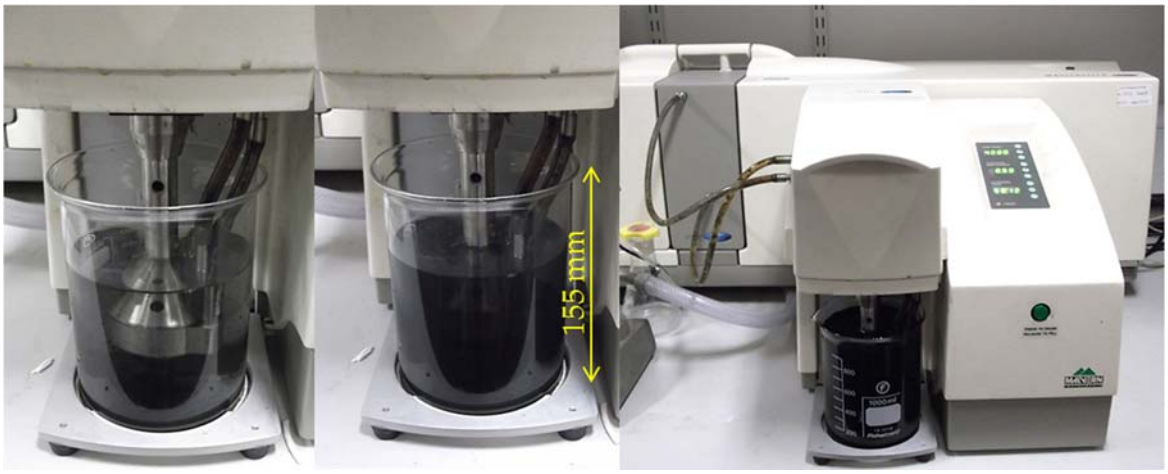

Figure 3.4 Dispersion of CNTs using a sonicator

3.3.3 Water

Normal tap water conforming to BS EN 1008, was used in this study. It is vital for foamed concrete stability that, the mixing water is not acidic or hot as these conditions exhibit higher drop out level of preformed foam (Mohammad, 2011).

3.3.4 Surfactant

There are several surfactant types available on the market, mainly protein-based and synthetic surfactants. It is suggested that protein surfactants yield foam with more stable and closed cells, thus higher foamed concrete strengths (Dransfield; McGovern, 2000). Therefore, commercially available protein-based surfactant (ProPump, Protein 40) was employed to produce preformed foam aiming to obtain low density foamed concretes with more stable microstructure. A neutral (pH 7.0), clear brown protein-based surfactant which has specific gravity of 1.12 g/cm^3 (Ansell, 2010) was used in this study.

3.4 MIX DESIGN AND MIX PROPORTIONS

The mix design method developed at the University of Dundee (Dhir et al, 1999; Brady et al, 2001; Giannakou and Jones, 2002) was used in this study. As described below, the developed method suggests that target plastic density, w/c ratio and cement content were considered as fundamental factors while designing the foamed concrete mixes. Target plastic density, cement content and w/c ratio were specified and the assumption of target plastic density is equal to the sum of solids and water in the mix was made as shown in Equation 3.1

$$D = C + W + F \qquad \text{Equation 3.1}$$

where; D = target plastic density, kg/m³

C = cement content, kg/m³

W = water content, kg/m³

F = fine aggregate content, kg/m³

At high/low densities (600 kg/m³ and above) where sand is used as fine aggregates water content was modified in order to satisfy the additional water requirement of the mix caused by water absorption of the sand. As the sand used is laboratory air dry with 1% of water absorption, water content of the sand mixes were increased by 1% of sand content. Water from the foam portion of the mix was not considered in the calculations as it is assumed to be minimal. However, due to foam collapse, of which the degree depends on the type of constituents and is not predictable in advance, actual w/c ratio of the mix was observed to increase slightly (Dhir et al, 1999).

To determine the foam content required for achieving the target plastic density, volume of air present in a unit volume of mix was calculated by using Equation 3.2.

$$V_C + V_W + V_F + V_{foam} = 1m^3 \qquad \text{Equation 3.2}$$

where V_C = Volume of cementitious materials, m^3

V_W = Volume of water, m^3

V_F = Volume of fine aggregate, m^3

V_{foam} = Volume of foam, m^3 ; then $M_{foam} = V_{foam} * \rho_{foam}$

For high/low densities cement content was kept constant at 300 kg/m^3 and reduced at densities below 600 kg/m^3, with an exception of 500 kg/m^3 density. Cement content was increased to 335 kg/m^3 to increase the 'fines' content as sand was not used at this density and below.

In this particular study w/c ratio was kept constant at 0.50 as it was observed to provide sufficient consistency at most densities with various material combinations. It should be borne in mind that w/c ratio plays a vital role on the quality and stability of foamed concrete (Brady et. al. 2001; Ramamurthy et. al, 2009). Therefore w/c ratio must be chosen considering the type of constituents used and their characteristics in order to provide the required workability of the base mix as well as maintaining the mix stability (Brady et al., 2001; Ramamurthy et. al, 2009). Insufficient water in the mix tends to cause extraction of water from the foam leading to disintegration of the foam, hence potential collapse of the mix. On the other hand, excess water in the mix favours segregation that may also lead to collapses and increased drying shrinkage (Kearsley, 1999b; Brady et al., 2001; Nambiar et al., 2006).

Table 3.2 shows the mix constituent proportions for the main study for a range of plastic densities considered in this study while Table 3.3 gives the mix proportioning for the alternative materials. Mixes considered for each test will be reported in corresponding sections.

Table 3.2 Mix constituent proportions for the main study

Plastic density, kg/m³	Cement combination	Combination name	Cement content, kg/m³			Sand content, kg/m³	Water† content, kg/m³	Air volume, %
			PC	CSA	FA			
1000	100% PC	PC	300	-	-	550	156†	55
600	100% PC	PC	300	-	-	150	152†	70
	50% PC/ 10% CSA/ 40% FA	40% FA	150	30	120	150		69
500	100% PC	PC	335	-	-	n.a	165	73
	95% PC/ 5% CSA	5%	318	17	-			73
	50% PC/ 10% CSA/ 40% FA	40% FA	165	35	135			71
400	100% PC	PC	267	-	-	n.a	134	78
300	95% PC/ 5% CSA	5% CSA	190	10	-	n.a	100	84
	90% PC/ 10% CSA	10% CSA	180	20	-			84
	60% PC/ 10% CSA/ 30% FA	30% FA	120	20	60			83
	50% PC/ 10% CSA/ 40% FA	40% FA	100	20	80			83
	40% PC/ 10% CSA/ 50% FA	50% FA	80	20	100			82
	30% PC/ 10% CSA/ 60% FA	60% FA	60	20	120			82
	20% PC/ 10% CSA/ 70% FA	70% FA	40	20	140			82
200	95% PC/ 5% CSA	5% CSA	126	7	-	n.a	67	89
	90% PC/ 10% CSA	10% CSA	120	13	-			89
	60% PC/ 10% CSA/ 30% FA	30% FA	80	13	40			89
	50% PC/ 10% CSA/ 40% FA	40% FA	67	13	53			88
150	90% PC/ 10% CSA	10% CSA	90	10	-	n.a	50	92
	50% PC/ 10% CSA/ 40% FA	40% FA	50	10	40			91

† water content increased by 1% of sand content considering the water absorption by sand; n.a: not applicable

Notes: 200 kg/m³ SF mix was produced with 85%PC/5%CSA/10%SF, where 26 g of SF, in slurry form, was used and the water content was reduced to 54 kg/m³ as 50% of the SF was water. 200 kg/m³ CNT mix was produced with 95%PC/5% CSA+ 0.05% CNTs (by mass of cement).

Table 3.3 Mix proportions for the alternative materials

Plastic density, kg/m³	Combination name	Cement content, kg/m³				Water* content, kg/m³	Air volume, %
		PC	PC2	CSA_p	MF		
300	PC2	-	200	-	-	100	84
	MF	-	-	-	200		
	5% CSA_p	190	-	10	-		
	10% CSA_p	180	-	20	-		
	20% CSA_p	160	-	40	-		
	40% CSA_p	120	-	80	-		
	50% CSA_p	100	-	100	-		
200	PC2	-	133	-	-	67	89
	MF	-	-	-	133		
	5% CSA_p	126	-	7	-		
	10% CSA_p	120	-	13	-		
	20% CSA_p	106	-	27	-		
	40% CSA_p	80	-	53	-		
	50% CSA_p	67	-	67	-		
150	PC2	-	100	-	-	50	92
	MF	-	-	-	100		
	5% CSA_p	95	-	5	-		
	10% CSA_p	90	-	10	-		
	20% CSA_p	80	-	20	-		
	40% CSA_p	60	-	40	-		
	50% CSA_p	50	-	50	-		
100	PC2	-	67	-	-	34	94
	MF	-	-	-	67		
	5% CSA_p	64	-	3	-		
	10% CSA_p	60	-	7	-		
	20% CSA_p	54	-	13	-		
	40% CSA_p	40	-	27	-		
	50% CSA_p	34	-	34	-		

* w/c ratio of 0.45 was used for PC2 mix, while 0.50 was used for the rest of the mixes.

3.5 FOAMED CONCRETE SPECIMENS PREPARATION

3.5.1 Foam production

In order to produce foam with density of 50±5 kg/m^3, 60g of surfactant was diluted in a litre of water to prepare the aqueous surfactant solution. Foam was produced with the foam generator shown in Figure 3.5. Measured foam densities were typically found to range between 45 and 50 kg/m^3.

As seen in Figure 3.6, there is a compressed air supply into the foam generator. As compressed air is directed to the pump air chamber, the surfactant solution is drawn into the fluid chamber by the pump. There is a diaphragm separating the two chambers. The pressure of the diaphragm forces the surfactant solution out of the pump discharge. The compressed air and the surfactant solution meet in the pump discharge and the combination is forced out through the foam lance which is filled with restrictions such as scouring pads.

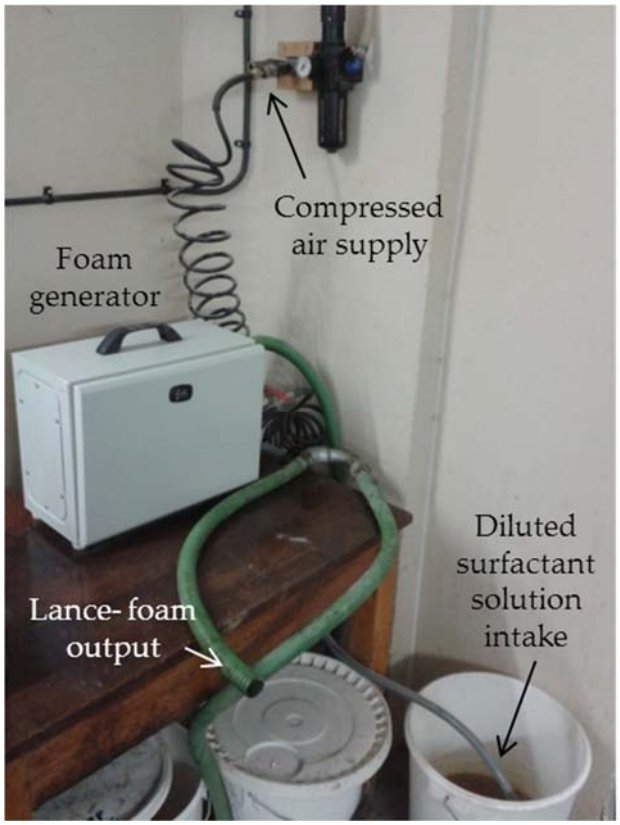

Figure 3.5 Foam generator

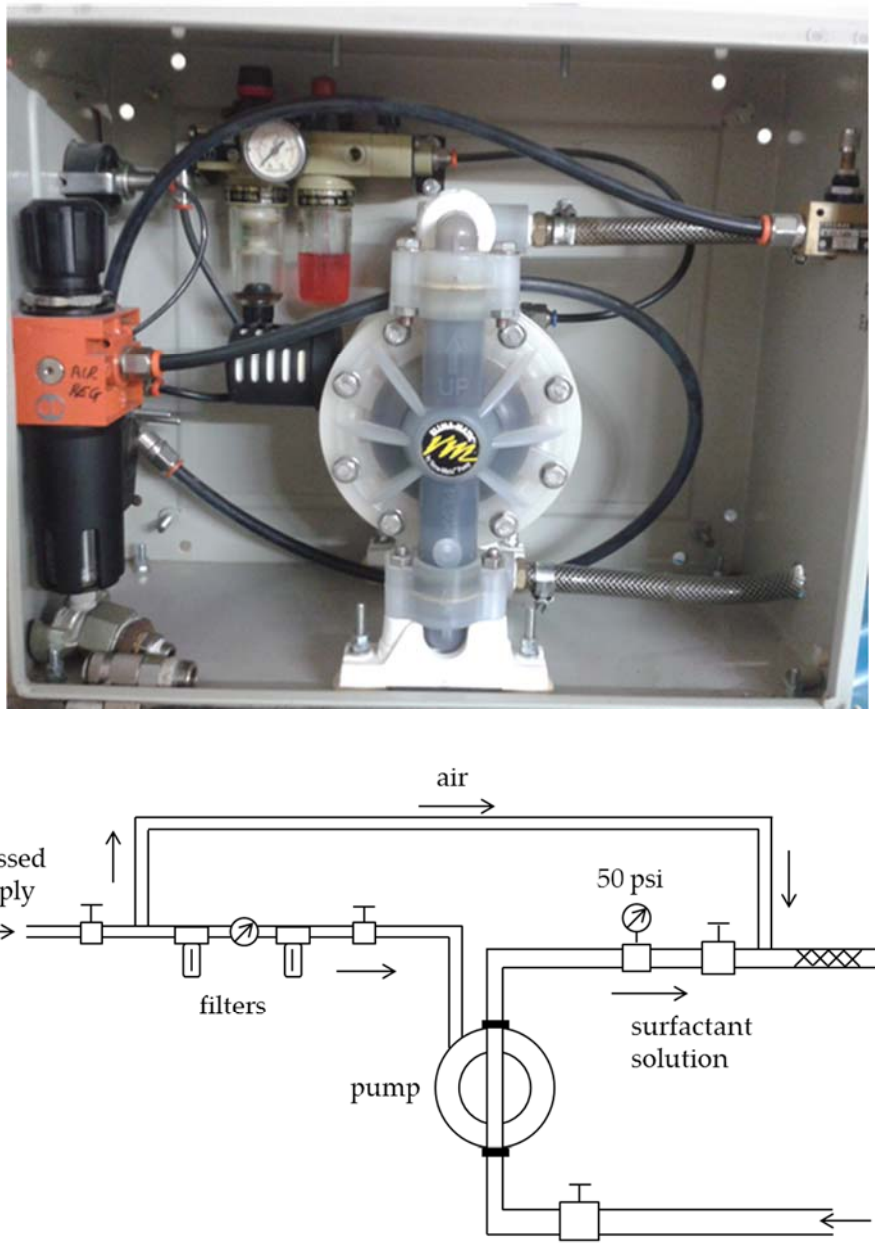

Figure 3.6 Operating system (top) and schematics of the foam generator (bottom)

Foam density was reported to be affected by the pressure applied in the foam generator (Jones, 2000). Therefore, as suggested by Jones (2000) and applied in the previous studies carried out at the University of Dundee, the pressure gauge of the foam generator was set to 50psi (345 kPa) in order to produce foam at the lowest density possible.

3.5.2 Foamed concrete production

Given the lack of a standard for foamed concrete production, the sequence described by Kearsley (1996) and followed by most others was applied for the production (see Figure 3.7). Therefore, the dry constituents (cement and fine aggregates) were combined in the mixer for around 30 seconds followed by the addition of the total amount of water. Base mix (mortar or slurry) was obtained following around 3-4 minutes of mixing, or until a homogeneous mix with no lumps was obtained.

Figure 3.7 Production of foamed concrete

Meanwhile, the pre-formed foam was produced by the foam generator and the calculated amount of foam was added to the base mix immediately. The mix was then combined for 2 minutes or until the foam is evenly distributed throughout the mix. Once the mixing was completed, the plastic density of the mix was measured as described in Section 3.6.1 to check whether the plastic density of the mix is within the stated limits of (±25 kg/m^3 for ultra-low and ±50 kg/m^3 for higher density mixes). Different from the common practice, ±25 kg/m^3 tolerance limit was chosen for ULFC mixes as ±50 kg/m^3 could represent 25 to 50% of the target plastic density at very low densities. If the measured plastic density was higher than the limits, additional foam was produced and added immediately until achieving the target density. On the other hand, mixes with plastic densities lower than the stated limits were rejected.

Although the production of foamed concrete was mainly carried out in a rotary drum (free-falling action) mixer, some of the mixes were produced in Hobart mixer (Figure 3.8) following the same procedure. Given the very little quantity of constituents that ultra-low density mixes contain, the base mix was found to stick on the walls of rotary drum leading to loss of the material. Therefore, it was found more efficient to produce foamed concretes with densities 200 kg/m^3 and below in a Hobart mixer. In the case of Hobart mixer, after combining the dry materials, foam was added and combined with hand mixing. This is because, high shear forces applied by the Hobart mixer could destroy the foam bubbles leading to collapses.

3.5.3 Preparation of forms and sampling

Prior to mixing, forms were prepared as described by Jones and McCarthy (2005a). All forms were lined with polythene film (cling film as its commercial name) as shown in Figure 3.9 to prevent any interaction between the preformed foam and the mould oil that yields a soft layer on the surface of the specimen (McCarthy, 2004). Then, the sampling was carried out and the samples were covered with cling film (Figure 3.10).

Figure 3.8 Foamed concrete mixing in rotary drum mixer (top) and Hobart mixer accompanied by hand mixing (bottom)

Figure 3.9 Preparation of moulds and sampling

Figure 3.10 Sampling of foamed concrete mixes

3.5.4 Curing

To obtain good quality concrete, curing is crucial for keeping the concrete saturated or almost saturated at required temperature and moisture levels, until the water-filled spaces at the fresh state are filled with the hydration products to the required extent (Neville, 1995). Unlike the common practice applied for curing conventional concretes, sealed curing at relative humidity of 65±5% and temperature of 20±2˚C was found to be the most effective curing regime for foamed concrete (Kearsley, 1999b).

Therefore, this curing regime was generally accepted and applied by most other researchers (Kearsley and Wainwright, 2001a; Jones and McCarthy, 2005a; Wee et al., 2006; Jones et. al, 2012). Within the frame of this study, sealed curing was used. Foamed concrete specimens were de-moulded 24 hours after casting, wrapped in polythene film (Figure 3.11) and kept at 65±5% RH and 20±2˚C. Different curing regimes applied for specific tests will be described in related sections.

Figure 3.11 Specimens wrapped in polythene film prior to curing

3.6 TEST METHODOLOGIES

3.6.1 Fresh state and early age tests

Plastic density

As foamed concrete is designed for a specified target density, plastic density of every mix produced is measured. In accordance with BS EN 12350-6:2009, plastic density was measured by filling and levelling the surface of a container of known volume and mass with freshly produced foamed concrete with no compaction applied. Measured plastic density should be within the range of ± 50 kg/m³ and ± 25 kg/m³ of target density for low/high and ultra-low density foamed concretes respectively. Plastic density (D, kg/m³) was obtained using Equation 3.3. Mixes with measured plastic densities out of the specified range were discarded and repeated.

$$D = \frac{m2-m1}{V} \qquad \text{Equation 3.3}$$

where m1 = mass of empty container, kg

m2 = total mass of container and sample, kg

V = volume of the container, m^3

Flow time (Marsh Cone method)

Flow behaviour of foamed concrete was assessed by modified Marsh cone method introduced by Dhir et al. (1999) and used by Jones and McCarthy (2003, 2005b). The set-up and dimensions of the modified Marsh cone is illustrated in Figure 3.12. Prior to testing, modified Marsh cone was dampened, the orifice was plugged and the cone was filled with 1.5 litres of foamed concrete sample immediately after mixing. A container with volumetric grades placed under the cone and the plug was removed in order to measure the time (to the nearest seconds) of flow for 1 litre of foamed concrete. Flow behaviour was then classified according to Table 3.4 considering both efflux time and flow continuity. Flow time test was carried out once for each mix.

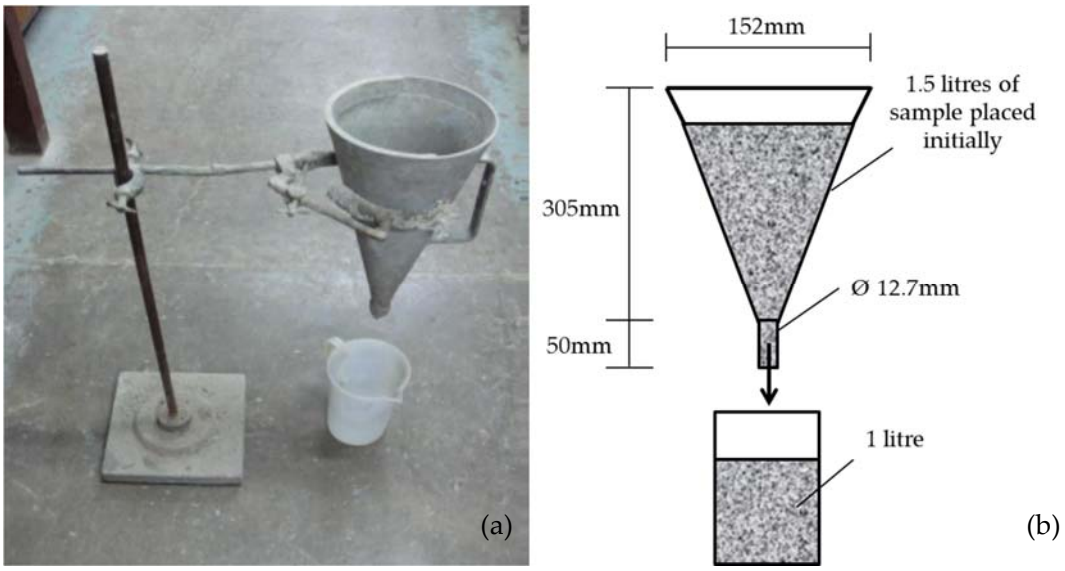

Figure 3.12 (a) Set-up and (b) schematics of modified Marsh cone apparatus

Table 3. 4 Classification of flow behaviour – Modified Marsh Cone (Dhir et al., 1999)

Main Class	Description	Sub-Class	Description
1	1 litre in < 1 min	A	Constant flow
2	1 litre in > 1 min	B†	Flow with breaks
3	0.5 litre < efflux < 1 litre	C†	Filling aided with gentle tamping
4	Efflux < 0.5 litre		
5	No flow		

† Only use with main Classes 1 and 2.

On the other hand, flow behaviour of ultra-low density mixes containing fly ash was assessed slightly different than this method. As ultra-lightweight mixes exhibited long flow times and incorporation of fly ash was not found to change these flow times significantly, instead of measuring the flow time for 1 litre efflux, efflux in 5 minutes was measured. 5 minutes was chosen to obtain enough efflux to make precise measurements.

Drop in level (stability) and collapse time

There is no standard test method for measuring the mix stability. Therefore, stability checks were carried out by placing foamed concrete mixes into 500 mm deep and 75 mm diameter polycarbonate cylinders that are lined with polythene film (cling film as its commercial name). Cylinders with these dimensions were chosen because severity of instability may not be observed at shorter depths, as Mohammad (2011) reported bigger drops in level when taller cylinders were used. Fresh foamed concrete mixes were then placed in the cylinders, surface was levelled and covered with polythene film and further observed over 24 hours. Any drop in the level of the mix was considered as instability (see Figure 3.13-a).

Collapse times of unstable mixes were measured observationally by using a stop watch (Figure 3.13-b). Stop watch was started with the addition of foam to the base mix. After the production, foamed concrete mixes were placed in cylinders as in mix stability measurements. Then mixes were observed for any drop in level occurring. Once the drop in the height of the sample can be observed visually, the time was recorded as the collapse time. Foamed concrete mixes with densities 600 kg/m^3 and below and 300 kg/m^3 and below were tested for drop in level and collapse time respectively.

Figure 3.13 (a) Drop in level test - example of a collapsed mix; (b) collapse time test

Figure 3.14 Temperature development set-up

Setting time

In order to determine the initial setting time, automatic Vicat apparatus was used in accordance with BS EN 196-3:2005+A1:2008. For the aim of current study where fast setting times are considered, it was not suitable to store foamed concrete prior to setting time testing as described by Dhir et. al (1999). Therefore, it was agreed to carry out setting time test on the base mixes with w/c ratio of 0.50. Additionally, it was thought controlling the initial setting time of the base mixes would be easier than the foamed concrete mixes which may comprise foam with varying density and quality.

Temperature development in a hot-box (semi-adiabatic)

The nature of foamed concrete and the apparatus were not suitable to use the isothermal hydration test. Therefore, the method described by Jones and McCarthy (2006) employing a hot-box was used to determine the temperature development due to heat of hydration of foamed concrete under semi-adiabatic conditions. Fresh foamed concrete sample from each mix was placed (immediately after mixing) in a 165 mm cube sitting in an insulated, timber hot-box which was lined with 150 mm thick expanded polystyrene (Figure 3.14). Then, a Type K thermocouple connected to a data logger was secured in the centre of the mix to monitor the core temperature development profile of the mix over 24 hours.

3.6.2 Hardened state tests

Compressive strength

As ULFCs have very low strength (< 600 kg/m^3), compressive strength was not the main focus of this study. The test was carried out on 100 mm cubes and 150mm diameter and 300 mm cylinders (3 specimens for each), in accordance with BS EN 12390-3 (2009) to provide a guideline for compressive strength values of ULFCs. The specimens were sealed cured for 28 days and the dimensions of the specimens were measured prior to testing. Compressive load was applied manually by using a compression testing equipment calibrated to apply low load values. The load was applied at the same rate continuously until the failure and the maximum load at failure was recorded for calculations. Compressive strength was calculated (to the nearest 0.1 N/mm^2) by using Equation 3.4.

$$f_c = \frac{F}{A_c}$$ Equation 3.4

where f_c = compressive strength, N/mm² (MPa)

F = max. load at the time of failure, N

A_c = cross-sectional area on which the load is applied, m²

Modulus of elasticity under compression (E-value)

The static modulus of elasticity was determined in accordance with BS EN 1352:1997, the standard method for autoclaved aerated concrete (AAC) or lightweight aggregate concrete. This standard method was chosen given the similarities of AAC and foamed concrete. The specimens used were three cylinders of 150mm diameter and 300mm high. Following the preparation, mixing and casting as described in Section 3.5, the specimens were demoulded after 24 hours and cured for 28 days in a controlled environmet with 20°C and 45 ± 5 % RH. Prior to testing the specimens were dried to mass related moisture content of 6±2% at 30°C followed by 24 hours storage in a dessicator.

Strain measurements were taken in two ways; (i) using demec points at three different points around the specimen (Figure 3.15) and (ii) using a frame equipped with a dial gage as shown in Figure 3.16. For the second method demec plates were secured at the point of contact between the frame and foamed concrete in order to avoid any damage to the specimens while securing the frame on the specimen. The gauge length used for both methods was 200 mm as it was stated in the standard test method.

The specimens sitted in the frame were placed in the compressive loading machine with rubber pads at the top and bottom of the specimens in order to level the surface perpendicular to the stress applied and aid the equal distribution of stress within the specimen. The specimens were exposed to cyclic loading (two repeats for each specimen) from 5% to 30% of their compressive strength which was determined earlier in the experimental programme. The E-value was then calculated as detailed in the standard. The averaged standard deviation of the measurements done by the frame was 0.09.

Poisson's ratio

Determination of Poisson's ratio was carried out in accordance with ASTM C469-02 by using a frame equipped to measure both lateral and axial strain (Figure 3.17). Two cylinders of 150mm diameter and 300mm high for each foamed concrete density considered were tested following 28 days of sealed-curing. The compressive strength values used for calculating the stress applied for determining Poisson's ratio were determined earlier in this study. As in the determination of E-value, rubber pads were placed both at the top and bottom of the specimens to provide equally distributed stress and prevent localised crashing upon loading. Similar to the installation of the frame for determination of E-value, demec plates were secured at the contact points of the frame and specimens, especially in ultra-low density specimens as they were prone damages when the frame was tightened. Standard deviation of the measurements taken was zero.

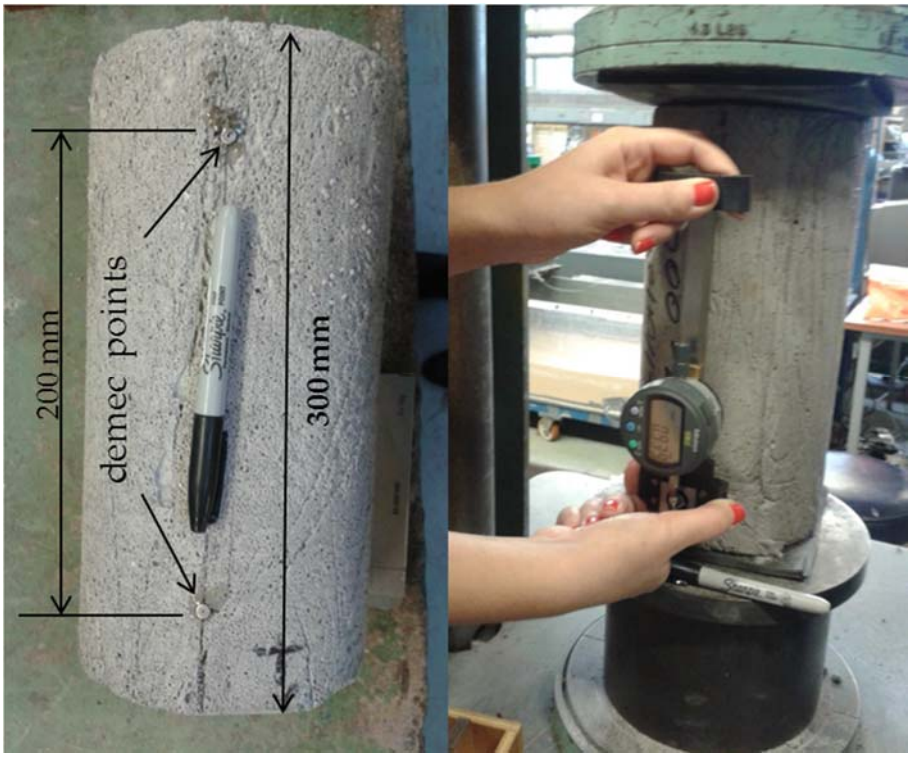

Figure 3.15 Strain measurements with demec points for determination of E-value

Figure 3.16 Strain measurements with a frame to determine E-value

Figure 3.17 Poisson's ratio apparatus

Drying shrinkage

Drying shrinkage was determined in accordance with BS EN 680:2005, determination of the drying shrinkage of autoclaved aerated concrete (AAC). As the microstructure of foamed concrete is more similar to AAC's than of normal weight concrete, this standard method was chosen to evaluate the drying shrinkage.

Three prisms of 40x40x160mm were produced as described in Section 3.5, instead of cutting from a pre-fabricated element as stated in the standard. As the ULFCs have weak structures with tendency to fracture at early ages, cast specimens were sealed-cured for 28 days in order to gain enough strength prior to the application of ball bearings. After 28 days, ball bearings were secured at the centre of the specimen ends by using epoxy resin and hardener, such that half of the ball was exposed. Mass of the samples with and without ball bearings was recorded.

Specimens were then conditioned in water for 72 hours (Figure 3.18-a). One third and two third of the thickness of the specimens were immersed in the water in the first and second 24 hours respectively, whereas the specimens were totally immersed in the water during the last 24 hours. Following the conditioning, the specimens were kept sealed for 24 hours in order to maintain even distribution of moisture. Then, initial length measurements were taken by a length comparator capable of measurements to 0.001mm and calibrated with 160mm invar bar (Figure 3.18-b). It is advised to calibrate the length comparator against the reference invar bar in every three specimen. The specimens were left to dry in a controlled environment (20°C, 45 ± 5% RH) with sufficient air circulation and length measurements were taken on a weekly basis as well as the corresponding mass change (to the nearest 1.0g).

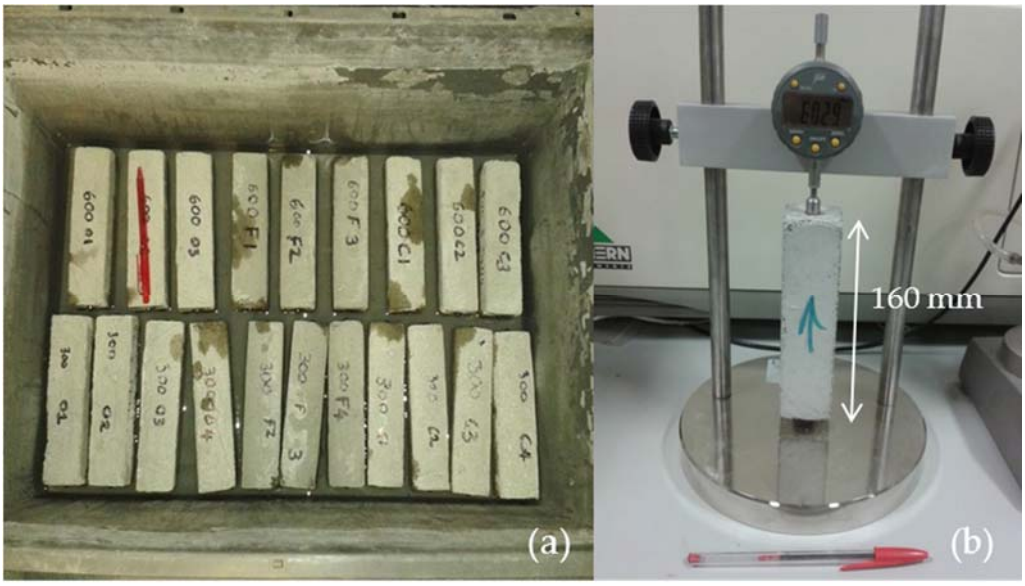

Figure 3.18 (a) Conditioning and (b) strain measurement for drying shrinkage

Coefficient of thermal expansion

The standard test method for determining the coefficient of thermal expansion (CTE) of concrete is AASHTO T336-11. However, given the unavailability of the apparatus required, the standard test method could not be strictly followed, but the assumptions made in the standard were followed. Accordingly, prior to testing the specimens were kept in water for 24 hours in order to reach the maximum expansion upon water saturation. Then it was assumed that any further expansion (during testing) is solely caused by the increase in temperature.

Four 40x40x160mm prisms were produced (smaller size than specified in the standard, as a small sized hot water tank was employed), cured for 28 days and then ball bearings were secured to both ends of the specimens as in drying shrinkage specimens. The specimens were then placed in a 20°C water tank for 24 hours in order to allow the specimens to expand upon saturation. Length measurements of the specimens were taken by using a length comparator as described in drying shrinkage test. Immediately after length measurements two of the specimens were put in a 50°C water bath (see Figure 3.19) whilst the other two specimens were kept in a 20°C water tank as control specimens. Following a further 24-hour of submersion, the length changes of the specimens both in the 50 and 20˚C water tanks were measured. Length changes of the control specimens were then

subtracted from the test specimens. Equation 3.5 (AASHTO T336-11) was then used to determine the coefficient of thermal expansion.

$$\Delta L = \alpha L_0 \Delta T \qquad \text{Equation 3.5}$$

where ΔL = change in length, mm

α = coefficient of linear expansion, microstrains/°C

L_0 = initial length of specimens at temperature T_1, mm

ΔT = change in temperature from temperature T_1 to T_2, °C

Figure 3.19 Coefficient of thermal expansion testing apparatus

Capillary sorption

Water sorptivity (S) was measured by using the capillary rise method described by Hall (1989) and used by Jones and McCarthy (2005b), Nambiar and Ramamurthy (2007b). Two 100mm cube specimens prepared as described in Section 3.5 were used for each mix. Following 28 days of curing, one side of each cube was slightly ground with sand paper in order to expose the pores. The specimens were then oven dried to constant mass at 30°C in order prevent any internal damage affecting the microstructure of the specimens when exposed to high temperatures (Alexander and Mackechnie, 1999). After the drying process the specimens were kept in a dessicator (along with silica gel for maintaining constant moisture) for 24 hours. The initial mass and dimensions of the specimens were measured prior to the test.

The ground surfaces of the specimens were then placed on a 3mm thick plastic mesh inside a tray. Water is added up to a height of 5mm above the base of the specimens as seen in Figure 3.20. The mass of the samples was measured every 10 minutes for an hour such that minimum of 5 readings obtained in 1 hour. Then, the change in mass as percentage of initial mass was calculated. Standard deviation averaged for the measured values was 0.021.

Sorptivity (S) was calculated by using Equation 3.6, where i (mm), is the slope of the line of the graph of cumulative water absorption per unit area of the surface exposed to water (Equation 3.7) against square root of time, t (minutes).

$$S = \frac{i}{t^{0.5}} \qquad \text{Equation 3.6}$$

$$i = \frac{\Delta w}{A\rho} \qquad \text{Equation 3.7}$$

where Δw = increase in mass with time, g

A = cross-sectional area of exposed surface, mm^2

ρ = density of water, g/mm^3

It must be noted that, materials with coarse pore structure were observed to show a downward curvature on the graph of cumulative water absorption against square root of time due to decreased suction (Hall, 1989). In that case Equation 3.8 was used instead of 3.7 (Hall and Tse, 1986) for calculating sorptivity.

$$i = A + St^{0.5} - Ct \qquad \text{Equation 3.8}$$

where C = sorptivity coefficient, mm/min

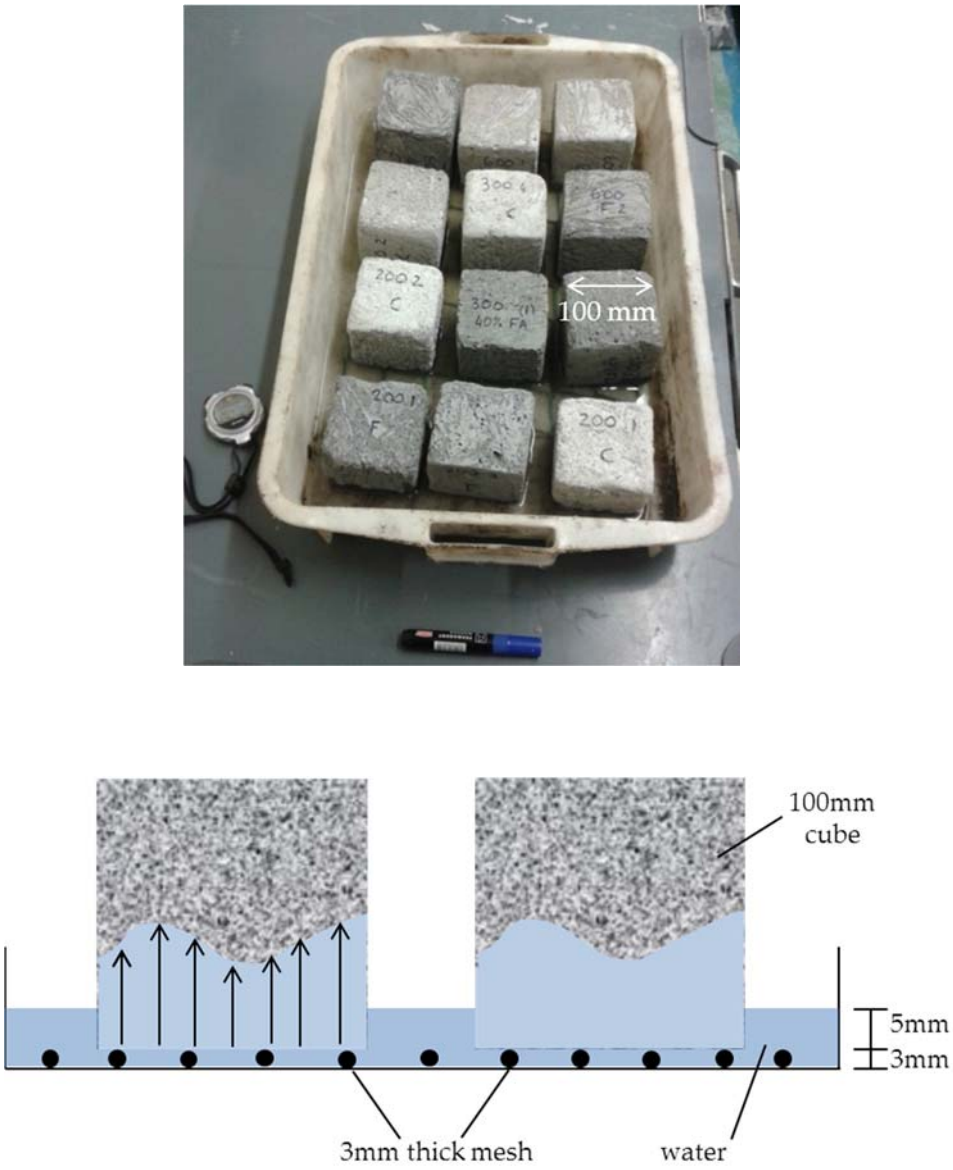

Figure 3.20 Water sorption test set-up (top) and schematics (bottom)

Thermal conductivity

Thermal conductivity was measured in accordance with the method developed at the University of Dundee and illustrated by Giannakou and Jones (2002) and McCarthy (2004). As the existing methods for measuring thermal conductivity were not suitable for foamed concrete specimens due to their small size and degree of flatness, another method originating from BS 874-3 (1990) was developed following discussions with the British Board of Agrément (McCarthy, 2004).

The modifications (Figure 3.21) made to the calibrated hot box described in BS 874-3 (1990) were; removal of the fan, reduction in the power of the heat source, addition of a refrigeration unit on the other side of the specimen and a plywood baffle in front of the heat source and increase in the number of thermocouples used (inside the refrigeration unit and in front of the baffle). During the calibration of the apparatus, it was also found that reliable thermal conductivity values could be obtained when the temperature on the heated side is 30°C, whilst the refrigeration unit was set to maximum (5°C) (McCarthy, 2004).

290mm square slabs with 50mm thickness were produced as described in Section 3.5 and cured for 28 days. After curing, specimens were oven-dried at 30°C until constant mass. High drying temperatures (105°C as suggested) were avoided in order to prevent any microstructural damage arising from rapid drying due to high temperatures (Alexander and Mackechnie, 1999). Prior to testing specimens were kept in a dessicator for 24 hours along with silica gel. Then, the mass (to the nearest 0.1g) and average thickness (to the nearest 0.1mm) of the specimen were recorded. As it was assumed that the heat flow will occur in one direction, the perimeter of the slabs were lined with an air-tight, thermally insulating tape (Figure 3.22) to prevent the heat loss through the edges of the specimen.

Calibration check of the test apparatus was carried out by testing a (1000 kg/m^3) foamed concrete specimen with a known thermal conductivity. Before placing the specimen in the apparatus, minimum of three thermocouples (ISO 8302) calibrated against a UKAS accredited glass thermometer were secured on each side of the specimen. Thermocouples were also secured on the insulation and between the plywood and styrofoam at the back of the heated side. The hot-box was then fastened, temperature on the heated and cold side

was set to 30 and 5°C respectively and the system was activated. For the first 24 hours no measurements were taken as the system was allowed to reach in equilibrium (i.e until the rate of heat transfer is steady). Upon reaching the equilibrium hourly readings were taken and thermal conductivity was calculated from the average of three hourly readings by using Equation 3.9.

$$\lambda = \frac{Q.d}{A.\Delta T} \qquad \text{Equation 3.9}$$

where Q = time rate of heat flow, W; Q = (15*counter reading)/(time between readings)

d = specimen thickness, m

A = area of the specimen exposed, m^2

ΔT = temperature difference between the heated and cold surface, °C

The test was repeated on two specimens for each mix and the standard deviation was 0.02.

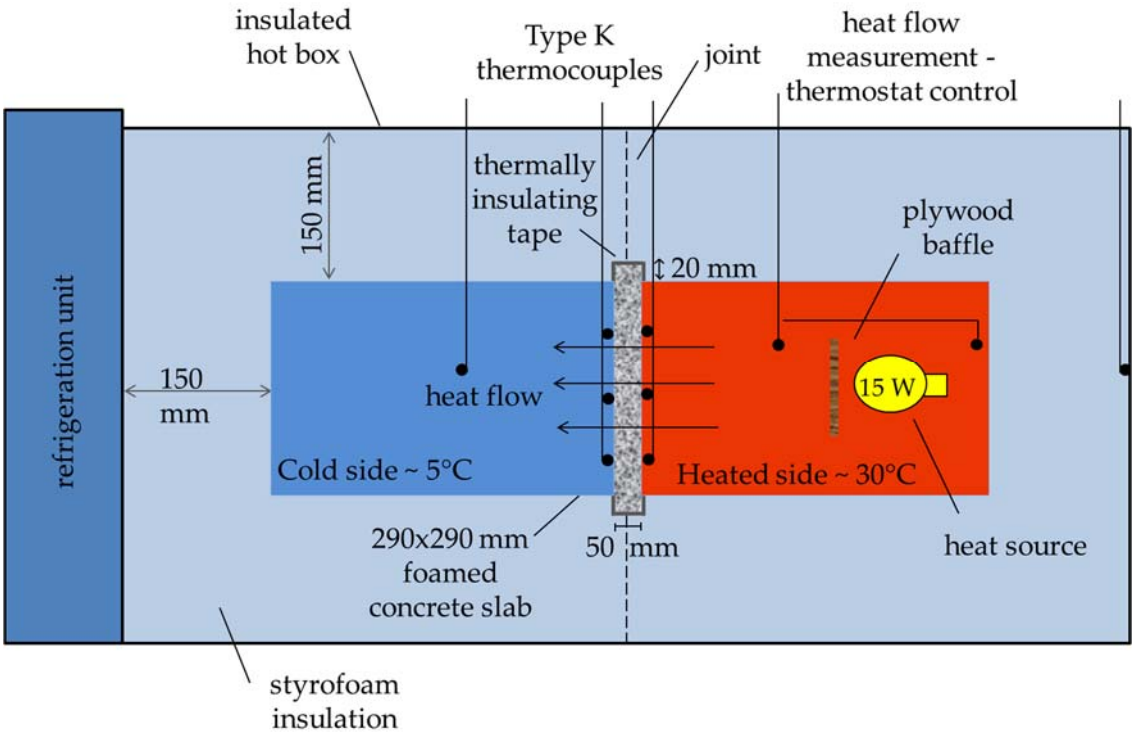

Figure 3.21 Schematics of modified calibrated hot-box (Giannakou and Jones, 2002)

Figure 3.22 Modified calibrated hot-box (top) and foamed concrete specimen ready for testing (bottom)

Sound absorption coefficient

Given its cellular characteristics foamed concrete is suggested to have good sound absorption performance (Ramamurthy et. al, 2009). However, there is no detailed investigation on the sound absorption potential of foamed concrete. Indicative sound absorption performance of foamed concrete was investigated in accordance with ISO 10534-1:1996 (E) by using a standing wave apparatus (provided by Brüel & Kjær, 1955). Unlike the conventional reverberation room method (BS EN ISO 354:2003) that requires large specimens, and costly test set-up, impedance tube requires small sized specimens and cheaper set-up that were more practical.

Figure 3.23 Standing wave apparatus and test specimens for determination of sound absorption coefficient

The test was carried out with frequencies ranging from 125 to 4000 Hz. Two different setups were used for the apparatus depending on the frequency under consideration. For frequencies ranging from 125 to 1000 Hz, an impedance tube of 100mm diameter was used, whereas a 29mm diameter tube was employed for the frequencies between 2000-4000 Hz (Figure 3.23 top and bottom left respectively).

Cylinders of 29mm and 100mm diameter and 25, 50 and 70mm depth (Figure 3.23) were prepared as described in Section 3.5 and cured for 28 days. Prior to testing, one must ensure that the impedance tube is clean (free of dust) and the specimen is placed in the sample holder such that there is no air gap at the edges of the tube (otherwise sealing the gaps with petroleum jelly is recommended).

Sound transmission loss

There was an attempt to measure the transmission loss of foamed concrete in accordance with ASTM 2611-09. The test kit (Figure 3.24) was constructed at the University of Dundee in accordance to the standard. However, it was not possible to run the test without a software which is able to calculate the measured data. Following the discussions made

with the Physics Department within the university and the University of Salford Acoustics Department, no further studies were carried out with this apparatus as these would lead the author away from the focus of this study.

Therefore, the specimens (cylinders of 29mm and 100mm Ø with 50mm thickness) were sent to University of Salford Acoustics Department to be tested for normal incidence transmission loss using impedance tube over the frequency range of 100 to 5000 Hz. Impedance tube method was chosen over traditional reverberation room as it was difficult to produce and transport 10-12 m^2 sized (BS EN ISO 354:2003) ultra-low density foamed concrete specimens at this stage.

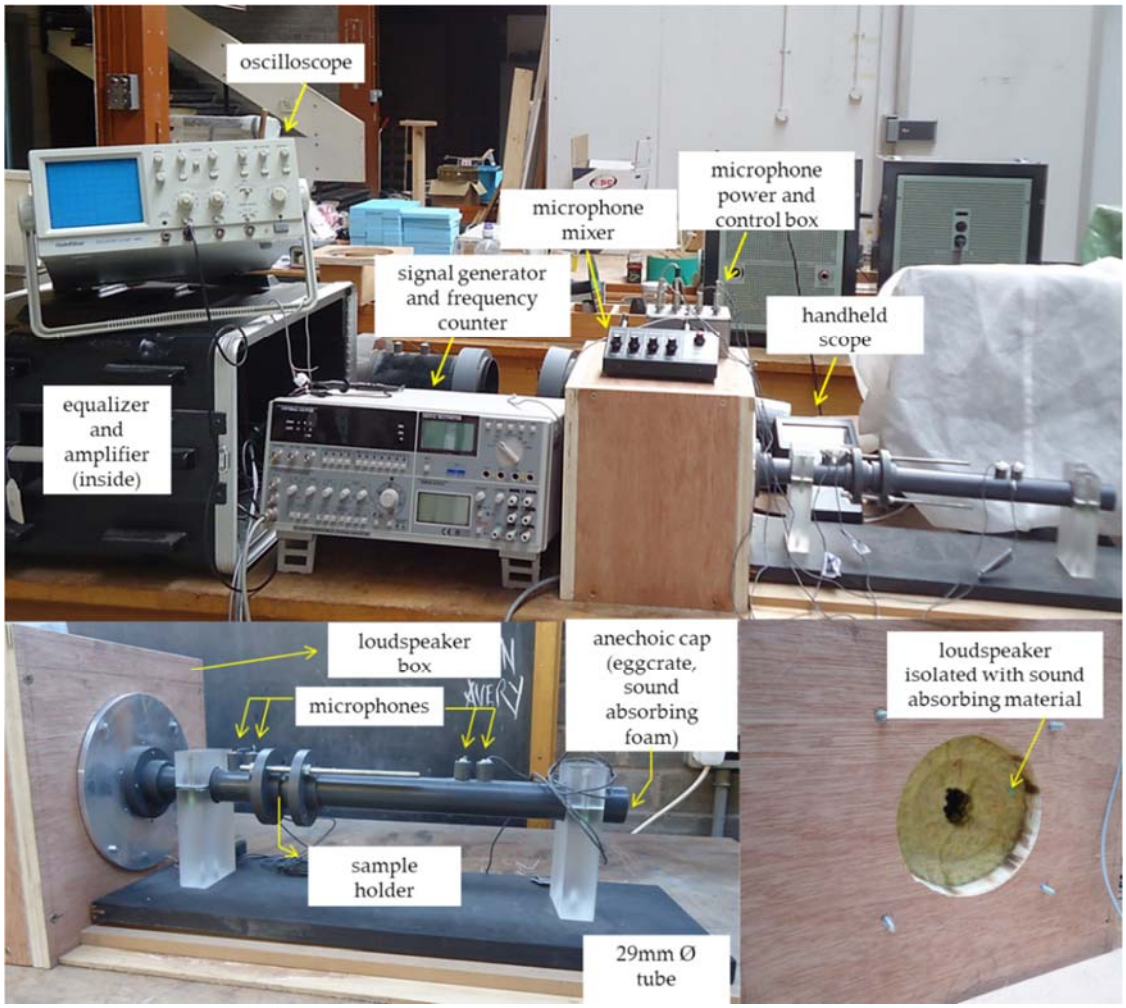

Figure 3.24 Sound transmission loss kit

2D image bubble analysis

Following the key observations obtained about the variations in the bubble size of foamed concretes with different plastic densities and constituents (Nambiar and Ramamurthy, 2007a; Mohammad, 2011), bubble analysis were carried out. 500mm high cylindrical specimens were produced for bubble analysis. After 28 days of curing, specimens were split longitudinally, and then sections from the top, middle and bottom (in the direction of cast) of the cylinder were taken to evaluate the bubble size throughout the specimen and increase the accuracy of the results. (The error bars on the bubble size data are based on standard error which is equal to standard deviation divided by the square root of number of measurements that make up the average).

Surfaces were brought to level and cleared from dust and residues of concrete pieces. Given the nature of foamed concrete, bubble walls are so thin to withstand traditional surface preparations that include polishing and grinding prior to image analysis (Aligizaki, 2006). Therefore, surfaces were sprayed with fluorescent paint to improve image contrast under UV illumination.

Then, a method which requires a good quality camera and image analysis software were adopted from a similar approach described in (Kearsley and Visagie, 1999a; Nambiar and Ramamurthy, 2007a). 2D image analysis was carried out by employing Image J software on images sized by 10 x 10 mm (Figure 3.25). Prior to the image processing, borders of the bubbles made visible by drawing lines where the borders are not clear in the black and white image in order to increase the accuracy of the results (Figure 3.25-right).

Microstructure analysis (ESEM)

Microstructure analysis was carried out for observing the effect of plastic density, constituents and age on the microstructure of foamed concretes by using Environmental Scanning Electron Microscopy (ESEM). Specimens for ESEM were obtained from foamed concrete specimens that were prepared as described earlier in Section 3.5 and cured until the desired age. Small specimens (as shown in Figure 3.26) were mounted on Aluminium stubs using carbon adhesive tabs. Prior to testing, the specimens were coated with 20-

30nm Gold/Palladium using a Cressington 208HR sputter coater in order to increase the conductivity of the specimens. Specimens were then examined using a Philips XL30 ESEM operating at an accelerating voltage of 15kV.

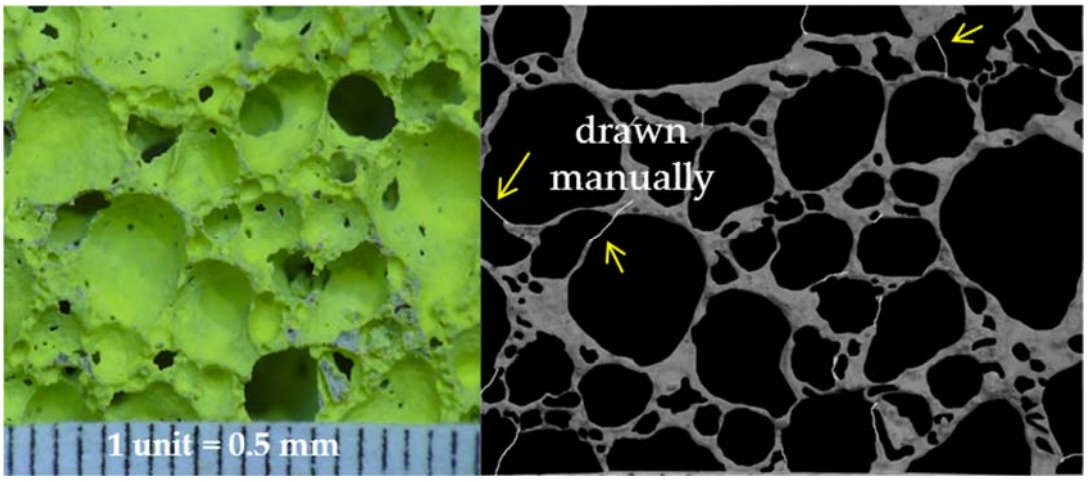

Figure 3.25 Image for bubble analysis (left) and a processed image in Image J (right)

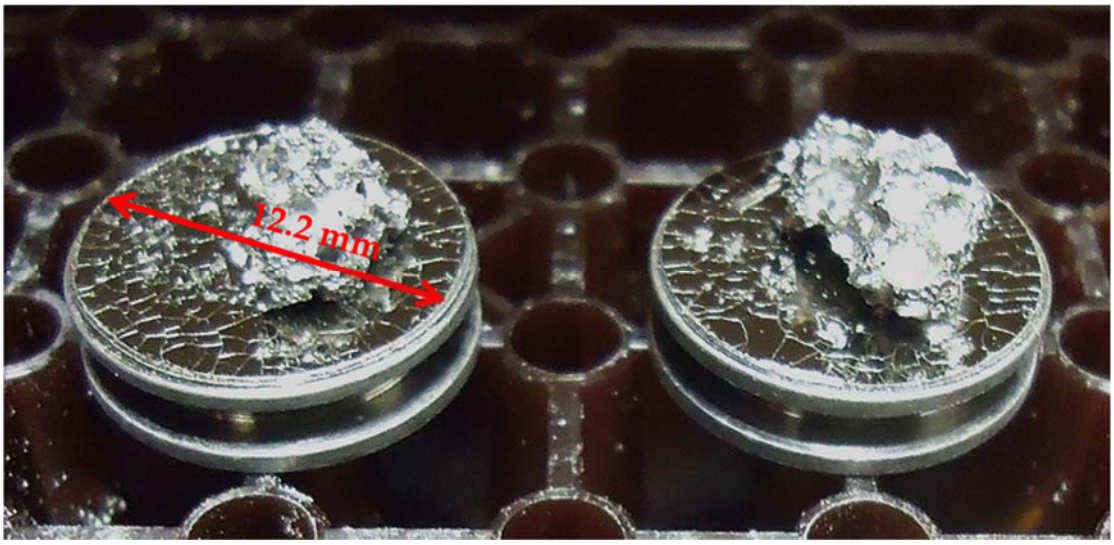

Figure 3.26 Specimens for ESEM

3.7 PRACTICAL OBSERVATIONS

Some key observations about maintenance of test equipment and storage of materials were done throughout the experimental studies. One of the most important observations made was on the maintenance of the foam generator. As suggested by Ansell (2010), the scouring pads packed inside the foam lance should be removed, washed and re-packed on a monthly basis in order to prevent the build-up of residues from the surfactant.
Furthermore, it was suggested to run clean water through the system after foam production is completed in order to flush out any surfactant solution and foam left in the system. It was reported that, in the absence of performing these maintenance, quality of the foam reduces such that it may even lead to failure of foamed concrete mixes. Moreover, the pressure at which the foam generator works (50psi, i.e 345 kPa) needs to be checked regularly, as lower pressure yields to low quality foam with fast rate of drainage.

Compared to the foam production in industry, pressure used to operate the foam generator is significantly lower. It was observed that the foam produced in industry applications is more stable with more uniform and smaller bubbles, yielding better quality mixes. Therefore, experiments carried out under laboratory conditions represent a worse case, indicating that quality and performance of a given foamed concrete mix could be better in industry.

Another key observation made was on the storage and life time of the materials used. Firstly, like all other cements CSA cement was stored in a sealed bag inside an air-tight tub. However, the shelf life of the CSA cement under consideration was found to be around one year. Beyond one year, it was reported to cause failure of foamed concrete mixes. Secondly, similar to CSA cement, surfactant which is stored under 65±5% RH and 20±2°C, was found to have a life time of around one year for producing good quality, stable foam.

Due to the low strength of ultra-low density foamed concretes, there were some difficulties observed while carrying out particular tests. For instance, the frame equipped for measuring E-value and Poisson's ratio could resulted in localised crushing, therefore, steel plates were secured at the contact points of the specimens and the frame. On the other hand, for drying shrinkage and coefficient of thermal expansion tests, steel ball-bearings

were required to be secured on the specimens. These were secured with great care and at the end of the curing period to avoid any damage to specimens. Furthermore, during the measurements of drying shrinkage and thermal expansion difficulties have arisen due to the movement of some of the ball-bearings. This may lead to errors in results as well as reducing the precision, however as the tests were only repeated once, it was not possible to quantify the errors.

Moreover, while preparing the specimens for bubble size and microstructure analyses, ultra-low strength foamed concretes were found to fracture into pieces, and therefore, great care was taken while preparing the specimens. Furthermore, due to the small specimen size required for SEM images and low strength of ULFCs, irregularities in specimen height could not be controlled. As a result variations in scales of SEM images were observed. Another reason for these variations is considered to be the use of two different machines.

CHAPTER 4

4. THE HYPOTHESES ON STABILITY OF FOAMED CONCRETE

4.1 INTRODUCTION AND BACKGROUND

The review of the literature showed that there is no clear understanding of how instability occurs in foamed concrete mixes, specifically in ultra-low density (< 600 kg/m^3) mixes and no successful solution to overcome this has been found until now. Clearly these mixes contain significant amount of foam and reduced solid content which is considered as the main source of the stability issues. Given the number of factors affecting the behaviour of foamed concrete such as plastic density, rheology, liquid drainage of foam and bubble size, it is extremely difficult to carry out fundamental scientific analyses of this.

Fresh foamed concrete mixes are complex, dynamic environments in which various processes occur from the time of mixing until hardening of the mix. Furthermore, as foamed concretes exhibit more Bingham-like behaviour than Newtonian behaviour (Basiurski, 2000; McCarthy, 2004; Mohammad, 2011), it is not suitable to apply the science for Newtonian liquids, which also contributes to the difficulties noted above.

Therefore, this Chapter summarises the hypotheses on the stability of foamed concrete which were constructed based on the previous observations made both under laboratory conditions at the University of Dundee and in practice. Additionally, although the medium surrounding the foam in foamed concrete mixes varies significantly from liquid foams, the mechanisms applied to these were adopted with an intention to explain the behaviour of bubbles in foamed concrete. Therefore, the Chapter provides a deeper understanding on the instability mechanism in foamed concrete and offers a solution to overcome this.

Instability of foamed concrete, in this case, can be described as the loss of bulk structure prior to initial setting, leading to the collapse of the structure. Previous research studies conducted at the University of Dundee (Mohammad, 2011) and the experience of its application in practice (Ansell, 2010) have shown that foamed concretes become more prone to instabilities as the plastic density decreases. More specifically, decreasing the

density of foamed concretes down to ultra-low levels (below 600 kg/m³) greatly increases the tendency for unstable mixes, with a significant risk of failure at plastic densities below 400 kg/m³ (Ansell, 2010; Mohammad, 2011). Therefore, industry does not generally use foamed concretes with plastic densities below 400kg/m³ (Ansell, 2010).

Figure 4.1 shows an example of a segregation type of failure of ultra-lightweight foamed concrete (ULFC) in practice (a project in Gerrards Cross in East London). The project required to facilitate the construction of a retail store above the tunnel. Therefore foamed concrete was chosen for topping up above incinerated bottom ash aggregate (IBAA) in order to reduce the self-weight of the materials above the tunnel. The foamed concrete mix produced with 100% Portland cement (PC) and plastic density of 350 kg/m³ was employed. However, there were incidences reported on the failure of foamed concrete shortly after pouring, indicating the susceptibility to instability. A similar failure mode was also noted on laboratory mixes (produced and tested as described in Sections 3.5.2 and 3.6.1 respectively) due to instability (see Figure 4.2).

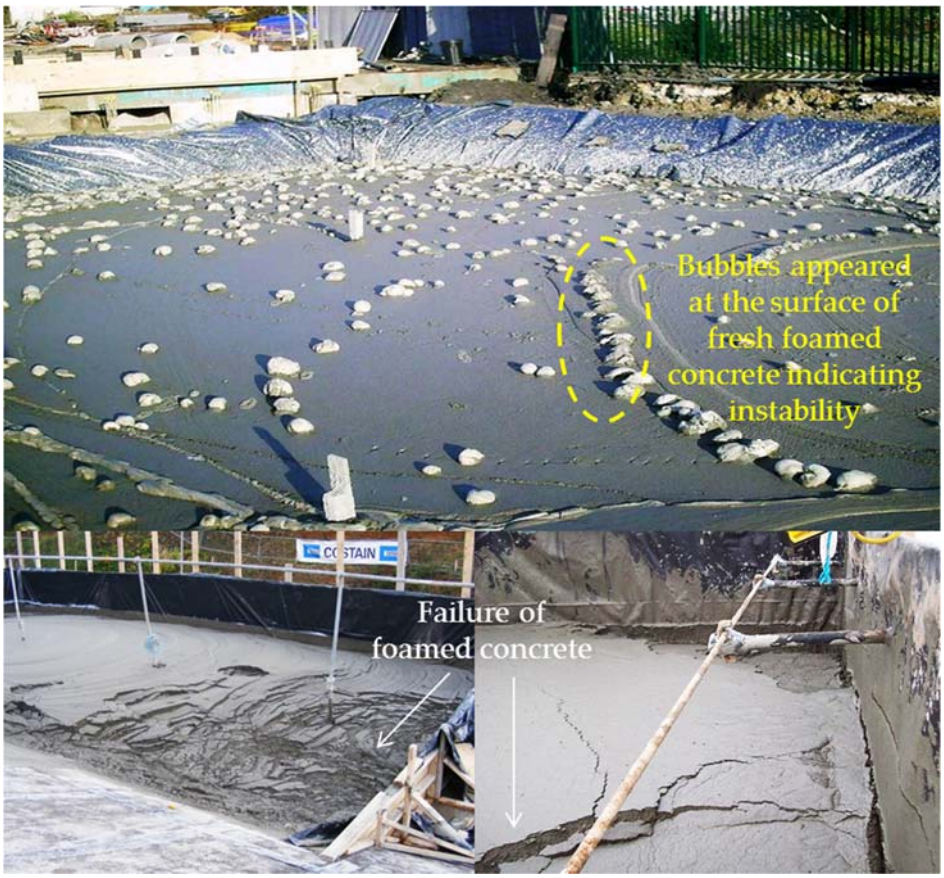

Figure 4.1 Observed failure of ultra-lightweight foamed concrete in practice

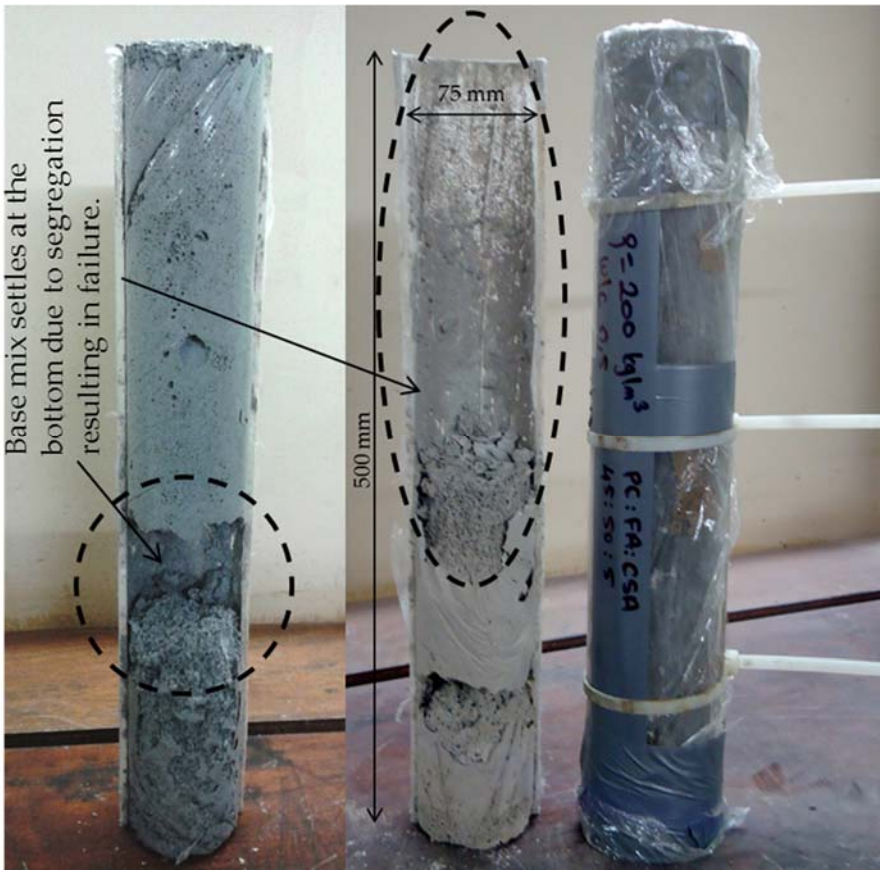

Figure 4.2 Failure due to segregation of 200 kg/m³ ULFC produced with 100% PC and protein surfactant in the laboratory

4.2 FUNDAMENTAL ISSUES AND OBSERVATIONS ON FOAMED CONCRETE STABILITY

4.2.1 Plastic density

Plastic density is the main factor governing the stability of foamed concrete, such that as this decreases, mixes become more prone to instability. As the density decreases down to ultra-low levels, firstly the solids content is reduced through the elimination of sand in mixes below 600 kg/m³, secondly, below 500 kg/m³, the cement content is reduced with decreasing density. On the other hand air (foam) volume increases with decreasing density. Hence, while the volume of foam to be surrounded by solids increases, the solid content reduces (Figure 4.3). Then, a stage is reached where the present solids are unable to fully surround and aid the stability of air-void system leading to instability hence collapses.

During the preliminary studies, a range of ULFC mixes comprising fixed w/c ratio of 0.50 were tested for stability as described in 3.6.1 in order to visually observe the rate and level of failure. Accordingly, it was observed that the risk of failure increases significantly for plastic densities below 600 kg/m³, whilst stable mixes were not achieved at densities below 400 kg/m³. Figure 4.4 shows the decreasing solid to air volume ratio and increasing likelihood of instability with decreasing density. Accordingly, solid to air volume ratio below 0.28 was found to lead to instability-dependent collapses.

4.2.2 Bubble size variability with plastic density

The key observation giving a better understanding on foamed concrete instability was the variation in bubble size at every density considered. Although the size of bubbles is assumed to be the same initially, when the foam is first produced (as fixed surfactant type and concentration as well as a foaming system were used), it was observed to change after mixing with the base mix, depending on the plastic density. It has been reported that the diameters of the bubbles increase with decreasing plastic density of foamed concrete, and consequently a reduced number of bubbles with thinner walls appear in lower density mixes (Kearsley and Visagie, 1999a; Nambiar and Ramamurthy, 2007a; Mohammed, 2011; Jones and Zheng, 2013, Wei et. al, 2014). As larger bubbles are reported to be less stable themselves (Dransfield, 2000; McGovern, 2000), they also affect the stability of the mix. Therefore, foamed concrete mixes comprising larger bubbles are more to instabilities.

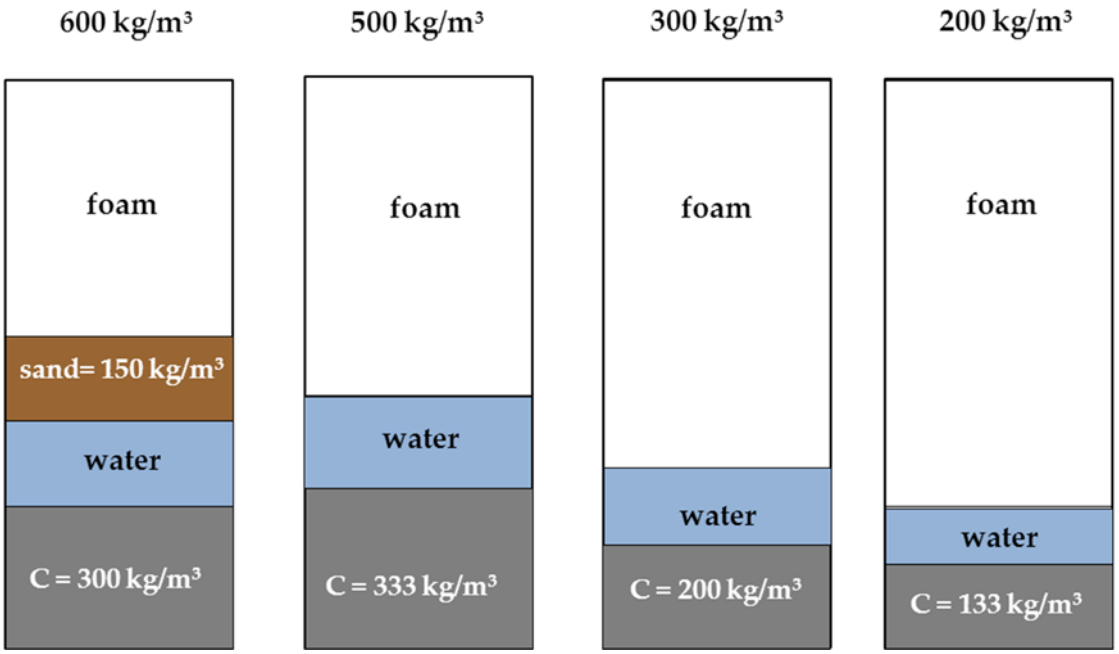

Figure 4.3 Change in the mix proportions as plastic density decreases

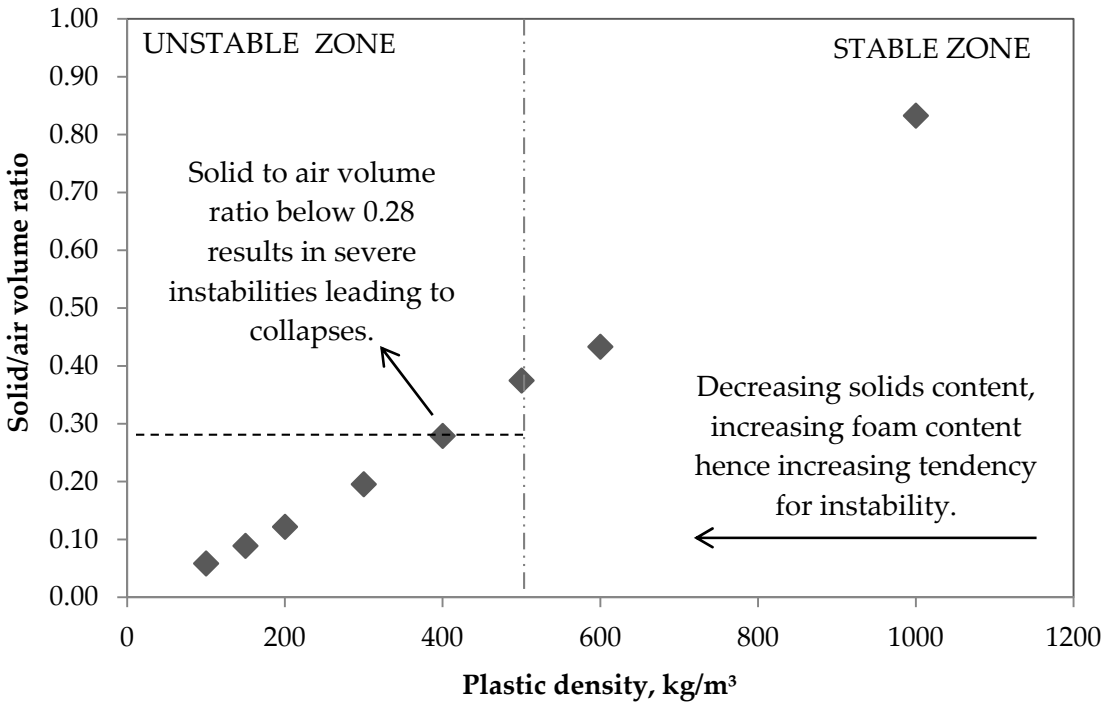

Figure 4.4 Influence of plastic density on stability of foamed concrete (based on visual assessment)

Figure 4.5 shows the changes in bubble distribution and size as the plastic density changes. This behaviour is mainly attributed to the change in the mix proportions that requires an increase in the air content with decreasing plastic density (as previously shown in Figure 4.3). Therefore, the balance of forces acting within a mix that controls the bubble size changes at every density. This balance of forces is further discussed in the following section which explains how bubbles change size within the mix.

4.2.3 Effective forces influencing bubble size in fresh foamed concrete

This section examines the forces acting within foamed concrete mixes and their effect on bubble size and stability. As there is no detailed information reported on the behaviour of foams in a cementitious medium, behaviour of liquid foams (Myers, 1992; Weaire and Hutzler, 1999; Somasanduran, 2006; Stevenson, 2011) was taken as a base in order to develop a hypothesis for the forces influencing the bubble size in fresh foamed concretes. In addition, observations made during the preliminary trials were also used to construct the hypothetical schematic shown in Figure 4.6. Although it was not practical to quantify these forces within the frame of this study, the parameters influencing their magnitudes are discussed.

Foamed concrete mixes reach equilibrium once the foam and the base mix are blended together and remain in equilibrium from the time when the mixing process is completed (t=0), until the time t=n, which is in order of minutes, hours or infinity depending on the effective forces interacting within the mix. The equilibrium state of the mixes is mainly due to the combination of bubble confinement force, $\mathbf{F_c}$, drainage force, $\mathbf{F_d}$, internal bubble pressure, $\mathbf{P_i}$, surface tension of bubbles, $\mathbf{F_{st}}$ and bubble buoyancy force, $\mathbf{F_b}$.

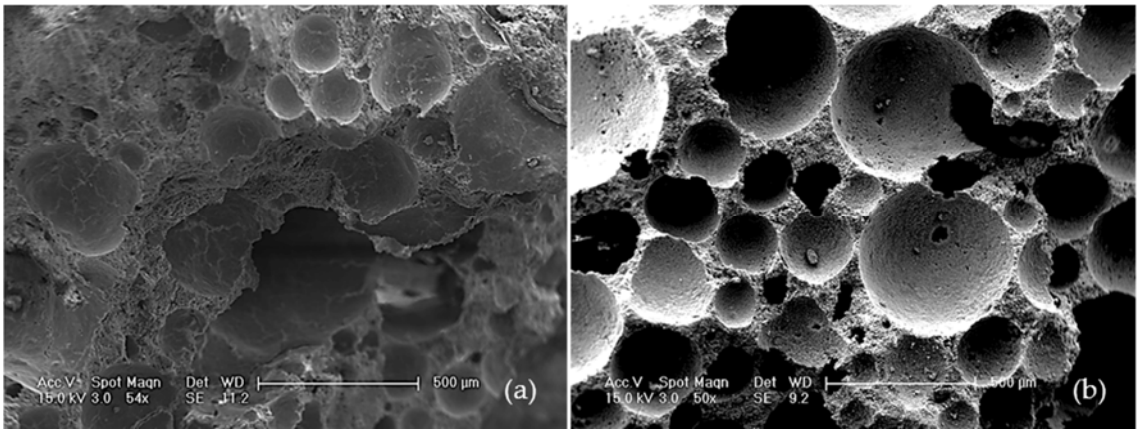

Figure 4.5 Influence of plastic density on the bubble size a) 1400 kg/m³ and b) 500 kg/m³

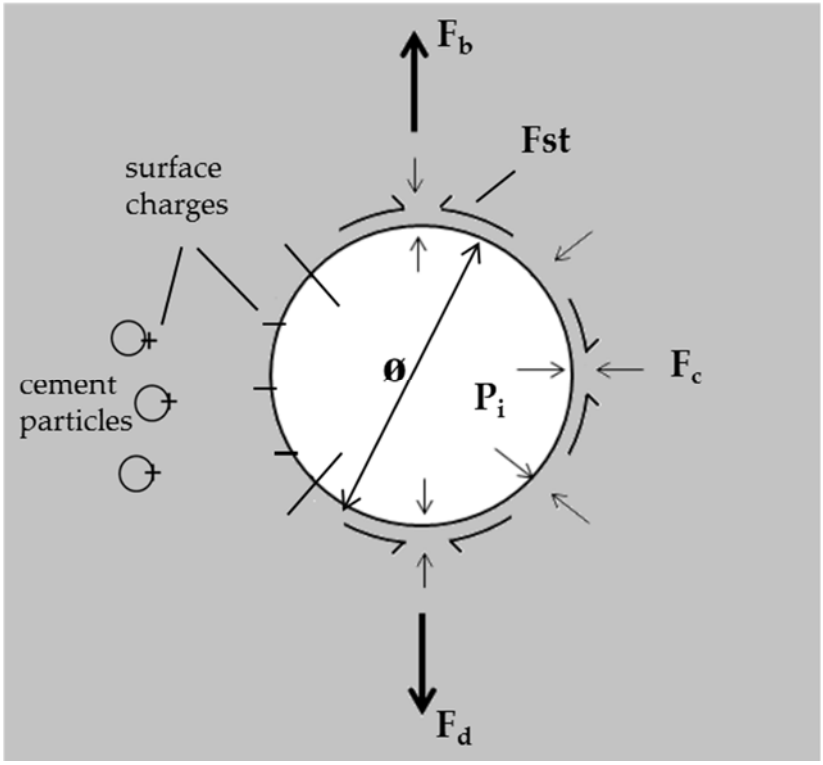

where; P_i = internal bubble pressure;

F_c = bubble confinement force;

F_{st} = surface tension force;

F_b = bubble buoyancy force;

F_d = drainage force

Ø = bubble diameter

Figure 4.6 Effective forces acting on a single particular bubble within a foamed concrete mix

$\mathbf{F_c}$ is mainly due to the plastic density of the fresh mix but the type of constituent materials such as use of different fillers (e.g. sand or fly ash) and cement type also affect this force. As the plastic density reduces, the solids content hence $\mathbf{F_c}$ reduces. In mixes with plastic densities below 600 kg/m^3, where sand is eliminated from the mix, there is a significant reduction in $\mathbf{F_c}$, given the relatively big change in the type of solids confining the bubbles. Below 500 kg/m^3, $\mathbf{F_c}$ continues to reduce due to the significant reduction in cement contents.

On the other hand, the use of finer cementitious materials also provides enhanced particle packing around the bubbles confining them (Nambiar and Ramamurthy, 2007a; Mohammad, 2011). As a result, $\mathbf{F_c}$ increases with fineness of cementitious materials. Moreover, in all mixes, as the foamed concrete starts to transform from the plastic to solid state, the cementitious medium surrounding the bubbles hardens, increasing $\mathbf{F_c}$ as the strength gain occurs.

Liquid drainage, $\mathbf{F_d}$, is driven by gravity and occurs on the foam proportion of the mix. As a result, the liquid fraction of the foam changes, so does the surface tension, $\mathbf{F_{st}}$ of the bubbles (which also changes with the changing bubble size such that larger bubbles have greater $\mathbf{F_{st}}$; Myers, 1992), breaking the equilibrium state of the mix (Weaire and Hutzler, 1999; Stevenson, 2011). Unlike liquid foams, bubbles in a cementitious matrix are mostly separated by the matrix surrounding them. Therefore, the drainage that occurs through the thin films separating the bubbles (lamellar film; Myers, 1992) and Plateau borders (channels formed where three neighbouring films meet; Stevenson, 2011) in liquid foams may change in the case of foamed concrete.

Moreover, Somasundaran (2006) stated that drainage occurs at a slower rate if the Plateau borders and thin films are rigid than if they are completely mobile (in the case of foamed concrete, presence of solid particles surrounding the bubbles is likely to reduce the mobility), whilst Stevenson (2011) reported a slower drainage rate in foams with smaller bubbles. Therefore, according to the statements made by Somasundaran (2006) and Stevenson (2011) decreased volume of solids and larger bubbles present in lower density foamed concretes possibly result in faster rate of drainage than higher densities.

Furthermore, surface charges on bubbles and cement particles are also likely to have an effect on the rate of drainage hence the stability (Jones and McCarthy, 2005b; 2006). If they are oppositely charged, cement particles will be attracted to bubbles making it more difficult for the liquid to drain while in the case of similarly charged constituents, liquid drainage occurs more readily and rapidly, even leading to instant failure (collapse) of the mix. As different surfactant types have different charges (Myers, 1992), interaction of foam and cement particles would vary. Figure 4.7 illustrates the case of similarly charged constituents assuming that anionic surfactant is used to produce the foam.

Internal pressure, $\mathbf{P_i}$, of the bubbles is assumed to be the same (due to same sized bubbles) when the foam is produced, as the surfactant type and foam generator pressure are constant. However, once the foam is mixed with the cementitious matrix, bubbles tend to increase in size (depending on the plastic density), whilst the internal pressure decreases, in order to maintain the equilibrium with the surrounding matrix. This process of bubble growth may happen elastically as the bubble surfaces covered with solid particles behaves purely elastically (Somasundaran, 2006). It must be noted that, if the bubbles behave elastically, they may also decrease in diameter at high densities where confining forces are greater. On the other hand, external forces applied during the mixing process may also cause a change in the bubble size. Figure 4.8 illustrates how plastic density influences the initial bubble size change once the foam and the base mix is blended together.

After placing the mix, given the internal pressure differential formed among the bubbles with small and big diameters, gas diffusion occurs. This is referred to as Ostwald ripening that takes place over a period of up to 10 hours in the case of liquid foams and is driven by the Laplace pressure (Weaire and Hutzler, 1999; Somasundaran, 2006; Stevenson, 2011). Laplace pressure is the pressure difference between inside and outside of a curved surface, a bubble, in this case. Laplace pressure is given by $2\gamma/r$ for spheres, where γ is the interfacial surface tension and r the bubble radius. During Ostwald ripening, the gas diffuses out from small bubbles into big bubbles. Therefore, bubbles smaller in diameter become even smaller and eventually disappear, while larger bubbles further increase in diameter. Furthermore, this process accelerates as the small bubbles reduce in size due to the increased driving force (i.e increased difference in Laplace pressure).

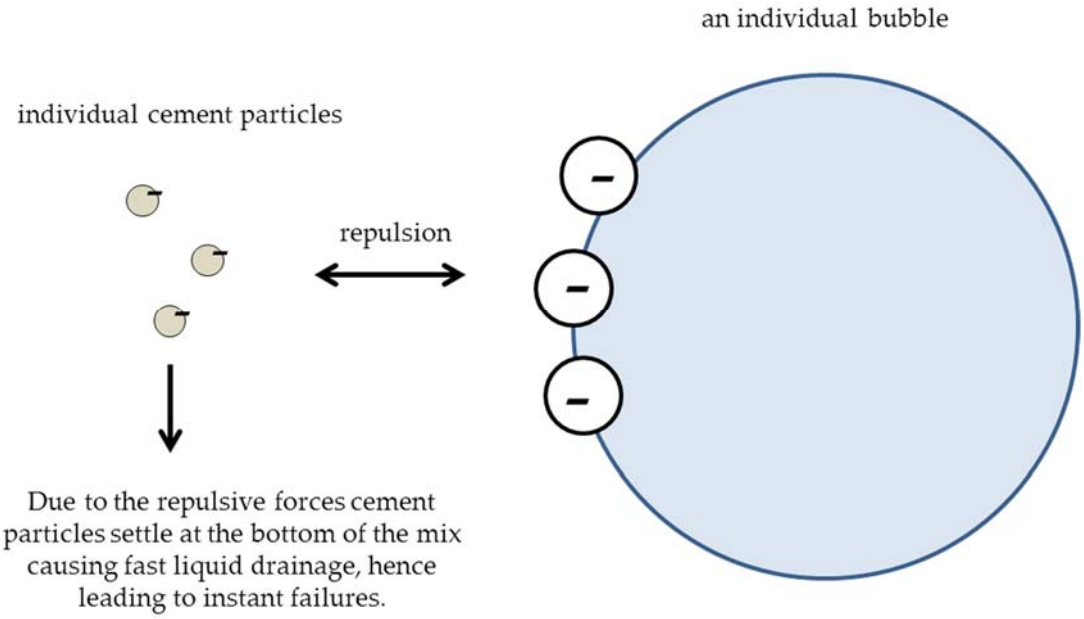

Figure 4.7 Influence of surface charges of constituents on stability (assumed charges)

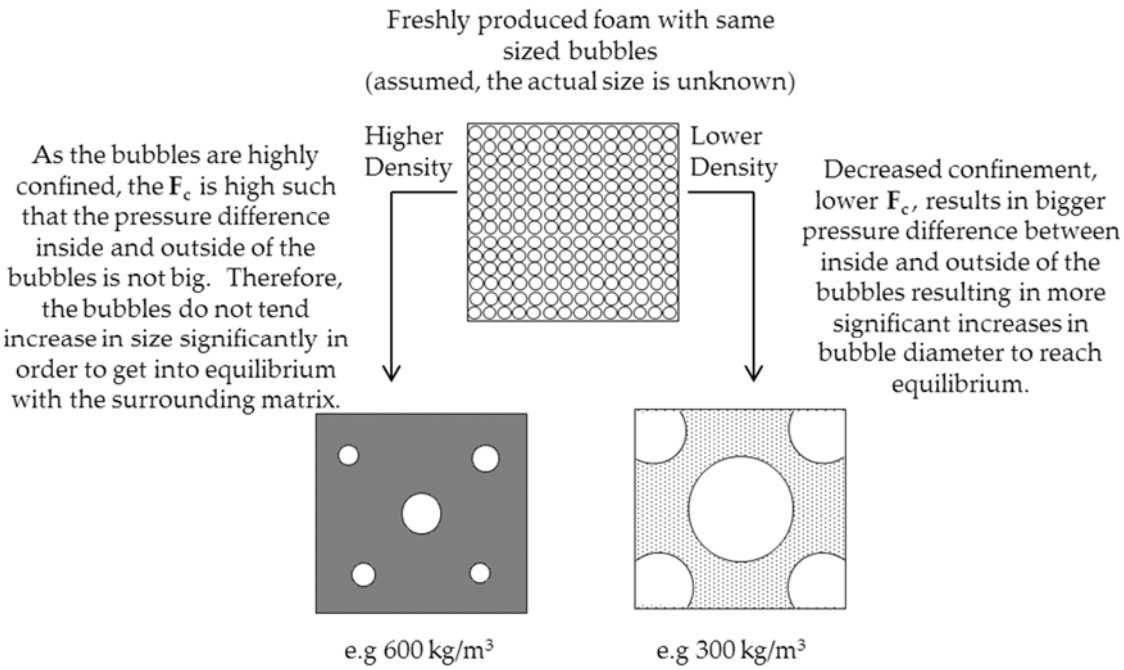

Figure 4.8 Change in the bubble size upon mixing the foam with the base mix

Although it was suggested for liquid foams that Ostwald ripening can even be stopped with the presence of particles sticking on the surface (Somasundaran, 2006), it is unlikely to happen in foamed concrete mixes, specifically at lower densities. This is because, formation of a range of bubble sizes was observed in foamed concretes that result in Laplace pressure differences driving the Ostwald ripening. It was again noted by Somasundaran (2006) that the presence of one big bubble surrounded by smaller bubbles causes the gas to diffuse rapidly into the big bubble. In that case Ostwald ripening can only be slowed down, rather than completely stopped. Therefore, it seems that the occurrence of Ostwald ripening in foamed concrete mixes is unavoidable, but its rate depends on the plastic density (i.e likely to be faster at ultra-low densities as the solids content surrounding the bubbles is lower).

As a result of the increase in bubble diameter, **Ø**, the bubble buoyancy force, $\mathbf{F_b}$, increases. However, the effect of buoyancy force is also dependent on $\mathbf{F_c}$. If $\mathbf{F_b}$ is high enough to overcome the surrounding $\mathbf{F_c}$, the bubbles rise towards the surface of the mix, displacing the surrounding solids and rupturing the surface.

Among these effective forces, the only force that is independent of others is the confinement force, $\mathbf{F_c}$ which is function of the plastic density and type of constituent materials used in the mix. As the plastic density and the type of constituents, and hence the $\mathbf{F_c}$ changes, other forces correspondingly change to maintain the equilibrium state within the mix.

Phase I - Equilibrium State (from time t=0 to t=n or t=∞)

As explained earlier, during mixing, bubbles in the mix tend to increase in diameter and change location in order to reach equilibrium. This process is a function of confinement force, $\mathbf{F_c}$, such that as the $\mathbf{F_c}$ decreases, bubble growth during mixing increases. For a very short period of time such that from the end of mixing (**t=0**) until the immediate placement of the mix, it is assumed that equilibrium is maintained. Once the mix is placed, as the liquid drainage continues (with the effect of gravity), causing the films separating the bubbles to get thinner, the equilibrium state of the mix tend to break.

Eventually, the liquid fraction (which determines if the foam is wet or dry; i.e lower the liquid fraction dryer the foam and more prone to coalescence; Stevenson, 2011) of the foam drops to a critical level at some point. The time and rate at which critical liquid fraction is reached are different for every plastic density and materials combination, as the drainage rate differs with changing medium surrounding the foam bubbles. Once the critical liquid fraction (at which film foam film rupture commences; Stevenson, 2011) is reached the bubbles tend to coalescence and increase in size due to rupture of the thinning film separating two neighbouring bubbles (Stevenson, 2011).

Besides coalescence of the bubbles due to liquid drainage, Ostwald ripening also occurs due to the presence of a range of bubble sizes resulting from mixing process and liquid drainage. As a result increase in the number of large bubbles is likely to occur. Given the increased size of these bubbles, their buoyancy, $\mathbf{F_b}$, increases as well. Consequently, they tend to rise to the surface of the mix (as previously shown in Figure 4.1) and rupture at time **t=n**, which indicates the start point of irreversible non-equilibrium state. However, this can only happen, if the total buoyancy force overcomes the confinement force of the mix ($\mathbf{F_b > F_c}$).

Therefore, when a foamed concrete mix maintains its equilibrium state from time t=0 to t=n or t=∞ (n is the time from placement of the mix until the non-equilibrium state is reached and ∞ is the time of initial set);

$$\mathbf{F_b \leq F_c}$$

This dynamic environment of bubble size and location changes exists until the mix hardens. When the mix hardens, time reaches t=∞ at when no more changes in the mix occur (i.e drainage, gas diffusion and dependent effects cease). Once the initial setting time of the mix occurs $\mathbf{F_c}$ becomes infinitely big, such that, if the mix is in an equilibrium state, it stays in equilibrium infinitely.

In high and low density (plastic densities ≥ 600 kg/m^3) foamed concretes with more paste/mortar present, as $\mathbf{F_c}$ is greater, size change and movement of the bubbles are restricted as it becomes harder to exceed $\mathbf{F_c}$, such that bubbles cannot grow in size or change location significantly. However, it must be noted that, at high and low densities, it

is the deceleration effect of $\mathbf{F_c}$ on liquid drainage and Ostwald ripening more than the magnitude of $\mathbf{F_c}$ that has a more dominant effect. Consequently, until the liquid drainage reaches critical levels or Ostwald ripening results in very large bubbles, low/high density mixes harden. Therefore, unless there is a significant change in environmental conditions disturbing the mix, such as extreme temperature changes and constituents of same surface charges, low and high density foamed concrete mixes tend to maintain the equilibrium state until they harden, yielding stable foamed concretes.

Phase II – Non-equilibrium State (from time t=n to t=∞)

Once the non-equilibrium state; ($\mathbf{F_b > F_c}$) is reached in a foamed concrete mix, it is irreversible. As the buoyancy force starts to exceed the confinement force, bubbles start to displace the surrounding solids, rise to the surface and coalesce with neighbouring bubbles. In consequence, bubbles at the surface start to rupture, leading to the loss of air volume of the mix, and hence collapse of the mix.

As mentioned earlier, in ultra-low density foamed concrete mixes, more specifically at densities below 400 kg/m^3, confinement force, $\mathbf{F_c}$, is significantly lower than at higher densities. Additionally, with reduced cement contents, the number of cement particles latching on the bubbles is reduced. This is thought to be a significant factor yielding unstable bubbles. These two main factors lead to faster drainage and, possibly, Ostwald ripening, allowing the bubbles to change size and location easily while trying to maintain the equilibrium in the mix. Therefore, the size of the bubbles, hence the buoyancy force, $\mathbf{F_b}$, increases faster compared to high density foamed concretes. Moreover, given the likelihood of larger bubbles in the ultra-lightweight mixes (as explained earlier), the spacing among bubbles is also smaller giving rise to easier coalescence of bubbles, hence shorter time to reach non-equilibrium state.

4.2.4 Summary

As mentioned earlier and demonstrated in Figure 4.7, bubbles change size during mixing, due to the pressure difference in the bubbles and surrounding environment in order to maintain the equilibrium. Moreover, high shear forces applied during mixing potentially urges the bubbles to get together and coalescence. As a result, a range of bubble sizes are is formed within the mix during the mixing process, depending on the confinement force, $\mathbf{F_c}$ which is a function of plastic density. Therefore, compared to high/low (high: above 1000kg/m^3; low: from 600 to 1000kg/m^3) densities, it is easier for the bubbles in ultra-low density mixes to expand resulting in bubbles with increased diameters. After placing the foamed concrete mixes, bubbles continue to change size as a result of liquid drainage, Ostwald ripening and coalescence.

The likelihood of coalescence due to liquid drainage in both high/low and ultra-low density foamed concretes is shown in Figure 4.9. Coalescing of bubbles occurs when two adjacent bubbles get into contact and the thin film separating the two bubbles ruptures resulting in one single bubble with a greater diameter. As seen in Figure 4.9, spacing among bubbles are bigger in high/low density mixes compared to ultra-low density mixes. On the other hand, as mentioned earlier, liquid drainage occurs at a slower rate in foams with smaller bubbles. Therefore, combining the spacing factor, liquid drainage rate and the magnitude of confinement force, that is considerably bigger in high/low densities, it is less likely for bubbles in high density mixes to overcome the confinement forces and coalescence, while it seems to happen readily at ultra-low densities.

Figure 4.10 demonstrates Ostwald ripening which occurs after placing the mix (as well as liquid drainage that is not shown in the schematics) and the onset of instability (non-equilibrium state). Due to the more uniform bubble size and the big bubble spacing of higher density mixes (Nambiar and Ramamurthy, 2007a) resulting from greater $\mathbf{F_c}$, it is likely that gas diffusion occurs at a slower rate at higher densities compared to lower densities.

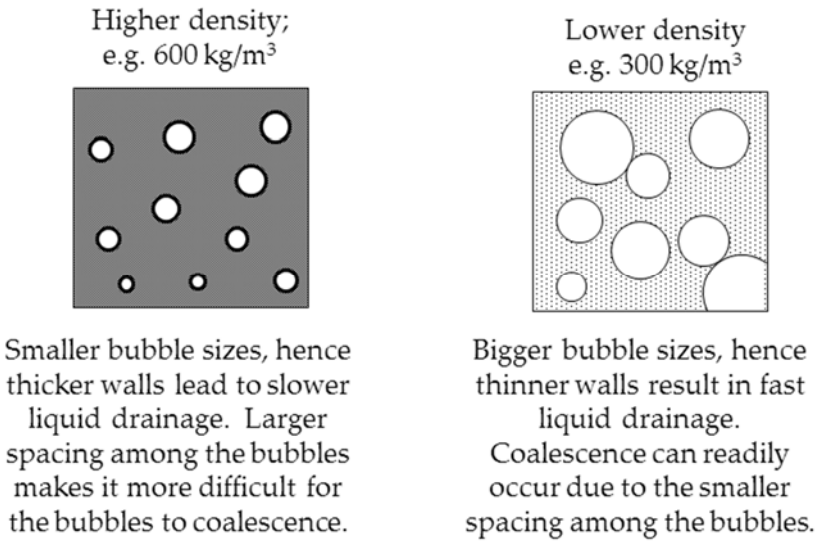

Figure 4.9 Likelihood of coalescence of bubbles due to liquid drainage

While the gas diffusion continues to occur in high/low density mixes, the process reaches an end in ultra-low density mixes, leaving a dynamic environment behind with the presence of bubbles having increased diameters and buoyancy, $\mathbf{F_b}$. Therefore, the likelihood of bubble coalescence greatly increases by the promoting environment of big bubbles with decreased spacing. Bubbles, then, start to rise towards the surface once the buoyancy force, $\mathbf{F_b}$, overcomes the confinement force, $\mathbf{F_c}$. The bubbles at the surface tend to rupture causing loss of the air phase of the mix. Eventually, loss of air from the mix through rupturing bubbles causes total collapse of the ultra-low density mix leaving the solid phase with fewer bubbles settled at the base.

At this point, it is not known whether the gas diffusion process is completed or still ongoing in high/low density mixes, when ultra-low density mixes collapse. It must be noted that, even if the gas diffusion is completed, yielding bubbles with bigger diameters compared to the ones at time t=0, it is unlikely for the resulting bubbles to have $\mathbf{F_b}$ that can overcome the $\mathbf{F_c}$ in the case of high/low densities. As a result, unlike ultra-low density mixes, high/low density mixes were observed to have bubbles with smaller diameter when hardened.

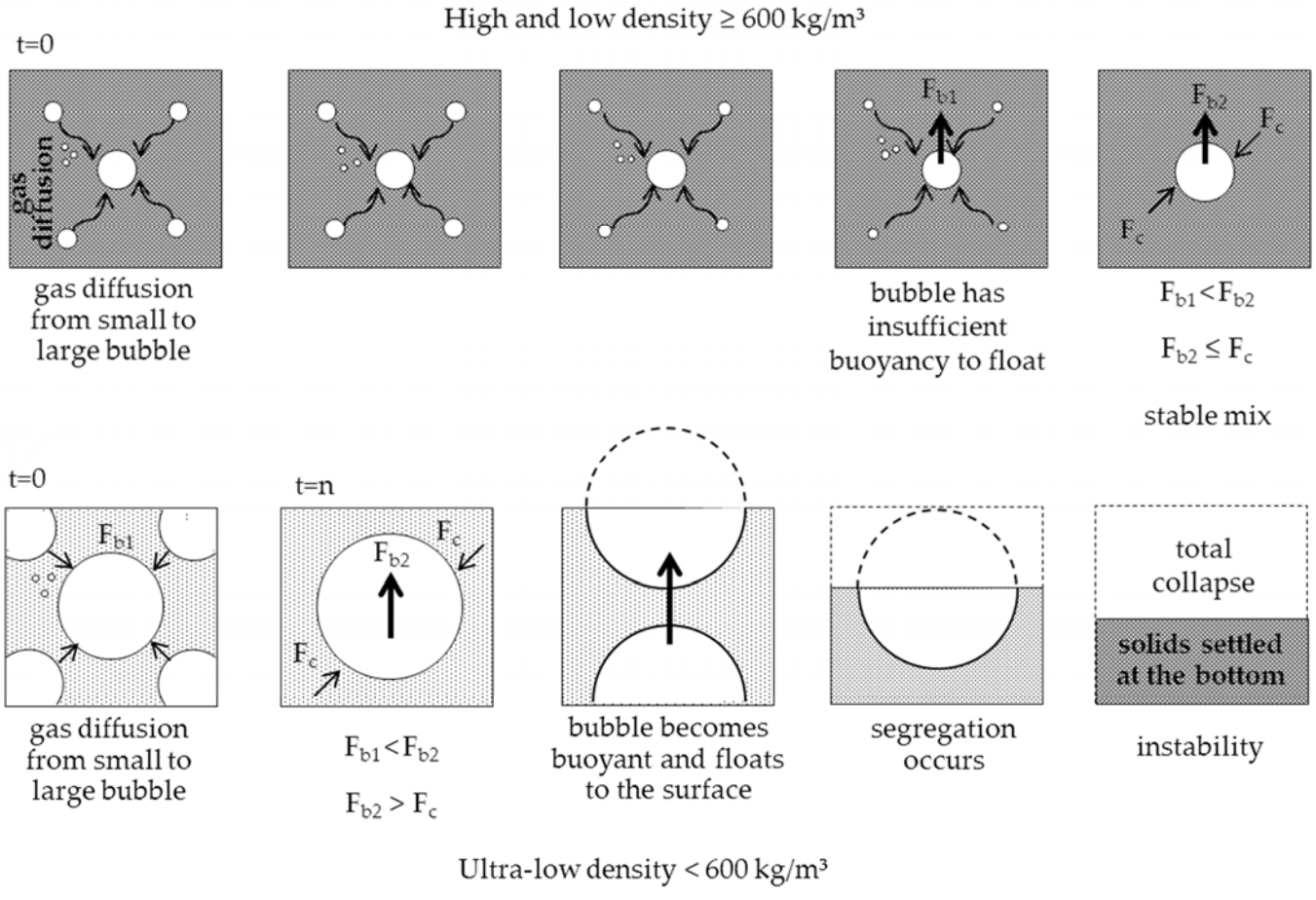

Figure 4.10 Schematic of inter-bubble gas diffusion and onset of non-equilibrium state (instability) in high/low and ultra-low density foamed concrete mixes

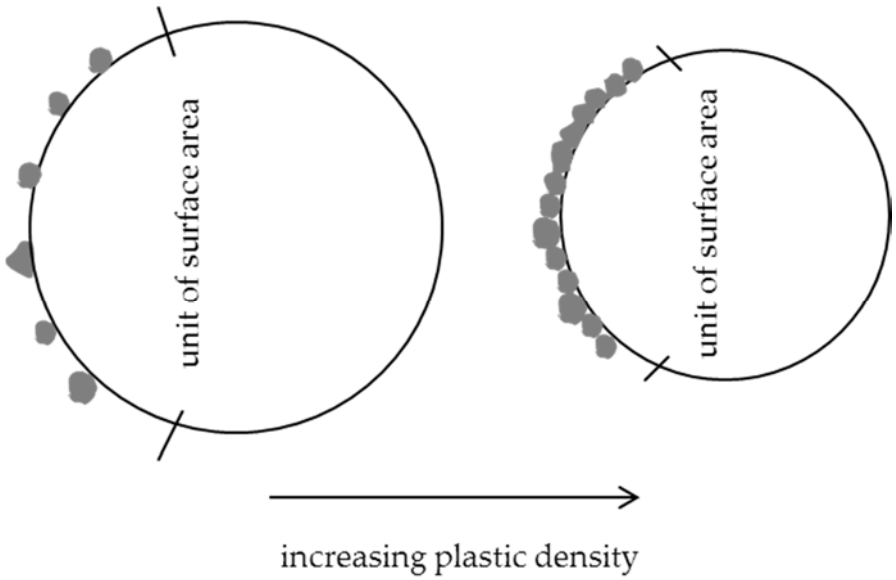

Figure 4.11 Influence of cement content on bubble stability

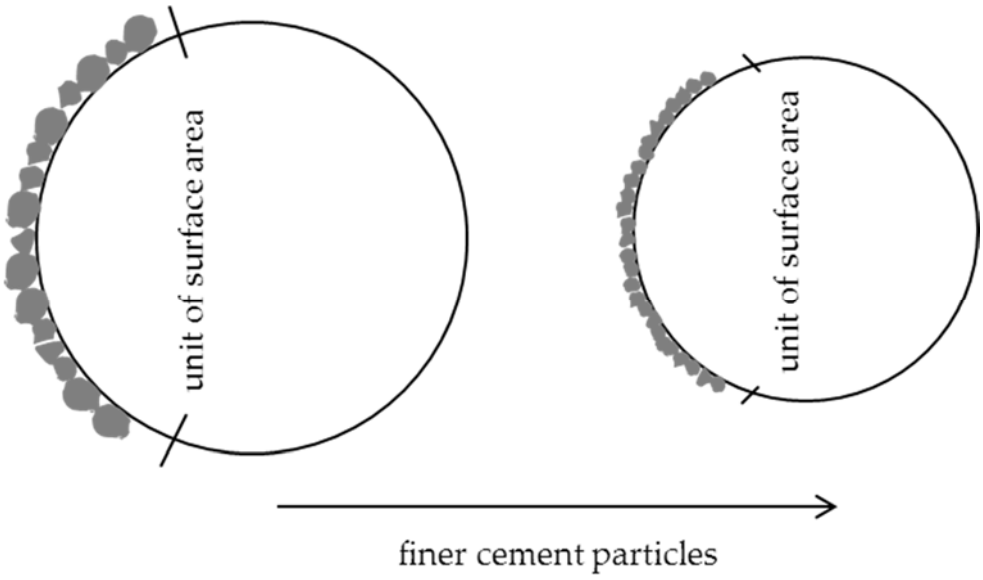

Figure 4.12 Influence of cement fineness on bubble stability

In addition to the hypotheses explained, more specifically the effect of a greater number of cement particles latching on to the bubble surface at higher cement contents resulted in smaller and more stable bubbles (Figure 4.11). Using finer cementitious materials at given cement contents, both at higher and lower densities, is likely to provide a similar effect on bubble stability (Figure 4.12). This is achieved by the 'closer packing' and presence of higher number of cement particles around the bubbles at a given cement content. Therefore, as in high cement content cases, utilisation of finer materials is also expected to decelerate the liquid drainage delaying the time to reach **t=n**, in other words onset of instability.

4.3 THE SOLUTION: LIQUID TO SOLID TRANSITION TIME

Over a specific period of time, the interaction of foam bubbles and forces within the mix results in failures in ultra-low density foamed concretes, specifically below 400 kg/m^3. While, the self-weight of foamed concrete is carried by the bubbles, the mix will be stable. However, the bubbles can only remain stable for a specific period of time depending on the environment that they are in. Over time, liquid drainage and gas diffusion result in coalescence of bubbles. Consequently, bubble diameters increase and the bubbles rise to the surface and rupture. This defines the period of stability and the onset of instability in foamed concrete.

However, at some point, the initial set of the mix will occur and the liquid foamed concrete becomes plastic and then hardens to solid. Once the initial setting occurs, bubbles stop changing size and location. Thus, there is a critical time before t=n, for any mix at which the initial set must occur or the mix will inevitably become unstable. Accordingly, a hypothesis was constructed for solving the instability issues. Therefore, by controlling the liquid to solid transition rate of an ultra-low density foamed concrete mix, failures upon instabilities will be prevented.

In order to achieve faster setting times, according to previous research done at the University of Dundee (Mohammad, 2011), neither adding accelerating set control admixtures (e.g calcium chloride which is considered the most effective for foamed

concrete; Dransfield, 2001) as this was known to cause mix instability (Jones and McCarthy, 2005b; 2006; Mohammad, 2011), nor adjusting temperatures (increasing the temperature of both environment and constituents to promote setting) were considered. Therefore, the need for utilisation of a fast-setting cement type was proposed to shorten the setting times, thus preventing the bubbles from changing size to an extent to cause instability.

Utilisation of Portland cement has been proven to work successfully with high/low density foamed concretes, yielding stable mixes consistently. However, as previously shown in Figure 4.10, onset of instability in ultra-low density mixes occurs much faster than in high/low density mixes. Therefore, the initial setting time provided by Portland cement was not considered fast enough to occur before t=n is reached, producing stable mixes at ultra-low density levels. For this reason, there was a need for fast setting cement, or combinations of cements that would provide initial setting times faster than PC (which is specified to have initial setting time of ≥ 45-75 minutes; BS EN 197-1:2011) to harden the mix before the t=n is reached. Furthermore, as the severity and the rate of collapse increases with decreasing density, a range of initial setting times were sought, to produce a range of stable ultra-low density mixes.

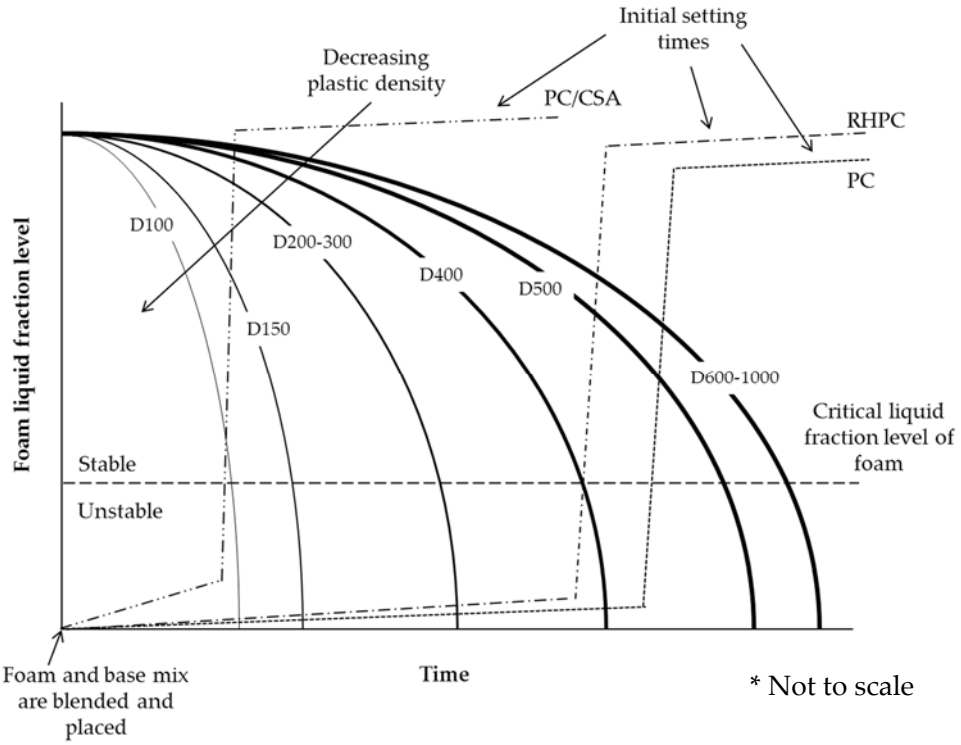

Figure 4.13 Schematic of hypothetical relationship of initial setting time to stability (based on observations)

As a result, calcium sulfoaluminate (CSA) cement, known with its rapid setting properties (BRE, 2007; Glasser and Zhang, 2001; Ioannou et. al, 2014), was proposed for producing stable ultra-low density mixes. Commercially available CSA cement compatible with PC, was chosen in order to provide adjustable initial setting times when blended with PC at various levels. Figure 4.13 demonstrates the hypothetical effect of different cement types/combinations on mix stability based on observations.

Accordingly, the lower the plastic density, the faster the liquid drainage, hence faster the onset of instability (t=n) will be reached. Therefore, as density decreases, initial setting time must occur faster, before the critical liquid fraction level of foam is reached in order to prevent the onset of instability.

4.4 CONCLUSIONS

The Chapter explained the underlying mechanism of foamed concrete instability. Therefore, the primary factor influencing the mix stability is the plastic density of the mix, such that as the plastic density decreases, mixes become more prone to instability. In ultra-low density mixes (< 600 kg/m^3) where no filler (sand) is used and cement contents are significantly reduced, the risk of instability is higher. Another factor affecting the mix stability is the bubble size which is proportional to the plastic density, such that the lower the plastic density the larger the bubble size, hence the more prone the mix to instability. However, bubble size as well as cement fineness have a secondary effect on mix stability.

Dynamic processes occurring in fresh foamed concrete densities such as liquid drainage, gas diffusion and bubble coalescence which directly affect the bubble size hence mix stability continues until the non-equilibrium state (onset of instability) is reached or until the initial setting occurs. Compared to high/low densities, these processes occur at a fast rate in ultra-low density mixes causing instability prior to hardening of the mix. Therefore, in order to produce stable ultra-low density foamed concretes, transition time of the mix from liquid to solid must be reduced.

As the initial setting time of Portland cement does not occur before the onset of instability in ultra-low density mixes, a fast-setting cement must be used to produce these mixes and initial setting times must be reduced with decreasing density. As a result, CSA cement compatible with PC was employed in this case to provide a range of fast initial setting times when used in combination with PC. Figure 4.14 illustrates the outcome of this Chapter.

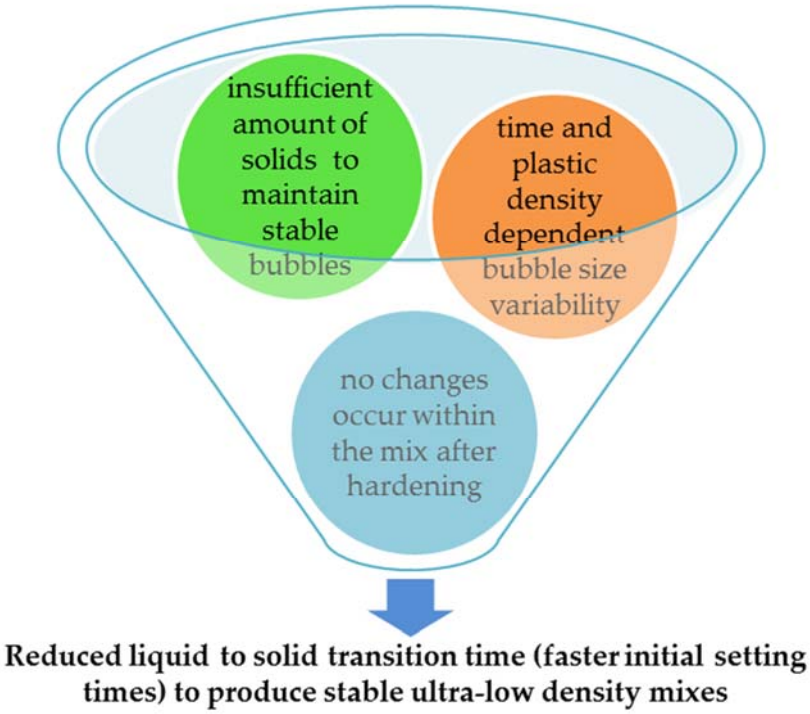

Figure 4.14 Outcome of the hypotheses on mix stability and the solution to produce stable ultra-low density foamed concretes

CHAPTER 5

5. OVERCOMING THE ISSUES OF MIX STABILITY

5.1 INTRODUCTION

Following the series of observations, hypotheses and the proposed solution for foamed concrete (FC) stability presented in Chapter 4, experiments were carried out on a range of materials. The experimental work covered in this Chapter comprises stability measurements, initial setting time of base mixes, collapse times of unstable mixes produced with PC, bubble size and microstructure analysis. Plastic densities ranging from 100 kg/m^3 to 500 kg/m^3 (from D100 to D500) were considered for this phase of the study.

A preliminary investigation was carried out in order to test the proposed solution with a range of materials and select the ones for the main study. In total, three Portland cements (PC) and two different calcium sulfoaluminate (CSA) cements were considered in FC mixes. Accordingly, one PC and one CSA cement was selected for the main study based on the performance, availability and cost of the materials.

Results are presented in two sections, as the main study and the alternative materials. The main study presents the data obtained from the materials analysed in the preliminary phase and selected to be employed for further analysis whereas, the preliminary study presents the data obtained from the materials that were only used at this initial phase of experimental work. Only the PC selected for the main study was presented in both sections, as the CSA (CSA_P) as an alternative material was used in combination with this PC. Materials reported in the alternative materials section can also be utilised for producing stable ultra-low density foamed concretes and concerns about these were also reported in this section.

5.2 MAIN STUDY

The main study provides performance data of the materials used throughout the study for producing stable ultra-low density foamed concretes. The chemical and physical properties of the cements used in the main study were reported earlier in Table 3.1, while the mix constituent proportions were given in Table 3.2.

5.2.1 Stability and initial setting times

Initially, densities 500 kg/m³ and below were produced with 100% PC and only the foamed concretes with densities above 300 kg/m³ consistently produced stable mixes. This indicated that, time t=n, onset of instability (as discussed in Chapter 4), was reached before the initial setting occurred at foamed concrete densities below 400 kg/m³ leading to failures. Figure 5.1 provides a schematic illustration of mix collapse due to instability where the base mix and air volume become increasingly more segregated, until the air portion is lost and the solids are left settled at the bottom. Cylinder height of 500 mm indicates the height of the cylinders used for drop in level test described in Section 3.6.1.

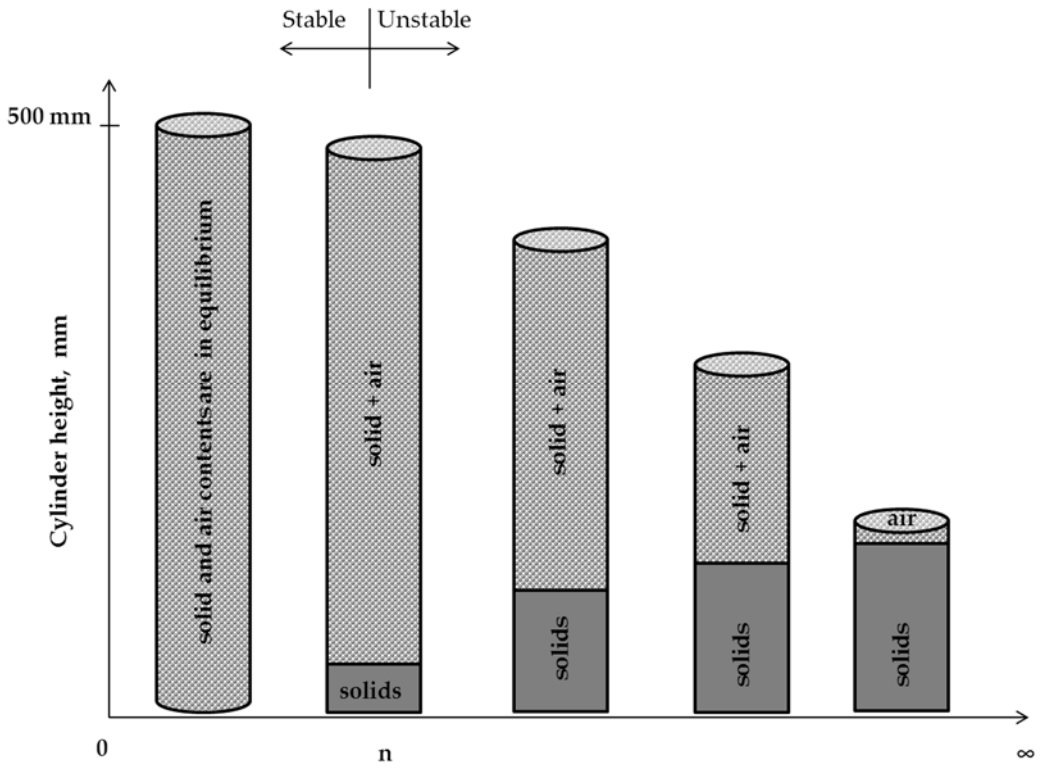

Figure 5.1 Schematic illustration of stages of collapse due to mix instability

On the other hand, Figure 5.2-a illustrates the increasing tendency of instability with decreasing plastic density which supports Figure 4.3 shown in Chapter 4. As the plastic density decreases, foam content (air volume) increases, making the mixes more prone to collapse as there are not enough solids to fully surround the bubbles and maintain their stability in the mix by slowing down the rate of drainage.

As seen in Figure 5.2-a, D300 mix exhibited a slight reduction in height, whilst the drop in level in D200 and D150 mixes were almost by two third of the full height. Although the drop in level seemed negligible in D300 mix on a 500mm tall specimen, in large scale or deeper pours this may be more severe. Therefore, plastic densities below 400 kg/m³ were deemed problematic for achieving stability and therefore selected for further investigation.

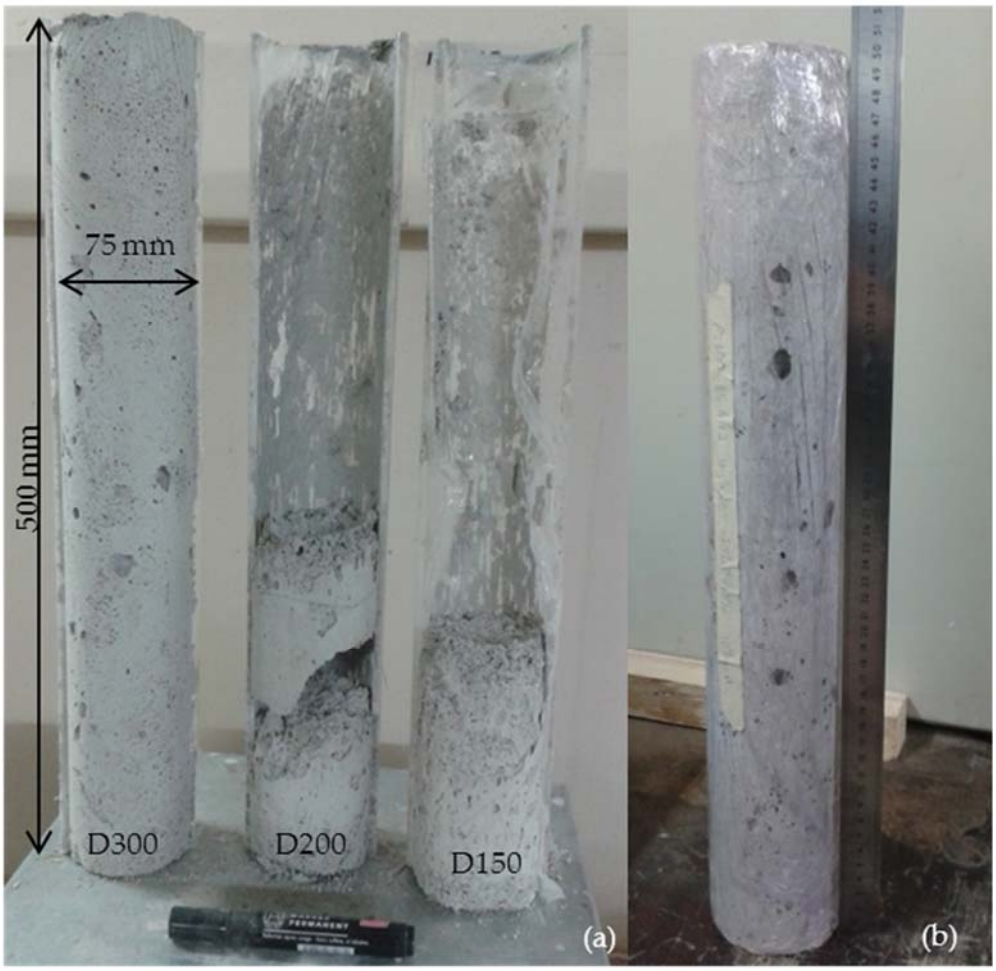

Figure 5.2 (a) Increasing severity of collapse with decreasing plastic density of PC concretes; (b) stable PC/CSA 200 kg/m³ mix

Initially, some trial mixes were produced by incorporating rapid setting CSA cement in the mixes partially replacing PC in order to achieve stable mixes. To start with, 5% of PC (by mass) was replaced with CSA cement, yielding stable mixes of 300 and 200 kg/m³ plastic densities (see Figure 5.2-b). However, the initial setting time achieved by 5% CSA addition was not rapid enough to yield stable foamed concretes with densities below 200 kg/m³. Therefore, CSA addition level was increased to 10%, which yielded stable 150 kg/m³ density mixes.

For the production of foamed concretes with plastic densities below 150 kg/m³, it was necessary to utilise CSA content beyond 10% by mass. However, utilisation of CSA at levels greater than 10% was found to result in ultra-rapid setting times such that the base mix started to harden during mixing. As there was not enough time to produce a homogeneous base mix, add the freshly produced foam and place the foamed concrete, CSA addition levels greater than 10% (by mass) were not considered for the given CSA cement type. Table 5.1 summarises the stability and initial setting times data obtained for different cement combinations at a range of densities.

Initial setting times of the base mixes were determined for each cement combination and the stability of the mixes produced with these combinations was measured. As mentioned earlier in Chapter 3, determination of initial setting times was carried out on base mixes as it would be easier to control the initial setting times of the base mixes than foamed concrete mixes during the production.

Table 5.1 Base mix initial setting times and stability

Cement type (% by mass)		Base mix initial setting time (hh:mm)	Stable (✓) / Unstable (x)			
PC	CSA		D150	D200	D300	>D300
100	-	03:25	x	x	x	✓
95	5	01:30	x	✓/x	✓	✓
90	10	00:20	✓	✓	✓	✓

Note: ✓ stands for mixes resulted in stable foamed concretes at a rate of 100%. ✓/x is used even if the rate of achieving stable mixes is 99%.

The addition of 5% CSA resulted in 56% reduction in the initial setting time, whilst the 10% CSA base mix was 10 times shorter than the 100% PC reference. The data therefore suggests that decreasing the initial setting times through the utilisation of 10% CSA (by mass) resulted in stable ultra-low density foamed concrete mixes down to 150 kg/m³. Moreover, the data shows that the lower the plastic density, the shorter the initial setting time should be for achieving stable mixes.

5.2.2 Collapse times

Following the production of stable ultra-low density mixes by blending PC and CSA, time of collapse of unstable mixes produced with 100% PC were determined for corresponding foamed concrete densities, in order to prove the relationship between the collapse and initial setting times. It must be noted that, as the base mixes (without foam) were used for determining the initial setting times, it is likely that reported initial setting times may increase upon incorporation of foam (due to the extra water resulting from the liquid drainage of the foam). Therefore, this should be considered while comparing the initial setting and collapse times.

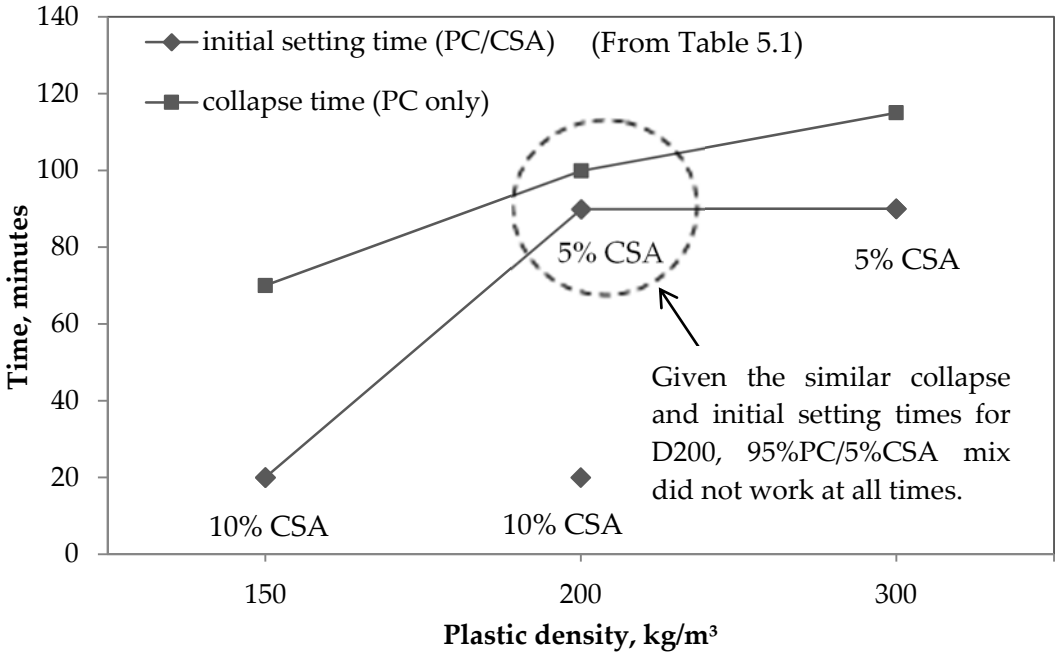

Figure 5.3 Comparison of collapse times of PC only mixes and base mix initial setting times of stable mixes for corresponding foamed concrete densities

Figure 5.3 shows the relationship between collapse times and initial setting times (from Table 5.1) of foamed concrete densities from 150 to 300 kg/m³. Clearly, initial setting times of the base mixes of stable mixes were shorter than the collapse times of corresponding mixes that were produced with 100% PC, indicating that mixes hardened before any collapse occurred, thus yielding stable mixes. It must be noted that collapse time is not equal to the time t=n (mentioned in Section 4.2.3) as the collapse does not occur instantly once the time t=n is reached. Therefore, time t=n for a specific mix is reached earlier than the collapse time.

5.2.3 Bubble size analysis

The influence of plastic density on bubble size was discussed in Section 4.2.2. Indeed, decreasing plastic density results in larger average bubble size (Mohammed, 2011) and median bubble size (Nambiar and Ramamurthy, 2007), thus increasing the tendency for instabilities (it was reported by Dransfield, 2000; McGovern, 2000; Brady et. al, 2001 that smaller bubbles are more stable). Therefore the bubble sizes of ultra-low density foamed concretes were evaluated.

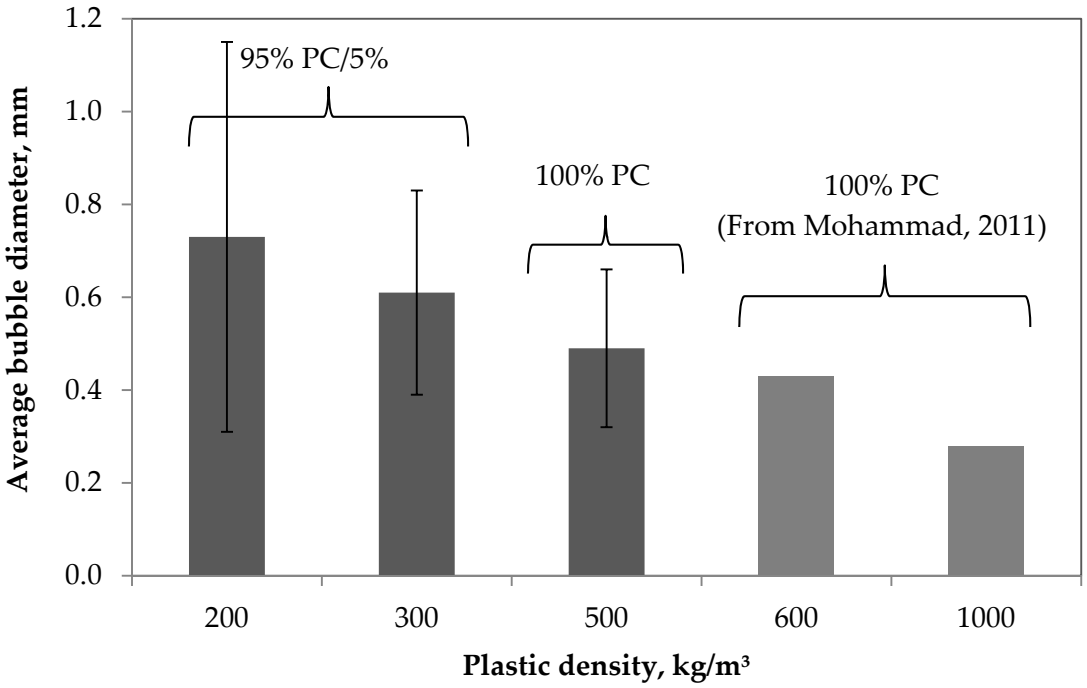

Figure 5.4 Influence of plastic density on the average bubble diameter

2D bubble size analysis was carried out on 200, 300 and 500 kg/m^3 densities as described in Section 3.6.2. D500 (produced with 100% PC) was chosen as a reference for bubble analysis to assess the elimination of sand on the bubble size and provide a transition from low to ultra-low densities. Additionally, bubble size data for 600 and 1000 kg/m^3 densities (produced with 100% PC and sand) obtained from Mohammad (2011) is also presented. It must be noted, while splitting the 150 kg/m^3 density specimens they were fractured into pieces, therefore it was not possible to carry out bubble analysis at this foamed concrete density. Figure 5.4 illustrates the bubble size analysis in terms of average bubble diameter for the foamed concrete densities considered.

As expected from the observations made by Mohammad (2011) and the hypotheses explained in Chapter 4, the average bubble diameter increased with decreasing plastic density. It was found that average bubble diameter increased up to around 2.5 times in ultra-low density foamed concretes when compared to high/low densities. This behaviour is attributed to the reduction in cement content as well as the elimination of sand at ultra-low densities. Although the cement content is higher in D500 than D600 (in order increase the 'fines' content as explained in Section 3.4), average bubble diameter of D500 was bigger due to the elimination of sand, hence the reduction in the confinement force ($\mathbf{F}_c$).

Given the faster initial setting time provided by 95% PC/5% CSA combination, the increase in average bubble diameter was stopped before it reaches to a critical level causing instability related failures. Therefore, it must be noted that the average bubble diameters obtained for D200 and D300 foamed concretes that were produced by 95% PC/5% CSA blend are likely to be smaller than a potential 100% PC mix.

As stated earlier, increased air (foam) content is a critical factor on stability of foamed concrete. This statement was supported with the 2D bubble analysis. Figure 5.5 shows the calculated bubble to solid area ratio obtained from 2D bubble analysis. Considering the increase in the bubble sizes within the fresh mix, this ratio is valid for the state of bubbles at the time of hardening (i.e in fresh state, the ratio is possibly smaller). Therefore, if 100% PC mixes were considered, the ratio would be higher as a result of the longer setting times allowing more time for bubble growth.

As the plastic density decreased, the ratio increased indicating the increased air content. At D300 where severe instability issues were observed in the case of PC, bubble to solid area ratio of 5% CSA mix was found to be almost 1. This may imply that at 300 kg/m³ density the bubbles and the solids try to dominate over each other within the mix, more likely causing instabilities. Moreover, at densities below 300 kg/m³, it is likely that the bubbles exhibit a dominant behaviour affecting the stability state of the mix and leading to instability more readily.

It must be noted that stable 100% PC, 300 kg/m³ mixes were observed occasionally in the laboratory conditions. This can be explained by the equal bubble and solid area observed, hence the $\mathbf{F_b}$ (buoyancy force of the bubbles) and $\mathbf{F_c}$ (confinement force applied by the solids) within the mix trying to overcome each other. Therefore, D300 was accepted as the critical density at which stability issues are observed clearly.

On the other hand, as the bubble analysis was carried out based on the 2D images, the values obtained are possibly smaller than the real bubble sizes. This is because during the specimen preparation, the bubbles may not be cut exactly through their centres hence the bubbles on the testing surface may not represent the real diameter. For this reason, the data was compared (see Figure 5.6) with the 3D bubble analysis (by X-ray computerised tomography) reported by Wei et. al (2014) to assess the efficiency of 2D bubble analysis.

However, it must be noted that for the given plastic densities, mixes reported in Wei et. al (2014) had higher cement contents of the were higher, no fine aggregates and lower w/c ratio of 0.35 in comparison to the current study. Moreover, for 3D analysis the data there was no data available for D200 and D600 mixes.

Average bubble diameters obtained from the 3D bubble analysis were bigger than the ones obtained from 2D analysis except 1000 kg/m³ density. The 2D average bubble diameter values were 36% and 30% lower than the 3D values for densities 300 and 500 kg/m³ respectively whilst it was 62% higher for 1000 kg/m³ density. Compared to D300 and D500 mixes, the biggest difference in the mixes for 2D and 3D analysis in terms of cement and sand content were at 1000 kg/m³, which seemed to exhibit a dominant effect on the average bubble diameter of D1000.

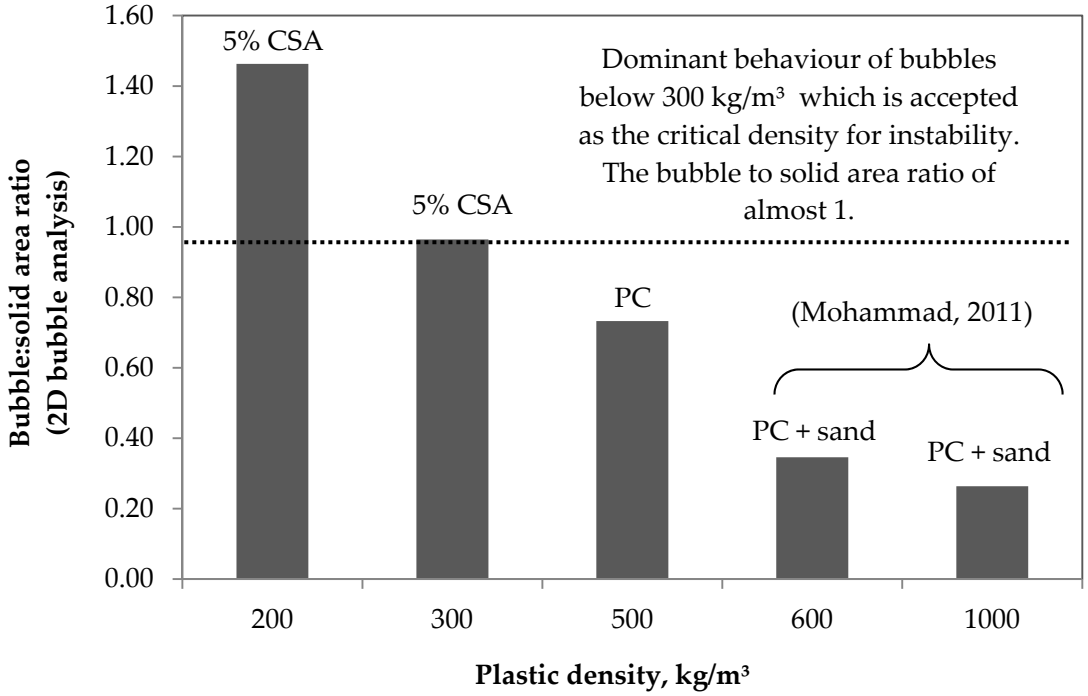

Figure 5.5 Relationship between bubble to solid area ratio (from 2D analysis) and stability

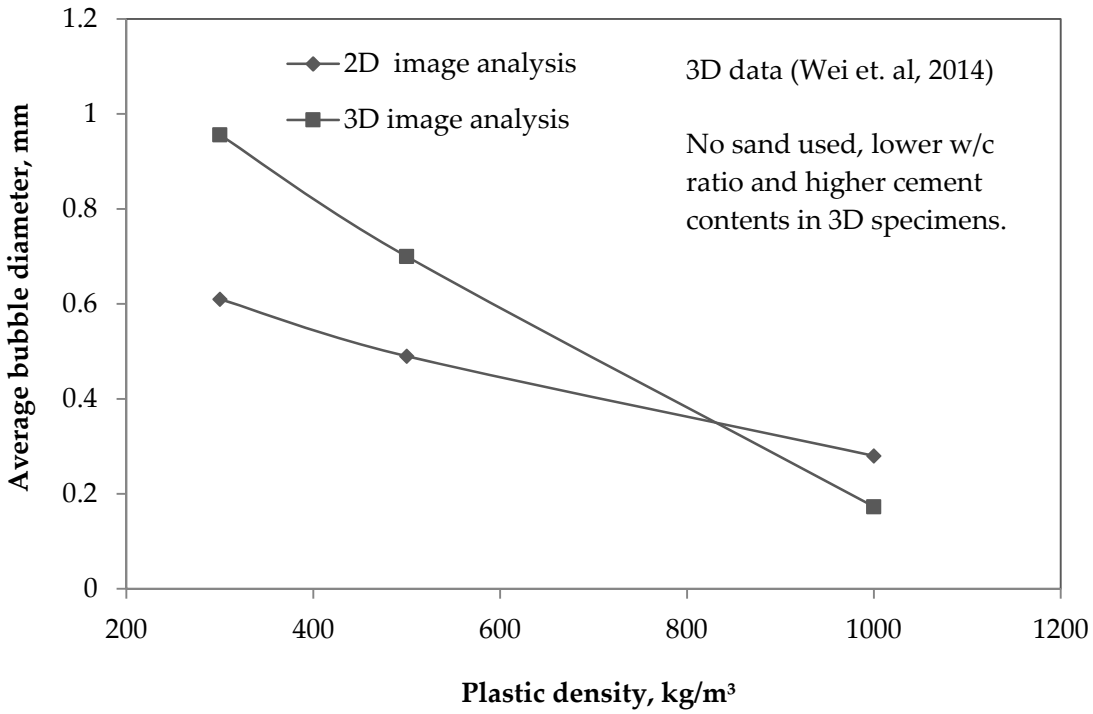

Figure 5.6 Comparison of 2D and 3D bubble analysis

As a result, 3D analysis yielded smaller average bubble diameter than expected. This behaviour can possibly be linked to very high cement content of D1000 mix in 3D analysis, that possibly provides enhanced particle packing and increased confinement force ($\mathbf{F}_c$) around the bubbles, preventing them from increasing in size. Moreover, absence of sand along with very high cement content in D1000 may also have an influence on lower bubble size reported in 3D analysis due to the presence of finer particles surrounding the bubbles.

It was difficult to draw any conclusions or relationships from the comparison made between 2D and 3D bubble analysis, as the foamed concretes used for the analyses had different constituents and mix proportions which were reported to have an influence on bubble size (Mohammad, 2011). Although, further analyses and comparison are required to draw solid conclusions, it can be said that 2D analysis generally underestimates the bubble sizes.

5.2.4 Microstructure

In order to distinguish the differences between high/low and ultra-low density foamed concretes, comparative microstructure analysis was also carried out on scanning electron microscopy (SEM) images at 28 days age. Foamed concretes with densities ranging from 150 to 1000 kg/m^3 were presented for a visual comparison. Figure 5.7 shows the changes in microstructure with decreasing plastic density.

As expected, foamed concrete (FC) microstructure was less dense with decreasing plastic density with holes forming in the bubbles, creating partially open cells. The holes in the bubbles are thought to appear as a result of the reduced cement contents in ultra-low density mixes (similar microstructure was also observed by Yakovlev et. al, 2006). Firstly, as there was no enough cement particles to fully cover the bubbles, the thin film at the uncovered parts of the bubble 'pop' leaving a hole as the hardening and drying occur. Secondly, due to the reduced cement contents, drainage occurs at a higher rate hence adjacent bubbles get in contact for coalescence quickly. Then, once the hardening or the initiation of coalescence followed by hardening occurs, the thin film separating the two bubbles possibly tears forming a hole.

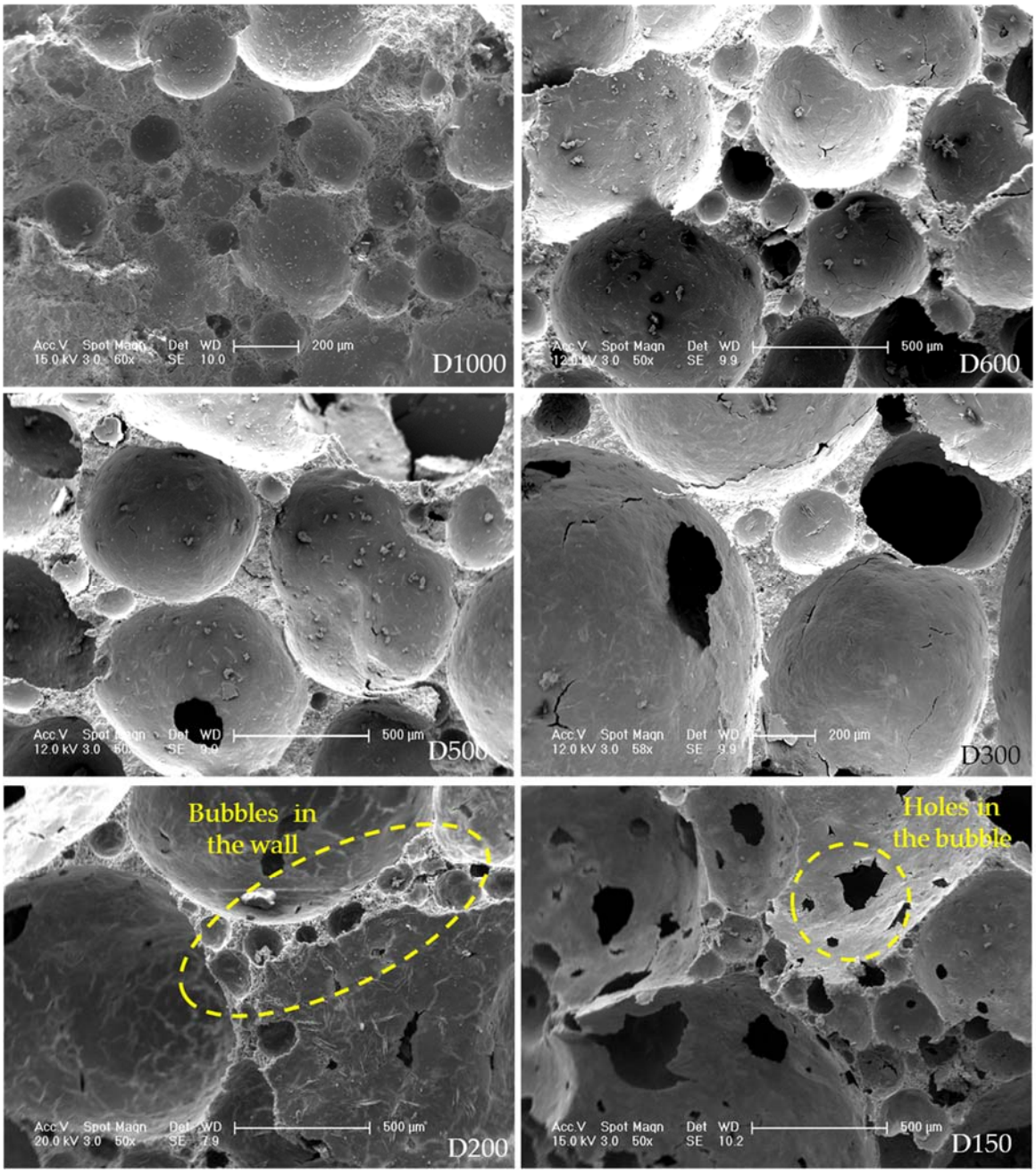

Figure 5.7 Influence of plastic density on the microstructure of FCs (100%PC for D1000-D500; 95%PC/5% CSA for D200, D300; 90%PC/10% CSA for D150)

Furthermore, the holes in the bubbles may also be formed by drying shrinkage strains which resulted in fractures like 'egg-shell' as well as cracks while some of the cracks and the holes may be formed mechanically during the preparation of the specimens for the SEM imaging. It is inferred that these holes form as a result of the gas diffusion where gas diffuses out through these opening.

On the other hand, smaller bubbles in the walls of bigger bubbles started to appear and increase in number with decreasing plastic density. This may be the sign of occurrence of Ostwald ripening in which the gas inside the smaller bubbles diffuses out towards the bigger bubbles, then into the bigger bubbles. Big bubbles surrounded by smaller bubbles result in faster rate of gas diffusion (Somasundaran, 2006) and therefore, the observed microstructure in the ULFCs supports the assumed behaviour in Chapter 4. Moreover, these bubbles in the walls may be due to entrapped air. It is likely that as the self-weight of the mix decreases significantly at ultra-low densities, self-compaction ability of foamed concrete may reduce leading to formation of entrapped air bubbles. Furthermore, supporting the bubble size data (in Figure 5.4), it was visually observed that the bubbles increase in size and the thickness of the bubble walls decrease as density decreases.

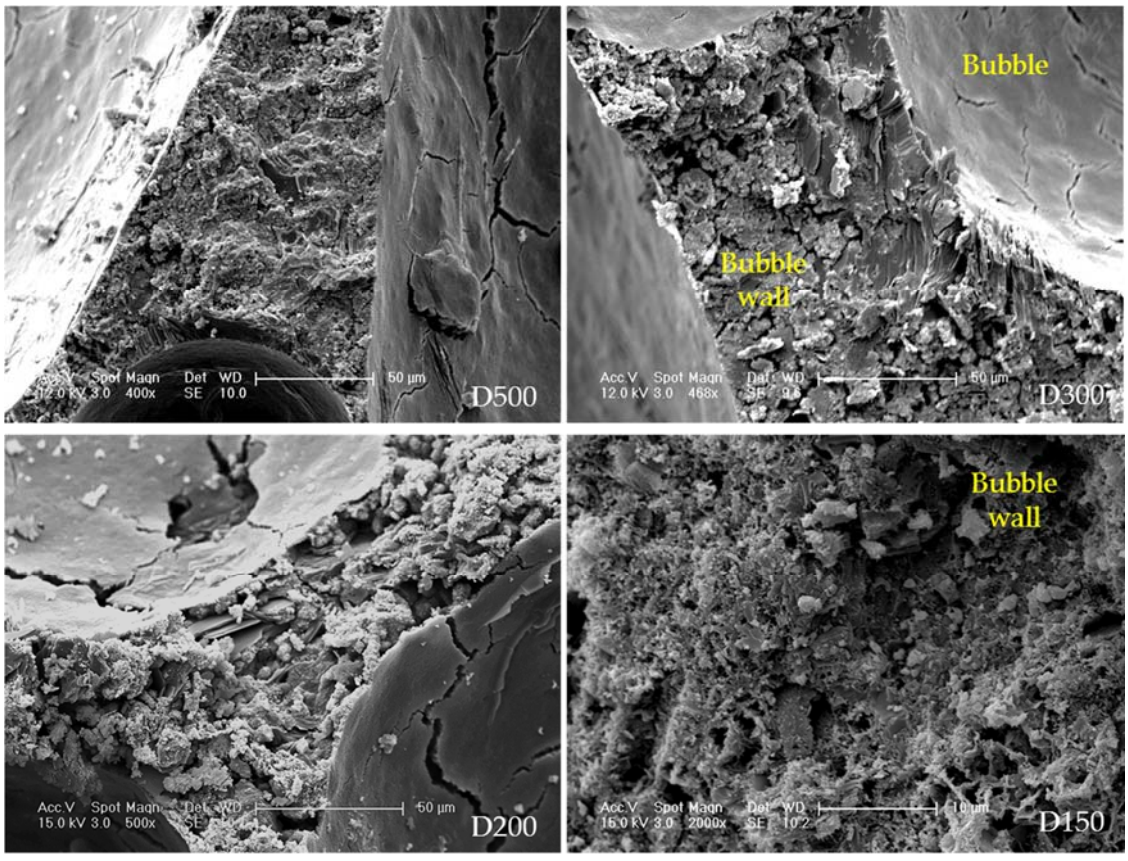

Figure 5.8 Influence of plastic density on the microstructure of bubble walls

Figure 5.8 illustrates how the microstructure of the bubble walls changes as the plastic density decreases. Therefore, at ultra-low density levels down to 300 kg/m^3 the bubble wall structure was observed to be highly dense. Below 300 kg/m^3 density, in D200 and D150 foamed concretes, significant reduction in the bubble wall density was observed due to the ultra-low cement contents (as low as 133 and 100 kg/m^3 respectively). It is seen in Figure 5.8 that bubble walls of D200 and D150 mixes are composed of more porous microstructure and reduced amount of hydration products.

5.3 USE OF ALTERNATIVE MATERIALS

The materials presented in this section were not employed for the main study, but they could be used as alternative materials for achieving stable, ultra-low density foamed concretes. Therefore, the performance of these materials was presented in order to provide a comparison among the alternative materials.

While PC and CSA_P were used in combination, PC2 (buxton lime) and MF which is a specialist type of PC, were used on their own. CSA_P was incorporated at levels up to 50% by mass of cement. Water to cement (w/c) ratio was fixed to 0.50 for all mixes whereas, PC2 mixes were produced with 0.45 w/c ratio (as recommended by colleagues from the industry). Properties of these materials were given in Table 3.1.

As in the main study section, the alternative materials tested were also assessed for their effectivity in producing stable ultra-low density mixes. Therefore, initial setting times in relation to stability and collapse times were presented. Moreover, bubble size and the microstructure of foamed concretes produced with the alternative materials were analysed to evaluate the influence of these materials on the given parameters.

The mix constituents proportions used for the alternative materials were given in Table 3.3. As stable foamed concretes down to 100 kg/m^3 could be produced in the preliminary phase, mix proportions for plastic densities ranging from 300 down to 100 kg/m^3 were shown. It must be noted that, only the mix proportions of the stable mixes were given.

5.3.1 Stability and initial setting times

The alternative materials tested also yielded stable foamed concretes with a range of ultra-low densities. Table 5.2 summarises the alternative materials and their performance on achieving stable ultra-low density mixes in relation to base mix initial setting time. Therefore, besides the PC/CSA combinations reported in the previous section, other materials can also be employed for producing stable ultra-low density foamed concretes.

Unlike PC, both PC2 and MF (on their own) yielded stable ultra-low density foamed concretes down to densities 200 and 150 kg/m^3 respectively. Given its higher fineness, MF yielded very rapid initial setting time. As a result, owing to high fineness and fast initial setting time in combination, it produced stable ultra-low density mixes down to 150 kg/m^3.

Table 5.2 Base mix initial setting times and stability

Plastic density (kg/m^3)					**100**	**150**	**200**	**300**
Cement proportions (%)				**Base mix initial setting time (hh:mm)**	**Stable (✓) / Unstable (x)**			
PC	**PC2**	**MF**	**CSA$_P$**					
100	-	-	-	05:00	x	x	x	x
-	100*	-	-	04:35	x	x	✓	✓
-	-	100	-	00:20	x	✓	✓	✓
95	-	-	5	04:00	x	x	x	✓
90	-	-	10	02:45	x	x	x	✓
80	-	-	20	00:30	x	x	✓	✓
60	-	-	40	00:30	x	✓	✓	✓
50	-	-	50	00:20	✓	✓	✓	✓

* w/c ratio of 0.45 was used for 100% PC2 mix, while 0.50 was used for the rest of the mixes. ✓ is used for mixes resulting in stable foamed concretes at a rate of 100%.

On the other hand, PC2 which is coarser than PC and exhibited similar initial setting times with PC (as well as longer initial setting times than collapse times of the ULFC mixes shown in Figure 5.9) yielded stable mixes down to 200 kg/m^3 density. Although the w/c ratio used for PC2 mix was 0.45 (while it was 0.50 for all other mixes), this did not have a dominant effect on stability as PC did not yield stable mixes with 0.45 w/c ratio either (observed during the initial trials). While it remains unclear how PC2 yielded stable ultra-low density mixes, experience of its trial application in industry was reported to be successful. However, given the lack of understanding on its underlying mechanism (possibly an additional chemical during its production), it is risky to utilise this material in ultra-low density mixes without further research.

On the other hand, CSA_P was combined with the PC to produce base mixes with a range of initial setting times. CSA_P contents from 5% to 50% by mass were utilised to produce stable mixes with densities down to 100 kg/m^3. As CSA cements can be very diverse, in terms of composition and origin (BRE, 2007), it was observed that CSA and CSA_P, performed differently. Compared to the CSA reported in the main study, CSA_P has greater fineness, but slightly longer initial setting time, as well as different chemical properties. Consequently, in order to achieve 20 minutes (requirement to achieve stable mixes down to 150 kg/m^3 density, as discussed in Section 5.2) of base mix initial setting time, 50% CSA_P (by mass) addition was required to combine with the PC, whilst for CSA it was only 10% by mass.

In the main study, the lowest stable foamed concrete density possible to produce was reported as 150 kg/m^3, provided the base mix initial setting time is 20 minutes. Contrarily, owing to 20 minutes initial setting time, 50% CSA_P yielded 100 kg/m^3 density stable foamed concretes. This performance may be attributed to the higher fineness of CSA_P compared to CSA as well as its higher incorporation level which affects the overall fineness of the PC/CSA combination. The same behaviour was also observed at 5%, 10% and 40% incorporation levels which yielded stable mixes with densities 300 kg/m^3 (with 5% and 10% CSA_P) and 150 kg/m^3 (with 40% CSA_P). This may further be supported by the longer initial setting times of 5% and 10% CSA_P compared to the collapse time of D300 produced with 100% PC (Figure 5.9).

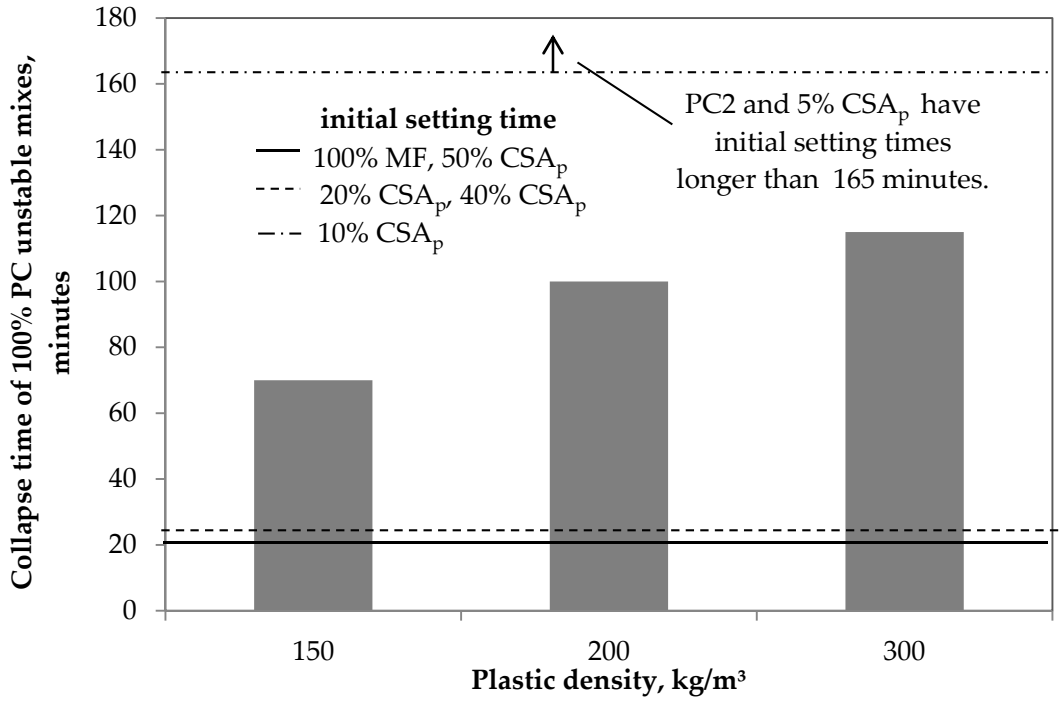

Figure 5.9 Initial setting times of the alternative materials in relation to collapse times

5.3.2 Bubble size analysis

Bubble analysis (in accordance with Section 3.6.2) was also carried out on the foamed concrete specimens produced with the range of alternative materials considered, to evaluate the influence of different cement types on the bubble size. Figure 5.10 provides the average bubble diameter data obtained, in comparison to the main study.

The data obtained suggested that foamed concretes produced with the alternative materials have larger bubble sizes in general. This may be mainly attributed to the quality of the foam used. During the time that these materials were produced, the foam was recorded to be fairly unstable as well as having fast liquid drainage. Therefore, it is likely to get bigger bubbles in a shorter time as a result of faster drainage. Moreover, as these were the first trials for determining the average bubble diameter, there might be some experimental errors. However, as these were not the main focus of the study, the mixes were not repeated.

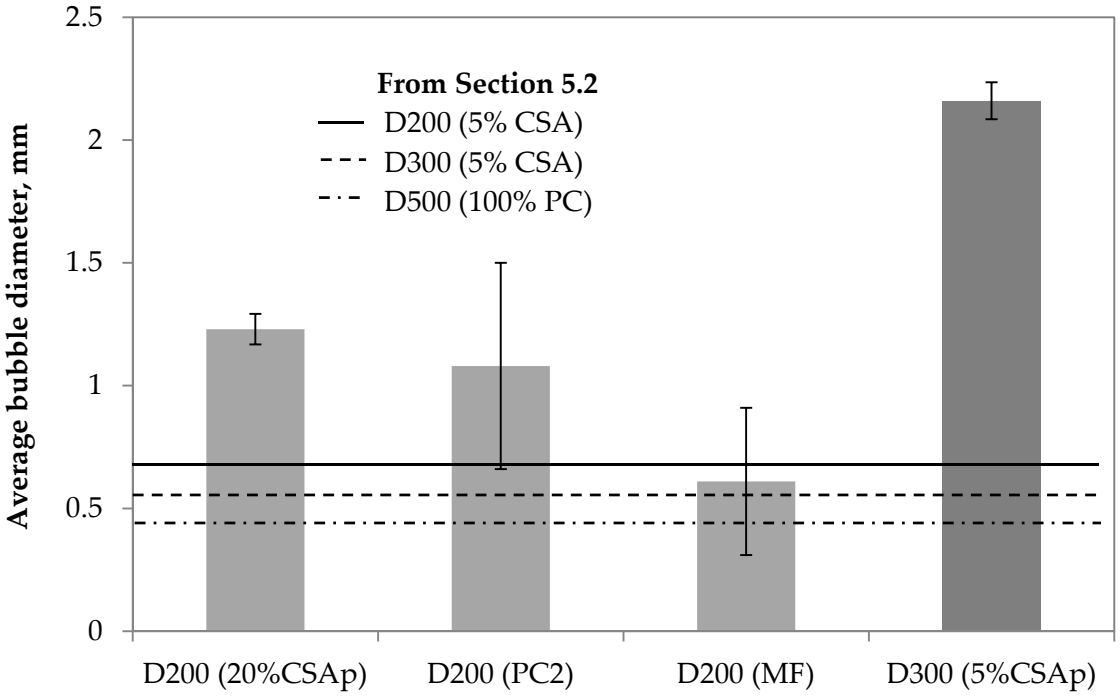

Figure 5.10 Average bubble diameter of FCs produced with the alternative materials

MF yielded the smallest bubble diameter for D200, probably due to the highest fineness and the fastest initial setting time among all materials considered in the studies. Having slightly longer initial setting times and overall coarser cement particles than MF, D200 80%PC/20%CSA_p combination exhibited larger bubbles. On the other hand, given its long initial setting time and fineness similar to PC, PC2 was expected to yield the largest bubble size for D200. However, performance of PC2 remained unclear as it produced smaller bubbles than 20% CSA_p mix.

Although D300 foamed concretes have higher cement contents (hence higher $\mathbf{F}_c$) and they are expected to have smaller bubble sizes than all D200 foamed concretes (decreasing bubble size with increasing density; Visagie and Kearsley, 1999; Nambiar and Ramamurthy, 2007a; Mohammad, 2011; Wei et. al, 2014), the 5% CSA_p mix produced significantly larger bubble size than D200. This may be attributed to the long initial setting time (4 hours) of this specific mix which gives enough time for the bubble growth.

5.3.3 Microstructure

For the alternative materials, microstructural analysis focused on 200 kg/m^3 foamed concretes, as this is likely the lowest density which can be used in practice due to the very-low strength of lower density mixes. The aim of this was to determine the influence of different cement types on the microstructure of 200 kg/m^3 mixes. Figure 5.11 illustrates the microstructure of D200 foamed concretes produced with PC2, MF and PC/CSA$_P$ combination respectively.

As can be seen in Figure 5.11-a, while the PC2 mix exhibited a rather 'open' bubble wall microstructure (similar to that of PC/CSA D200 specimen presented in the main study), no holes in the bubbles were observed. Moreover, fewer bubbles appeared in the walls. This may suggest that PC2 mixes may have an unknown mechanism preventing/retarding the occurrence of gas diffusion which requires further research. In addition, the shape of the bubbles seemed to be less rounded whilst owing to smoother surfaces.

The MF mix, seen in Figure 5.11-b, resulted in more 'open' structure and increased number of holes in the bubbles compared to the PC/CSA mix presented in Section 5.2.4. It is possibly the high fineness of MF which resulted in higher shrinkage and tendency to cracking (Neville, 2011), if the holes in the bubbles are caused by drying shrinkage. Although MF was not chosen for the main study, the more open microstructure may increase the sound absorption capacity as it has bubbles with more open cells. Moreover the bubbles seemed to be mostly rounded.

The microstructure of the 80%PC/20%CSA$_P$ mix (Figure 5.11-c) comprised closed cell bubbles with fewer bubbles with holes, while having significantly less dense bubble walls, compared to the 95%PC/5%CSA mix in the main study. In line with stability, initial setting time and bubble size observations, the CSA$_P$ behaved differently to the CSA, however, the reason for this is unclear requiring future investigation.

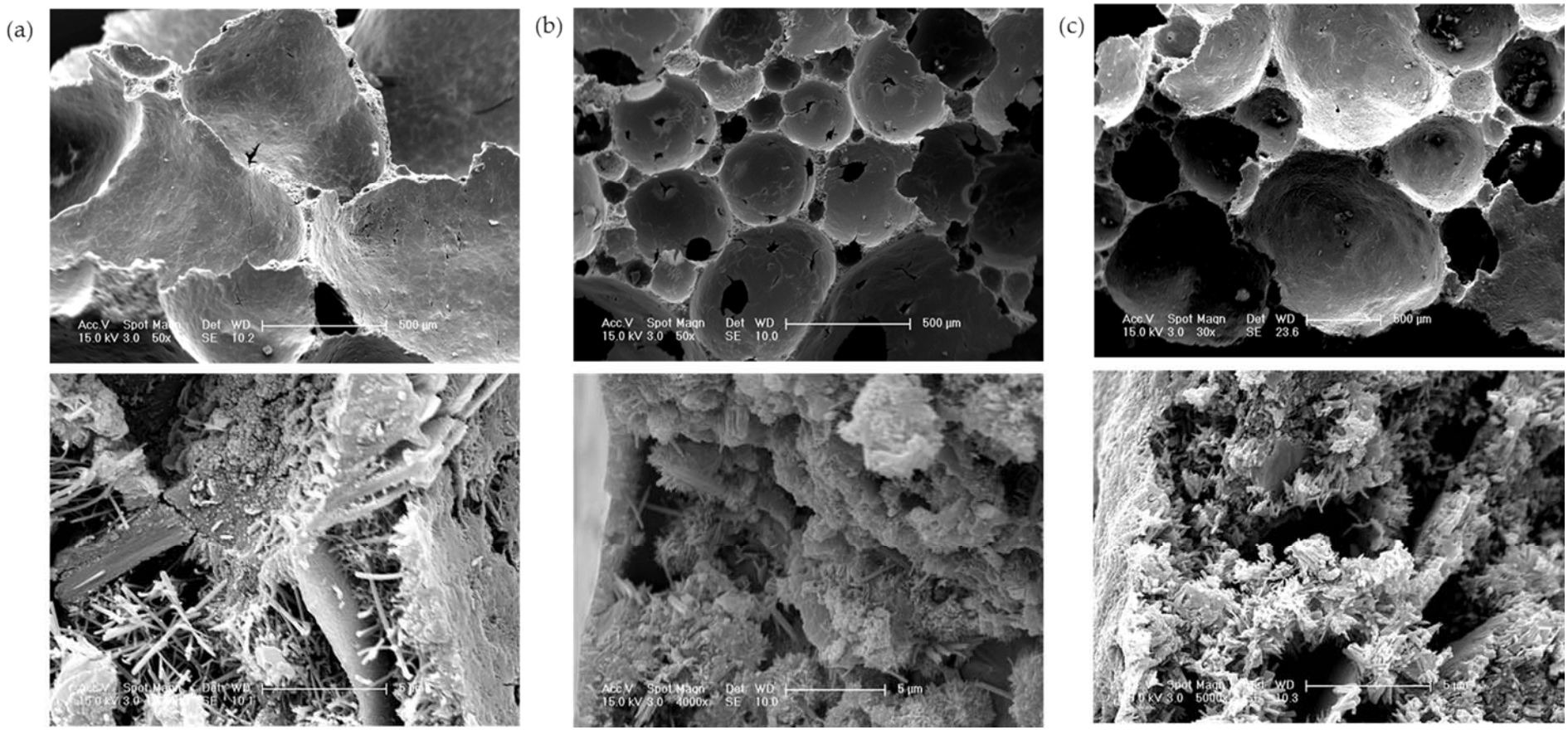

Figure 5. 11 Microstructure of D200 foamed concrete produced with (a) 100% PC2; (b) 100% MF; (c) 80% PC/20% CSA_p

Overall, the materials tested in the preliminary study were found to be successful in overcoming the stability issues. Although the combinations of PC and CSA_P were successful in achieving stable mixes at plastic densities down to 100 kg/m³, CSA_P was eliminated from the study, as it was not readily available and cost-effective.

The use of MF in foamed concrete also resulted in stable mixes down to 100 kg/m³ density, but the concretes were found to have weak and open microstructure. Although PC2 mixes down to 200 kg/m³ were stable, with 'reasonably good' microstructure, it was deemed preferable to have a control over the initial setting time of the cements used. Therefore, for the scope of this study, a lower plastic density limit of 150 kg/m³ was set for achieving stable ULFCs and assessing the key properties.

5.4 CONCLUSIONS

The stability of foamed concretes with plastic densities ranging from 100 to 600 kg/m³ and w/c ratio of 0.50 was evaluated, in order to assess the effectiveness of the proposed solution for overcoming such issues, discussed in Chapter 4. Therefore, based on the observations and recommendations for foamed concrete stability in Chapter 4, efforts were made to produce stable ultra-lightweight foamed concretes (ULFCs) by controlling the initial setting time of the base mix.

Data obtained in this Chapter proved the viability of the proposed solution of 'reducing the liquid to solid transition time' for overcoming the stability issues in ULFC mixes. Therefore, combinations of PC/CSA that accelerate the initial setting times of the susceptible mixes provided an alternative solution for the production of stable ULFCs by preventing the onset of instability. Moreover, the bubble size data supported the observed trend of increasing average bubble diameter with decreasing density. Detailed conclusions and key observations obtained were as follows;

Stability and initial setting times

i. Plastic density, hence the solids content (combined cement and fine aggregate contents) which determines the confinement force, $\mathbf{F_c}$, of foamed concrete mixes, was found to be the main parameter affecting the stability of the mix. As proposed in the hypotheses, the visual observations and the collapse times confirmed that, susceptibility to instability, as well as the degree of instability, increase with decreasing plastic density.

ii. As the plastic density decreases below 500 kg/m^3, cement contents of the mixes decrease significantly, providing insufficient amount of solids to support the bubbles within the mix. Therefore, in the absence of fine aggregates, cement contents below 260 kg/m^3 (at 400 kg/m^3 density), were found to always cause failure due to instability.

iii. Over the years, industrial and laboratory experience has confirmed the suitability of utilising PC at foamed concrete densities down to 600 kg/m^3 without any problems. Therefore, there was a need to stop the changes occurring in the bubbles within the mix before the onset of instability. This was achieved by, replacing a maximum of 10% of PC, by mass of cement content, with CSA cement, which consistently resulted in stable mixes down to 150 kg/m^3 density, with setting times no longer than 20-25 minutes.

iv. Comparison of collapse times of the unstable PC mixes and the (base mix) initial setting times of the stable mixes supported the need to reduce initial setting times in order to achieve stable ULFCs.

v. Stable foamed concrete mixes with densities down to 150 kg/m^3 can be produced. However, below 200 kg/m^3 density, there are handling issues at very early ages (1-2 days) as the material has high tendency to fracture due to the significantly reduced cement contents, hence strength.

vi. As no additional calcium sulphate source was added to the mix to maintain fast reacting properties of CSA cement (described in Section 3.3.1), it probably consumed

the gypsum in the PC to react faster. Consequently, the reaction rate of PC may be altered, resulting in ultra-rapid initial setting times at CSA levels beyond 10% (by mass). However, by adding an additional sulphate source, it may be possible to control the rate of hardening and strength gain of PC/CSA combinations more effectively.

vii. In terms of practical applications, placing foamed concretes that have base mixes with initial setting times of 20-25 minutes is extremely demanding, especially in the case of ready-mix base mixes. Therefore, further research is needed in order to retard the CSA until foam is added and activate it immediately when hardening is needed.

viii. Although the main approach for overcoming the stability issues was the utilisation of PC/CSA combinations, alternative materials were also found to yield stable ULFC mixes given their fast setting properties. Only the performance of one cement type, PC2, which had similar properties with PC and yielded stable D200 mixes could not be explained and remained unclear requiring further research.

Bubble size and microstructure

i. Increasing bubble diameter with decreasing plastic density was the key observation for understanding the stability behaviour of foamed concrete mixes. The bubble analysis data for ultra-low density mixes was found to be in line with the observed behaviour.

ii. It was found that, foamed concretes with average bubble diameters above 0.5 mm (at D500) were prone to collapse. The risk of instability increased significantly as the average bubble diameter increased beyond 0.6 mm, as in 300 kg/m^3 density foamed concrete.

iii. When the bubble size data obtained by 2D analysis was compared with 3D bubble analysis reported by Wei et. al (2014), 2D analysis was found to yield smaller values (at a given plastic density). Although the difference might have arisen from different

mix proportions, an improved method or utilisation of 3D analysis for the determination of bubble size is required.

iv. The microstructure of ULFCs were observed to be more porous and open (partially open-cell bubbles) in comparison to the high/low density foamed concretes. Although it reduces the strength, more porous microstructure may favour the insulation performance in general, whilst open-cell bubbles may specifically provide an advantage for sound absorption performance.

v. While the cause of holes in the bubbles of ULFC concretes is unclear, it may be the reduced cement contents, hardening at the time of coalescing or drying shrinkage causing these holes.

vi. Similar to the holes in the bubbles, cause of increased number of bubbles in the walls of ULFCs is not known. However, they may indicate the occurrence of Ostwald ripening with a big bubble surrounded by many smaller bubbles.

vii. The bubble size data and observed microstructure for the alternative materials showed that type of constituents have an influence on the physical properties of foamed concretes.

CHAPTER 6

6. REDUCING EMBODIED CARBON DIOXIDE (eCO_2)

6.1 INTRODUCTION

In response to the increased demand for low embodied carbon dioxide (eCO_2) construction materials and activities (EU Construction Products Regulation; European Commission, 2011a; concrete industry sustainable construction strategy; MPA, 2012a), this Chapter focuses on reducing the eCO_2 contents of ultra-lightweight foamed concretes (ULFCs). As fly ash has an eCO_2 content of as low as 4 kg CO_2/tonne in comparison to 930 kg CO_2/tonne of PC (MPA, 2011a), fly ash (FA) was used to meet this aim. Two types of ashes, FA1 and FA2 (properties given in Table 3.1), were tested to evaluate their efficiency in producing stable ULFCs with the maximum fly ash addition levels possible.

Mixes with plastic densities ranging from 150 to 500 kg/m³ and w/c ratio of 0.50 were examined. As the trial mixes with PC/FA combinations were found to result in unstable ULFC mixes, combinations of PC/CSA/FA were considered to benefit from the fast setting properties of CSA cement. Therefore, from the data obtained in Chapter 5, CSA addition of 10% by mass (which yielded stable mixes down to 150kg/m³) was kept constant and PC was replaced with fine FA was added with an increasing rate.

This Chapter evaluated the effect of FA addition in ULFCs in terms of collapse and initial setting times, stability, bubble size and microstructure. As the strength of the ULFCs was not the focus of this study, long-term strength development of fly ash was not monitored. Given its high fineness, the influence of FA on stability in relation to the cement fineness hypothesis (explained in Section 4.2.4, Figure 4.11) was also considered. Moreover, eCO_2 contents of a range of foamed concretes (high/low and ultra-low density) were presented to identify the influence of plastic density and fly ash.

6.2 EFFECT OF FLY ASH ON STABILITY

The effect of fly ash on stability, in relation to collapse and initial setting times, was evaluated. Jones et. al (2003) reported that addition of fine fly ash in foamed concrete at a rate of 30% (by mass) increased the long-term strength, reduced the drying shrinkage and the peak core temperatures due to hydration while improving the thermal insulation. Although reduced flow was also reported with the addition of fine fly ash, it was not considered as an issue in the case of ULFC mixes, as they were found to be not self-flowing (which will be discussed in Chapter 8). Therefore, utilisation of FA contents of 30% (by mass) and above were considered.

As proposed in Section 4.2.4, utilisation of finer cement particles are thought to lead the formation of smaller hence more stable bubble, at a given cement content (Mohammad, 2011). This is because finer cements would provide a higher number of cement particles for a given cement content, providing more coverage of the bubbles surfaces. Consequently, this would slow down the rate of liquid drainage, restricting the bubbles from increasing in diameter and coalescing easily.

Owing to its high fineness, fly ash was expected to improve the stability of the bubbles, hence the mix. In order to evaluate the influence of higher cement fineness, on foamed concrete stability, collapse times of PC/FA2 combinations were compared with PC only mixes, for a given density. In addition, the influence of fly ash content on the initial setting times of PC/CSA/FA base mixes were evaluated, as well as the stability of the corresponding foamed concrete mixes.

6.2.1 Initial setting times

As the key factor for achieving stable ULFC mixes, the initial setting times of FA mixes were measured. Base mixes with combinations of PC/CSA/FA with constant 10% CSA addition and w/c ratio of 0.50 were considered. Fly ash was introduced into mixes at levels 30% to 70% by mass whilst FA1 was only used at 30% and 40% addition levels.

In general, the influence of fly ash on setting time is dependent on its content and composition, w/c ratio of the mix, type and amount of cement, as well as the temperature of the mix (RILEM, 1991). Figure 6.1 illustrates the initial setting times of the PC/CSA/FA combinations considered, in comparison to the non-fly ash reference, while Table 6.1 covers the initial setting times of the range of PC/CSA/FA combinations in relation to stability. As can be seen, the data suggest that CSA cement is likely to be the governing factor controlling the initial setting times.

Compared to the reference mix (90% PC/10% CSA), the effect of 30% to 50% fly ash addition on setting times was found to be negligible. Indeed, the 40% fly ash (by mass) provides the same initial setting time of 20 minutes while 30% and 50% FA addition levels result in 25 minutes. This is perhaps due to, the heat evolved from the rapid reaction of CSA, possibly preventing the retarding effect of fly ash by increasing the temperature of the mix. As a result of the increased mix temperature, fly ash reacts faster (Neville, 2011). Furthermore, fly ash also brings sulfate sources which may further accelerate the reactions of CSA (as explained in Section 3.3.1). However the solubility of these sulfates was not determined hence, their effect on the initial setting time is not known.

Table 6.1 Initial setting times of fly ash base mixes

Plastic density, kg/m³				**150**	**200**	**300**
Cement type (% by mass)			**Base mix initial setting time (hh:mm)**	**Stable (✓)/Unstable (x)**		
PC	**CSA**	**FA2**				
100	-	-	03:25	**x**	**x**	**x**
95	5	-	01:30	**x**	✓/x	✓
90	10	-	00:20	✓	✓	✓
60	10	30*	00:25	**x**	✓	✓
50	10	40*	00:20	✓	✓	✓
40	10	50	00:25	**x**	✓	✓
30	10	60	00:40	**x**	✓/x	✓
20	10	70	00:45	**x**	✓/x	✓

* Valid for both FA1 and FA2

Note: ✓ stands for mixes resulted in stable foamed concretes at a rate of 100%. ✓/x is used even if the rate of achieving stable mixes is 99%.

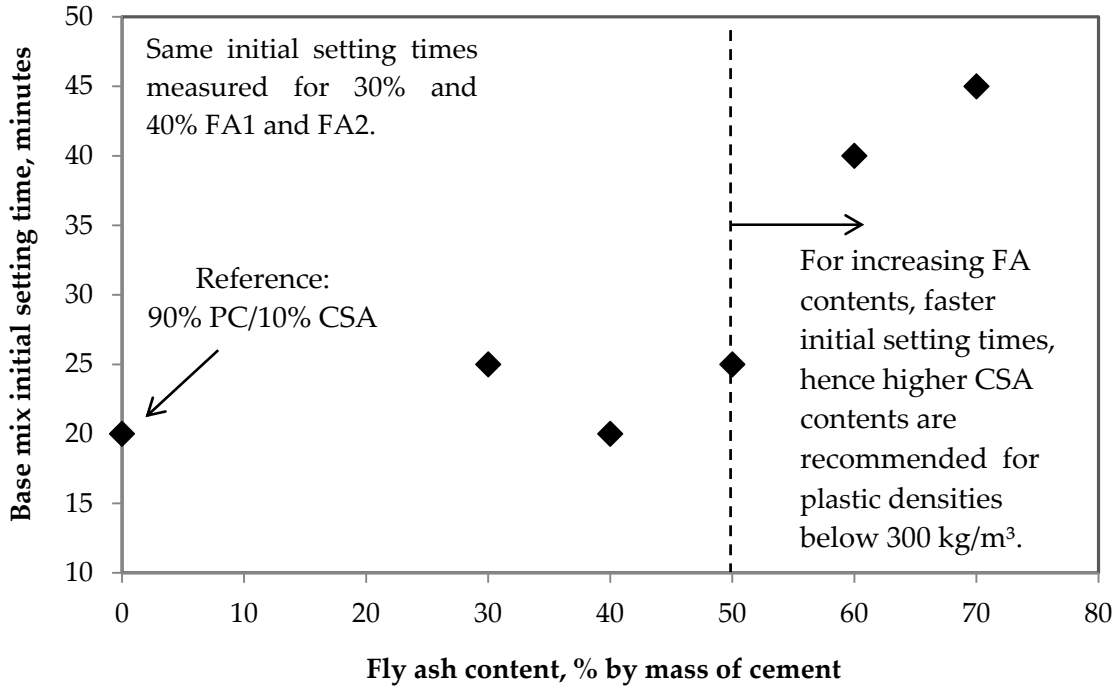

Figure 6.1 Effect of varying fly ash content on initial setting times of the base mixes containing 10% CSA

On the other hand, at fly ash levels greater than 50%, retardation in initial setting times was observed. This behaviour may be attributed to the reduced PC content, which provides the lime and calcium sulfate for the rapid reaction of CSA cement. Therefore, due to the reduction of the lime and calcium sulfate contents available, the CSA reacted slower. A similar behaviour was also observed in the initial setting times of ternary blends of calcium sulfoaluminate/calcium sulfate/fly ash cements reported by Ioannou et. al (2014) that suggested the incorporation of fly ash had no effect on the initial setting time. However, it must be noted that, in that case, the fly ash levels were ranging from 5 to 15% by mass and while doing so, the presence of calcium sulfate was kept at levels such that the required strength was maintained, no dimensional instability was caused and the formation of ettringite was ensured.

Overall, 30% to 70% fly ash levels were found to satisfy the required initial setting times presented in Section 5.2.1 (Table 5.1) to produce stable foamed concretes at plastic densities down to 200 kg/m³, while only 40% fly ash level was found to yield stable D150 foamed concretes mixes. As reported by Jones and McCarthy (2006), incorporation of fine fly ash replacing PC may cause slight foam instability in some cases, requiring addition of more

foam than the calculated amount. Although this was observed in the current study, it was occasional and did not occur in all mixes. However, it is recommended to increase the CSA cement content for 200 kg/m³ mixes with fly ash contents beyond 50% to ensure a base mix initial setting time of 20-25 minutes as a safety margin for achieving stability.

6.2.2 Collapse time

The collapse times of 60%PC/40%FA2 mixes for densities from 150 to 300 kg/m³ were measured to assess the effect of fly ash on bubble and, hence, the mix stability. The data obtained for collapse times of PC/FA2 mixes showed that FA enhanced the stability, as longer (up to 1 hour 15 minutes for densities from 150 to 300 kg/m³) collapse times were observed in comparison to PC only mixes (Figure 6.2).

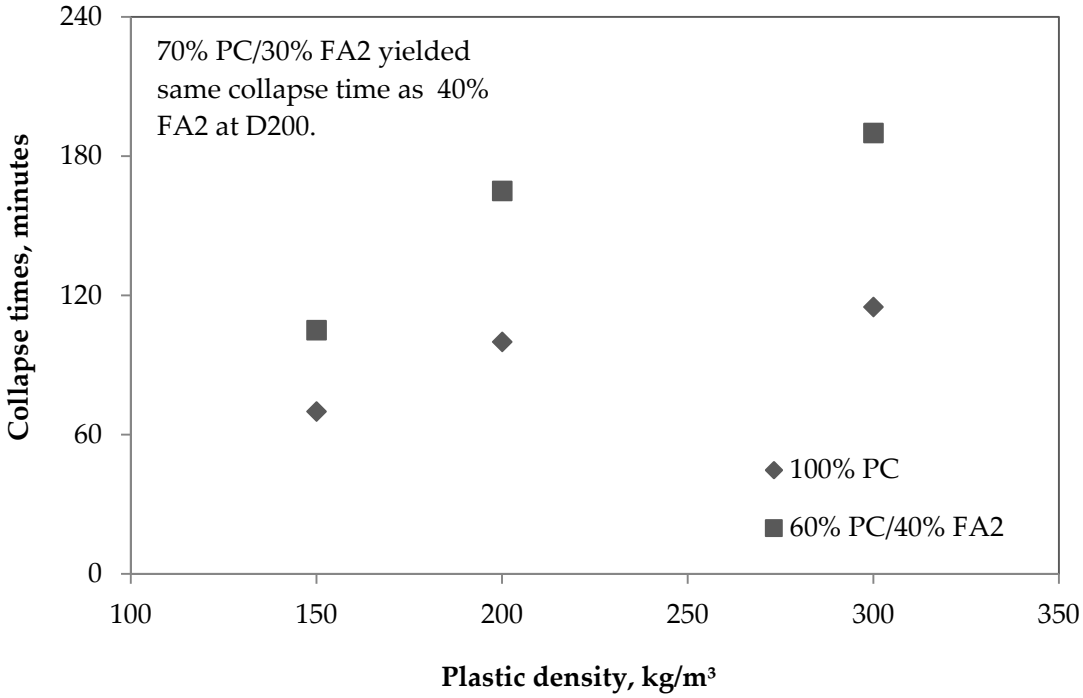

Figure 6.2 Influence of fly ash on collapse times of unstable ULFC mixes

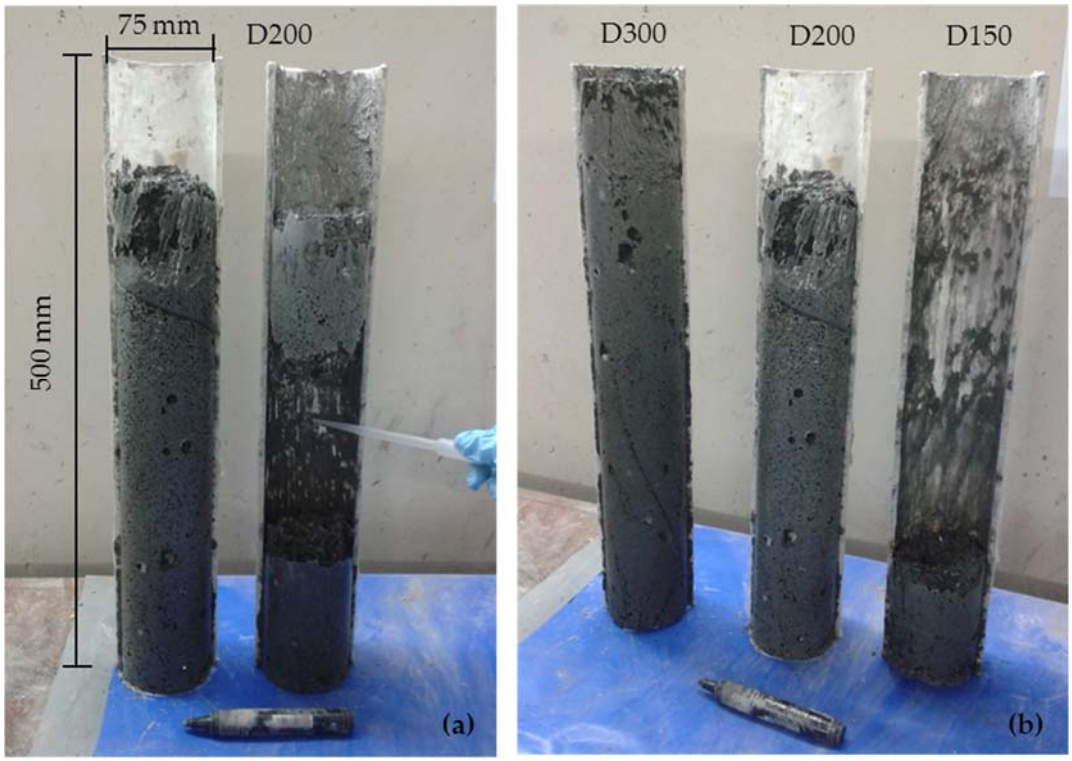

Figure 6.3 Failure of unstable PC/FA2 ULFC mixes (a) 200 kg/m³ with 40% (left) and 30% FA2 (right); (b) 300, 200 and 150 kg/m³ with 40% FA2 by mass

For D200 mixes, collapse time of 30% FA2 was also determined, in order to identify any differences in mix stability due to fly ash content. It was found that, the mix containing 30% FA2 collapsed slightly faster, when compared to the 40% FA2, however this is probably within the repeatability limits. Therefore, the collapse times were taken as equal. On the other hand, when the level of collapse was considered, the 40% FA2 mix was found to exhibit less drop in level, as shown in Figure 6.3-a. In line with the observations on collapse behaviour of 100% PC mixes presented in Chapter 5, the degree of instability of PC/FA mixes increased with decreasing plastic density (Figure 6.3-b).

6.3 EFFECT OF FLY ASH ON BUBBLE SIZE

Besides the cement fineness hypothesis constructed in Section 4.2.4, the effectiveness of replacing sand with fly ash (coarse) on obtaining more uniform and finer bubble structure at high/low densities was reported by Nambiar and Ramamurthy (2007). On the other hand, Wei et. al (2014) reported that replacing PC with fly ash at levels of 20%, 40% and

60% by mass of cement resulted in increased bubble diameter at 1000 kg/m³ density possibly due to longer setting times of FA mixes.

Given the longer collapse times of PC/FA mixes (Figure 6.2), FA was thought to yield smaller bubble sizes. This is because smaller bubbles are considered as more stable, as stated by Dransfield (2000), McGovern (2000) and Brady et. al (2001). Therefore, with the expectation of obtaining smaller bubble sizes in comparison to non-fly ash ULFCs, bubble size analysis was carried out on D200 and D300 fly ash ULFC specimens. Only the specimens produced with FA2 were assessed for bubble size, whilst for D300 mix effect of 40% FA1 was also evaluated.

Figure 6.4 shows sections from D200 foamed concretes produced with 95% PC/5% CSA and 50% PC/10% CSA/40% FA2. The difference between the bubble size of non-fly ash and fly ash mixes can be distinguished visually, with the fly ash mix exhibiting smaller bubble sizes. Accordingly, data obtained from the bubble analysis of 50% PC/10% CSA/40% FA2 mixes (see Figure 6.5) proved that, in the presence of fly ash, bubbles in ULFCs are smaller. In this case, the reason for this is unclear as there is also CSA cement included in the mix, however, it may possibly be attributed to (i) utilisation of a finer cementitious material and (ii) fast initial setting times of the mixes. The combination of these two factors is thought to affect the bubble size.

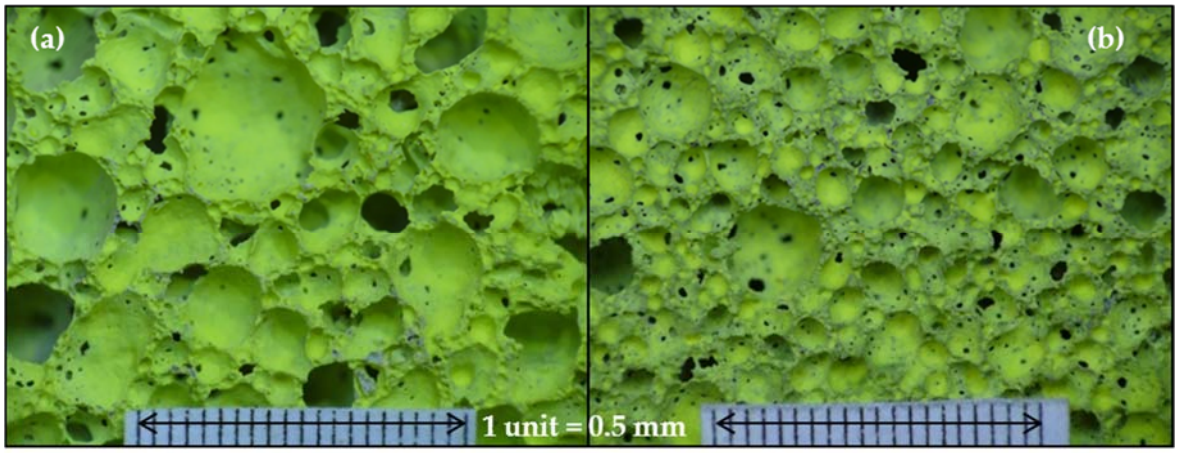

Figure 6.4 Influence of fly ash on the bubble size of D200 (a) 95% PC/5% CSA and (b) 50% PC/10% CSA/40% FA2

As assumed in Section 4.2.4 and shown by the collapse times (Figure 6.2) and bubble size (Figure 6.5) data, the fineness of the cementitious portion of the mix has an effect on bubble size, hence the stability of the mix. Secondly, fast initial setting times controlled the bubble sizes by preventing the bubbles from increasing in diameter. In other words, before the bubble sizes reach a critical size that would lead to collapse, the mix hardens, leaving the bubbles smaller in diameter.

Accordingly, the utilisation of 5% CSA addition restricted the increase in average bubble diameter through decreasing the initial setting time from almost 3.5 down to 1.5 hours, yielding stable ULFCs (as discussed in Chapter 5). At this stage, the increase in cement fineness caused by 5% CSA addition was considered negligible. Thus, it was dominantly the shorter setting times resulting in smaller bubble diameters.

On the other hand, introducing 40% FA2 and adding a further 5% CSA cement in the mixes (to form 50%PC/10%CSA/40%FA) increased the combined fineness of the cement blend by 7% compared to 95% PC/5% CSA mix. Therefore, shifting from 95% PC/5% CSA mixes to 50% PC/10% CSA/40% FA2 mixes resulted in a decrease of 26% and 31% in average bubble diameter at densities 200 and 300 kg/m^3 respectively (Figure 6.5). In the case of D300 40% FA1, the decrease in the average bubble diameter was found to be slightly less 10%, which may be attributed to the lower specific surface area of FA1.

It must be noted that the setting times of the mixes considered in Figure 6.5 are different. The PC/CSA mixes have initial setting time of 90 minutes, while the PC/CSA/FA2 mixes have an initial setting time of as short as 20 minutes. Therefore, the faster initial setting times of PC/CSA/FA mixes in combination with higher fineness were also effective in yielding smaller bubble sizes.

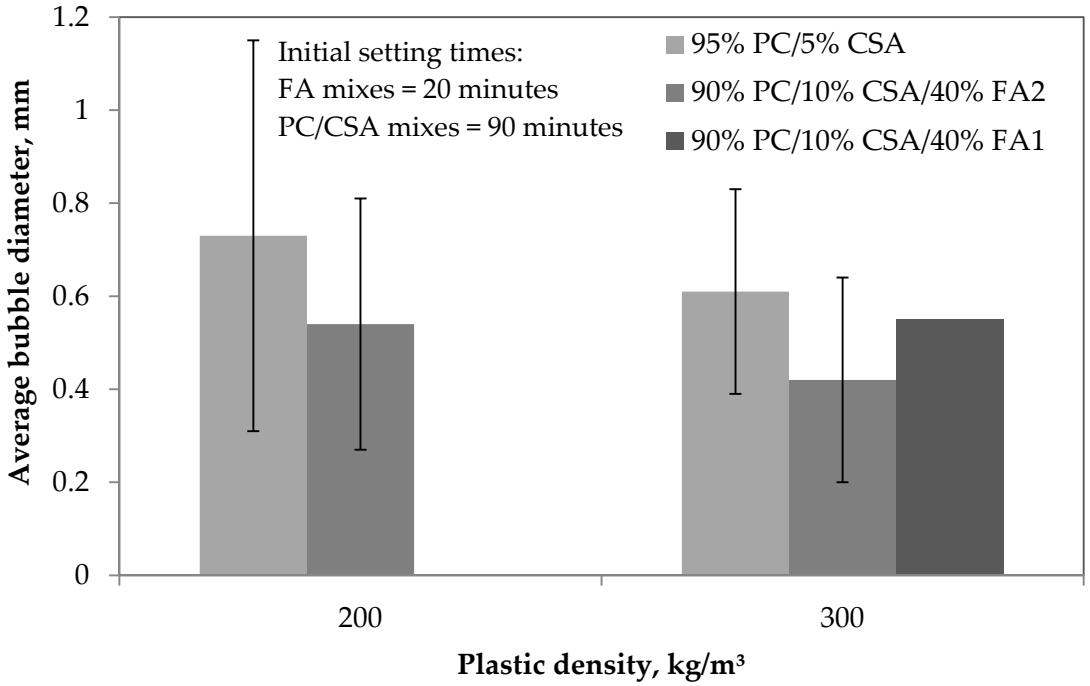

Figure 6.5 Effect of utilisation of fly ash on average bubble diameter

6.4 EFFECT OF FLY ASH ON MICROSTRUCTURE

Microstructural analysis was carried out on the fly ash foamed concretes, in order to evaluate the effect of finer particles and long-term strength gain of fly ash on the microstructure. ULFCs with plastic densities of 200 and 300 kg/m^3 and comprising FA levels of up to 70% by mass were analysed at 28 days age. Furthermore, as FA hydration continues beyond 28 days (Neville, 2011), in comparison to PC/CSA mixes, the microstructure of fly ash ULFCs was expected to improve in long-term and, therefore, comparative microstructural analysis was also carried out on specimens at an age of beyond 6 months.

Figure 6.6 shows the microstructure of 28 days old D300 foamed concretes with varying fly ash levels and types. As noted on the PC/CSA foamed concretes, holes in the bubbles were also observed in the D300 fly ash mixes. From 30% to 50% (by mass) fly ash levels, the bubble walls were found to be reasonably dense for 28 days age. However, beyond 50% fly ash, at 70% (by mass) fly ash level the overall microstructure was found to be weaker with bubble walls packed with fly ash spheres.

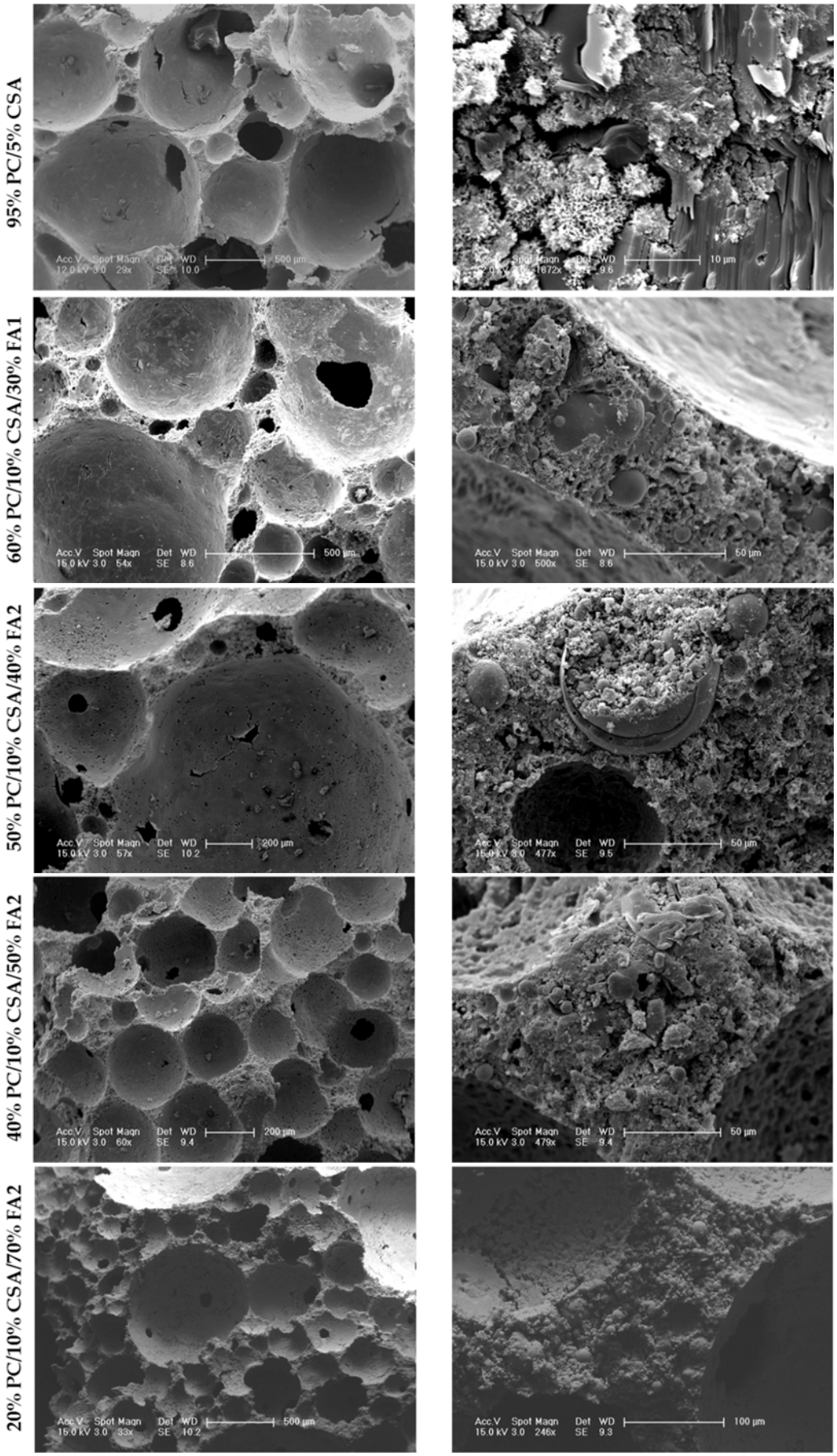

Figure 6.6 28-day microstructure of 300 kg/m^3 FCs with varying FA levels and types

On the other hand, like PC/CSA foamed concretes, bubbles are present in the walls, however, their numbers decreased with increasing fly ash content. Furthermore, the texture of the inner surface of the bubbles appeared to be rough at fly ash contents beyond 40% (by mass). This may possibly be the consequence of a decreased amount of lime available for fly ash to react at reduced PC contents within the PC/CSA/FA combination (as CSA cement is also thought to use the lime from PC to react faster).

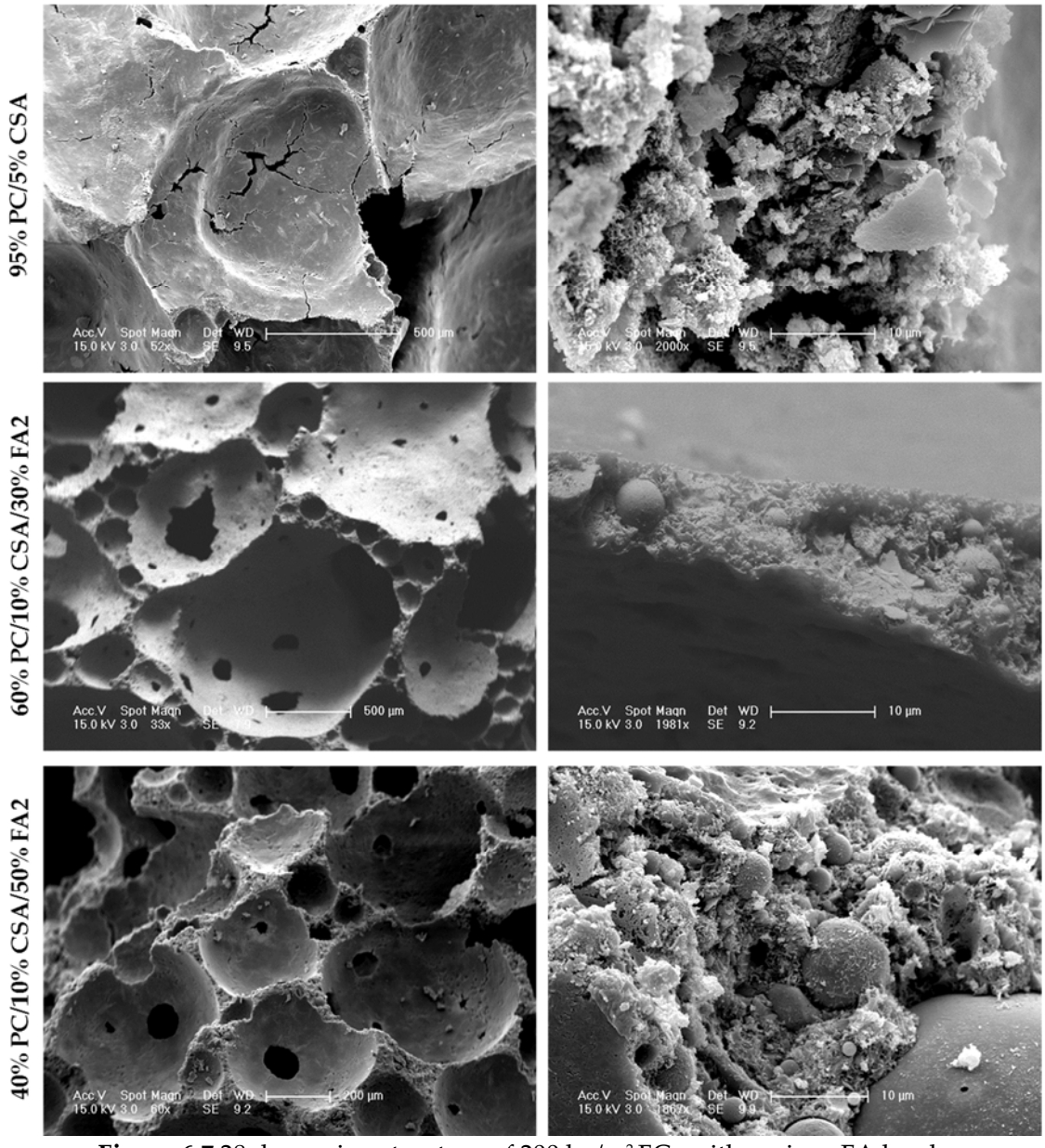

Figure 6.7 28 days microstructure of 200 kg/m^3 FCs with various FA levels

Figure 6.7 illustrates the 28 days microstructure of D200 foamed concretes produced with no fly ash as well as 30% and 50% fly ash (by mass). Compared to the PC/CSA mixes, D200 fly ash mixes were observed to have denser microstructure, especially the bubble wall microstructure which improved with increasing fly ash content at 28 days age. This may be attributed to the increased number of cement particles in fly ash mixes for given cement content resulting in formation of denser microstructure around the bubbles.

On the other hand, Figure 6.8 shows the influence of fly ash particles in reinforcing the bubble walls, hence giving stability to the system. Comparing the non-fly ash and fly ash mixes, the reinforcing effect of fly ash particles is more visible in D200 specimens than D300. This is possibly due to the lower cement contents and more porous microstructure of D200 mixes. Moreover, the reduced number of bubbles in the walls in fly ash mixes may be attributed to the reinforcing effect of fly ash particles.

Given the known long-term strength gain of fly ash concretes, microstructural analysis was carried out on specimens of beyond 6 months age, with the expectation of observing an enhanced microstructure. When comparing the long-term SEM images of fly ash specimens shown in Figure 6.9 and 6.10. to 28-day images shown in Figure 6.8, it can be seen that there is an improvement in the microstructure of fly ash specimens in long-term, which was observed at all fly ash levels and types at foamed concrete densities considered.

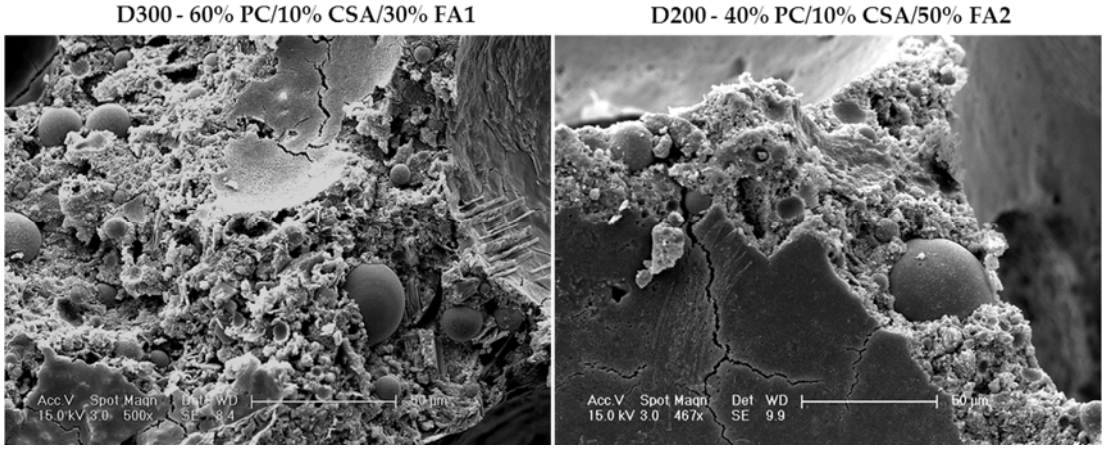

Figure 6.8 Walls reinforced with fly ash particles

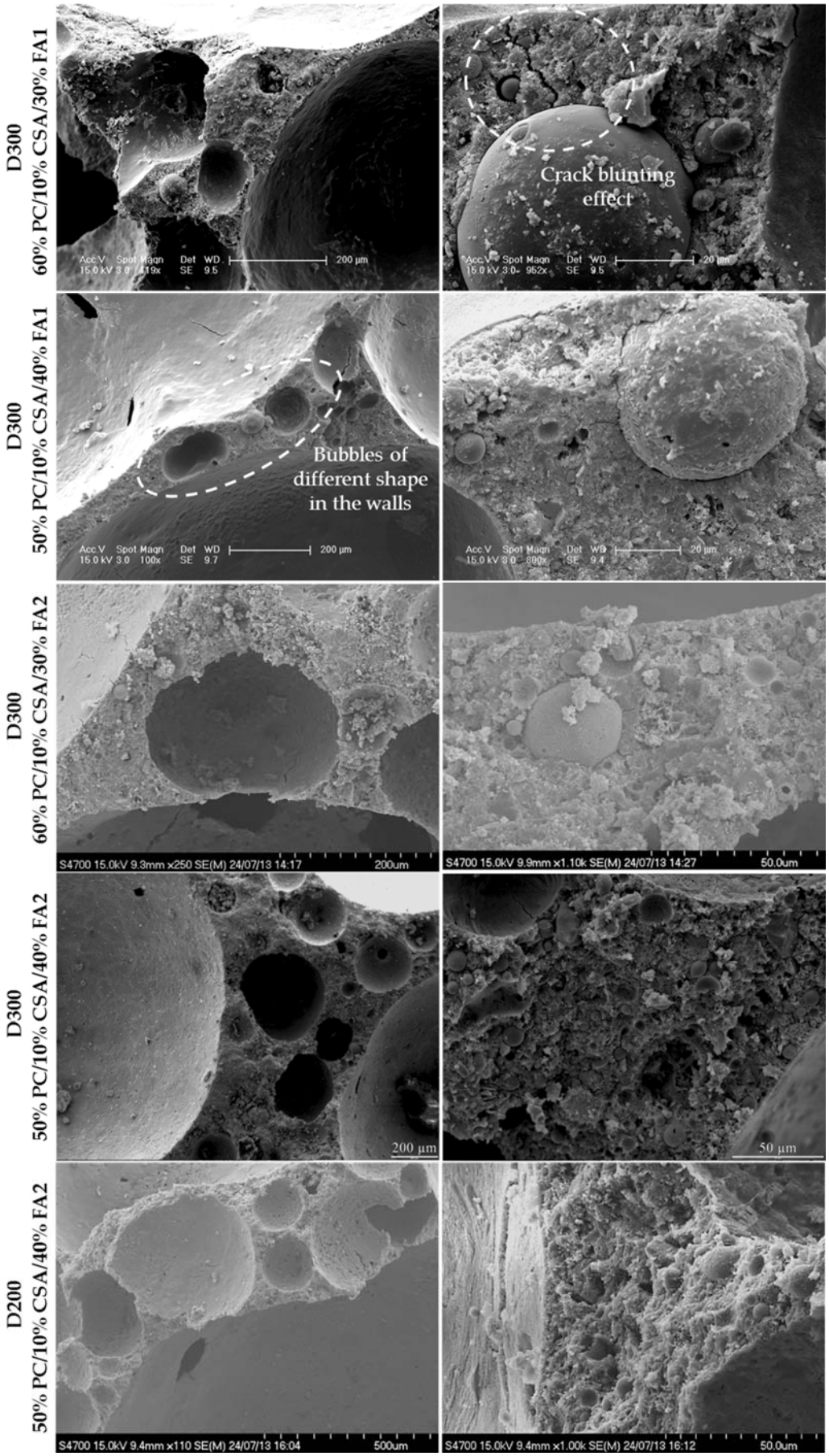

Figure 6.9 8-month microstructure of D300 and D200 fly ash FCs

More sprecifically, Figure 6.9 illustrates the 8-month microstructure of D200 and D300 foamed concretes with fly ash levels of up to 40% by mass. The texture of the inner bubble surfaces was smoother, with finer cracks or smaller holes, possibly as a result of self-healing ability due to long-term strength gain of fly ash, whilst the bubble walls appeared to get denser. Although no significant difference was observed between FA1 and FA2 specimens of D300, FA1 seemed to yield slightly denser microstructure. Furthermore, fly ash particles were also observed to have 'crack blunting effect', stopping further growth of cracks as seen in Figure 6.9.

Moreover, bubbles of different shapes were observed in the walls, some of them were rounded whilst others were elliptical in shape (Figure 6.9), however these may not be unique to fly ash mixes. It is possible that the origins of these bubbles may be different; entrapped air or surfactant sourced. The elliptical shaped bubbles may even be the sign of coalescence or 'squeezed' bubbles due to thinning of the bubble walls.

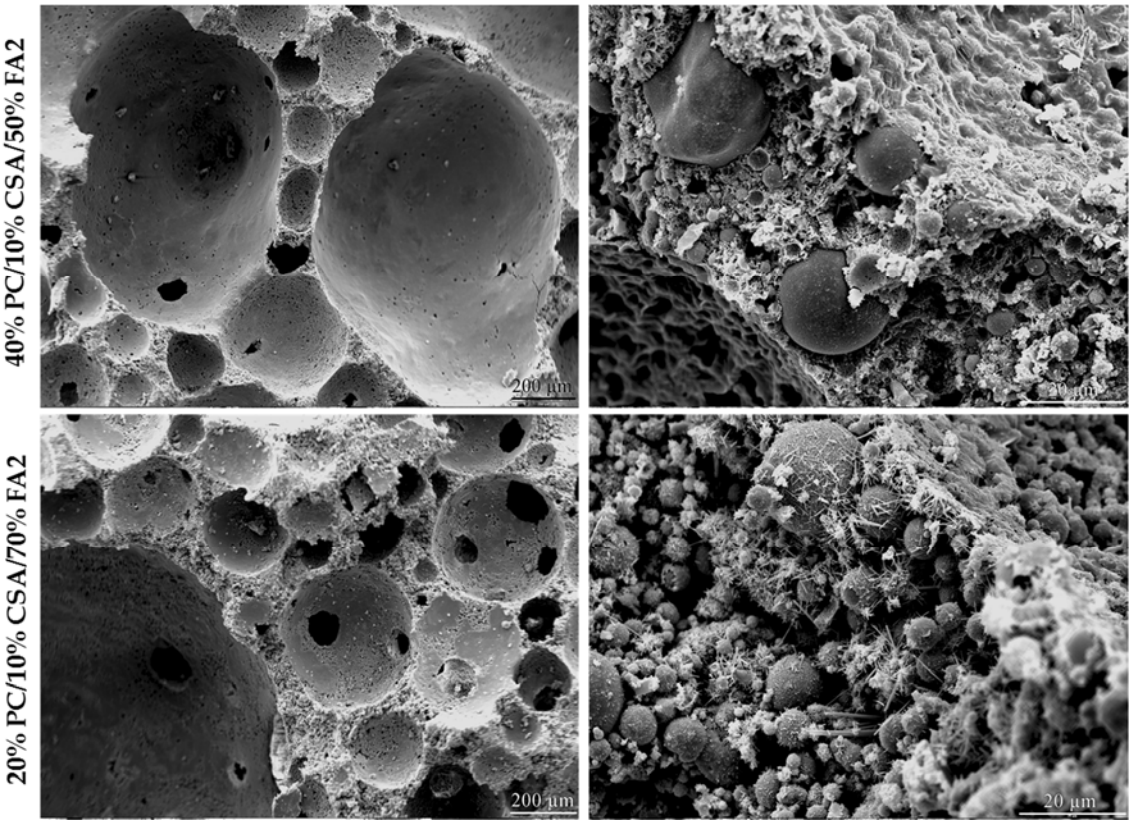

Figure 6.10 Microstructure of 16-month D300 foamed concretes

On the other hand, when D300 foamed concretes with fly ash levels of 50% and 70% by mass were analysed at a further age of 16 months age (Figure 6.10), the microstructure was not found to be as good as in lower fly ash contents. The long-term microstructure of 50% and 70% FA2 foamed concretes perhaps suggested that most of the fly ash particles in these mixes seemed to stay unreacted possibly due to to lack of enough calcium hydroxide and water. Although the microstructure of 50% FA2 foamed concretes were 'reasonably acceptable', fly ash levels beyond 50% (by mass) are not recommended for PC/CSA/FA combinations as employed in this study.

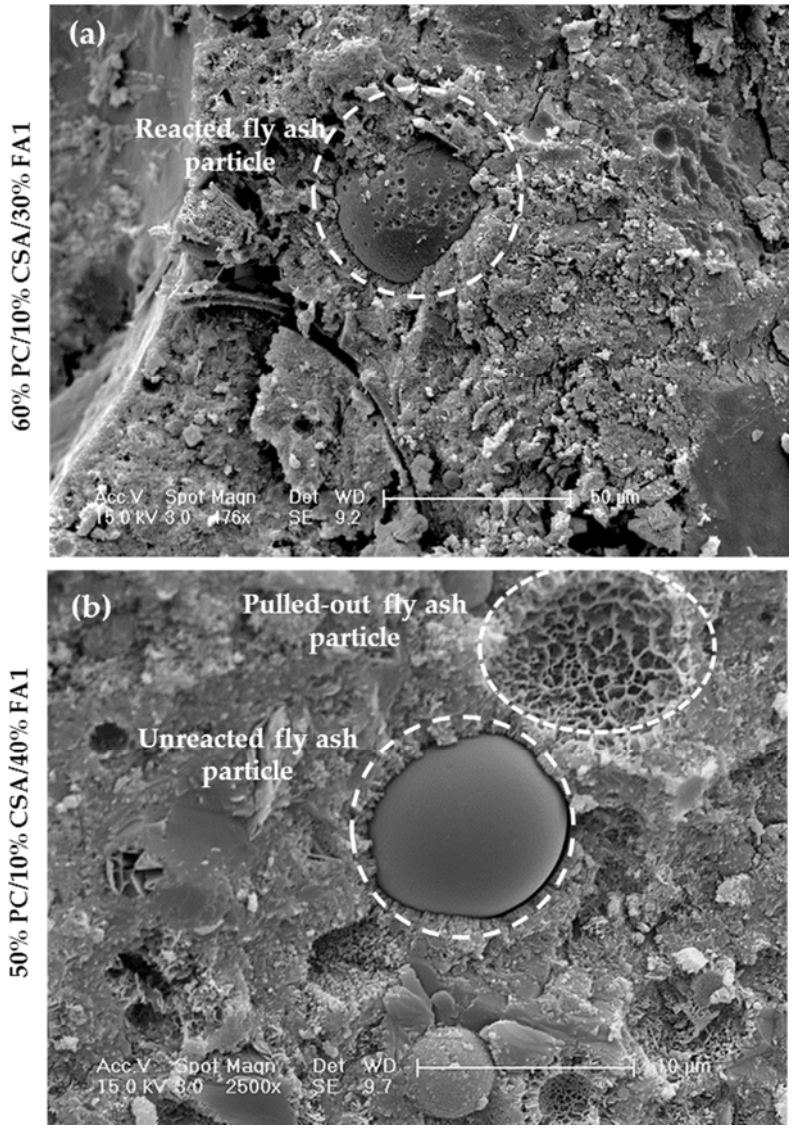

Figure 6.11 (a) Reacted and (b) unreacted fly ash particles in 300 kg/m^3 FCs

Figure 6.11 shows reacted and unreacted fly ash particles in D300 fly ash mixes. The etched surface of the fly particle shown in Figure 6.11-a indicates that it has reacted, while the smooth, glassy surface of the one shown in Figure 6.11-b indicates that it remained unreacted (RILEM, 1997). Moreover, the fly ash particles surrounded with ettringite may stay unreacted, as ettringite may restrict the $Ca(OH)_2$ required for the hydration of fly ash to penetrate through. Therefore, unreacted fly ash particles can be 'pulled out' easily. The spherical holes with internal surfaces coated, possibly, with ettringite may be the evidence of this (Figure 6.11-b).

6.5 EFFECT OF FLY ASH ON EMBODIED CARBON DIOXIDE (eCO_2)

Targets set for sustainable construction and reducing carbon emissions in the sustainable construction strategy (MPA, 2012) urge for the production of low eCO_2 concrete. Specifying sustainable concrete (MPA, 2011a) and the framework standard BES 6001 (BRE, 2009) provide a guideline on achieving these targets and maintaining the performance through the use of responsibly sourced materials. In the competitive environment of construction industry, which has been satisfying the targets set (MPA, 2013), foamed concrete also needs to meet the requirements of sustainability and responsible sourcing. Therefore, this section focused on the environmental impact of foamed concrete from the embodied carbon dioxide (eCO_2) point of view.

The eCO_2 of a range of foamed concretes (of high to ultra-low density class) was calculated, considering the cradle to gate eCO_2 contents only. As it is well-established in terms of properties and behaviour, supplying conventional PC foamed concrete with plastic densities of 600 kg/m^3 and above is fairly common practice in industry. Owing to its high air contents, foamed concretes may be considered to have low eCO_2 in comparison to normal weight concrete. However, comprising minimum cement contents of 300 kg/m^3, high and low density foamed concretes have high eCO_2 contents.

On the other hand, at ultra-low densities (below 500 kg/m^3) where cement contents are less than 300 kg/m^3, the eCO_2 contents of the mixes decrease naturally even without the utilisation of low eCO_2 constituents. Further reduction in the eCO_2 is provided by replacing the PC with fly ash at all density classes. The method described by CICSF (2008)

was followed to calculate the eCO_2 contents of foamed concretes and an example calculation is shown in Appendix (C). Table 6.2 shows the eCO_2 values of the constituents used in the calculations.

The embodied carbon dioxide (eCO_2) contents of foamed concretes with densities ranging from 150 to 1000 kg/m^3 are shown in Figure 6.12. As the mixes with plastic densities from 600 to 1000 kg/m^3 have cement contents of 300 kg/m^3 (which is the dominant factor affecting the eCO_2), the eCO_2 of these foamed concretes were calculated to be the same, hence shown together in Figure 6.12.

The ULFC mixes had up to 67% lower eCO_2 in comparison to high/low densities, due to their lower cement contents. It must be noted that only the ULFC with plastic densities below 500 kg/m^3 were considered. Since 500 kg/m^3 density mixes were produced with increased cement content (333 kg/m^3, which is higher than the high/low density mixes) and without incorporating fine aggregates, their eCO_2 content was higher than that of high/low density mixes.

On the other hand, the incorporation of fly ash in the mixes at a rate of 40% by mass (50%PC/10%CSA/40%FA) reduced the eCO_2 contents by 39% to 42%, in comparison to non-fly ash mixes. Therefore, eCO_2 contents ranging from 55 to 160 kg eCO_2/m^3 of foamed concrete were calculated for densities ranging from 150 to 1000 kg/m^3 respectively. When comparing 100% PC conventional foamed concrete (D600 and above) with 40% FA D200 foamed concrete (which is likely to be the lowest density to be used in the industry), combined effect of reduced cement content and utilisation of FA results in a 75% of reduction in the eCO_2.

Table 6.2 ECO_2 of the constituents (MPA, 2011a)

eCO_2 of the constituents, kg CO_2 / tonne	
Portland cement	930
CSA cement	744*
Fly ash	4
Surfactant	0.22
Water	0.3

* Calculated as around 80% of eCO_2 of PC (MPA, 2011b)

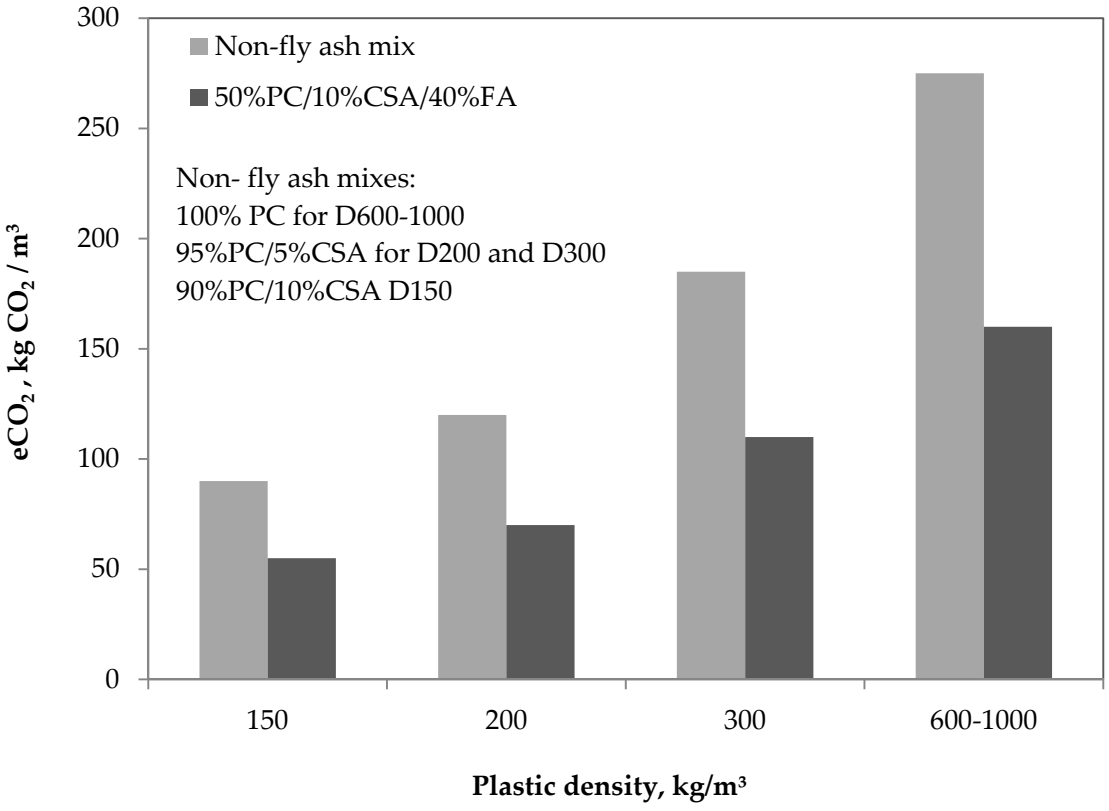

Figure 6.12 Influence of plastic density and fly ash on the eCO_2 of foamed concrete

6.6 CONCLUSIONS

The aim of this Chapter was to produce ultra-lightweight foamed concretes with low eCO_2 by utilising fly ash. The calculated data and observations made showed that fly ash can be incorporated into ULFCs successfully, providing substantial benefits on environmental impact. The conclusions drawn from the influence of fly ash on ULFCs are summarised below.

Stability and initial setting times

i. Fly ash levels of up to 50% by mass can be utilised to produce stable ULFCs with plastic densities down to 200 kg/m^3. For 150kg/m^3 density mixes, a maximum fly ash content of 40% (by mass) can be used. Increased fly ash contents may potentially be used along with increased CSA cement contents to maintain the required initial setting times for achieving stable mixes.

ii. Both FA1 and FA2 could be used to achieve stable ULFC mixes, as no significant difference in the performance of two ashes was observed.

iii. As no additional lime and calcium sulfate sources were added for the reactions of CSA cement, it is thought that they were taken from the PC, and possibly from the sulfate sources of fly ash. Therefore, it is possible that the maximum benefit could not be obtained from the utilisation of fly ash in terms of microstructure and strength (although it was not measured some specimens with high fly ash contents had such low strengths that they could not be handled. Although strength of FA specimens were not measured, very low strength of high level fly ash mixes led to handleability issues.

iv. By providing additional lime and calcium sulphate sources for the reactions of CSA cement, more control over the initial setting times and strength may be obtained such that strength might be increased as well as optimum fly ash levels in ULFC mixes.

v. Longer collapse times may indicate the influence of fly ash on stability proving the hypothesis in Chapter 4 that utilisation of finer particles improve bubble stability.

vi. Initial setting times seemed to be governed by CSA cement but mix temperature (due to fast reaction of CSA) and the sulphate sources in fly ash may have an effect on hindering the retarding effect of fly ash.

Bubble size and microstructure

i. In 200 and 300 kg/m³ density mixes cement contents are low, thus not providing sufficient cement particles to fully surround the bubbles. Therefore, once the combined cement fineness is increased at a given cement content with the inclusion of fly ash, sufficient cement particles are provided to surround the bubble surfaces resulting in decreased bubble diameters.

ii. Besides the effect provided by the fineness of fly ash, fast initial setting time of 50%PC/10%CSA/40%FA2 combination is also thought to have an effect on reducing the bubble size. Therefore, average bubble size was found to decrease by up to 26% and 31% for D200 and D300 mixes respectively.

iii. The 28-day microstructure of both D200 and D300 foamed concretes with fly ash contents up to 40% by mass was observed to be comparable with non-fly ash mixes but slightly weaker.

iv. Fly ash contents greater than 40% by mass resulted in less dense microstructure in comparison to lower addition levels.

v. Significant improvement in the microstructure of long-term (6 months and beyond) fly ash foamed concretes was observed at all fly ash levels; the bubble walls became denser, the cracks got finer and the holes got smaller in the bubbles, compared to 28-day microstructure.

vi. Additional lime and calcium source (for CSA cement to react) potentially increase the strength, by improving the microstructure of fly ash foamed concretes.

Environmental impact

i. Due to the minimum cement content of 300 kg/m^3, low/high density foamed concretes produced with 100%PC have considerably high eCO_2 (275 kg CO_2/m^3).

ii. The reduction in cement contents of ULFC mixes resulted in a decrease of up to 67% in eCO_2, in comparison to high/low density mixes.

iii. The addition of fly ash at a rate of 40% by mass in order to replace the PC resulted in a 39% to 42% reduction in eCO_2 at all foamed concrete densities.

iv. There is a 75% reduction in eCO_2 when 100%PC conventional foamed concrete (eCO_2:275 kg CO_2/m^3) is compared to D200 40%FA mix (eCO_2: 70 kg CO_2/m^3). This can lower the high environmental impact of foamed concretes reported in BRE (2004) due to the reduced cement and PC contents of ULFCs.

v. According to the Magcon (minimal or no primary aggregate content) pilot study (BRE, 2004), elimination of primary aggregate content in ULFC, provides further advantages on reducing the environmental impact by lowering the minerals/primary aggregate extraction impacts.

CHAPTER 7

7. INSULATION PROPERTIES

7.1 INTRODUCTION

Operational energy use and corresponding carbon dioxide emission of the buildings represent their environmental impact regardless of the type of materials used in the construction. One of the most energy demanding operational use is heating that result in considerable carbon footprint. On the other hand, environmental, airborne and impact noise have been causing significantly high social impact, disturbing the health and comfort of people. Consequently, increasing number of requirements have been specified by the regulations such as Building Regulations Part L (Conservation of Fuel and Power) and Part E (Resistance to the Passage of Sound) as well as European Union Construction Products Regulations in order to improve the insulation capacity of the buildings. Therefore, construction products and buildings are expected to be thermo-acoustically insulating maintaining the performance, cost and sustainability.

Foamed concrete is a relatively cheap, sustainable and inorganic material which can be an alternative to conventional insulating materials such as expanded polystyrene foam and mineral wool. Owing to its cellular nature, foamed concrete is expected to have good thermal insulation and sound absorption capacity. While thermal insulation properties of conventional foamed concretes are well-established, there is little information in the literature regarding the sound insulation behaviour of foamed concrete. Current study intends to evaluate the insulation performance of a range of foamed concretes in terms of thermal conductivity, sound absorption and sound transmission loss.

As reported in Chapter 3, thermal conductivity of foamed concrete was evaluated by using a modified test apparatus and the sound insulation performance was not assessed by using the 'conventional' reverberation room method. Moreover, it was not possible to calculate a single value to reflect the sound absorption and transmission loss performance of foamed concrete. Therefore, it is reasonable to name the data obtained 'indicative' (e.g indicative thermal conductivity).

7.2 Thermal insulation

Increasing emphasis on energy efficient design has increased the popularity of thermally insulating materials as well as their competitiveness. On the other hand, increasing demand for the utilisation of sustainable construction products has been increasing the pressure on the manufacturers to produce high performance, durable and lightweight insulating materials. As an inorganic, durable, incombustible and insect resistant material (Jones and McCarthy, 2005a) which can be produced with secondary materials and reused at the end of its service life (Jones et. al, 2009; 2012), foamed concrete is a good alternative to many other insulation materials as well as providing cost benefits. Therefore thermal conductivities of a range of foamed concretes were measured to assess their thermal insulation capacity.

7.2.1 Thermal conductivity

Earlier studies showed that foamed concrete exhibits excellent thermal insulation properties that improve with decreasing plastic density and vary with different material combinations (Giannakou and Jones, 2002; Demirboğa and Gül, 2003; Jones and McCarthy, 2005c; Othuman and Wang, 2011, Wei et. al, 2013). With the expectation of obtaining an improved thermal insulation performance, current study evaluated the thermal conductivity of ultra-lightweight foamed concretes (ULFCs) as well as the influence of different material combinations on the performance. Moreover, the data was analysed in relation to the microstructure of the corresponding foamed concrete.

Foamed concretes with plastic densities ranging from 1000 down to 200 kg/m^3 were tested with the main focus given to ultra-lightweight foamed concretes of D300 and D200. D150 foamed concretes could not be tested as the test specimens were fractured due to low strength. Table 7.1 summarises the different material combinations used and their corresponding names for all the foamed concretes considered. Standard deviation of thermal conductivity measurements was averaged as 0.02.

Table 7.1 Material combinations used for thermal conductivity

Material combinations	Combination name	Plastic density, kg/m³
100% PC	PC	1000, 600, 500
100% PC2	PC2	200
95% PC : 5% CSA	5% CSA	200, 300
90% PC : 10% CSA	10% CSA	200, 300
95% PC : 5% CSA + 0.05% CNTs*	5% CSA + CNT	200
85% PC : 5% CSA : 10% SF	SF (silica fume)	200
60% PC : 10% CSA : 30% FA1,2	30% FA1,2 (fly ash)	200 (FA2 only), 300
50% PC : 10% CSA : 40% FA2	40% FA2 (fly ash)	300
20% PC : 10% CSA : 70% FA2	70% FA2 (fly ash)	300

* Addition of 0.05% by mass of total cement content

Effect of plastic density

Thermal conductivity of foamed concrete is largely affected by the plastic density, hence the volume of air within the mix (Narayanan and Ramamurthy, 2000; Giannakou and Jones, 2002; Othuman and Wang, 2011) due to the ultra-low thermal conductivity of air (0.025 W/mK at 25°C; Kreith and Bohn; 2011). Therefore, a range of foamed concretes were compared to evaluate the influence of ultra-low plastic density on thermal conductivity.

Increased air volume of ultra-low density foamed concretes contributed to the thermal insulation capacity (Figure 7.1). This behaviour is mainly attributed to the low thermal conductivity of air which is the lowest among the thermal conductivity of other constituents of foamed concrete (Kim et. al, 2003). Therefore, when the air content dominates over the solids content of foamed concrete, significant decrease in the thermal conductivity is observed.

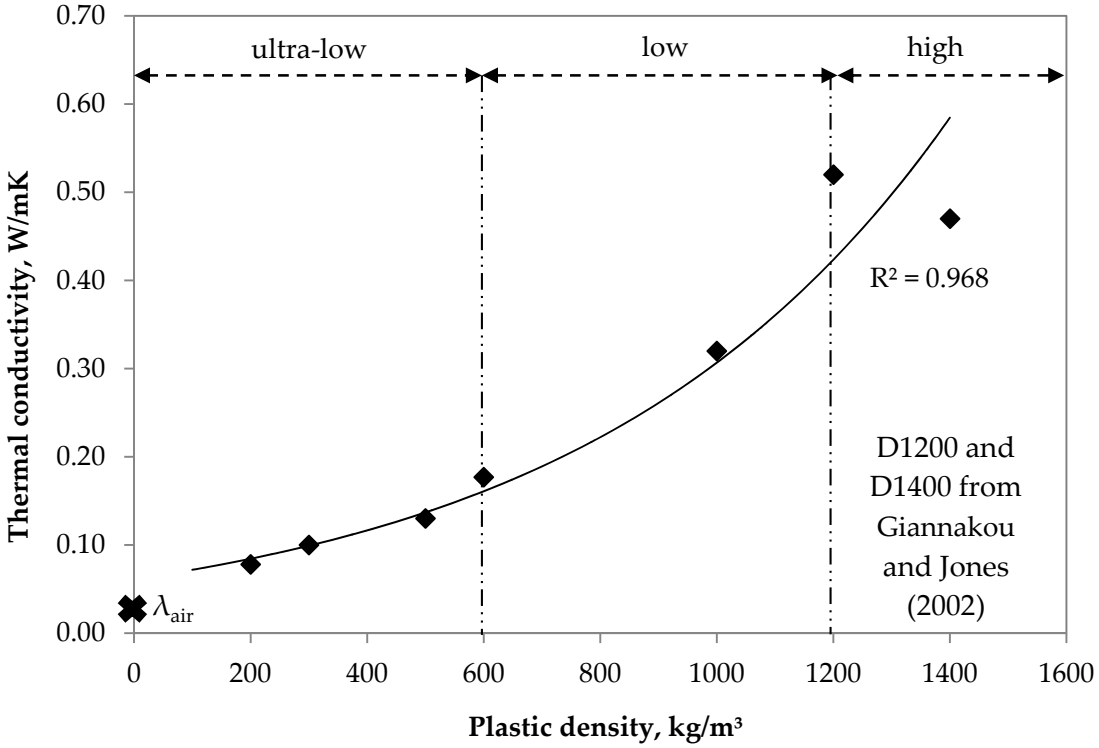

Figure 7. 1 Influence of plastic density on thermal conductivity of FC

As shown in Figure 7.1 thermal conductivity values of foamed concretes with plastic densities from 200 to 1400 kg/m³ ranged between 0.073 and 0.52 W/mK. Clearly, the decrease in the thermal conductivity with decreasing density is more significant at low and high density ranges as the difference in the air contents of densities considered in the these ranges are bigger compared to ultra-low density range mixes (air contents are given in Section 3.4, Table 3.2).

Moreover, it is possible that, the equipment used is unable to efficiently measure the changes in the thermal conductivity of ULFCs as the density range of the specimens approaches to the density of the insulating material (styrofoam) lining the modified hot-box (test equipment used was described in Section 3.6.2). Due to the similar densities of the test specimen and the surrounding material, heat may be lost to the surrounding insulating material, yielding higher indicative thermal conductivities than the real values. This will further be discussed under the title of discussions on the test method.

Figure 7.2 illustrates the changes in the microstructure with decreasing foamed concrete density. Therefore, increased air volume with decreasing plastic density resulted in less solid area for the heat to conduct through. Moreover, decreased bubble wall thickness (resulting from higher volume of air and bigger bubble sizes) in lower densities also restricted the conduction of heat. However, with an adverse effect, for a given foamed concrete density, presence of bigger bubbles (Narayanan and Ramamurthy, 2000) and more holes in the bubbles in ULFCs could increase the thermal conductivity.

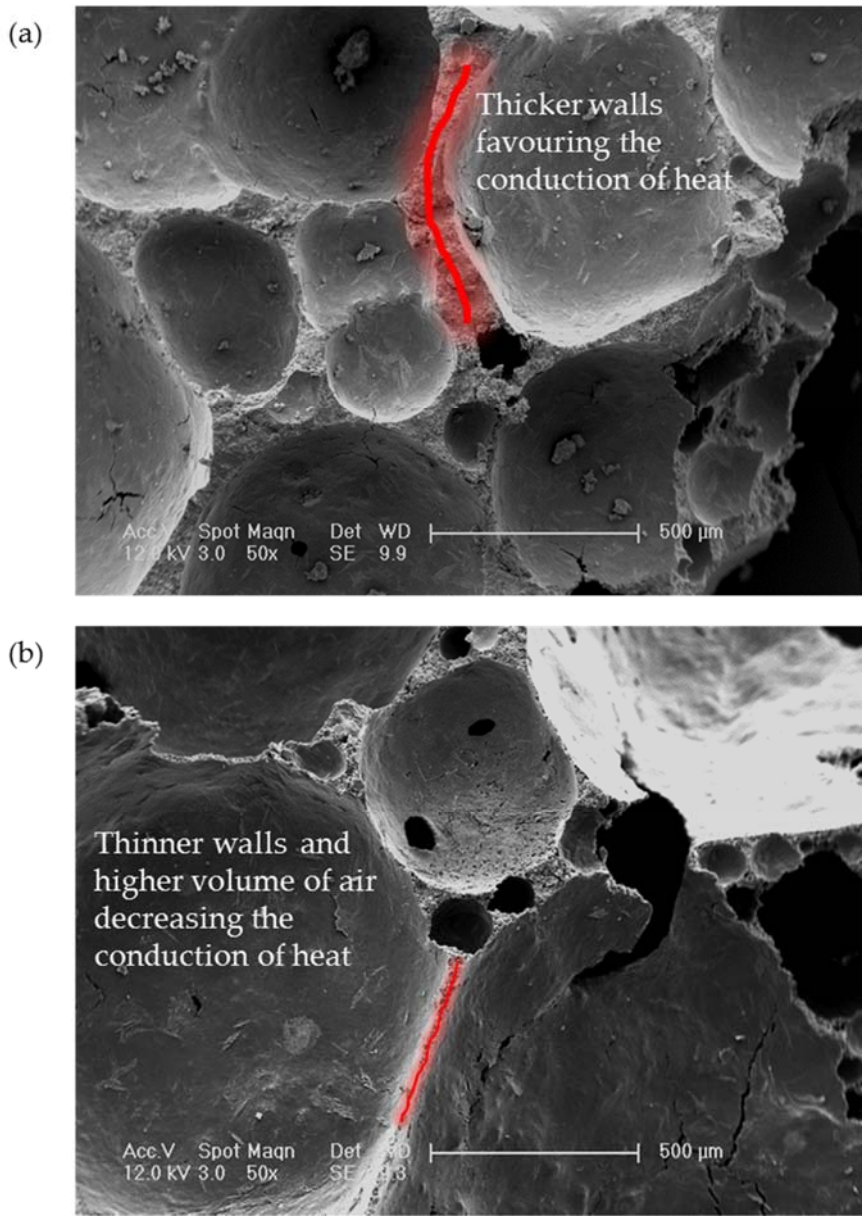

Figure 7.2 Microstructure of (a) D500 (100% PC) and (b) D200 (95%PC/5%CSA) FCs

The thermal conductivity values were found to be higher than the data provided by Wei et. al, (2013) for a given foamed concrete density. This was mainly attributed to the higher testing temperature employed (0-40°C) and smaller bubble size of the specimens used by Wei et. al (2013), exhibiting lower thermal conductivity values (Kim et. al, 2003; Narayanan and Ramamurthy, 2000).

Relationship between plastic density and thermal conductivity of foamed concrete could be approximated ($R^2 = 0.97$) by using Equation 7.1. Figure 7.1 shows that, it is possibly more reliable to employ Equation 7.1 for predicting the thermal conductivity of low and ultra-low density range foamed concretes.

$$\lambda = 0.061\, e^{0.0016(\text{Plastic density})} \qquad \text{Equation 7.1}$$

However, it must be noted that predictions of indicative thermal conductivity should not solely depend on plastic density (i.e air content). A theoretical model or equation should consider the effect of other mix constituents, properties of the materials used, moisture content and bubble size/distribution of the specimens as well as the testing conditions such as temperature.

Effect of constituents

Different constituent materials are known to influence the thermal conductivity behaviour. Therefore, a focus was given to assess the effect of various materials on the thermal conductivity of ultra-low density foamed concretes D200 and D300. Given the lowest density under consideration, and perhaps the best thermally insulating foamed concrete (because of the higher volume of air present in the mix), D200 foamed concretes produced with wider range of material combinations than D300 were tested in order to optimise the best thermally insulating mix. Material combinations and specified plastic densities given in Table 7.1 were utilised to evaluate the thermal conductivity of a range of foamed concretes.

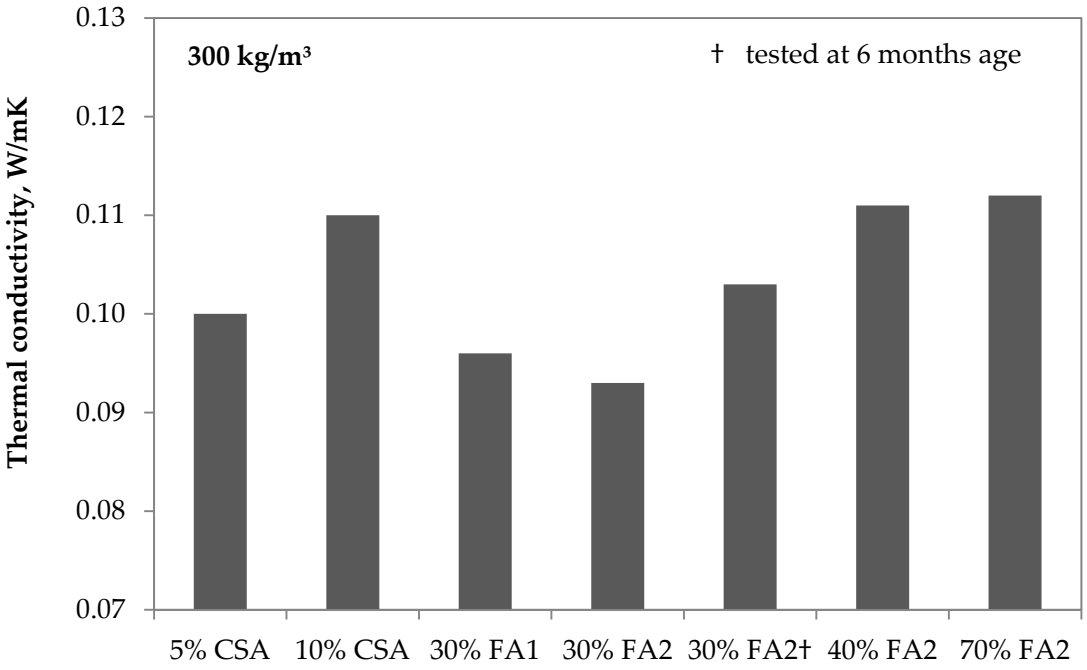

Figure 7.3 Influence of various material combinations on thermal conductivity of D300

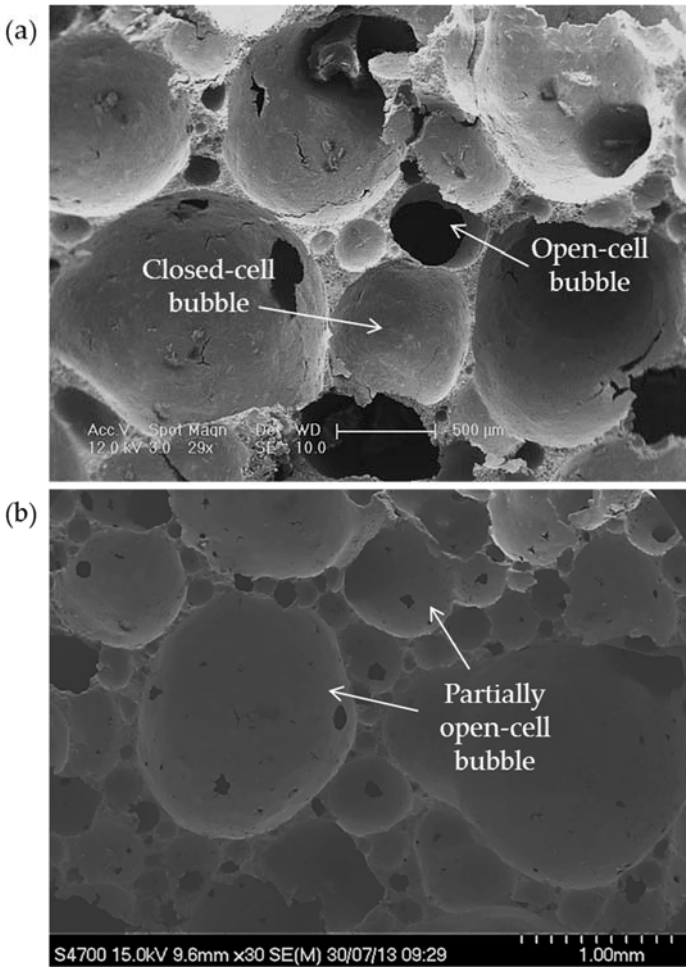

Figure 7.4 Microstructure of (a) 95%PC/5%CSA and (b) 90%PC/10%CSA D300 FC

Figure 7.3 shows the behaviour of D300 foamed concretes produced with various material combinations. The thermal conductivity values for D300 ranged from 0.093 to 0.112 W/mK. 5% CSA mix was found to have a thermal conductivity of 0.1 W/mK which is the lowest of D300 non-fly ash mixes. Addition of 5% more CSA cement by mass (10% CSA mix) resulted in an increase in thermal conductivity by 10%. This behaviour may be attributed to the slightly different microstructure of 10% CSA mix which seemed to have higher number of holes in the bubbles (open/partially open-cell bubbles which leads to higher thermal conductivity; Yakovlev et. al, 2006; Lyons, 2010) (Figure 7.4), adversely affecting the thermal insulation performance of D300 foamed concrete.

The lowest thermal conductivity for D300 was obtained by the 28-day 30% FA2 mix, which was followed by 30% FA1 mix. Comparing 30% FA1 and FA2 mixes to 10% CSA mix, there is 13% and 15% reduction (respectively) in the thermal conductivity provided by the utilisation of fly ash. This expected behaviour of fly ash mixes over the non-fly ash mixes was possibly the consequence of low particle density of fly ash (2200 kg/m^3) in comparison to PC (3150 kg/m^3) and thermal conductivity of fly ash (UKQAA, 2003), given the air-filled nature of fly ash cenosphere cores (Giannakou and Jones, 2002; Demirboğa and Gül, 2003; Ramamurthy et. al., 2009). Moreover, larger surface area of fly ash may increase the heat flow paths and increased interface area may act as a thermal barrier decreasing the amount of heat transfer (Xu and Chung, 2000).

Moreover, better thermal insulation performance of fly ash specimens may be attributed to the bubble size of these foamed concretes. Bubble size is known to have an effect on the thermal conductivity such that the smaller the bubbles the lower the thermal conductivity (Narayanan and Ramamurthy, 2000) for a given density of concrete. As fly ash mixes were found to have smaller average bubble size in comparison to non-fly ash mixes (as presented in Section 6.3), it is likely that bubble size also had an effect on reduction of the thermal conductivities obtained on the 30% fly ash mixes.

Given the long-term hydration of fly ash, D300 30% FA2 mix was tested after 6 months sealed-curing in order to evaluate the effect of age on thermal conductivity of fly ash foamed concretes. Consequently, 11% increase in the indicative thermal conductivity of 30% FA2 mix was observed when tested at 6-months age. This increase is attributed to the

improvement and densification observed in the microstructure of all long-term fly ash concretes as discussed in Section 6.4.

Figure 7.5 shows the differences in the microstructure of 28 days and 8 months old 30% FA1 D300 specimens. Although the long-term thermal conductivity data was only provided for 30% FA2 mixes, Figure 7.5 is an example of the enhanced microstructure of all fly ash specimens in long-term. Denser wall structure of long-term fly ash samples provides ease for the heat transfer in comparison to the more open and porous microstructure of 28-day fly ash concretes that are still at the early stages of hydration process. This is because more porous wall structures comprising higher volume of air results in less conduction of heat (Kim et. al, 2003. As a result, data obtained from the 6-month old fly ash specimens are considered to reflect the real behaviour of fly ash foamed concretes.

Furthermore, D300 foamed concretes with higher fly ash contents of 40% and 70% were also tested to evaluate the influence of increased fly ash contents. It was found that additional fly ash adversely affected the thermal conductivity of D300, such that 28 days 40% FA2 mix delivered 19% higher thermal conductivity in comparison to 28 days 30% FA2 mix. Although further reductions in the thermal conductivity with increased fly ash content was expected, the data indicated that there might be an optimum fly ash content to obtain the best insulation performance as also concluded by De Rose and Morris (1999).

Figure 7.6 illustrates the performance of various material combinations for D200 foamed concrete. Thermal conductivities of various material combinations for D200 ranged from 0.073 to 0.095 W/mK. Out of three 5% CSA mix with different w/c ratios, the lowest thermal conductivity (0.078 W/mK) was obtained from the mix with w/c ratio of 0.5. Decreased w/c ratio (from 0.50 to 0.45) led to increased conduction of heat possibly due to the higher thermal conductivity of cement (Kim et. al, 2003), and decreased porosity resulting from a denser microstructure (McCarthy, 2004).

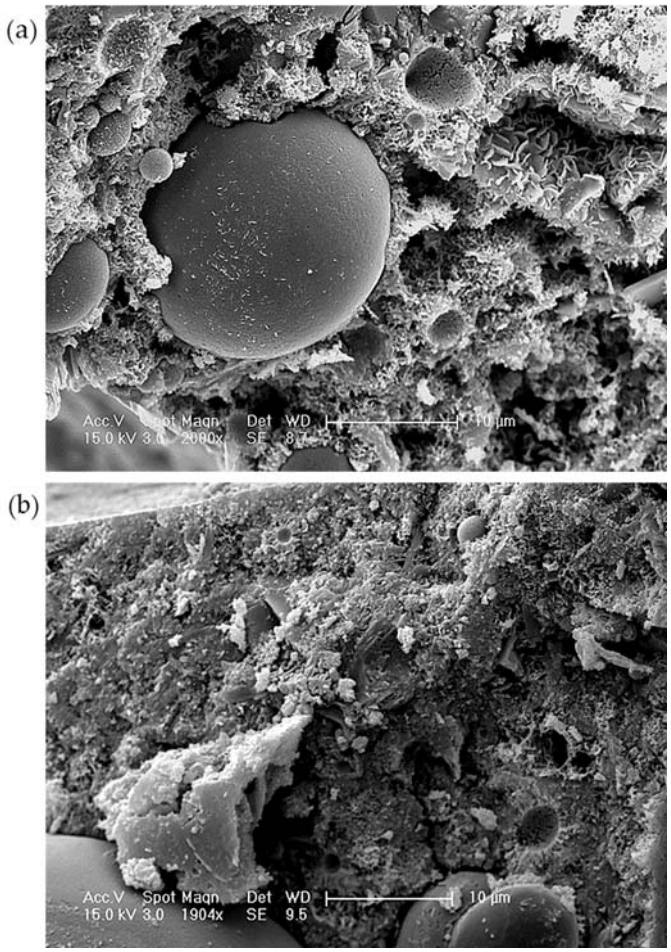

Figure 7. 5 Typical microstructure of D300 30% FA1 FC at (a) 28 days and (b) 8 months old

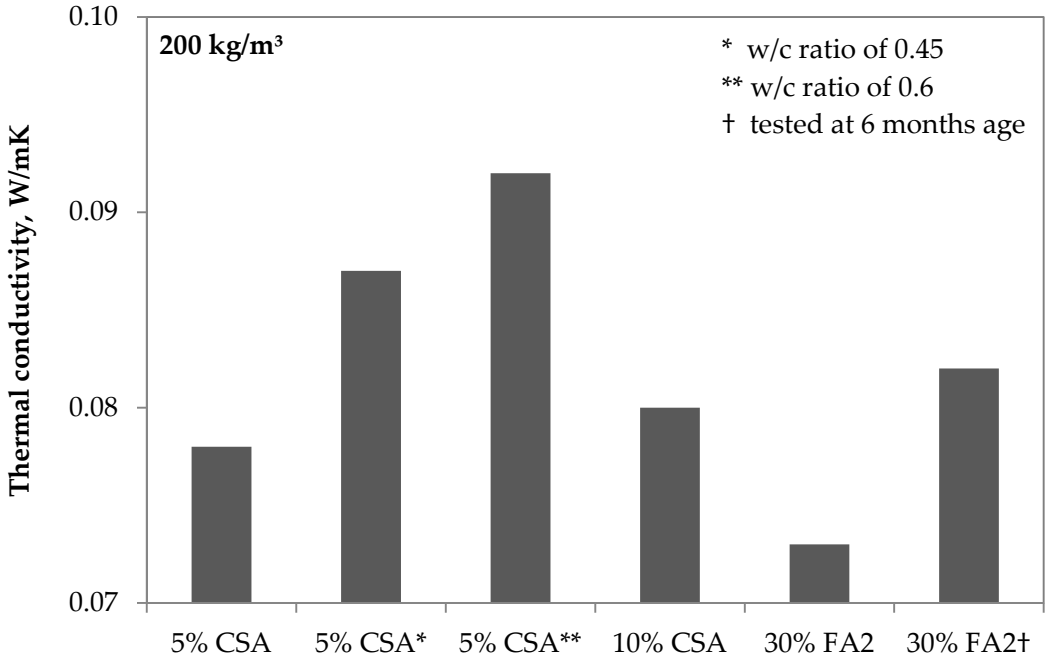

Figure 7.6 Influence of various material combinations on thermal conductivity of D200

On the other hand, increased w/c ratio (from 0.50 to 0.60) exhibited an unexpected increase in thermal conductivity as higher w/c ratios lead to more porous hence less conductive structure. As CSA cement requires higher w/c ratio (in comparison to PC) for complete hydration (Winnefeld and Lothenbach, 2010) the employed w/c ratio of 0.50 may not be enough for the complete hydration. Thus increased w/c ratio may lead to complete hydration of CSA resulting in denser, hence more conductive microstructure. However, there is a need for detailed further work on the influence of w/c ratio on the thermal conductivity of ULFCs. Moreover, it is possible that w/c ratio of 0.60 yielded larger bubble sizes increasing the thermal conductivity. On the other hand, similar to D300, D200 10% CSA mix was also found to have higher thermal conductivity in comparison to 5% CSA mix, but with a slight difference of 2.6%.

When fly ash mixes are considered, utilisation of 30% fly ash (by mass) resulted in almost 9% decrease in thermal conductivity (from 0.08 to 0.073 W/mK) compared to 10% CSA mix. Furthermore, thermal conductivity of 6 months old D200 fly ash concrete was found to increase by 12% compared to 28 days old fly ash foamed concrete. As discussed earlier, it is not realistic to use the thermal conductivity values obtained for 28-day fly ash mixes for design, as the thermal conductivity will increase in long-term with improving (denser) microstructure.

Further investigations on the influence of material combinations on thermal conductivity were carried out with the utilisation of PC2 (an alternative material discussed in Section 5.3), carbon nanotubes (CNTs) and silica fume (SF) (of which the microstructure images are presented in Appendix B). It must be noted that, during the production of these foamed concretes, the foam was observed to drain faster (before incorporating with the base mix) and exhibit a weaker structure, however, there was no instability observed in the mixes. However, as the assessment of these mixes was not the main focus of this study, the mixes were not repeated.

Comparing the 5% CSA mixes in Figure 7.6 and Figure 7.7, the difference in the thermal conductivity values (0.078 and 0.095 W/mK respectively) was attributed to the quality of the foam used for the production of the mixes. Lower quality of the foam (which leads to faster drainage and hence coalescence) potentially led to more 'open' bubble

microstructure in the latter mix, thus causing a slight increase in the density. Therefore, considering the difference in the quality of the foam the mixes used for further investigations were only compared among themselves.

D200 5% CSA+CNT mix was produced in an attempt to decrease the indicative thermal conductivity as suggested by Yakovlev et. al (2006). Consequently, addition of CNTs resulted in almost 10% decrease in thermal conductivity similar to the results obtained by Yakovlev et. al (2006). The improvement in the thermal insulation capacity was attributed to the ability of CNTs to reinforce the perforated foamed concrete bubbles (forming closed bubbles). Although, CNTs provide an advantage on improved thermal insulation, the difficulty of dispersing the CNTs to provide even distribution within the mix (as reviewed in Section 2.3.3) and their high cost make them impractical for industry applications.

Given the known effect of silica fume on reducing the thermal conductivity (Xu and Chung, 2000; Demirboğa and Gül, 2003), influence of silica fume on the ultra-low density foamed concretes was assessed. Thermal conductivity decreased by almost 14% in comparison to 5% CSA mix. The reduction was mainly attributed to the low thermal conductivity of silica fume, its ability to increase the specific heat and increased interface between silica fume and cement matrix (like in fly ash) due its high specific surface area (Xu and Chung, 2000). However, similar to CNTs, using silica fume in industry applications can be costly hence impractical.

Finally, the utilisation of PC2 (at 0.45 w/c ratio) yielded indicative thermal conductivity of 0.092 W/mK which is higher than that of D200 5%CSA+CNT and SF mixes. As analysed in Section 5.3, PC2 produced foamed concrete with dense bubble wall microstructure which potentially increases the heat conduction. Moreover slightly low w/c ratio (0.45 instead of 0.50 as mentioned in Section 5.3) used may be the cause of higher thermal conductivity.

Although the trends obtained in this further investigation are correct, the degree of improvement and the thermal conductivity values obtained with the incorporation of CNTs and silica fume may have some errors given the low quality of foam during the production of these mixes. Therefore, further research needs to be carried out on these mixes.

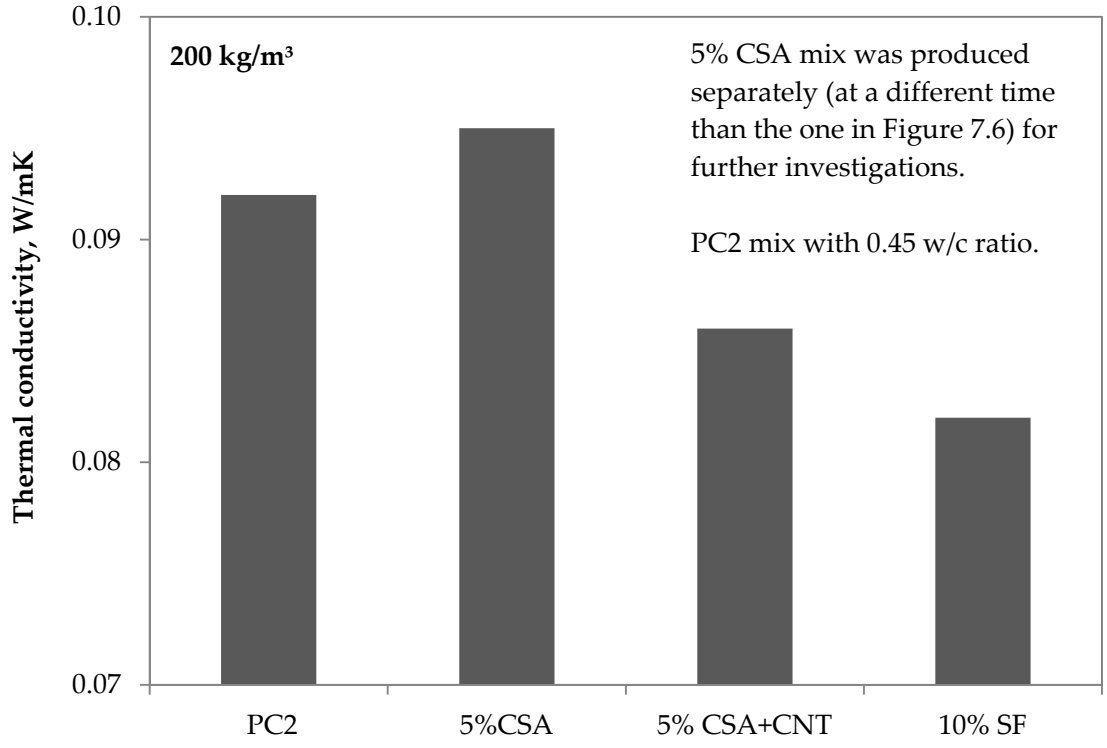

Figure 7.7 Further investigations on influence of different material combinations on indicative thermal conductivity of D200 foamed concrete

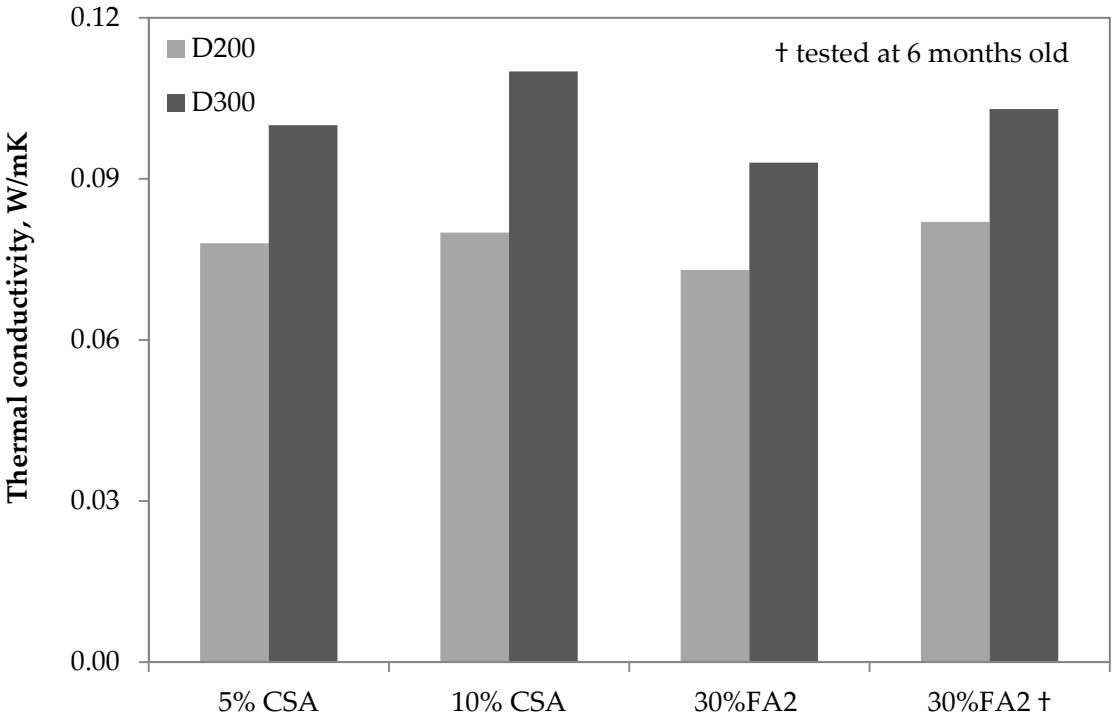

Figure 7.8 Comparison of D200 and D300 mixes

Figure 7.8 compares the performance of D200 and D300 foamed concretes produced with PC/CSA and PC/CSA/FA blends. Given the high air content of D200 (≈ 90% by volume), it seems that the air content dominates over the other parameters influencing the indicative thermal conductivity, resulting in smaller changes in the performance when various material combinations are applied.

Other properties

Although the effect of different cements on thermal conductivity was examined, water/cement ratio, fine aggregate fraction and type of admixture also have an effect on thermal insulation as they affect the hydration reactions and products, hence the microstructure of concrete (Kim et. al, 2003).

Besides air content, constituents of the mix, moisture content and temperature also have an effect on thermal conductivity (Kim et. al, 2003). Given the high thermal conductivity of water (0.61 W/mK as noted by McCarthy, 2004) concretes with higher moisture contents exhibit higher thermal conductivities (Kim et. al, 2003) such that 1% (by mass) of increase in the moisture increases the thermal conductivity by 42% (Narayanan and Ramamurthy, 2000). On the other hand, it was reported that increased temperature of the concrete results in lower thermal conductivity.

In this study, moisture content was not monitored as all the specimens were oven-dried to a constant mass at 30°C (as described in Section 3.6.2) and the results were compared on this basis. Moreover, only one temperature setting (30°C on the hot side and 5°C on the cold side) was used for testing the specimens therefore, influence of concrete temperature on the thermal conductivity was not examined.

Although it was reported that the age of specimens were not considered to affect the thermal conductivity, except early ages like 2 days (Kim et. al, 2003), the situation is possibly different in fly ash concretes (McCarthy, 2004). Given the long-term hydration of fly ash, some of the specimens containing fly ash were also tested at later ages (6 months). Consequently, it was found that thermal conductivity of fly ash specimens increases in long-term.

Like air volume and porosity, bubble characteristics such as size, shape and distribution also affect thermal conductivity (Narayanan and Ramamurthy, 2000). While the presence of ellipsoidal voids were reported to yield more rigid and less thermally conductive materials than spherical voids (Malou and Cabrillac; 1999), finer bubbles were reported to result in lower thermal conductivity (Narayanan and Ramamurthy, 2000). Although the influence of these aspects was not examined, it was observed that fly ash specimens which exhibited lower thermal conductivities possess smaller bubbles. As the microstructure, bubble size, shape and distribution of foamed concretes were observed to change at ultra-low density levels as well as with the incorporation of different constituents, further work is required to analyse the influence of bubble characteristic and microstructure in detail.

Discussions on the test method

As reported by McCarthy (2004) there are concerns about the test method regarding the conditioning of the test specimens. Low temperatures (30°C instead of 105°C) were used while conditioning the specimens in order to prevent any microstructural damage due to rapid drying (Alexander and Mackechnie, 1999). However, occurrence of micro-cracking due to drying shrinkage could still occur (observed to be higher in ULFCs) leading to 'disconnected' regions of paste that increase the thermal conductivity.

Moreover, there are some concerns about the test equipment used while testing the ultra-low density foamed concretes. Compared to high/low density foamed concretes, densities and indicative thermal conductivities of ULFCs are closer to those of styrofoam (thermal conductivity value of 0.033-0.040 W/mK; Lyons, 2010) that is used to insulate the test apparatus to prevent the heat losses (as described in Section 3.6.2). It is possible that, due to the closer density and thermal conductivity values of ULFCs and styrofoam, the heat could potentially be lost to the surrounding (possibly into the styrofoam) hence resulting in higher thermal conductivity values for ULFCs.

As the main focus was on the ULFCs which do not comprise fine aggregates, influence of fine aggregate fraction was not examined. Although specimens produced with different cement types and combinations were tested, influence of heat of hydration and corresponding thermal cracks (which may increase the thermal conductivity; Kim et. al, 2003) was not examined in relation to thermal conductivity.

7.3 Sound insulation

Recently, increasing level of disturbance caused by the environmental noise (due to urbanisation, increased demand on the use of motorised transport and inefficient urban planning; EC, 2011b) as well as airborne (e.g people's speech) and impact sound (e.g people walking) in dwellings (BRE, 2014) is a rising social issue. This issue can be solved by correct design of new buildings or installing sound insulation treatments to the existing buildings.

Given the porous and relatively open-cell structure of ultra-low density foamed concretes (as discussed in Chapter 5 and 6) they are expected to exhibit good sound absorption performance. On the other hand, foamed concretes are not considered to exhibit good transmission loss (Ramamurthy et. al, 2009) as transmission loss (or sound reduction index) is mainly the function of weight of the material per unit area (NRCC, 1990; Arenas and Crocker, 2010). Therefore, sound absorption coefficient and transmission loss of a range of foamed concretes were measured to evaluate the sound insulation properties of foamed concretes hence the potential to be used as an alternative, sustainable material providing further benefits in addition to that have been discussed in Section 7.2.

7.3.1 Sound absorption coefficient

Sound absorption in porous materials occurs through the vibration of air molecules at the surface and within the pores of the material and hence losing part of their original energy upon being exposed to incident sound waves. The energy loss occurs, as part of the energy of the air molecules is converted into heat as a result of thermal and viscous losses in the walls of the internal pores and tunnels of the porous material (Kutruff, 2000, Arenas and Crocker, 2010).

There are numerous parameters that affect the sound absorption capacity of a material. The most common parameters are listed as porosity (pore size, characteristic, orientation and closed/open pores), tortuosity, air flow resistance, viscous thermal characteristic length and thermal characteristic length (Mosanenzadeh et. al, 2013). Additionally, surface texture (the rougher the surface, the higher the sound absorption) and the exposure level of

interconnected voids and pores to the outside air affect the sound absorption of materials (Kutruff, 2000). Moreover, Arenas and Crocker (2010) emphasised the influence of frequency, material composition and thickness, surface finish and method of mounting (with/without air gap between sound absorbing layers or between the wall and insulating layer) on the sound absorption capacity. Finally, Dong et. al (2009) reported that combination of low modulus and high porosity yields good sound absorption capacity.

Standing wave apparatus was used to determine the sound absorption coefficient, α, which ranges from 0 to 1, where 0 indicates no absorption and 1 indicates 100% sound absorption. Sound absorption coefficient at frequencies ranging from 125 to 4000 Hz was measured on specimens with thicknesses of 20, 50 and 70mm in accordance with ISO 10534-1:1996. A range of densities were considered in order to determine the influence of density on the sound absorption capacity of foamed concrete. Therefore, plastic densities ranging from 200 to 600 kg/m^3 were analysed with a greater focus on ultra-low density foamed concretes (D200 and D300).

Further investigations were carried out on 300 kg/m^3 foamed concretes produced with utilisation of fly ash, in order to evaluate the effect of fly ash on the sound absorption. Finally, 200 kg/m^3 foamed concretes produced with nano-materials, silica fume (SF) and carbon nanotubes (CNTs), were tested with the expectation of increasing the tortuosity and the surface area within the foamed concrete bubble walls hence the sound absorption. Foamed concrete densities and material combinations tested are given in Table 7.2. The data provided a comparison in terms of plastic density, specimen thickness and utilisation of fly ash as well as nano-materials.

Table 7.2 Foamed concretes tested for sound absorption coefficient

Density (kg/m³)	Material combinations	Combination name
600	100% PC	D600
500	100% PC	D500
300	95% PC : 5% CSA	D300
	60% PC : 10% CSA : 30% FA1	D300 FA (fly ash)
200	95% PC : 5% CSA	D200
	85% PC : 5% CSA : 10% SF	D200 SF (silica fume)
	95% PC : 5% CSA + 0.05% CNTs*	D200 CNT

* 0.05% by mass of total cement

Effect of plastic density

Figure 7.9 illustrates the comparison of sound absorption coefficient of 70, 50 and 25mm thick specimens of plastic densities of 200 to 600 kg/m^3. Overall foamed concretes with lower densities exhibited higher sound absorption capacity at frequencies 500 Hz and below with the exception of D600 foamed concretes. This behaviour is attributed to the increased porosity and more open microstructure as well as open-cell bubbles of ultra-low density foamed concretes (shown in Figure 7.4). Therefore, the surface area available for the sound energy to be absorbed and converted into heat is increased. Furthermore, owing to the lowest stiffness and possibly the highest porosity value, D200 foamed concretes exhibited a higher sound absorption (Dong et. al, 2009).

On the other hand D600 foamed concretes performed better than D500 foamed concretes. This is thought to be due to the presence of sand in D600, whilst it is eliminated in D500 foamed concretes. As reported by Kim and Lee (2010), sand may increase the tortuosity and flow resistivity so that more sound is absorbed along the path that sound waves travel. Moreover, higher cement content of D500 (as explained in Section 3.4) may yield a denser and smoother bubble wall microstructure compared to D600, thus absorbing less sound.

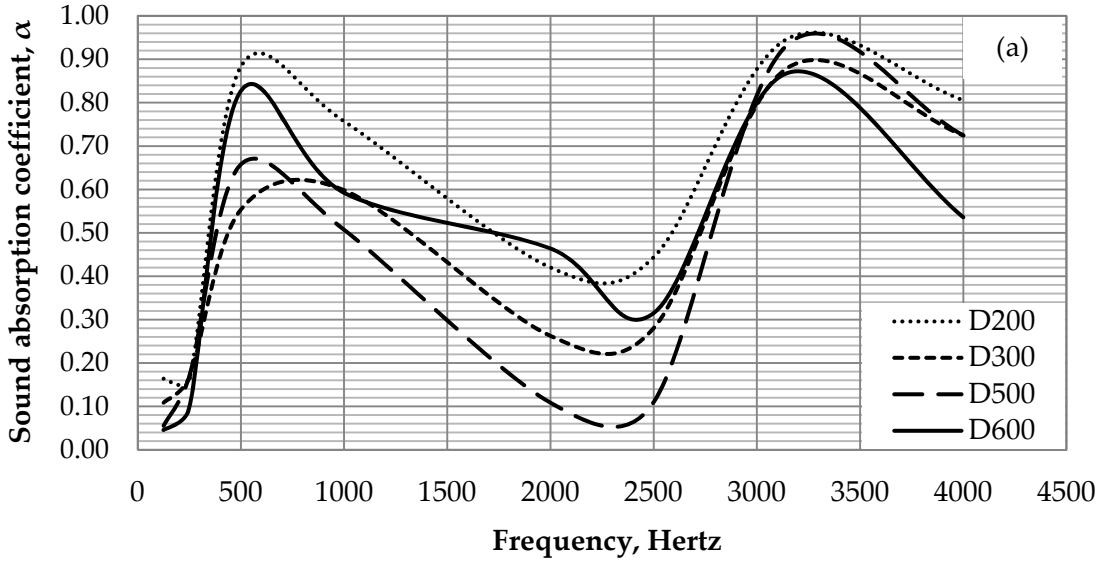

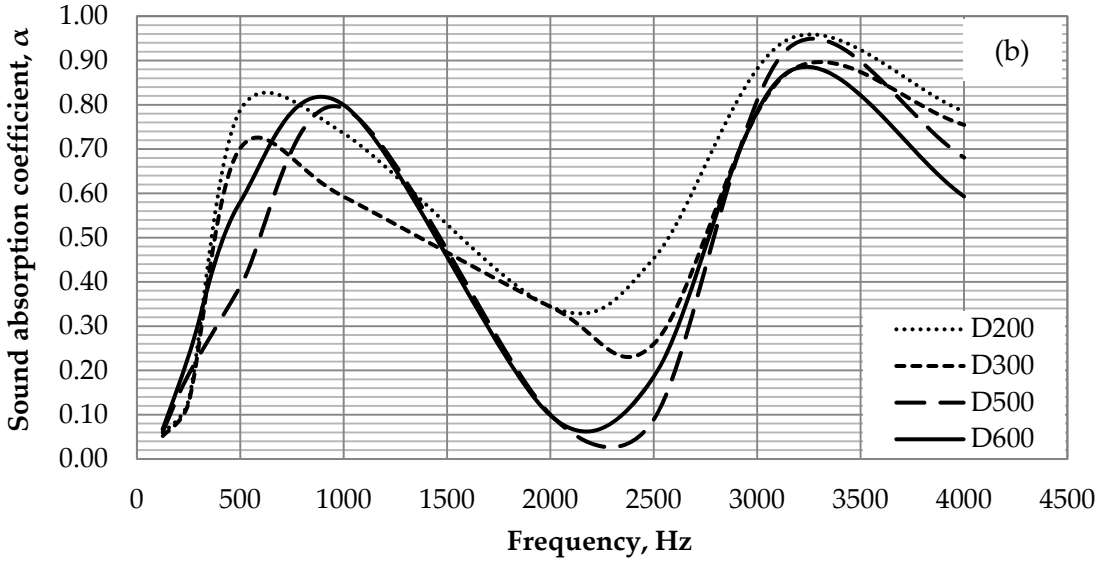

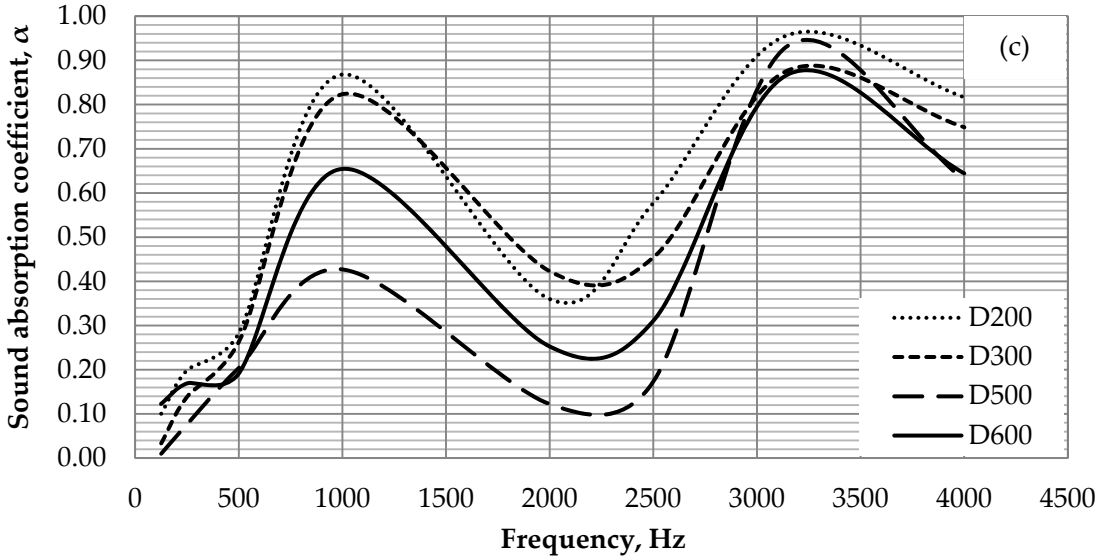

Figure 7.9 Influence of plastic density on sound absorption coefficient in (a) 70mm (b) 50 mm and (c) 25 mm thick specimens

Comparing the foamed concretes tested, D200 foamed concrete exhibited the best performance overall at all thicknesses for the range of frequencies under consideration. However, at very low frequencies, little or no sound was absorbed by any foamed concrete density. This is because most materials are unable to absorb low frequency sounds as a result of their long wavelength (Kutruff, 2000; Berger et.al, 2003; Lyons, 2010). On the other hand, at high frequencies, most materials are able to absorb close to 100% as sound waves at high frequencies have a very small wavelength. Therefore, to absorb low frequencies either an increased material thickness or incorporation of air gap between sound absorbing layers is needed (Kutruff, 2000; Zhang et. al, 2011).

Effect of sample thickness

Comparing different specimen thicknesses, sound absorption coefficient was found to change, but no relationship could be established between thickness and sound absorption coefficient, except D500 foamed concretes. Lack of correlation is mainly attributed to the varying microstructure of the specimens of different thicknesses, due to the difficulties in producing homogeneous small-sized specimens. D500 specimens exhibited increasing sound absorption coefficient with increasing specimen thickness.

Furthermore, the peak sound absorption coefficients occurring around 500-1000Hz frequencies were observed to shift towards higher frequencies with increasing specimen thickness. On the other hand, Laukaitis and Fiks (2006) reported that change in the specimen thickness affect the sound absorption capacity of aerated autoclaved concrete only up to 30-35 mm thicknesses (i.e specimens thicker than this do not exhibit significant changes in the sound absorption capacity).

Effect of porosity and bubble connectivity

Determination of porosity and bubble connectivity was out of the scope of this study. However, CT scanning was carried out on 100mm cubes (images are shown in Appendix B) obtained from preliminary trial mixes to check the porosity and bubble connectivity of a range of foamed concretes as shown in Figure 7.10. Accordingly, over 90% connectivity was obtained for the foamed concretes considered, while porosity was observed to decrease with increasing foamed concrete density.

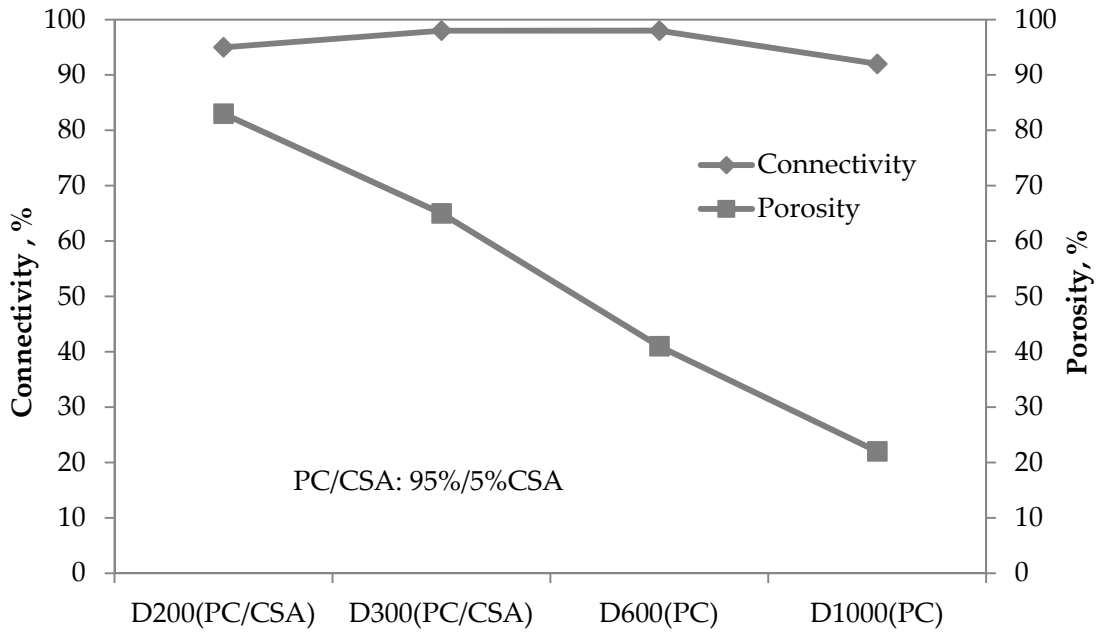

Figure 7.10 Bubble connectivity and porosity measured by CT scanning

Porosity data explains the improved sound absorption behaviour of lower plastic density foamed concretes as it was suggested that higher porosity leads to higher sound absorption (Dong et.al, 2009). Furthermore, high percentages of connectivity of all foamed concrete specimens may be the indication of open cell bubbles which improves the sound absorbing capacity.

Effect of fly ash

D300 foamed concretes produced with the utilisation of 30% fly was tested in order to determine the influence of fly ash on the sound absorption capacity. Figure 7.11 shows the influence of fly ash at various specimen thicknesses. Considering the sound absorption curves show in Figure 7.11, fly ash foamed concretes seemed to absorb more sound than the non-fly ash ones, especially at 70mm thickness. This can be attributed to the potential ability of fly ash cenospheres to increase the tortuosity, in other words the complexity of the path that sound waves follow resulting in higher absorption capacity (Laukaitis and Fiks, 2006). Moreover, Han et. al (2003) and Lee et. al (2011) reported that foams with smaller cell size show higher sound absorption. This statement may explain the better sound absorption performance of fly ash concretes that have smaller bubble size (as discussed in Section 6.3).

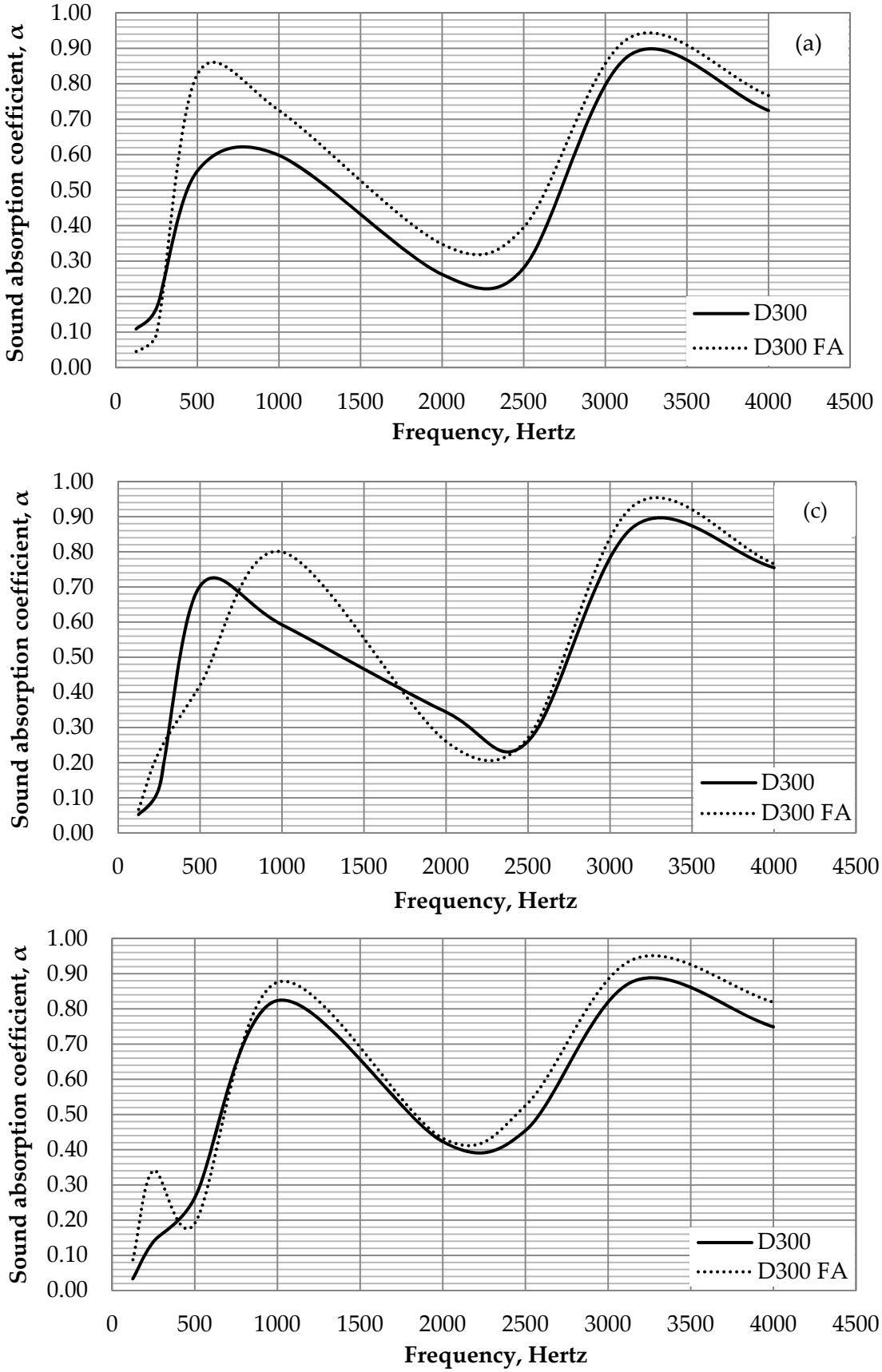

Figure 7.11 Influence of fly ash on the sound absorption of (a) 70mm, (b) 50mm and (c) 25mm thick D300 specimens

Although 70mm thick D300 FA specimens absorbed less sound than D300 specimens at 125 and 250 Hz frequencies, this behaviour was not observed at other thicknesses. Similar to other foamed concretes tested relationship between specimen thickness and sound absorption capacity could not be established.

Effect of nano-materials

Figure 7.12 shows the influence of nano-materials on the sound absorption of D200 foamed concretes with varying specimen thicknesses. Accordingly, in 70 and 50mm thick specimens, incorporation of CNTs in D200 foamed concrete was found to increase the overall sound absorption in comparison to the reference PC/CSA specimen. Like fly ash CNTs may increase the tortuosity of the bubble walls resulting in higher absorption of sound energy. However, in 25mm specimens, sound absorption of D200 CNT mix was only higher than the reference mix at around 1000 and 2500 Hz frequencies. Although CNTs were found to seal the open-cell bubbles and decrease the thermal conductivity (Yakovlev et. al, 2006) as reported in Section 7.2.1, their effect on increasing the tortuosity may be more dominant than sealing the bubbles, thus resulting in higher sound absorption.

On the other hand, D200 SF specimen exhibited the lowest sound absorption overall in comparison to D200 reference and CNT specimens. This behaviour is attributed to the potential ability of silica fume to produce closed cell bubbles (see Appendix B for the microstructure of D200 SF) as supported by the thermal conductivity measurements (Section 7.2.1). Although, D200 SF exhibited the lowest sound absorption over the range of frequencies considered, only at frequencies ranging from 1500 to 3000 Hz it performed better than the reference. Due to its high fineness SF may be expected to yield smaller bubbles hence higher sound absorption as in fly ash specimens, however, it is possible that it formed finer but closed-cell bubbles which do not favour sound absorption.

Overall, no consistent relationship could be established between specimen thickness and sound absorption coefficient of foamed concretes produced with nano-materials. Moreover, incorporation of nano-materials did not provide any significant improvement in the sound absorption capacity except 50mm D200 CNT specimen. However, difficulties to disperse CNTs and their cost paralyse its effect on increasing the sound absorption coefficient.

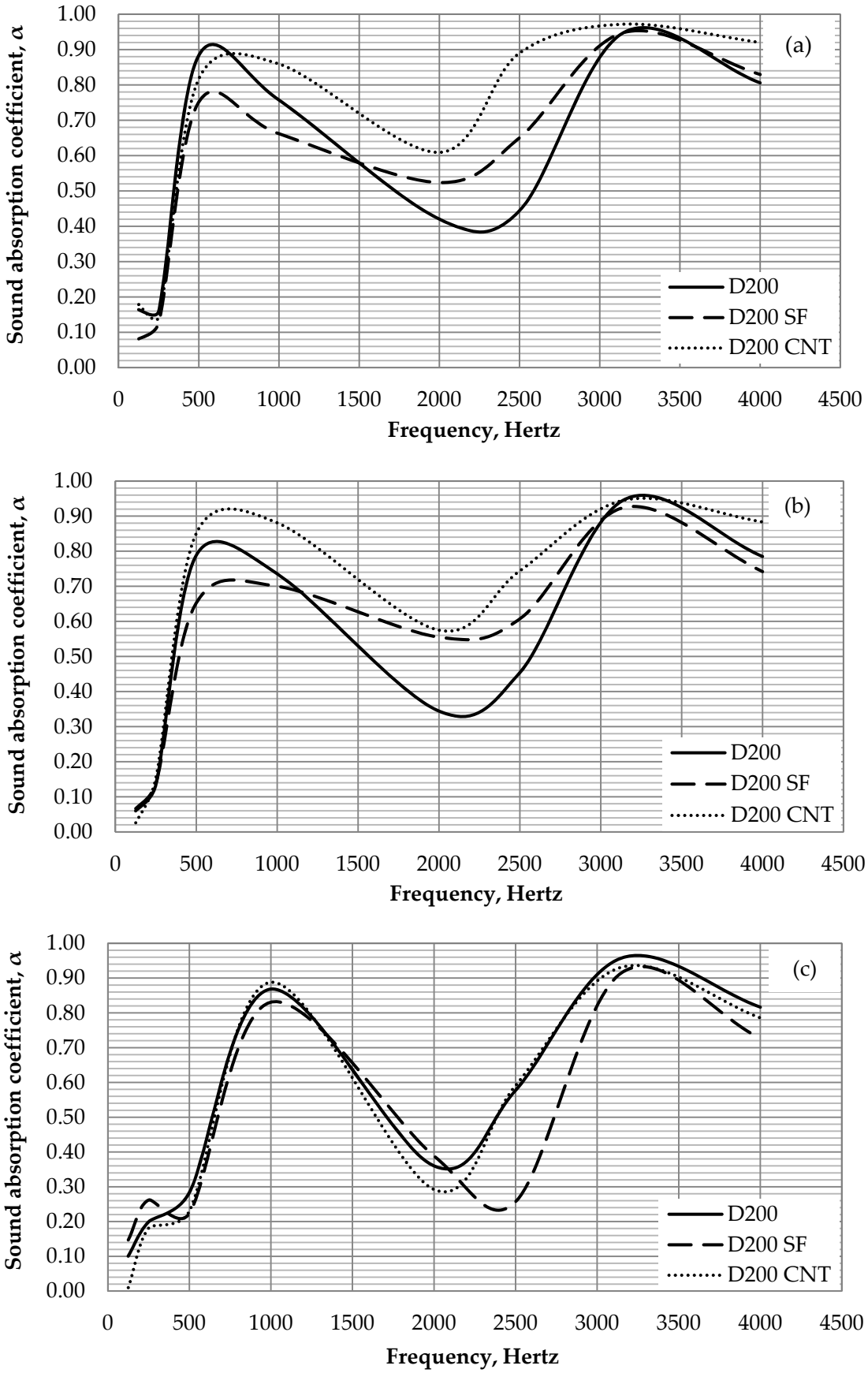

Figure 7.12 Influence of nano-materials on sound absorption of (a) 70mm, (b) 50mm and (c) 25mm thick D200 specimens

Overall, sound absorption performance of foamed concretes were observed to be similar to the behaviour of a single layer, open-cell Aluminium foam mounted with 50mm air-gap backing (Figure 7.13) which enhances the sound absorption especially at low densities. This is achieved by creating a micro-resonator effect, where the air passages inside the material are considered as the neck and the air-gap as the cavity. As a result, the sound wave propagating inside the material is dissipated through the vibration of the air molecules inside the cavity, if the frequencies of the sound wave are same with the resonance frequencies of the micro-resonator (Zhang et. al. 2011).

Although the sound absorption pattern of foamed concretes under consideration was similar to the open-cell Aluminium foam shown in Figure 7.13, frequencies at which peak absorption occurs are differing, such that peaks occurred at lower frequencies in the case of foamed concretes. This is believed to be mainly caused by the air-gap backing of the Aluminium foam, different sample thicknesses and microstructure.

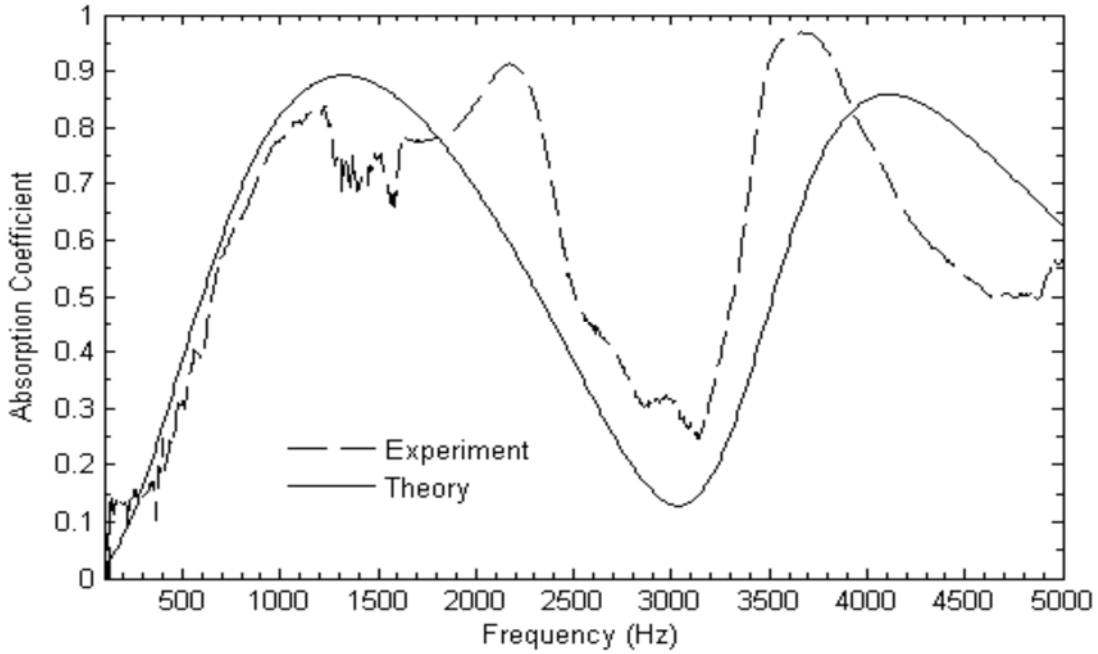

Figure 7.13 Sound absorption coefficient of single layer Aluminium foam (10mm thick) mounted with a 50mm air-gap (Zhang et. al, 2011)

7.3.2 Sound transmission loss

Transmission loss is dependent on the mass law, which is a function of frequency and surface density (Ramamurthy et. al, 2009) at states that, doubling the weight of a wall increases the transmission loss by 5 dB (NRCC, 1990). Sound transmission of a cellular concrete may be 2-3% higher compared to normal weight concrete when exposed to most of the audible frequencies (Ramamurthy et. al, 2009).

Although foamed concretes are stated to have low sound transmission loss, foamed concrete specimens with plastic densities of 200, 300 and 600 kg/m³ and 50mm thickness were tested for sound transmission loss at the University of Salford by using an impedance tube. As the standard reverberation room method was not employed, calculation of a single number weighted value for sound transmission loss could not be possible, thus frequency dependent transmission loss was presented.

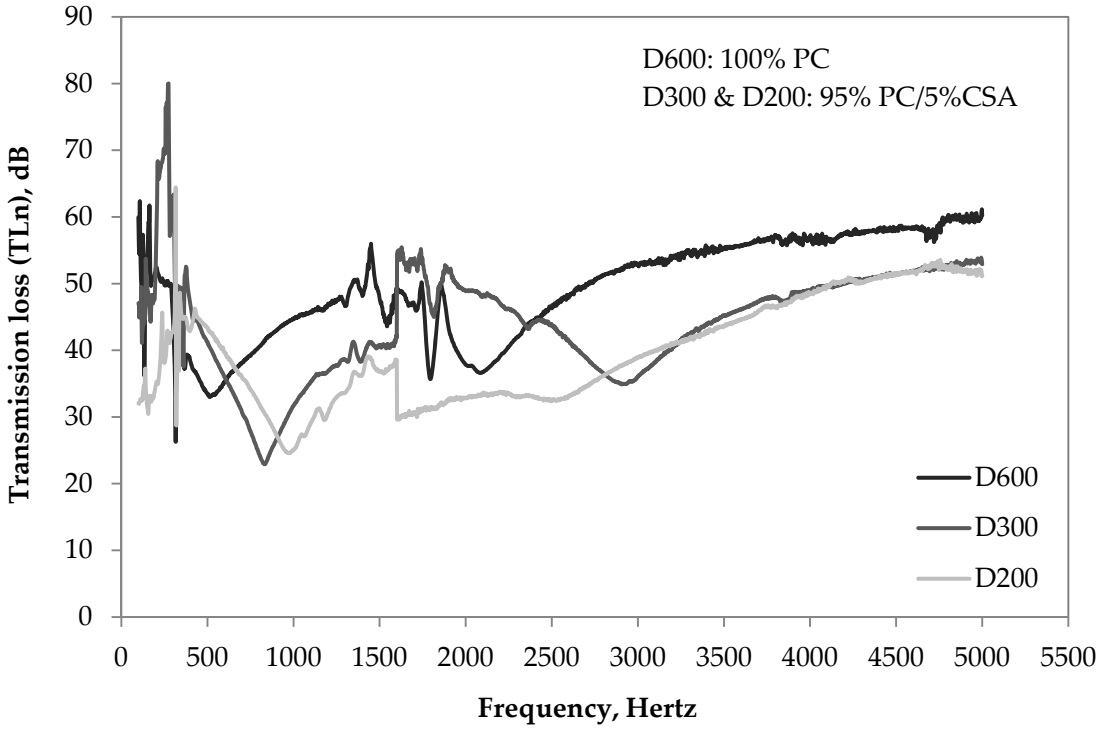

Figure 7.14 Transmission loss of D600, D300 and D200 foamed concretes

Data provided in Figure 7.14 shows that materials with high stiffness and porosity exhibit low sound transmission which was also reported by Dong et.al (2009). Out of the three foamed concrete densities tested for sound transmission loss, D600 has the highest stiffness (which will be discussed in Chapter 8) and it showed the highest sound transmission loss, thus the lowest sound transmission. However, at frequencies below 800 Hz, D300 specimen seemed to outperform D600. This may be attributed to the utilisation of two different impedance tubes (29 and 100mm diameter), hence different specimens for the measurement of low (up to 1000 Hz) and high (above 1000 Hz) frequencies. Given the small-sized specimens used, it is likely that there were lack of homogeneity in the specimens tested for both frequency classes.

Discussions on the test methods

Due to its practicality on quick and lower cost of set-up as well as the use of small size specimens, using impedance tube for the determination of sound insulation properties can be more advantageous over the conventional reverberation room method. However, correct mounting of the specimens inside the tube is of great importance for obtaining reliable results. Existence of gaps around the edges of the sample and compressing the samples inside the tube in a way to cause changes in the microstructure, lead to inaccurate measurements (Mosanenzadeh et. al, 2013). Moreover, the size of the specimens used for the impedance tube is challenging to produce homogeneous foamed concretes. Reduced flow of ultra-low density foamed concretes (discussed in Chapter 8) resulted in lack of compaction which affects the formation of the microstructure, hence the sound insulation performance.

7.4 CONCLUSIONS

A range of foamed concretes with varying material combinations were tested for evaluating the insulation performance of ultra-low density foamed concretes. Ultra-low density foamed concretes were found to exhibit better thermal insulation and sound absorption performance than higher densities, while exhibiting a poorer performance on transmission loss. More detailed conclusions on the insulation performance of ULFC are listed below:

Thermal insulation

i. At ultra-low density levels, thermal conductivity of foamed concrete was found to decrease down to 0.078 W/mK as it is mainly the function of density (i.e volume of air in the mix). Type of constituents was also found to influence the thermal insulation performance of foamed concrete.

ii. Addition of 30% FA2 was found to yield the lowest thermal conductivity values at 28 days. However, when tested at 6 months age, foamed concretes comprising fly ash exhibited higher (up to 12%) thermal conductivity due to the formation of denser microstructure caused by long-term hydration of fly ash. Moreover, the data suggested that 30% is the optimum fly ash level for obtaining the lowest thermal conductivity.

iii. Addition of nano materials like silica fume and carbon nano-tubes (CNTs) found to decrease the thermal conductivity. However, due to their cost and difficulties in dispersing the CNTs, these are not practical for industry applications.

iv. Overall, 5% CSA mix was found to be the best thermally insulating mix among the D200 and D300 foamed concretes tested at 28 days. Indeed, the performance of 5%CSA and 6 months old 30% FA2 mixes are comparable for both D200 and D300 as there are only 5% and 3% difference respectively in thermal conductivity values that can potentially be adjusted for the design needs. Moreover, sustainability benefits of utilising 30% FA replacing the PC is more advantageous than using a non-fly ash mix.

Sound insulation

i. Sound absorption behaviour of foamed concretes under consideration exhibited a similar trend regardless of the density of the specimens. Foamed concretes appeared to have maximum sound absorption between the frequencies of 500 and 1000 Hz followed by a reduced sound absorption at the frequencies between 1000 Hz and 2500 Hz. A general trend showed that foamed concretes have another peak in sound absorption at frequencies around 3150 Hz.

ii. Addition of fly ash and nano-materials except silica fume, resulted in enhanced sound absorption capacity.

iii. Overall, varying the thickness of the specimens led to changes in the sound absorption values as well as the frequencies at which the peak sound absorption is obtained. However, sound absorption capacity was mostly affected at frequencies below 2500 Hz whereas at frequencies above 2500 Hz it did not seem to be affected with the varying specimen thickness. In general, correlation between specimen thickness and sound absorption could not be established.

iv. Competitive performance of D600 foamed concretes with lower density foamed concretes may be due to the presence of sand (which increases tortuosity) and smaller bubbles in D600. However, as the porosity and tortuosity are considered as more dominant parameters, higher porosity and tortuosity (due to open-cell bubbles) of D200 and D300 concretes offset the bubble size effect.

v. Over the range of frequencies considered, transmission loss of foamed concrete was found to increase with increasing density. At frequencies between 250 and 600 Hz as well as 1600 and 2500 Hz, D300 specimens outperformed D600. The highest transmission loss of 80 dB was obtained at 270 Hz by D300 foamed concrete, whereas the lowest transmission loss was recorded at 800 Hz.

vi. The sound insulation data suggested that, foamed concretes of various densities can potentially be used in a multilayer system, in combination with other materials and air gaps provided among the layers. However, further research is required on both sound absorption and transmission loss of foamed concrete.

CHAPTER 8

8. PROPERTIES OF ULFC

8.1 INTRODUCTION

Properties of foamed concrete which were divided into three categories as fresh, early age and hardened state properties were examined and presented in this Chapter. Although most of the properties considered are well-established for high/low densities, behaviour of ULFCs is not known. Therefore, this Chapter aimed to examine the behaviour of ultra-lightweight foamed concretes (ULFCs) in respect to high/low density foamed concretes regarding the engineering properties including, flow behaviour, temperature development (due to heat of hydration), compressive strength, modulus of elasticity, Poisson's ratio, drying shrinkage, coefficient of thermal expansion and sorptivity. It was also aimed to provide a guideline to the users of foamed concrete (especially the ULFC) regarding its behaviour in order to specify the most suitable foamed concrete mix for a given application.

Therefore, depending on the nature of the test method, foamed concretes with densities down to 200 kg/m^3 were tested for ultra-low density class while densities up to 1000 kg/m^3 were tested to provide comparison. Foamed concrete densities and cement combinations used for each test are stated in the relevant Section.

8.2 FRESH STATE PROPERTIES

Fresh state of foamed concrete is generally described by its mix stability and flow behaviour. Stability of ULFC was discussed in Chapter 5 and 6, therefore, only the flow behaviour of foamed concrete was considered in this Chapter as a fresh state property.

8.2.1 Flow behaviour

Foamed concrete is well-known with its highly flowing and self-compacting characteristics. In general, flow behaviour of foamed concrete is well characterised and mainly affected by the foam content of the mix, as well as the type and proportion of the constituents. More specifically, increased foam content reduces the flow due to reduced self-weight, increased cohesion and increased adhesion between the bubbles and solids (Jones and McCarthy, 2005b; Nambiar and Ramamurthy, 2006; Ramamurthy et. al, 2009). However, there is limited information on the flow behaviour of ULFCs. Thus, current study evaluates the flow characteristics of foamed concrete at ultra-low density levels as well as the influence of constituent materials on the flow behaviour.

Effect of plastic density

Previous studies suggested that reducing the density of foamed concrete reduces the consistency due to the reduced self-weight and increased cohesion of the mix (Jones and McCarthy, 2005b; Nambiar and Ramamurthy, 2006). Therefore, it was expected that consistency of foamed concrete would decrease significantly at ultra-low density levels given the foam is the dominant constituent in these mixes. Flow time data obtained from the modified Marsh cone showed that there is a significant difference in the flow behaviour of ultra-lightweight foamed concretes was observed as presented in Table 8.1 and from Figure from 8.1 to 8.4.

Figure 8.1 shows the significant change in the flow behaviour of foamed concrete when shifting from low to ultra-low density foamed concrete class. It was visually observed that self-flowing ability of foamed concrete was lost in ULFCs. While D600 mix flows constantly, D300 mix exhibits a flow pattern in drops.

Figure 8.2 presents the data obtained from the modified Marsh cone test, while Table 8.1 gives the classification (according to Section 3.6.1, Table 3.4) of flow behaviour of the mixes considered, providing more detailed information for the visual observation made in Figure 8.1. When the flow behaviour of mixes from D200 to D600 was checked against their flow time, the values ranged from 1 litre/0.67minutes for D600 to 1 litre/15.5 minutes for D200. This behaviour is mainly attributed to the reduced self-weight of the mixes below D500.

Figure 8.1 Influence of plastic density on the flow behaviour of foamed concrete; (a) D600 low density and (b) D300 ultra-low density foamed concrete

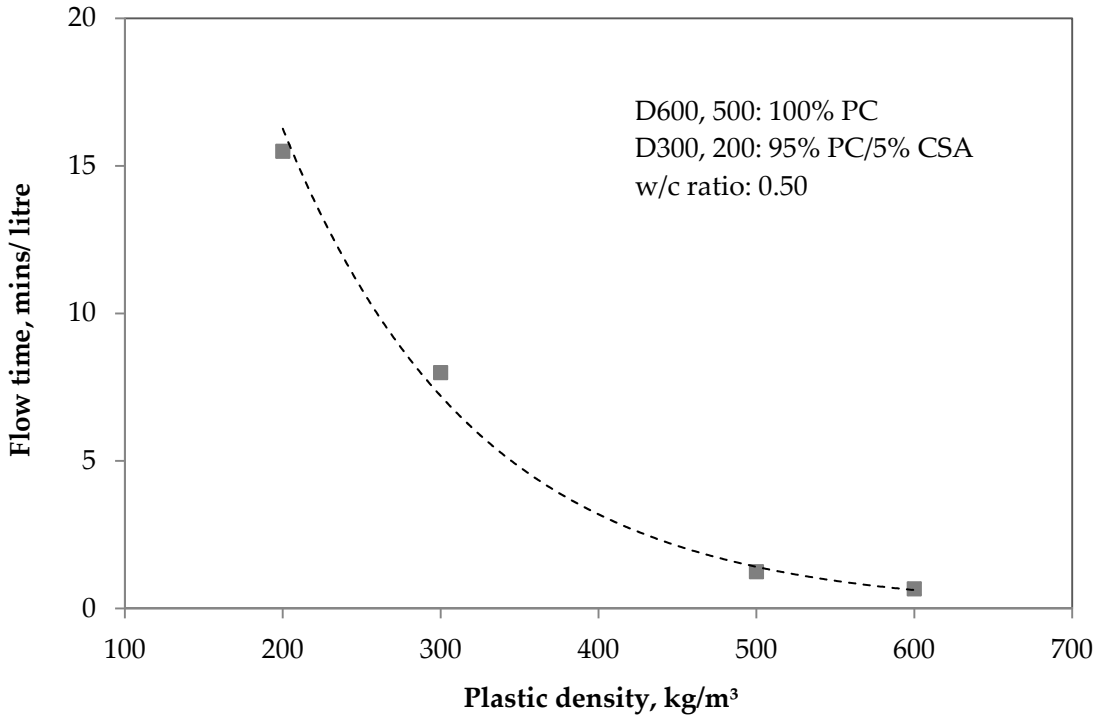

Figure 8.2 Influence of plastic density on flow time

Table 8.1 Classification of flow behaviour of a range of foamed concretes

Flow Class	Plastic density, kg/m³
C1- Fills 1 litre < 1 min	D600
C2- Fills 1 litre > 1 min	D500
C3- Fills < 1 litre > 0.5 litre	-
C4- Fills < 0.5 litre	D150*-D300
C5- No flow	-

* D150 mix produced with 10% CSA/90% PC was assesed visually.

According to the data obtained, D600 foamed concretes are classified as both self-flowing and levelling, whilst at 500 kg/m³ density flow is slightly reduced compared to the D600 mixes that contain sand. In addition to the increased foam content in D500 mixes, it is believed that mainly the elimination of sand at 500 kg/m³ density causes the reduction in the flow. On the other hand, as D500 is the cross-over density at which sand is eliminated from the mix, cement content had been increased (from 300 to 333 kg/m³) to increase the 'fines' content. Consequently, this may offset the effect of elimination of sand and reduced density on flow behaviour causing only a slight change in the flow. Although flow reduces with increasing foam content, it is thought that flow behaviour is dominated by the solids within the mix down to 500 kg/m³ density and the bubbles act as a lubricant making the mix to flow easier.

Given their significantly reduced self-weight, foamed concrete mixes with densities below 500 kg/m³ were not self-flowing and levelling. At ultra-low densities, as the volume of air increases foam content dominates the solids content. Therefore, unlike densities 500 kg/m³ and above, flow behaviour is dominated by the bubbles. As a result of significantly decreased solids content at ultra-low densities, bubbles get closer to each other with decreasing wall thicknesses. Therefore, the adhesion between bubbles and solid particles increases significantly. Consequently, the mix tends to get 'sticky' reducing the flow. At this stage it is thought that the self-weight effect competes with the gravity resulting in a mix that would hardly flow.

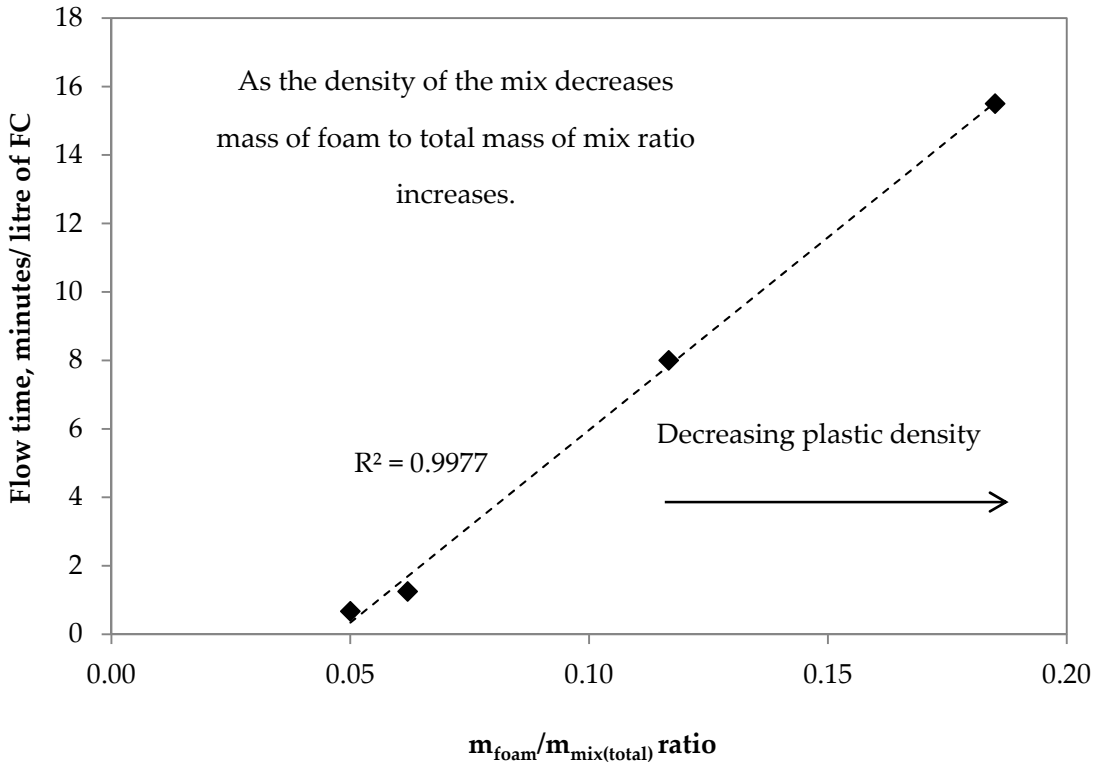

Figure 8.3 Relationship between flow time and ratio of mass of foam to total mass of the mix

Figure 8.3 shows the relationship between flow time and the ratio of mass of foam per 1m³ of mix to the total mass of 1m³ mix ($m_{foam}/m_{mix(total)}$). There is a linear relationship between the flow time and $m_{foam}/m_{mix(total)}$ ratio with an excellent correlation obtained ($R^2 = 0.998$). Therefore, flow time could be predicted by using Equation 8.1. However, it must be noted that Equation 8.1 is only suitable for foamed concretes with densities 600 kg/m³ and below (produced with PC and PC/CSA combinations) where foam starts to act as the dominant parameter controlling the flow behaviour. Contrarily, when checked against the flow time data reported by Jones and McCarthy (2005b), for densities 1000 kg/m³ and above, it was found that Equation 8.1 is not suitable to predict the flow behaviour of foamed concretes at these densities. Moreover, as there was no flow time data available, accuracy of Equation 8.1 could not be checked for plastic densities between 600 and 1000kg/m³.

$$\text{Flow time} = 112.54 * [m_{foam}/m_{mix(total)} \text{ ratio}] - 5.284 \qquad \text{Equation 8.1}$$

Effect of constituents

Previous studies carried out regarding the influence of constituents on the flow behaviour of foamed concrete were mainly focused on the effect of filler type and w/c ratio (Jones and McCarthy, 2005b; Nambiar and Ramamurthy, 2006). Indeed, McCarthy (2004) and Mohammad (2011) reported that utilisation of 30% (by mass) fine fly ash in combination with PC reduced the flow time at densities 1000 and 600 kg/m^3, due to the reduced yield stress values. For ULFCs, this may indicate reduced attraction among the bubbles through the confinement of the bubbles, thus making the mixes to flow easier. However, there is no information regarding the influence of fly ash on the flow behaviour of ULFC mixes.

Current study evaluated the influence of various fly ash addition levels on the flow behaviour of D200 and D300 ULFCs. As explained in Section 3.6.1, evaluation of influence of fly ash on the flow behaviour was carried out by comparing the amount of efflux obtained in 5 minutes. Figure 8.4 illustrates the influence of fly ash addition on the flow behaviour of ultra-low density foamed concrete mixes. FA1 was only tested at 30% addition level while FA2 was tested up to 50%. Consequently, was shown that influence of fly ash on the flow behaviour varied with plastic density, fly ash level and type.

As expected, utilisation of fly ash the ultra-low density foamed concrete mixes was found to improve the flow. Compared to the reference mixes, it was found that utilisation of 30% FA1 yielded the maximum improvement (based on the amount of efflux) in the flow D300 and D200 mixes at a rate of 33% and 144% respectively. On the other hand, similar to FA1, 30% FA2 also enhanced the flow of D200, however, approximately 2 times less than the former. Unlike D200, flow of D300 reduced by more than 2.5 times when 30% FA2 was used.

It is unclear why FA1 outperformed FA2 in regard to flow behaviour. Although FA2 is a finer ash with a slightly wider particle size distribution, the difference between FA1 and FA2 is not significant. Un-burnt carbon contents of the two ashes are not significantly varying from each other, where FA2 possess lower loss on ignition (LOI). Comparing the SEM images of two ashes (as shown in Appendix B), their microstructure looks similar with more agglomeration observed in FA2. Although it is unlikely to be the main reason,

agglomeration of fly ash cenospheres due to fineness, may interrupt the ease of flow reducing the flow in the case of FA2. However, the adverse effect of 30% FA2 on the flow behaviour of D300 could not be explained while 30% FA1 exhibited the maximum improvement on the flow of D300.

Beyond 30% FA, utilisation of 40% and 50% FA was not found to have a significant effect on the flow behaviour of both D200 and D300. In comparison to the reference mixes, addition of 40% FA2 resulted in a slight increase in the flow of both densities whilst 50% FA2 yielded slightly less flowing mixes. Therefore, the data suggests that, 30% FA is the optimum level for improving the flow of D200 and D300 ULFC mixes. It must be noted that, further work is required in order to evaluate the effect of different types of ashes and varying w/c ratios on the flow behaviour of ultra-low density mixes.

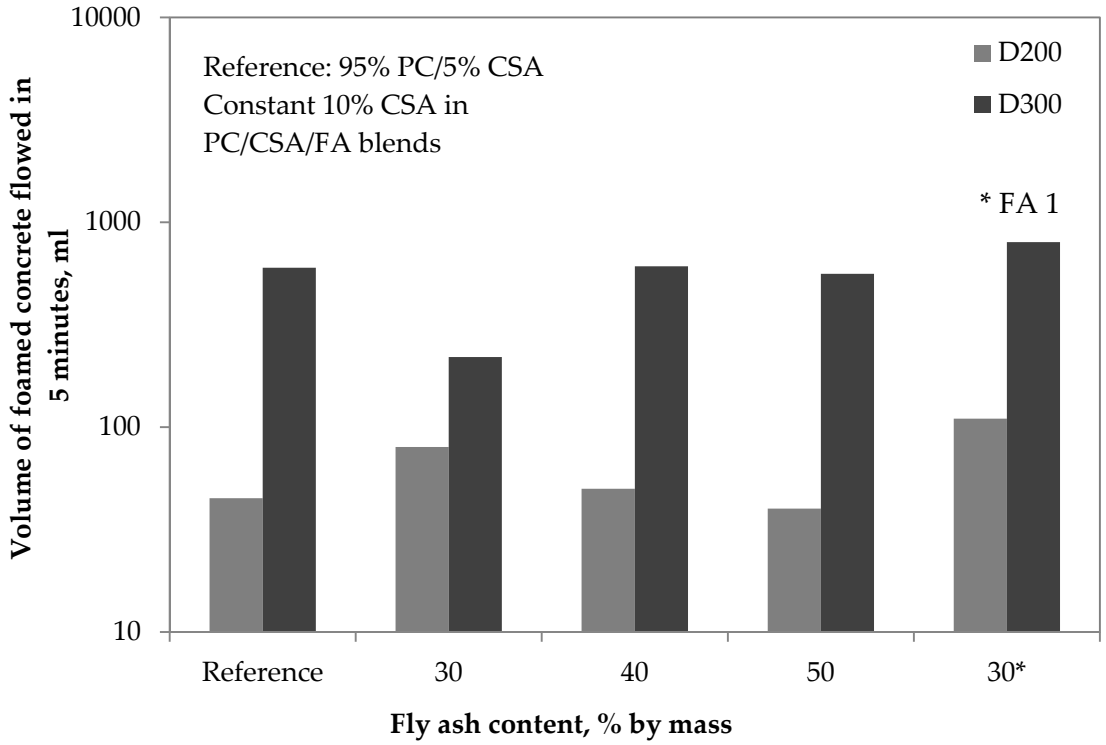

Figure 8.4 Influence of fly ash on the flow behaviour of ULFCs

8.3 EARLY AGE PROPERTIES

Early age properties considered within the frame of this research were rate of hardening and heat of hydration. As rate of hardening was discussed in Chapter 5 and 6, along with the stability, only heat of hydration was presented in this Chapter.

8.3.1 Temperature development

Given its one of the most popular application as a fill material and its highly insulating characteristics, when used in large volumes, foamed concrete can lead to high core temperatures as a result of the heat evolved due to hydration. Owing to a higher air content, ULFCs exhibit higher insulation capacity hence, a higher tendency for significant temperature rises due to hydration. Both Jones and McCarthy (2006) and Tarasov et. al (2010) reported the increase in peak temperatures with decreasing foamed concrete density at a given cement content and combination.

Current study focused on monitoring the heat development due to the cement hydration in ULFC mixes. Therefore, mixes with plastic densities 600, 300 and 200 kg/m^3 were evaluated, whilst D600 was chosen in order to provide a link between low and ultra-low density foamed concretes. Mixes produced with 100% PC for D600 and 95%PC/5%CSA for D300 and D200 were tested as well as an additional cement combination of 90%PC/10%CSA for D200. Furthermore, knowing the influence of fly ash on reducing the peak core temperatures (from the literature), 50% PC/10%CSA/40% FA mixes produced with two different ashes, FA1 and FA2, were tested for all foamed concrete densities.

As it was not possible to produce ULFC mixes with 100% PC, minimum requirement of 95% PC/5% CSA combination was used for D200 and D300 densities as non-fly ash mixes. As 95% PC/5% CSA D200 mix collapsed during the temperature development profiling, 90% PC/10% CSA mix was also evaluated for D200. As a result 90% PC/10% CSA mix was also found to collapse during testing as well as the fly ash mixes. Although the data obtained for D200 was not accepted as reliable due to the collapsing mixes, the data recorded was found to be in line with D600 and D300 mixes.

Table 8.2 Summary of heat development data

Plastic density, kg/m³	Cement combination, % by mass	PC content, kg/m³	Peak temperature, °C	Time of peak, hours	Max. rate of rise, °C/hour
600	100% PC	300	55.8	12.8	6.1
	50% PC/10% CSA/40% FA1	150	27.5	1.6	7.9
	50% PC/10% CSA/40% FA2		28.9	2.1	5.9
300	95% PC/5% CSA	190	38.3	10.4	2.6
	50% PC/10% CSA/40% FA1	100	27.1	1.7	5.5
	50% PC/10% CSA/40% FA2		27.9	1.4	7.8
200	95% PC/5% CSA	126	31.0	13.3	1.6
	90% PC/10% CSA	120	27.9	1.6	5.0
	50% PC/10% CSA/40% FA1	67	25.4	1.7	2.9
	50% PC/10% CSA/40% FA2		26.3	1.9	4.1

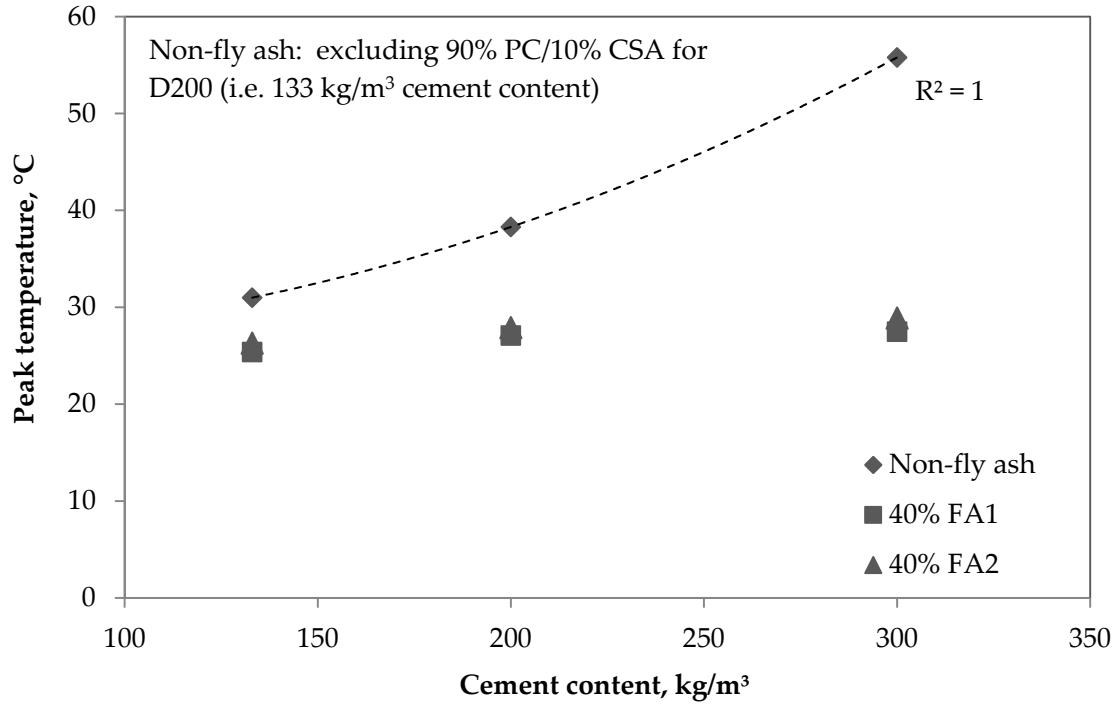

Figure 8.5 Influence of cement content on the peak temperature

Table 8.2 and Figures from 8.5 to 8.9 show the temperature development profiles of the mixes considered. It must be noted, given their varying densities, cement contents (300, 200 and 133 kg/m^3 for D600, D300 and D200 respectively), insulation capacity and microstructure, it is difficult to make a detailed comparison among these mixes.

Effect of plastic density

Effect of plastic density was found to be the function of cement content, as all foamed concrete densities considered had different cement contents. Accordingly, higher cement contents resulted in higher peak temperatures. The data suggested that peak core temperatures of non-fly ash (100% PC, 95% PC/5% CSA) mixes are highly dependent on the cement content, while fly ash mixes exhibited slight dependence on the cement content (Table 8.2 and Figure 8.5). The maximum core temperatures for the non-fly ash mixes considered ranged from 55.8 to 31°C with the order of decreasing cement content. More specifically, elimination of fine aggregates as well as 33% decrease in cement content of D300 resulted in 32% decrease in the core temperature of PC/CSA mix compared to D600 PC mix.

A predictive equation, Equation 8.2, (with R^2 =1) can be used to determine the peak core temperatures of a foamed concrete mix with a given cement content. However, as the pour volume directly influences the peak temperatures, this equation can only be applied for mixes tested in 165 mm cubes (as described in Section 3.6.1). Moreover, Equation 8.2 was not found to be predictive for the mixes comprising 10% CSA and fly ash (90% PC/10% CSA and 50% PC/10% CSA/40% FA respectively), as these were found to behave differently (as will be discussed in the next section, covering the effect of constituents).

$$\text{Peak temperature} = 0.0004*(C)^2 - 0.0227*(C) + 27.029 \qquad \text{Equation 8.2}$$

Where C = cement content, kg/m^3

When checked against the data reported by Tarasov et. al (2010) for foamed concretes produced with 100% PC and without aggregates, Equation 8.2 was found to be predictive, specifically at lower cement contents. Although the pour volumes reported were different

than the current study, expected peak core temperatures were approximated with interpolation. As a result, the approximated and predicted peak temperatures for a foamed concrete mix with 350 kg/m^3 plastic density and 220 kg/m^3 cement content, were found to be equal. On the other hand, predicted peak temperature for a 465 kg/m^3 mix with cement content of 300 kg/m^3 was found to be 14% higher than the approximated value. Furthermore, approximated peak temperatures for D350 (42.0 °C) and D465 (49.2 °C) mixes presented by Tarasov et. al (2010) were found to be in line with the data for D300 and D600, shown in Table 8.2.

Although the addition of fly ash reduced the peak temperatures for all foamed tested, unlike non-fly ash mixes, cement content was not found to have a significant influence on the peak temperatures. However, the data obtained was found to be in line with the trend (the lower the cement content, the lower the peak temperature). The difference between the peak core temperatures yielded by the maximum and minimum (300 and 133 kg/m^3) cement contents was measured as only 2.1 and 2.6°C for FA1 and FA2 respectively, whereas it was 24.8°C for non-fly ash mixes. However, this behaviour should not be solely attributed to the incorporation of fly ash. As can be seen from Table 8.2 (D200 data), utilising 10% CSA in the mix also has an effect on reducing the peak temperature. It can be speculated that, the addition of 10% CSA may have an unknown dominant effect offsetting the influence of cement content or it leads to a flash set.

The reviewed literature suggested that lighter foamed concretes are expected to have higher peak temperatures given their higher insulation capacity that results in retention of the evolved heat inside for longer periods. However, this behaviour was observed in a range of foamed concrete densities with constant cement content which does not apply to this particular study, where cement content was reduced with decreasing density. In this case, cement content was found to be the dominant factor offsetting the higher insulating effect of lower density foamed concretes as predicted by Brady et. al (2001). In consequence, lower density foamed concretes yielded reduced peaks compared to heavier foamed concretes.

Furthermore, cement content was not found to have a consistent relationship with the time of peak temperature where the time of peak varied from 10.4 to 13.3 hours. It is likely that

either an interaction (possibly due to test conditions; closed lid hot box) caused D200 mixes to collapse and extended the time of setting hence the time of peak or vice versa. Therefore, time of peak for 95%PC/5%CSA D200 mix was not in line with D600 and D300 non-fly ash mixes. On the other hand, maximum rate of rise for non-fly ash (only 95% PC/5% CSA for D200) and FA1 mixes was found to decrease with decreasing density whilst FA2 mixes were not in line with this trend.

Effect of constituents

In regard to evaluate the influence of constituents on the heat development profile, cement combination of 50% PC/10% CSA/40% FA was employed with the utilisation of two types of ashes, FA1 and FA2, for all the foamed concrete densities considered. Expectedly, data obtained suggested that incorporation of fly ash decreased the peak core temperatures at all densities, whereas the effect is more noticeable at higher densities (and cement contents). Figures from 8.6 to 8.8 shows the detailed influence of fly ash on the heat development of D600, D300 and D200 foamed concretes respectively.

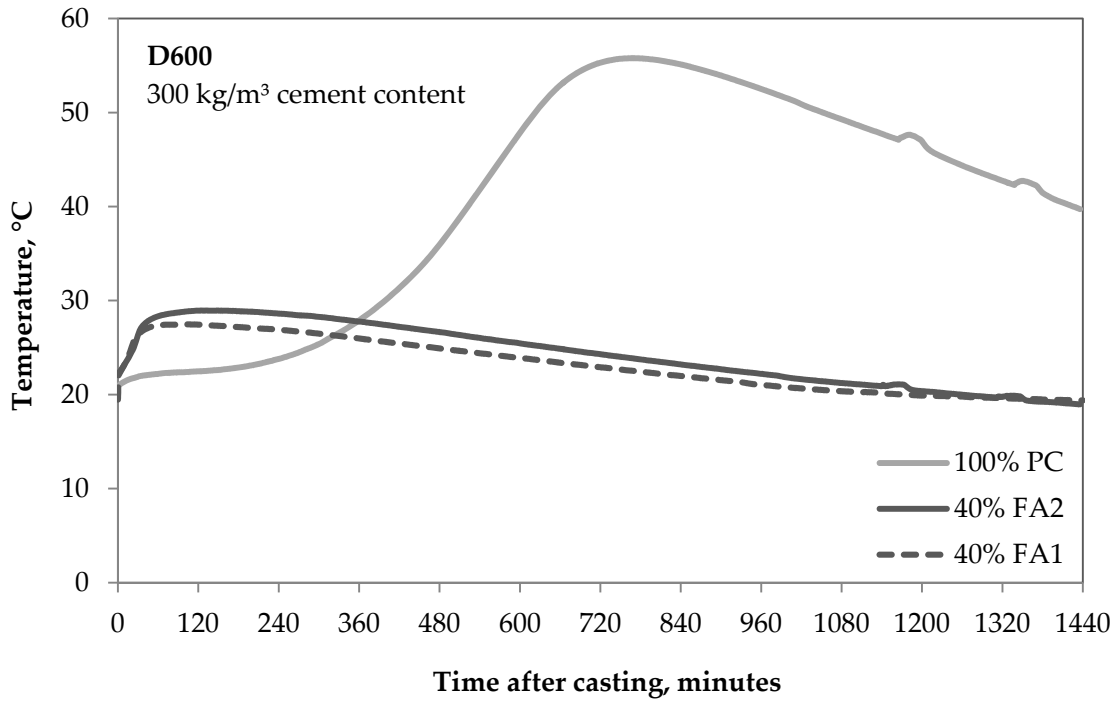

Figure 8.6 Influence of fly ash on the heat development of 600 kg/m³ foamed concrete

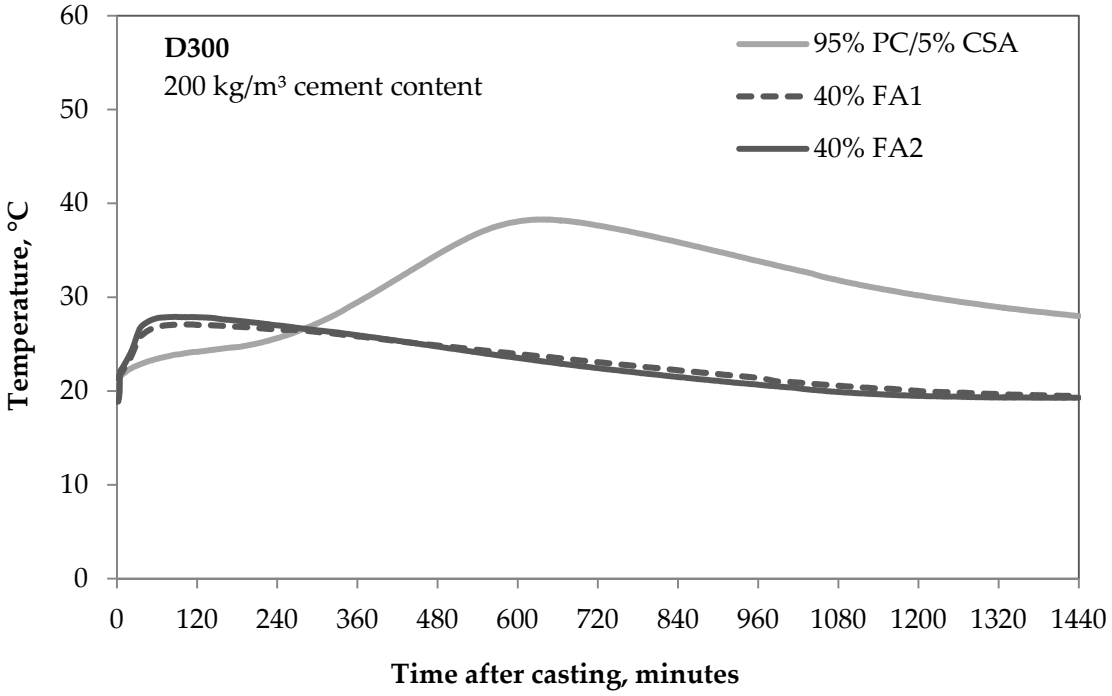

Figure 8.7 Influence of fly ash on the heat development of 300 kg/m³ foamed concrete

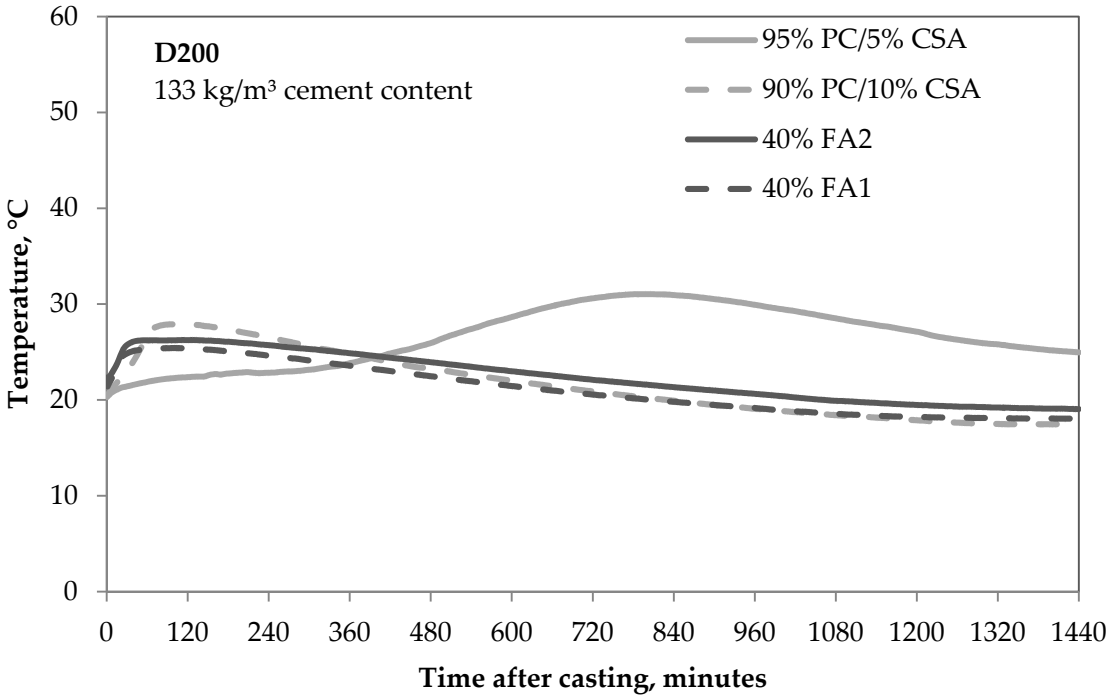

Figure 8.8 Influence of fly ash on the heat development of 200 kg/m³ foamed concrete

Comparing the foamed concrete densities under consideration, it was observed that the heat development curves obtained for the non-fly ash mixes (excluding 90% PC/10% CSA) showed similar trends at all densities, while the heat development curve yielded by D200 90%PC/10%CSA mix was similar to those of all other 50%PC/10%CSA/40%FA mixes (Figure 8.8). This behaviour is thought to indicate the dominant role of increased CSA content (10% CSA by mass of cement) on reducing the peak temperatures. Accordingly, increasing CSA content by 5% by mass of cement was found to reduce the peak temperature of D200 by 10% when compared to 95% PC/5% CSA mix. Therefore, the reduction provided purely by fly ash, FA1 and FA2, was only 9% and 6% respectively when 50%PC/10%CSA/40%FA mixes were used.

The effect of CSA cement on reducing the peak temperatures may be due to lack of enough calcium sulfate available in the mix for controlling the hydration of CSA cement (Winnefeld and Lothenbach, 2010), however further research is needed to prove this. Similarly, the peaks occurred in 90% PC/10% CSA and fly ash mixes may be associated with the depletion of calcium sulfate and the formation of sulfoaluminate and aluminate hydrates as suggested by Ioannou et. al (2014).

Furthermore, Jones et. al (2012) reported that, presence of higher volume of anhydrite leads to evolution of more heat due to hydration of CSA cement. However, this must be studied in more detail in order to evaluate the behaviour of CSA cement in PC/CSA and PC/CSA/FA blends as well as the behaviour of these combinations in foamed concrete. Moreover, short initial setting times (20 minutes, as discussed in Chapter 6) of these cement combinations (90%PC/10%CSA and 50%PC/10%CSA/40%FA) containing 10%CSA can possibly be due to a flash set not generating appreciable heat.

As 90% PC/10% CSA combination was not tested for D300 and D600 foamed concretes, the precise effect of fly ash on reducing the peak temperatures could not be calculated for these densities. However, it is expected that the influence of 10% CSA on reducing the peak temperatures is also the same at these foamed concrete densities. This can be supported by the similar heat development curves obtained for D600 (Figure 8.6) and D300 (Figure 8.7) in comparison to D200 (Figure 8.8) when fly ash mixes were employed.

Therefore, regardless of the cement content, fly ash mixes (as well as 90%PC/10%CSA D200 mix) yielded similar core temperatures with the effect provided by the presence of 10% CSA. For this reason, it is more convenient to do a comparison between fly ash and non-fly ash mixes taking the effect of 10% CSA into account. Consequently, D600 exhibited the maximum reduction in the peak core temperatures followed by D300 with the incorporation of PC/CSA/FA combinations for both fly ash types. FA1 performed slightly better than FA2 in reducing the core temperatures such that FA1 resulted in up to 3% higher reduction rate in comparison to FA2, yet the reason for this is not clear.

In this study, as plastic density was found to be the function of cement content mainly, percentage reduction in the peak temperatures (in comparison to non-fly ash reference mixes) was plotted against cement content. Figure 8.9 summarises the effectiveness of 50% PC/10% CSA/40% FA cement combination on reducing the peak temperatures in foamed concretes with varying cement contents (and/or plastic densities). Besides reducing the peak core temperatures, utilisation of 50%PC/10%CSA/40%FA combination (as well as 90%PC/10%CSA for D200) also had an influence on the time of peak, such that the peaks were shifted earlier by 8.7 to 11.6 hours. It is likely that this effect is due to the presence of 10% CSA and possible flash set rather than the presence of fly ash. Moreover, fly ash mixes increased the maximum rate of temperature rise at all foamed concrete densities tested.

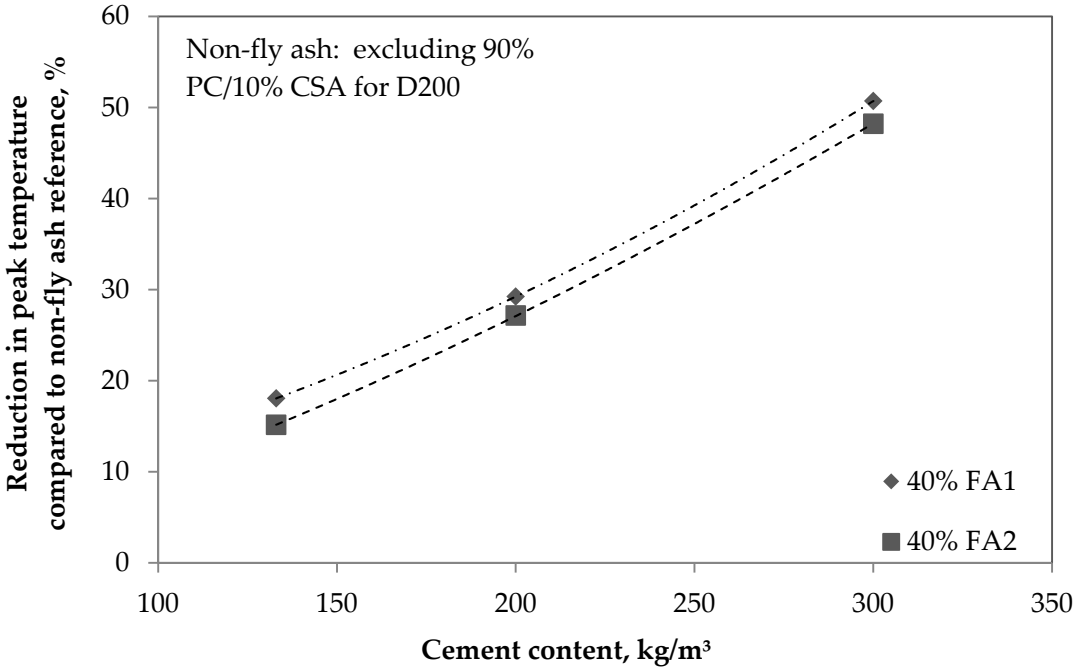

Figure 8.9 Effectiveness of 50% PC/10% CSA/40% FA cement combination on reducing the peak temperatures

8.4 HARDENED STATE PROPERTIES

For the hardened state, engineering properties including compressive strength, modulus of elasticity and Poisson's ratio were considered. Additionally, drying shrinkage, coefficient of thermal expansion and sorption of a range of foamed concretes were also evaluated.

8.4.1 Compressive strength, modulus of elasticity and Poisson's ratio

Given the ultra-low cement contents, high air contents and lack of fine aggregates, ULFC mixes were expected to have low strength values. Therefore, strength and strength related properties of ULFCs were not the main of this study. However, in order to provide an overall guideline for the properties of ULFC foamed concrete, compressive strength, modulus of elasticity and Poisson's ratio were measured. Although compressive strength and modulus of elasticity of conventional foamed concrete is well-established, there is no data on Poisson's ratio which is an important factor especially for the applications that cannot accommodate high lateral strains, such as restoration of ancient arch bridges.

Foamed concrete densities ranging from 300 to 1000 kg/m^3 were considered to evaluate the load dependent properties. As the compressive loading machine used for the tests were unable to apply loads as low as to test D200 foamed concretes, D200 mixes were not tested for any load dependent test.

Compressive strength

Strength is considered as one of the most valuable hardened state properties of concrete (Neville, 2011). Although foamed concretes (of high/low density range) are used in non- and semi-structural applications (Ramamurthy et. al, 2009) where high strengths are not required, compressive strength of high/low density foamed concretes are well established. On the other hand, there is no sufficient information on the compressive strength range of ultra-low density foamed concretes.

Owing to decreased cement contents and no sand (fine aggregate) content, ULFCs were observed to have lower strengths in comparison wth high/low density foamed concretes. Observed handleability issues of ULFCs with plastic densities below 200 kg/m^3 clearly

suggest that application areas for ULFCs should be selected carefully if they will be exposed to any loading. Although ULFCs are not likely to be eligible for semi-structural applications, compressive strength of D300 foamed concrete was measured in order to check the strength range to which ULFCs belong. Therefore, 28-day 100mm cube sealed-cured specimens of D300 foamed concrete as well as D600 and D1000 were tested for compressive strength.

Figure 8.10 shows the 28-day compressive strength of D300, D600 and D1000 foamed concretes. As expected from the fundamentals (the higher the porosity, the lower the strength of the concrete; Neville, 2011) and reported in earlier studies (Kearsley, 1999b; Jones and McCarthy, 2005a; Ramamurthy et. al, 2009) compressive strength was found to decrease with decreasing plastic density. Accordingly, compressive strengths ranged from 1.8 down to 0.23 MPa in the order of decreasing plastic density. Consequently, decreasing the plastic density from 1000 to 600 kg/m^3 resulted in 37% reduction in the strength while shifting from D600 to ultra-low density D300, 80% reduction in strength was observed.

The bigger drop in the strength of D300 is attributed to the reduced cement content (decreased from 300 to 200 kg/m^3) and absence of sand in D300 foamed concretes. Moreover, Nambiar and Ramamurthy (2007a) as well as Visagie and Kearsley (1999a) reported a drop in the strength with increased void diameter. Increasing average bubble diameter with decreasing plastic density (presented in Section 5.2.3) supported the lower strengths obtained at lower densities.

Compressive strength for D300 was found to be lower than any reported comparable ultra-low density foamed concrete such as 280 kg/m^3 density foamed concrete (reported by Ramamurthy et. al, 2009 and produced with cement-sand/fly ash) which has 0.6 MPa compressive strength, but at 91 days age. On the other hand, Ramamurthy et. al, 2009 reported the 28-day compressive strength for 240 kg/m^3 (dry density) foamed concrete with no sand as 0.48 MPa which is also higher than the measured value of 0.23 MPa in this study. Compressive strengths of D600 and D1000 foamed concretes were found to be in an agreement, but higher than the values reported by Jones et.al (2012), 0.5 and 0.9 MPa respectively.

Furthermore, an observed failure mode of D300 cube specimens is shown in Figure 8.11. According to the BS EN 12390-3:2009, D300 cube specimen seemed to exhibit a satisfactory failure. It must be noted that D300 ULFC failed by gradual consolidation rather than an explosive failure given the presence of high volume of air providing space for compaction as the specimens, hence the bubble walls crashes.

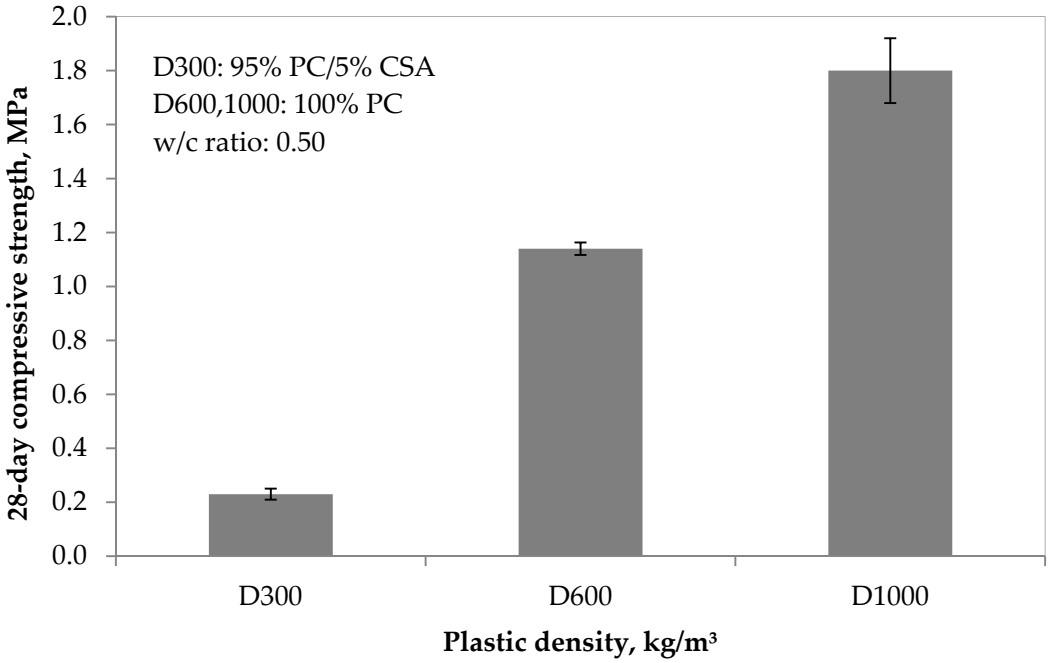

Figure 8.10 Comparison of compressive strengths of D300, D600 and D1000 FCs

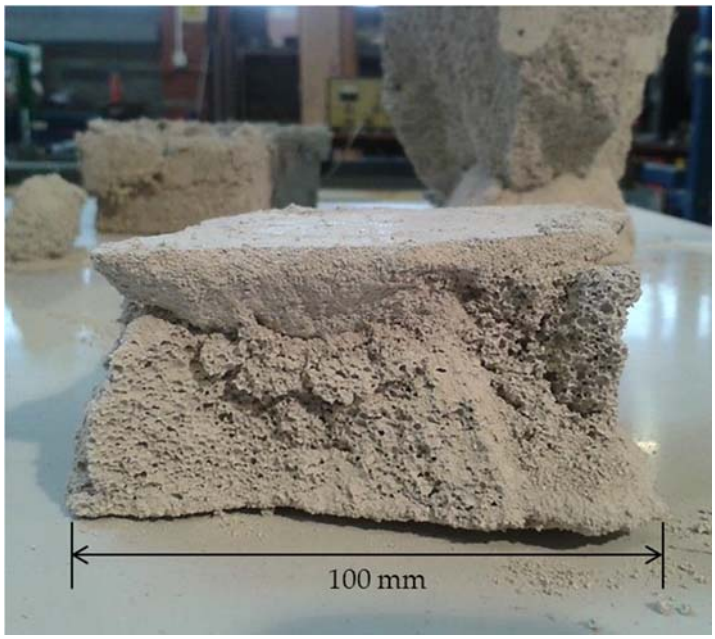

Figure 8.11 Failure mode of D300 cube specimen under compressive loading

E-value and Poisson's ratio

Modulus of elasticity (E-value) of foamed concrete was measured by determining the strains with two methods; using (i) demec points and (ii) a frame (Section 3.6.2). As a result, the strain values recorded using the frame were found to result in more realistic E-values than the demec points such that a linear relationship between density and E-value was obtained, as expected from the literature. It is likely that inaccuracies in strain measurements using demec points occurred because of the localised crushing of foamed concrete upon installation of demec points (given its low strength) and possible movement of the demec points. Figure 8.12 shows the E-values obtained using both demec points and the frame.

The E-values measured in this study were found to be lower than the values reported in the literature (0.8 to 8 kN/mm^2 for dry densities ranging from 400 to 1500 kg/m^3; Dransfield 2000; Concrete Society, 2009). This may be due to the higher compressive strengths of those foamed concretes reported in the literature. Furthermore, localised crushing and micro-cracking of the foamed concrete specimen at the contact points with the frame may lead to inaccurate strain measurements.

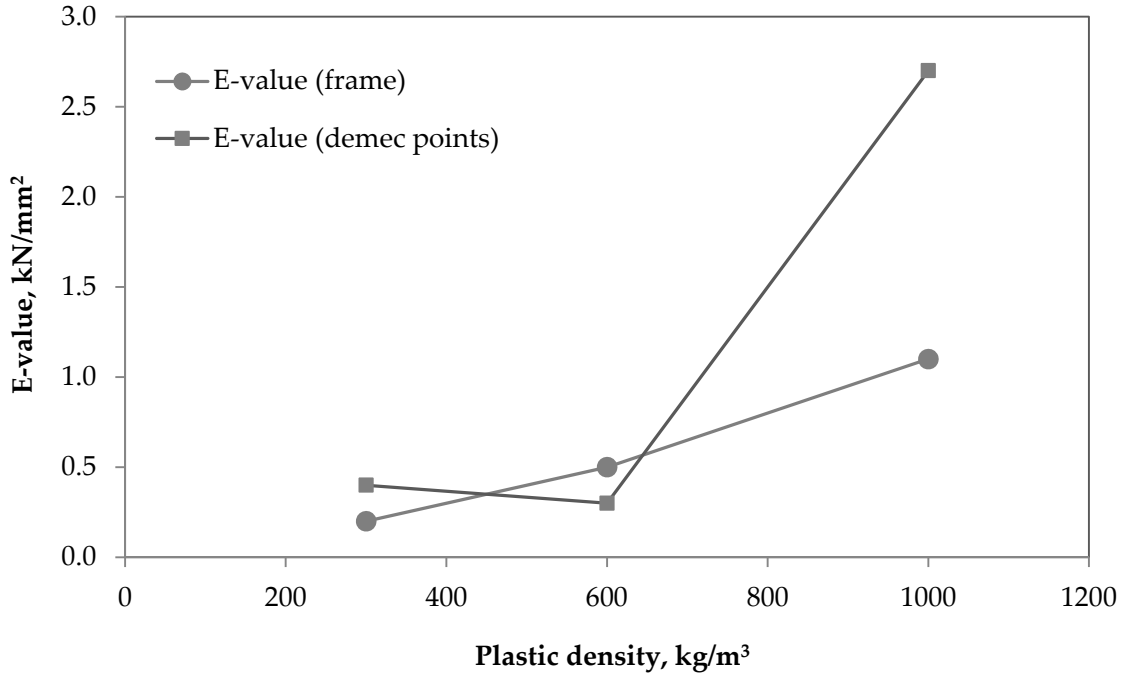

Figure 8.12 E-value of foamed concrete measured with (i) demec points and (ii) a frame

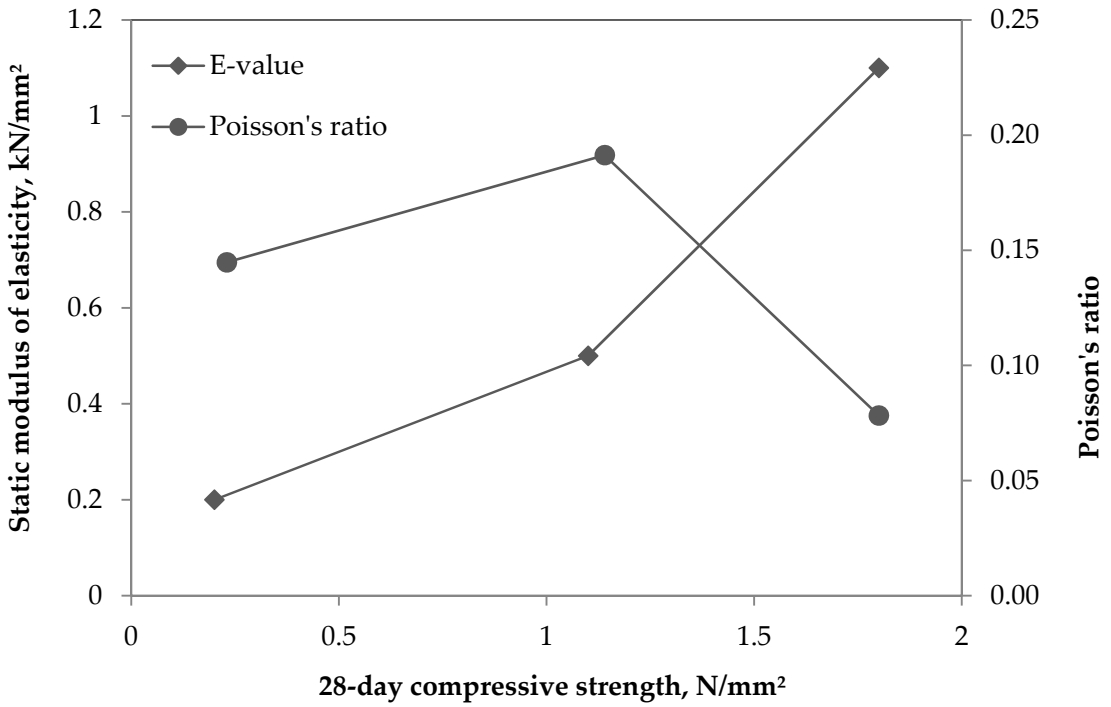

Figure 8.13 E-value and Poisson's ratio of FC in relation to compressive strength

Modulus of elasticity of foamed concrete was reported to be directly proportional to the compressive strength (Jones and McCarthy, 2005a; Concrete Society, 2009). Moreover, when there is no sand in the mix, E-value tends to be lower due to the lack of interlocking effect of sand (Brady, et. al, 2001). When the E-values are compared against the compressive strength of corresponding mixes in Figure 8.13, it shows that the same trend reported in earlier studies was obtained. However, the prediction equation (function of compressive strength) for E-value provided by Jones and McCarthy (2005a) underestimated the E-value of D300 and D1000 by 50% and 27% respectively, whilst well-predicting the value for D600.

Similarly, another equation (function of density and compressive strength) by McCormick reported in Ramamurthy et. al (2009) well predicted the E-value for D600 while under-estimating D300 and over-estimating D1000 mixes. On the other hand, the equation provided by Tada (Ramamurthy et. al, 2009) for predicting the E-value as a function of concrete density over-estimated all of the foamed concrete densities considered. It is likely that, these variations occur as a result of different mix designs and compressive strengths assigned while developing the prediction equation. For instance, in the case of D300 mixes which has no sand, it is only the cement paste providing the deformation resistance.

Equation 8.3 obtained from the data presented in Figure 8.13 approximates (R^2= 0.999) the E-value in relation to 28-day compressive strength. However, as there are only three data points, the equation may not be highly reliable.

$$E = 0.16e^{1.06fc} \qquad \text{Equation 8.3}$$

where E is modulus of elasticity under compression (kN/mm^2) and fc is 28-day compressive strength (N/mm^2).

Figure 8.13 shows the Poisson's ratio of D300, D600 and D1000 foamed concretes in relation to 28-day compressive strength. For normal weight concrete the Poisson's ratio usually varies between 0.15 and 0.22, while the values for lightweight aggregate concrete is at the lower edge of the range (Neville, 2011). There is almost no information available on the Poisson's ratio of foamed concrete. The only data reported by Lee et. al (2004) suggests that foamed concretes with no sand and nominal densities of 1000 and 1400 kg/m^3 have Poisson's ratio range of 0.13 to 0.16 and 0.18 to 0.19 respectively.

The values measured were 0.14, 0.19, and 0.08 for D300, D600 and D1000 foamed concretes respectively. Therefore, in comparison to the data available on foamed concrete as well as normal weight concrete, Poisson's ratio values obtained for the foamed concretes tested are either within the ranges reported or lower. The variability in the results was thought to be within the repeatability limits as very low microstrains and difficulties (such as localised crushing of the specimens) were involved during the testing of such low strength materials. Therefore, the Poisson's ratio of foamed concretes ranging from D300 to D1000 can be given in the range of 0.1 to 0.2 with D300 ULFC showing no extraordinary behaviour.

Similar to E-value measurements, due to the low strength of foamed concrete, localised crushing at the contact points between the frame and specimen were observed, possibly leading to inaccuracies in the strain measurements. Moreover, errors in the measurements

may also arise from the contact points of the frame not being attached tightly enough to avoid localised crushing. Consequently, this may cause potential slipping of the frame yielding readings with errors. As the test method employed for this test was for normal weight concrete (given the lack of standard test method for foamed concrete), suitability of this test method for yielding reliable results is of concern to be considered.

8.4.2 Drying shrinkage

Foamed concretes are reported to undergo high drying shrinkage strains due to the absence of coarse aggregates that restrain the volumetric changes (Ramamurthy et. al, 2009), high water contents of the mixes and high paste to fine aggregate contents (McCarthy, 2004). While Ramamurthy et. al (2009) reported lower drying shrinkage strains at lower foamed concrete densities (due to the lower paste content of affecting the shrinkage), McCarthy (2004) and Concrete Society (2009) reported contradicting data such that lower foamed concrete densities of exhibited higher shrinkage. Therefore, ULFCs (that does not comprise fine aggregates) are highly prone to drying shrinkage strains and corresponding crack developments which can be problematic in many applications including ground supported slabs and multi-layer wall systems.

In order to obtain an indicative drying shrinkage range for ULFCs D300 and D600 foamed concretes produced with blends of 95%PC/5%CSA, 90%PC/10%CSA and 50%PC/10%CSA/40%FA2 were examined for drying shrinkage profiles as well as moisture loss over a period of 6 weeks. Given the similar characteristics of foamed concrete and for autoclaved aerated concrete (AAC) , determination of drying shrinkage was carried out following the standard method described for AAC (BS EN 680:2005). Different from the standard methods for normal weight concrete and masonry units, test specimens were saturated in the water prior to testing as the test specimens are considered to be cut from already existing elements. For this reason, foamed concretes were cast and cured for 28 days prior to testing as well proving sufficient strength gain prior to securing the steel ball bearings on the specimens (as described earlier in Section 3.6.2).

Effect of plastic density

Figure 8.14 shows the drying shrinkage profiles of D300 and D600 foamed concretes. Drying shrinkage strains ranged from 0.018% to 0.057% (180 and 570 μstrain) for D300 mixes while ranging from 0.021% to 0.047% for D600 mixes. Clearly, the trend reported by McCarthy (2004) and Concrete Society (2009) was observed and D300 foamed concretes exhibited higher drying shrinkage strains in comparison to D600 for all cement combinations. Although the cement content of D300 mixes (200 kg/m^3) is lower than that of D600 mixes (300 kg/m^3) which implies a lower paste content exposed to shrinkage strains, absence of fine aggregates (that restrain the strains) in D300 mixes were observed to have more dominant effect on the drying shrinkage profiles of D300. On the other hand, Neville (2011) suggested that concretes with lower compressive strength and more 'open' structure would result in faster loss of moisture hence yielding higher drying shrinkage strains which fits the trend obtained.

Compared to the values reported by McCarthy (2004), Jones and McCarthy (2005a) and Concrete Society (2009) which range from 0.35% down to 0.06% for dry densities of 400 to 1600 kg/m^3 respectively, measured values of D300 and D600 foamed concretes were found to be significantly lower (i.e reported values were found to be 80% higher than the measured values for D600 mixes). This is mainly attributed to the differences in the test methods used, i.e while values reported in the literature were measured on drying specimens just after de-moulding, specimens in this study were tested after curing for 28 days and pre-conditioning (saturation in water as described in Section 3.6.2). Therefore, it is possible that, during the curing period, specimens may have shrunk prior to saturation leading to lower shrinkage strains than expected.

On the other hand, increasing rate of drying shrinkage development of foamed concretes at both densities and all cement combinations (except D300 FA mix which resulted in scattered data with no apparent trend) was observed over the testing period. McGovern (2000) and McCarthy (2004) reported that in most cases development of drying shrinkage levels off between the 3rd and the 10th week of testing period. As there were time limitations while performing this test, further measurements could not be taken beyond 6 weeks and the test was ceased while the rate of drying shrinkage development was still increasing. This may be another reason of obtaining lower drying shrinkage strains than expected. From another point of view, Narayanan and Ramamurthy (2000) related drying

shrinkage to the size and distribution pores which may likely be case in this study, however, further research is required for relating the microstructure to drying shrinkage.

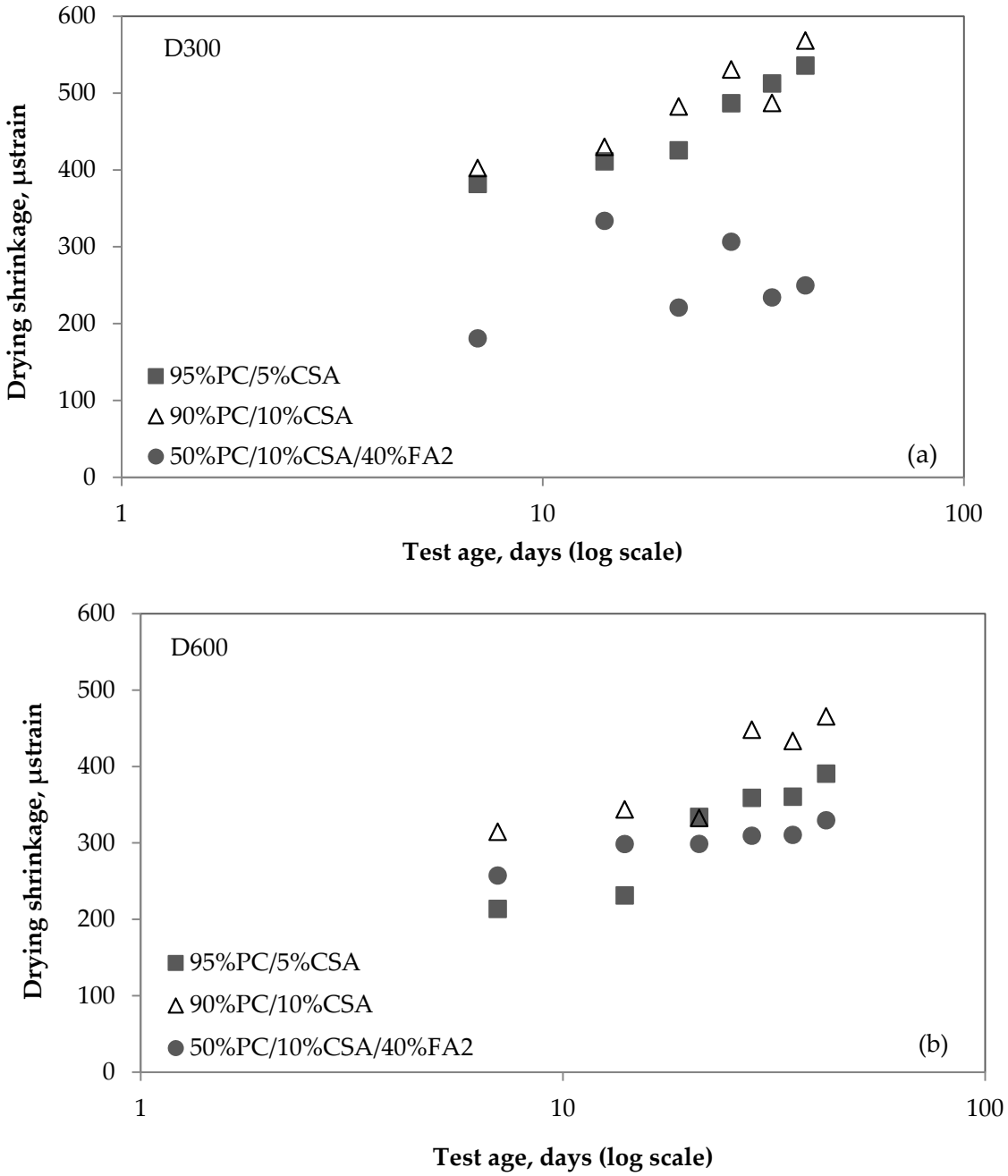

Figure 8.14 Drying shrinkage strain development of (a) D300 and (b) D600 FCs

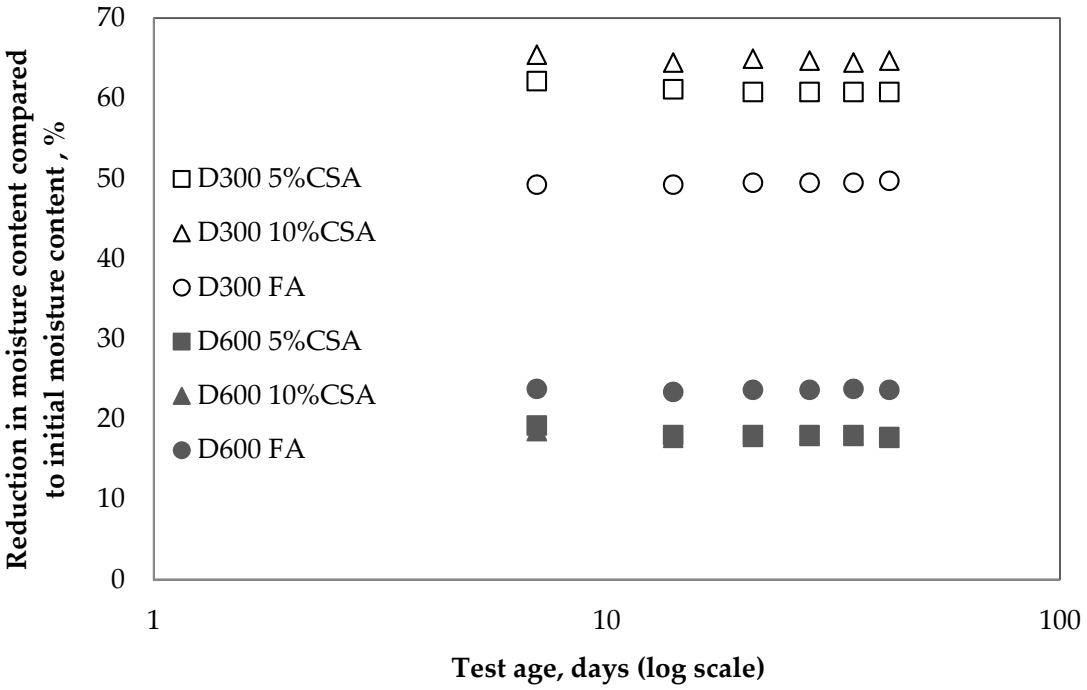

Figure 8.15 Moisture content profiles of D300 and D600 FCs upon drying

Figure 8.15 illustrates the reduction in moisture content of test specimens in respect to the initial moisture content prior to drying. As seen in the Figure, there is no apparent reduction in the moisture content of the test specimens after the first week of drying as all the evaporable water was lost in the first week. Data reported by McCarthy (2004), mass loss instead of reduction in moisture content, exhibited an increasing reduction in the mass of the specimens with time.

Effect of constituents

Overall, at both foamed concrete densities, 90%PC/10%CSA blend was found to yield the highest drying shrinkage strains followed by the 95%PC/5%CSA blend. This behaviour is attributed to the more 'open' and porous microstructure of 90%PC/10%CSA blends (as visually observed and shown in Section 7.2.1). On the other hand incorporation of fly ash in the mixes at a rate of 40% by mass (50%PC/10%CSA/40%FA2 blend) reductions of up to 56% and 31% in the drying shrinkage strains of D300 and D600 foamed concretes were observed respectively. The trend obtained with the incorporation of fly ash is in line with the findings by McCarthy (2004), Jones et. al (2003) and Jones and McCarthy (2005a) who

reported reductions in drying shrinkage strains of foamed concretes with higher reductions at lower densities.

Lower drying shrinkage strains of fly ash mixes are attributed to the slower reaction rate of fly ash which results in lower volume of shrinkable paste in comparison to PC mixes at any given time, concrete density and fine aggregate type (RILEM, 1991; McCarthy, 2004). Moreover, RILEM (1997) and Neville (2011) attribute the reduced drying shrinkage strains of fly ash mixes to the unreacted fly ash particles (that were observed in this study in Chapter 6) which act as filler providing a level of restraint. Apart from the cement types, influence fine aggregate content was covered earlier that absence of fine aggregates leads to higher shrinkage strains. Furthermore, influence of different w/c ratios was not examined in this study.

Discussions on the test method

As mentioned earlier, standard test method used for determining the drying shrinkage (BS EN 680:2005 for autoclaved aerated concrete) was different than the tests used to obtain the comparable data reported by McCarthy (2004) and Jones and McCarthy (2005a) who used the test method for mortars. As the test method used in this study required pre-conditioning of the specimens in water, further research is required to determine the correlation between test methods. Moreover, influence of curing prior to testing (which was required for ULFCs to gain sufficient strength for securing the ball bearings) needs to be examined, as the specimens may have shrunk already during this period.

8.4.3 Coefficient of thermal expansion

As there is no available data on the coefficient of thermal expansion (CTE) of foamed concrete, foamed concretes with plastic densities of 300 and 600 kg/m^3 were tested to obtain an indicative range. Cement combinations of 95%PC/5%CSA, 90%PC/10%CSA and 50%PC/10%CSA/40%FA2 were employed with the intention of evaluating the influence of varying mix composition. Neville (2011) states that it is mainly the hydrated cement paste and aggregate controlling the CTE, whereas hydrated cement paste possessing higher CTE. Importance of aggregate on reducing the CTE was also reported with the decreasing CTE with increasing aggregate content.

As described in Section 3.6.2, control specimens left in the 20°C water tank during the test and the CTE measurements were corrected by subtracting the measurements taken from the control specimens in order to eliminate any further expansion caused by any other means than thermal changes. Accordingly, Figure 8.16 shows the initial CTE of the specimens tested and the control specimens. As seen in the Figure, all of the control specimens apart from 90%PC/10%CSA blends have undergone prolonged expansion at both foamed concrete densities. Although it was assumed that immersion of the specimens in 20°C water tank for 24 hours (prior to testing) would result in full saturation of the specimens and expansion due to saturation, further expansion was observed upon prolonged saturation. Shrinking control specimens of 90%PC/10%CSA blends may be within the repeatability limits and possibly caused by the difficulties arising during the strain measurements of fully saturated specimens. Therefore, they were not taken into account as correction factors.

Effect of plastic density

Figure 8.17 shows the resultant CTE of D300 and D600 foamed concretes which ranged from 8.1 to 41.7x10^{-6}/°C and exhibited no definite trend. As there is no aggregate in D300 mixes, it was expected to have higher expansion in these mixes. However, D300 foamed concretes generally exhibited lower CTE than D600 mixes except for 95%PC/5%CSA blend where both densities exhibited equal rate of expansion. Lower CTE of D300 specimens can be attributed to the more porous and 'open' microstructure of these specimens that can accommodate expansion strains without undergoing any volumetric changes. Therefore, although the absence of aggregates is considered to lead higher CTE, in the case of D300, porous microstructure of D300 paralysed the effect of expansive thermal strains. Moreover, given the lower paste content which influences shrinkage and expansion (Jones et. al, 2005a; Ramamurthy et. al, 2009). , D300 foamed concretes exhibit lower expansion owing to lower volume of shrinkable paste.

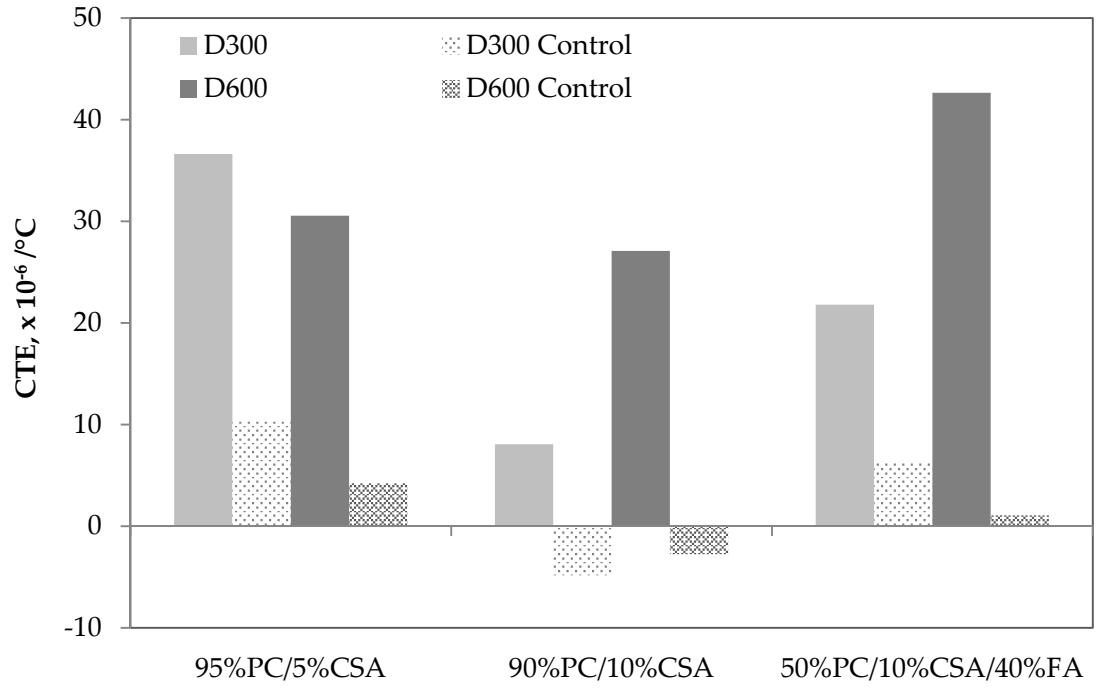

Figure 8.16 CTE of D300 and D600 foamed concretes and the control specimens

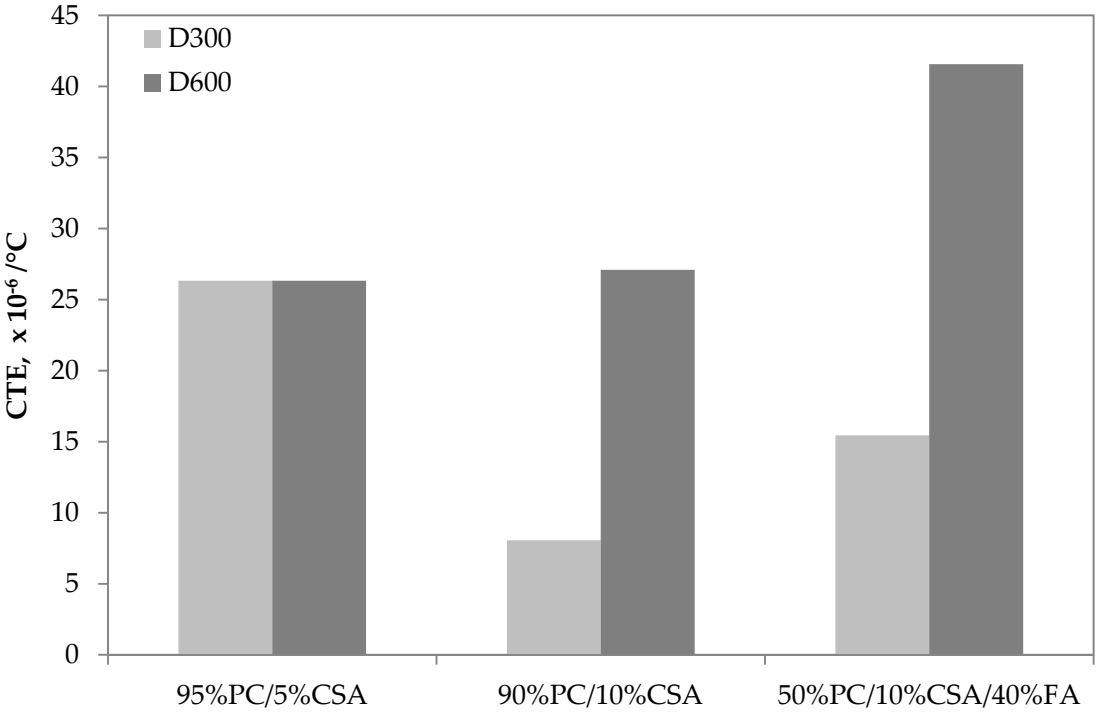

Figure 8.17 Corrected CTE of D300 and D600 foamed concretes

Effect of constituents

Different cement blends resulted in varying CTE values at both foamed concrete densities except 95%PC/5%CSA and 90%PC/10%CSA D600 specimens which exhibited similar CTE values. More porous microstructure of 90%PC/10%CSA specimens specifically in D300 mixes (shown in Section 7.2.1, Figure 7.2) which already possess 'open' microstructure can accommodate higher strains compared to 95%PC/5%CSA yielding lower CTE. On the other hand, given its higher density and presence of aggregates which have more dominant effect than the microstructure, D600 mix did not seem to exhibit any significant change in CTE when 90%PC/10%CSA blend was used.

Moreover, when fly ash specimens are considered, CTE of D300 decreased in comparison with 95% PC/5%CSA blends whilst increased compared to 90% PC/10%CSA blends. This may be attributed to the microstructure properties of fly ash mixes which are more porous and 'open' than 95%PC/5%CSA blends but denser and more 'close' than 90% PC/10%CSA blends (as discussed and shown in Sections 6.4 and 7.2).

On the other hand, D600 specimens seem to exhibit significantly increased CTE with the incorporation of fly ash and the reason behind this behaviour stays unclear. There is insufficient data on influence of fly ash on CTE, while Joshi and Lohtia (1997) stated that fly ash does not really affect the CTE.

Discussions on the test method

Standard test method of AASHTO T336-11 for determination of CTE of concrete was not strictly followed given the unavailability of the test apparatus. Firstly, changes made to specimen size and smaller test specimens were used which may lead to higher CTE readings. Secondly, the lower end temperature used in the current study was higher than the specified temperature (20˚C instead of 10˚C) which may possibly have an influence on the measurements. Given the unavailability of a temperature controlled big water tank, hot and cold environments were created separately and the measurements from the specimens could not be taken while the specimens are in the water tank. From the same reason, expanding and shrinking cycles could not be recorded as gradual cooling/heating of the water was not possible within one water tank. Consequently, all these factors are considered to yield measurements with errors requiring detailed, further research.

8.4.4 Sorptivity

Most foamed concrete applications including trench fills and thermally insulating ground slabs requires interaction with the soil. Therefore, foamed concrete in the ground is susceptible to attacks by deleterious agents such as acids and sulfates, potentially leading to expansion of foamed concrete. Although foamed concrete was reported to exhibit good resistance to aggressive chemical attack up to 12 months (Jones and McCarthy, 2005b; Ramamurthy et. al, 2009), it is beneficial to examine the capillary sorption of the foamed concretes under consideration as it gives an indication on susceptibility to expansions caused by aggressive environments (Jones and McCarthy, 2005b).

Sorptivity of foamed concrete specimens produced with 90%PC/10%CSA and 50%PC/10%CSA/40%FA2 blends were measured utilising the capillary rise method described by (Hall, 1989). Plastic densities of 200, 300 and 600 kg/m^3 were considered. The specimens were evaluated at testing ages of 28 days and 4 months to identify the effect of age (which likely changes the microstructure, especially in fly ash specimens) in relation to sorptivity. Sorptivity indices of foamed concretes ranged from 0.06 to 0.18 mm/min$^{1/2}$ and are shown in Figure 8.18.

Effect of plastic density

It was expected from the literature (Jones and McCarthy, 2005b; Nambiar and Ramamurthy, 2007b; Ramamurthy et. al, 2009) that for a given type of aggregate, sorptivity indices will decrease with increasing foam content and decreasing volume of sorbing paste (i.e decreasing density). However, a contrasting trend was obtained for foamed concretes with densities ranging from D200 to D600 such that sorptivity was found to increase with decreasing plastic density. This behaviour may be attributed to the absence of sand which would possibly provide obstruction to the movement of water in ULFCs. Although Kearsley and Wainwright (2001a) suggested that inclusion of aggregates in foamed concretes may not reduce the permeability as the small air voids already act as aggregates stopping the movement of water, presence of open-cell bubbles in ULFCs may not effectively achieve this leading to high permeability in the absence of aggregates.

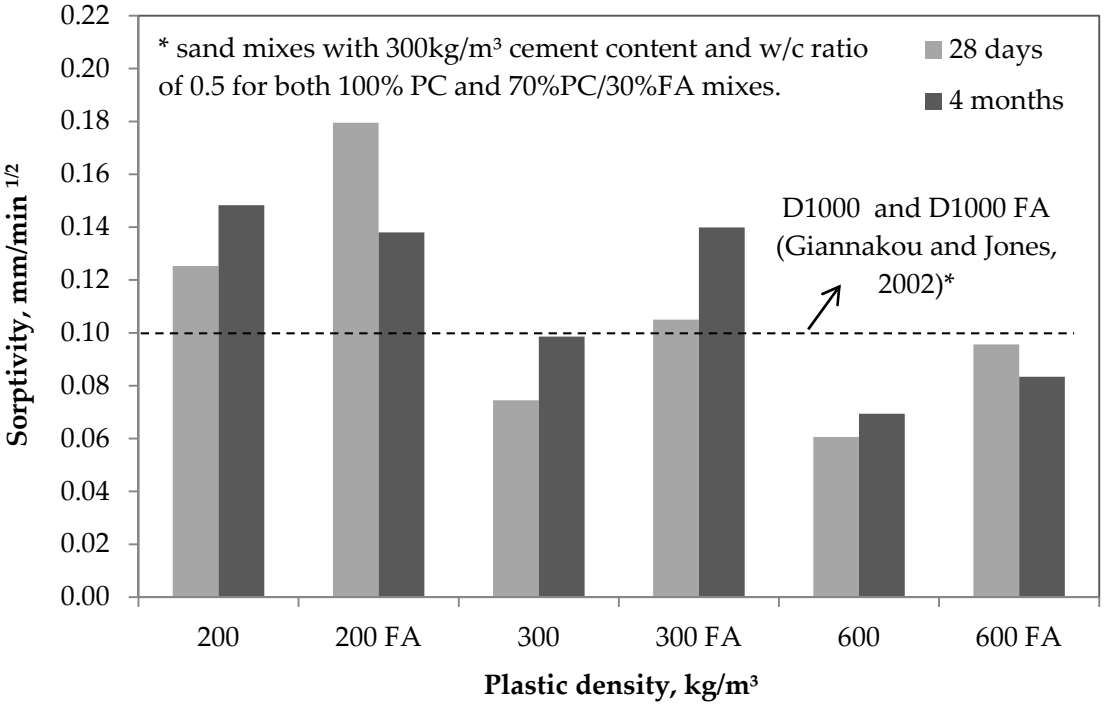

Figure 8.18 Sorptivity indices of D200, D300 and D600 90%PC/10%CSA and 50%PC/10%CSA/40%FA2

It must be noted that, although Jones and McCarthy (2005b) reported decreasing sorptivity with decreasing density, sorptivity indices for mixes produced with sand were reported to be similar, but slightly higher on the lower side of the density range. Moreover, during the conditioning of the specimens prior to testing (drying to a constant mass at 30°C as described in Section 3.6.2) shrinkage cracks are likely to occur, specifically at ultra-low densities. Consequently, this modifies the pore structure increasing the permeability (Kearsley and Wainwright, 2001a) as well as the capillarity hence the sorptivity indices of ULFCs.

Although larger and more interconnected pores present in the ULFCs were expected to lead lower capillary forces, hence lower sorptivity indices, effect of sand obstructing the movement of water within the concrete may be more dominant. Furthermore, more open structure of ULFCs may possibly increase the number of flow channels increasing the water intake (McCarthy, 2004). In contrast, observations reported by Hall (1989) suggest that decreased cement contents lead to increased sorptivity which supports the findings for the mixes considered.

On the other hand, in comparison to the sorptivity indices reported for D1000 (Jones and McCarthy, 2005b), sorptivity of D600 (comprised of equal volume of sorbing paste but lower volume of sand than D1000) was found to decrease. However, it still stays unclear why ULFC specimens exhibited higher sorptivity indices requiring detailed further research.

Effect of constituents

Foamed concretes produced with 50%PC/10%CSA/40%FA2 blends were found have higher sorptivity indices in comparison to 90%PC/10%CSA blends. Giannakou and Jones (2002) reported that 70%PC/30%FA foamed concretes have similar sorptivity indices compared to 100%PC comprising sand as fine aggregate. In the current study increased sorption of fly ash mixes may be attributed to the formation of finer flow channels and more importantly finer pores (as shown in Section 6.3) resulting from incorporation of fly ash. Moreover, as suggested by McCarthy (2004), slower hydration of fly ash hence more 'open' microstructure may increase the number of flow channels yielding higher sorption values. On the other hand, this behaviour can be attributed to the increased water requirement of mixes containing fly ash which results in a more pervious matrix, as also concluded by Nambiar and Ramamurthy (2007b) who also reported higher sorptivity levels with increasing fly ash contents.

The trend of increasing sorptivity indices with decreasing plastic density obtained for PC/CSA mixes was also observed in the fly ash mixes. On the other hand, similar to PC/CSA mixes, D600 fly ash specimens exhibited lower sorptivity than the D1000 specimens (70%PC/30%FA) reported by Giannakou and Jones (2002).

Effect of age

Fly ash is reported to decrease the permeability of concrete by time (around 180 days) as a result of its pozzolanic activity. Fly ash reacts with calcium hydroxide (produced by Portland cement hydration) in the water filled capillary channels producing calcium silicate and aluminate hydrates which are insoluble in water and tend to fill in the capillary channels (Joshi and Lohtia, 1997). Therefore, reduced sorptivity is expected in fly ash foamed concretes in long-term. While D200 and D600 specimens exhibited the expected trend, sorptivity of D300 fly ash specimens increased in long-term (Figure 8.18). The

behaviour of D300 specimens are considered to be in the repeatability limits and possibly caused by the presence of shrinkage cracks within the tested specimens. However, it also be noted that, if the hydration products of fly ash did not fully fill the capillary channels, but made them finer, it may lead to increased capillary forces, hence sorption.

Although the testing age is considered to mainly influence the fly ash mixes, it was found that sorptivity of PC/CSA mixes were also affected in long-term. Accordingly, compared to 28-day specimens, 4-month specimens were found to exhibit increased sorptivity. This behaviour may be attributed to the changes in the microstructure due to any prolonged hydration of cement which left unhydrated in the earlier stages. The 10% CSA cement in the non-fly ash mixes is likely to undergo prolonged hydration when exposed to additional water (provided during the 4-month sealed curing) causing expansion (Chen et. al, 2012) hence changing the pore structure of the specimens. Consequently, capillary channels become finer exhibiting higher capillary forces which yield higher sorptivity.

Discussions on the test method

Complexity of liquid transport and permeation mechanism in porous media which has variable, evolving microstructure and pore structure (resulting from different constituents, specifically fly ash used for production) was reported by Jones and McCarthy (2005b). Given the variations in foamed concrete microstructure, sorptivity test is not sufficient to provide enough information on pore network including size, distribution, interconnectivity (McCarthy, 2004).

Due to the combined effect of low-strength and lack of fine aggregates in ultra-low density foamed concretes, shrinkage cracks upon drying of specimens (even at much lower temperatures than specified; 30°C instead of 105°C) were observed. These cracks may possibly lead to errors in the measurements by increasing the permeability of the concrete (Kearsley and Wainwright, 2001a). Furthermore, although it was required to seal the testing specimens such that only one face of the cubes is exposed to water to maintain one-dimensional sorptivity, the specimens were not sealed. This was done in order to follow the same procedure with McCarthy (2004) and make comparisons with the reported data. Consequently, even if this may yield sorptivity values with errors, the trend would be the same.

8.5 CONCLUSIONS

Behaviour of ultra-low density foamed concretes were evaluated in regard to fresh, early age and hardened properties and compared to low/high density ones. The data suggested that, overall performance of ultra-low density foamed concrete does not restrict its use in the potential applications and in some aspects it provides further advantages compared to higher density foamed concretes. The detailed conclusions drawn from the evaluation of properties of ULFC are as follows:

Fresh and early age properties

i. The flow time data obtained by the modified Marsh cone method showed that ULFCs with densities below 500 kg/m^3 do not have the self-flowing and levelling ability due to the significantly reduced self-weight. Moreover, as the foam content increases significantly at ultra-low density levels, the flow behaviour is mainly governed by the foam bubbles.

ii. Addition of fly ash was not found to change the flow behaviour of ULFCs significantly, to an extent to provide self-flowing ability. Moreover, the type of fly ash was also found to have an influence on the flow behaviour, where in this case FA1 was found to have a greater effect at 30% addition level. In the case of FA2, addition level greater than 40% was found to reduce the flow in ULFCs. Furthermore, influence of pour volume on the heat development profile of ULFCs, was not considered in this study and needs to be analysed in further research.

iii. Peak core temperatures developed due to heat of hydration were found to decrease with reducing cement contents, hence plastic density. Therefore, the maximum peak temperature obtained was, 55.8 °C for 100% PC D600 mix (300 kg/m^3 cement content), while the minimum temperature was 25.4 °C for 50% PC/10% CSA/40% FA1 D200 mix (cement content of 133 kg/m^3).

iv. Addition of 40% fly ash reduced the peak temperatures by up to 51%, with a pattern of increasing reductions with increasing cement contents. The maximum peak temperature recorded for fly ash mixes was 28.9 °C for D600 mix. Besides the

addition of fly ash, it was observed that 10% CSA addition has a dominant effect on reducing the peak temperatures, which is thought to be due to flash set.

v. Due to the high thermal insulating capacity of foamed concretes with decreasing density, heat developed due to hydration can be retained, leading to higher core temperatures at lower densities. However, influence of cement content was found to be more dominant on the peak core temperatures of ULFCs, which has the higher thermal insulating capacity and lower cement contents than D600 mixes.

Hardened properties

i. Compressive strength was found to reduce with decreasing plastic density. Due to the absence of sand and low cement content, 300 kg/m^3 foamed concretes were found to have 28-day compressive strength of as low as 0.23 N/mm^2.

ii. Modulus of elasticity was found to increase with increasing compressive strength and ranged from 0.2 to 1.1 kN/mm^2 for D300 to D1000 foamed concretes respectively.

iii. Poisson's ratio of foamed concrete did not exhibit an apparent trend for densities from 300 to 1000 kg/m^3. However, the values were found to be in line with the reported values and suggested that lateral strain development of foamed concrete under compression is unlikely to cause any problems.

iv. Due to the lack of fine aggregates, ULFC exhibited higher drying shrinkage strains compared to the low density ones. Addition of 40% fly ash was found to reduce the drying shrinkage strains by up to 54%. Overall, drying shrinkage strains obtained were found to be lower than the values reported in the literature, which was mainly attributed to the test method used in this study. However, drying shrinkage would not be an issue for ULFC pre-cast elements, as they would shrink prior to use.

v. Coefficient of thermal expansion (CTE) of both D300 and D600 concretes were found to be higher than the values reported for cellular and autoclaved aerated concretes, except 10% CSA D300 mix which exhibited the value of 8x10^{-6}/$^{\circ}$C, same as the

reported values. Addition of fly ash increased the CTE when compared to 10% CSA mix.

vi. Although neat cement paste exhibits higher CTE, ULFCs in this case were found to have lower CTE, suggesting that the reduced cement content (hence expansive paste) has a more dominant effect than the absence of sand. Furthermore, as the standard test method was not followed strictly, further research is required using the specified test apparatus.

vii. Sorptivity indices increased with decreasing density, addition of fly ash (at all densities) and specimen age (for all mixes except D200 FA and D600 FA mixes). Overall, while the D600 specimens exhibited the expected behaviour, ultra-low density specimens did not.

viii. High sorptivity indices and larger pores present at lower densities may indicate higher risk of attacks by aggressive environments. However, larger pores and more porous microstructure of lower density foamed concretes possibly well-accommodate the high expansion strains, leading to less expansion than it would be in a less porous concrete.

CHAPTER 9

9. OVERALL CONCLUSIONS, PRACTICAL IMPLICATIONS, APPLICATIONS AND RECOMMENDATIONS FOR FURTHER RESEARCH

9.1 INTRODUCTION

Following extensive consideration of the results in each Section, the detailed conclusions drawn were presented at the end of each relevant Chapter. This Chapter therefore concentrates on presenting the major findings of this research project. More specifically, the Chapter identifies the practical outcomes, applications and implications of the research as well as identifying the opportunities for further research.

9.2 OVERALL CONCLUSIONS

The overall aim of the study was achieved by carrying out laboratory-based investigations and trials which:

i. identified potential materials and their combinations and evaluated their performance in order to develop and produce stable ultra-lightweight foamed concretes (ULFCs),
ii. characterised the developed system,
iii. evaluated performance in terms of insulation and key fresh, early age and hardened properties.

The detailed conclusions drawn from the main focuses of the study, which were stability, microstructure, insulation and properties (fresh, early age and hardened) of ULFCs, are summarised in the relevant Chapters. The following is, however, a summary of the major conclusions.

9.2.1 Stability

The proposed solution of controlling the rate of hardening hence, the change in bubble size, was successfully utilised to produce stable ultra-lightweight foamed concretes with plastic densities down to 150 kg/m^3. Although in the main study calcium sulfoaluminate (CSA) cement was employed to achieve stable mixes through fast initial setting times, other alternative materials could potentially be utilised, provided the initial setting time of the base mix is kept to 20 minutes.

Ultra-low density mixes, more specifically plastic densities below 200 kg/m^3, were found to ultra-low strength foamed concretes that had to be handled with care at early ages. Besides the primary effect of plastic density (i.e amount of foam and solids), cement fineness was also found to have an influence on bubble size which directly affects stability (i.e finer cements enhance stability), however this had a secondary effect.

Fine fly ash of up to 40% by mass was found to produce stable, 150 kg/m^3 ULFCs when used in combination with PC and CSA. Although, it was found that fly ash contents of up to 70% by mass yielded stable mixes at 300 kg/m^3 density, long-term hydration of fly ash resulted in very soft and low strength ULFCs with handleability issues at early ages.

Since fast initial setting-times of base mixes of ULFCs are likely to restrict utilisation in ready mix situations, ULFCs are more appropriately produced by on site mixing or in precast manufacturing.

9.2.2 Microstructure

Average bubble sizes in foamed concretes were found to increase by decreasing plastic density thereby increasing susceptibility to instability at ultra-low density levels. Type of constituents was also found to influence the average bubble size at a given density such that finer materials yielded smaller bubble diameters. Fly ash mixes were observed to yield up to 31% smaller average bubble diameter.

Comparing the microstructure (SEM) images of a range of foamed concretes showed that, in comparison to high/low density foamed concretes (≥ 600 kg/m^3), ULFCs exhibit a rather 'open' and porous microstructure with holes present in the bubbles. Furthermore, due to the decreased cement contents, absence of fine aggregates and increased average bubble size, the bubble walls were observed to become thinner indicating lower strength. Use of fly ash was found to improve the microstructure in the long-term (up to 1 year); strengthening the bubble walls and healing the holes present on the internal bubble surfaces.

9.2.3 Insulation performance

Thermal insulation

Compared to low density FCs, ULFCs exhibited increased resistance to the conductance of heat, providing thermal conductivities of down to 0.078 W/mK in 200 kg/m^3 mixes. Addition of 30% fly ash resulted in further reductions in the thermal conductivity. However, as the microstructure of fly ash mixes get denser over time, thermal conductivity values slightly increased in the long-term when compared to 28-day values.

Sound insulation

Owing to higher porosity and more open microstructure, foamed concretes with plastic densities of 200 kg/m^3 exhibited the highest sound absorption capacity overall. Therefore, sound absorptions of a maximum of 96% were recorded for frequencies ranging from 125 to 4000 Hz, where the peaks were observed around 500-1500 Hz and 3000-3500 Hz. Addition of fly ash was found to increase the sound absorption. On the other hand, given its higher mass and stiffness, 600 kg/m^3 foamed concrete exhibited better sound transmission loss performance than ULFCs.

9.2.4 Properties of ULFC

Fresh properties

In contrast to conventional foamed concretes, ULFC mixes with plastic densities below 500 kg/m^3 were not found to be self-flowing and compacting. Addition of 30% fly ash (by

mass) was found to slightly improve the flow of ULFCs, yet not to an extent provide self-flowing and levelling ability.

Early-age properties

Peak temperatures reached due to the heat of hydration was measured to be reduced by up to 45-50% in 200 kg/m^3 mixes in comparison to 600 kg/m^3 mixes. As expected, incorporation of fly ash provided further reductions in peak temperatures. Therefore, ULFCs can be used for large volume applications without the risk of thermal cracks.

Hardened properties

Although compressive strength, modulus of elasticity and Poisson's ratio were not studied in detail, some indicative values were obtained as a response to an increasing number of industry originated requests for these values. The conclusion is that, ULFCs exhibited lower strengths and E-values compared to low density foamed concretes. For Poisson's ratio, no apparent trend was obtained. 300 and 600 kg/m^3 mixes exhibited higher Poisson's ratio compared to 1000 kg/m^3 whilst 300 kg/m^3 was recorded to be lower than 600 kg/m^3.

ULFCs exhibited increased drying shrinkage in comparison to low density foamed concretes, yet lower drying shrinkage strains reported in the literature for low/high density foamed concretes. Addition of 40% fly ash (by mass) was found to reduce drying shrinkage strains of ULFCs by up to 54% in comparison to PC/CSA mixes.

Owing to the more porous structure, 300 kg/m^3 foamed concretes were found to be better in accommodating the expansive strains developed upon temperature rises, hence exhibiting a 37% lower coefficient of thermal expansion compared to 600kg/m^3 mixes. Use of fly ash was not found to further reduce the lowest thermal expansion coefficients.

For densities from 200 to 600 kg/m^3 sorption indices increased with decreasing density and overall ultra-lightweight foamed concretes exhibited higher sorption than low density ones. Incorporation of 40% (by mass) fly ash was found to increase the sorption.

9.2.5 Environmental Impact

ULFCs can have up to 200 kg/m^3 lower cement contents at plastic density 150 kg/m^3 in comparison to 600 kg/m^3 low density foamed concrete mixes. Additionally, fine aggregates are eliminated in ULFC which further contribute to resource efficiency and reduction of the use of primary resources.

Compared to foamed concretes with plastic densities 600 kg/m^3 and above, ULFCs have up to 67% lower eCO_2 (in 150 kg/m^3 mixes) while with the addition of 40% fly ash further 13% reduction was obtained.

9.3 POTENTIAL APPLICATIONS

The findings of this research can be used to expand the application areas for foamed concrete as well as improving the performance for the current areas including the following:

Being an inorganic, fire and insect resistant and relatively cheap material, ULFC can potentially be used as an alternative insulation material, possibly in combination with other materials and/or higher density foamed concretes constructed into a multi-layer system, to serve as thermo-acoustic insulation. It can also be used to pre-cast ultra-lightweight insulating blocks or panels.

Due to low Poisson's ratio and ultra-low self-weight, it is advantageous to employ ULFC for the restoration of historic structures such as masonry arch bridges where minimum self-weight is required (as the load bearing capacity of such structures may not be known). Low peak temperatures developed due to heat of hydration and low eCO_2 combined with ultra-low self-weight make ULFC advantageous to use as large volume fill material.

Table 9.1 provides guidance on the performance of a range of foamed concretes enabling the specification of the most suitable foamed concrete to be selected to satisfy the needs of the application.

9.4 PRACTICAL IMPLICATIONS

Due to the nature of ultra-lightweight foamed concrete, there are some constraints which may affect its use in practical applications. Therefore, it is beneficial to review these in order to provide guidance for its use in industry. The practical constraints related to setting times, flow behaviour, long-term performance and sorption properties are listed respectively, as follows:

- In the case of the ready mixed base mixes, short initial setting times required for ULFC can be problematic, considering the potentially long travel times and the possible delays in placing the mix. Therefore, using ready mix base mix for ULFCs is not really practical unless a mechanism is developed to retard and immediately accelerate the initial setting when required. On-site mixing of base mix is however recommended for the applications of ULFCs.

- At ultra-low density levels, foamed concrete loses its self-flowing and levelling properties. Therefore, it should be considered to include external forces to aid placing and levelling of ULFC mixes in a way that the nature of the mix is not destroyed (i.e avoiding actions causing foam collapse).

- Long-term performance of fly ash mixes should be considered in design, particularly when assigning them for thermal and sound insulation purposes where microstructure greatly affects the performance.

- High sorption indices indicate higher susceptibility to the flow of solutions into ULFCs. Therefore, precautions should be taken, such as installing water-poof membranes, when using these materials in the ground.

Table 9.1 Typical range of properties on the performance of foamed concrete

Plastic density, kg/m³		Peak temp. upon heat of hydration, °C	28-day compressive strength, MPa	E-value, GPa	**Drying shrinkage, %	‡Thermal expansion, μstrains/°C	†Sorptivity, mm/min$^{1/2}$	*Thermal conductivity, W/mK	eCO_2, kg CO_2/m^3 of concrete
200	O	31.0	-	-	-	-	0.148	0.078	120
	FA	26.3	-	-	-	-	0.138	†0.082	80
300	O	38.3	0.2	0.2	0.05	26	0.099	0.100	185
	FA	27.9	-	-	0.03	15	0140	†0.103	125
600	O	55.8	1.1	1.1	0.04	26	0.069	0.177	275
	FA	28.9	-	-	0.03	42	0.083	-	185
1000	O	49.0	1.8	1.8	0.19[1]	-	0.101[1]	0.320	275
	FA*	46.0	0.7[2]	-	0.07[1]	-	0.102[1]	0.280[1]	218

Notes: In. setting times: min. setting time of 20 minutes for fly ash (FA) mixes of D200, D300 and D600. Min. 1.5 hours for ordinary (O) mixes.

Poisson's ratio: 0.08-0.19 for D300- D1000; sound absorption increases, transmission loss reduces with decreasing density.

† Long-term performance (4-6 months)

‡ Lower values obtained for D300 with different non-fly ash cement combination. Needs further research.

* 30% FA used to replace PC, otherwise 40% (by mass)

** 6-week drying shrinkage; 60-day drying shrinkage for the quoted values of 1000 kg/m³ foamed concrete.

[1] Giannakou and Jones (2002); [2] Jones et. al (2003)

9.5 RECOMMENDATIONS FOR FURTHER RESEARCH

The findings of this research suggest that there is a need for further research on particular aspects of ultra-lightweight foamed concretes. These mainly focus on understanding the behaviour of ULFC in order to improve its performance and widen the application areas. The proposed areas requiring further research are as follows:

Retardation mechanism for ULFC

In order to enable the use ready mix base mixes and improve the practicability of ULFC mixes generally, development of a retardation mechanism compatible with foamed concrete (i.e. a mechanism not interacting with the foam) is needed. Such a mechanism, which possibly comprises two different chemicals, is required to retard (switch off) the fast setting base mixes for as long as required and accelerate (switch on) the initial setting immediately when needed.

Rheology of ultra-lightweight foamed concretes

Rheology of ULFC, which is one of the most important parameter affecting the developing behaviour of the concrete and its performance in the practical applications, needs to be studied in detail. This needs to be carried out considering the effect of plastic density, type of constituents, presence of sand, w/c ratio and bubble size. Moreover, further research is required to improve the flow behaviour of ULFC, which is associated with its rheology, making ULFC self-flowing and compacting.

3D bubble analysis and microstructure

To obtain more accurate bubble size data, 3D bubble analysis needs to be carried out with respect to density, constituents and stability. Analysis also needs to be carried out on the samples taken from different heights of the specimen. CT scanning can potentially be used for this purpose. Moreover, changes in the bubble size needs to be monitored CT scanning from the time of production of the mix until hardening.

Reinforcement of foamed concrete bubble walls

ULFCs with densities of 200 kg/m^3 and below tend to be fragile especially at early ages. Although sealed curing improves the handleability through strength gain, further studies need to be done to strengthen the ULFCs. This can be done by utilising lightweight and short length fibres to reinforce the bubble walls, increasing the strength.

Sound insulation behaviour

Sound absorption and sound transmission loss capacities of foamed concretes over a range of densities would value from further research. The analysis needs to be carried out in respect to foamed concrete density, type of constituents, hardened properties like stiffness, bubble size and microstructural properties such as porosity and tortuosity.

Full scale trials

Full scale trials of ULFC need to be designed and tested in possible application areas, including restoration of historic masonry bridges and more specifically, as a multi-layer composite wall for thermo-acoustic insulation.

Behaviour of PC/CSA/FA blends

In general, there is no information on the behaviour of PC/CSA/FA blends. Therefore, analysis of the behaviour of such cement systems, including its effects on foamed concrete properties (fresh, early age, hardened and insulation), needs to be carried out.

Specification for ULFC

Development of a specification for ultra-lightweight foamed concretes is necessary. Given the changes in the nature of the mix (i.e mix constituents; elimination of sand) at ultra-low density levels, it would be beneficial to develop a specification, specifically covering the testing methods for ULFCs.

REFERENCES

AASHTO T336-11 (2011). Standard method of test for coefficient of thermal expansion of hydraulic cement concrete. American Association of State Highway and Transportation Officials.

ALDRIDGE, D. (2005). "Introduction to foamed concrete: What, why, how?" in 'Use of foamed concrete in construction' by Dhir, R.K., Newlands, M.D. and McCarthy A. from the proceedings of the International Conference in the University of Dundee, Scotland, 5 July 2005, pp.1-14.

ALEXANDER, M.G. and MACKECHNIE, J.R. (1999). "Discussion of 'A water sorptivity test for water and concrete' ". Materials and Structures, Vol. 32, pp. 695-696.

ALIGIZAKI K.K. (2006). "Pore Structure of Cement-based materials". Taylor and Francis, pp 286 – 331.

ANSELL, T. (2010). Private communication, Propump Engineering Ltd.

ARENAS, J.P., CROCKER, M.J. (2010). "Recent trends in porous sound-absorbing materials". Sound and Vibration Magazine, July 2010, Materials Reference Issue.

ASTM International

ASTM C469-02 (2002). Standard test method for static modulus of elasticity and Poisson's ratio of concrete in compression.

ASTM E2611-09 (2009). Standard test method for measurement of normal incidence sound transmission of acoustical materials based on the transfer matrix method.

BASIURSKI J. (2000). "Foamed concrete for void filling, insulation and construction". One day awareness seminar 'Foamed concrete: properties, applications and potential', University of Dundee, Scotland, pp. 42-52.

British Cement Association (BCA)

BCA (1991). "Foamed concrete - a Dutch view" by Van Dijk, S. BCA Reprint 2/91. British Cement Association.

BCA (1994). "Foamed concrete- Composition and properties". First published in 1991, British Cement Association.

BERGER, E.H., ROYSTER, L.H., ROYSTER, J.D., DRISCOLL, D.P, LAYNE, M. (2003). "The noise manual". American Industrial Hygiene Association, 5th edition.

Building Regulations

Building Regulations Part E (2013). "Approved Document Part E, Resistance to the passage of sound".

Building Regulations Part L (2013). "Approved Document Part L, Conservation of fuel and power"

BRADY, K.C., WATTS, G. R. A. and JONES, M. R. (2001). "Specification for foamed concrete". Quality Services, Civil Engineering, Highways Agency. Application Guide 39. TRL Ltd.

Building Research Establishment (BRE)

BRE (2004). "Concrete with minimal or no primary aggregate content. The MAGCON pilot study." by Nixon, P. J. BRE Information Paper, IP 12/04.

BRE (2007). "Calcium sulfoaluminate cements. CO2 reductions, concrete properties and applications" by Quillin, K. BRE Report No. 496.

BRE (2009). "Responsible Sourcing of Construction Products, Framework Standard for the Responsible Sourcing of Construction Products - BES 6001". BRE Information Paper, IP 6/09.

BRITISH STANDARDS (British Standards Institution (BSI))

BS EN ISO 354:2003. Acoustics. Measurement of sound absorption in a reverberation room.

BS EN ISO 8990:1996. Thermal insulation. Determination of steady-state thermal transmission properties. Calibrated and guarded hot box.

BS EN ISO 6946:2007. Building components and building elements. Thermal resistance and thermal transmittance. Calculation method.

BS EN 1008:2002. Mixing water for concrete —Specification for sampling, testing and assessing the suitability of water, including water recovered from processes in the concrete industry, as mixing water for concrete.

BS EN 1352:1997. Determination of static modulus of elasticity under compression of autoclaved aerated concrete or lightweight aggregate concrete with open structure.

BS EN 12350-1:2009. Testing fresh concrete. Sampling.

BS EN 12350-6:2009. Testing fresh concrete. Density.

BS EN 12620:2013. Aggregates for concrete.

BS EN 13263:2005 + (A1:2009). Silica fume for concrete. Definitions, requirements and conformity criteria (+A1:2009).

BS EN 196-3:2005+A1:2008. Methods of testing cement. Determination of setting times and soundness.

BS EN 197-1:2011. Cement. Part 1: Composition, specifications and conformity criteria for common cements.

BS EN 450:1-2012. Fly ash for concrete. Part 1: Definition, specifications and conformity criteria.

BS 874:3.2-1990. Methods for determining thermal insulating properties. Tests for thermal transmittance and conductance. Calibrated hot-box method.

CHANDLER, J.W.E. (2000). "Highway reinstatement with foamed concrete". One day awareness seminar 'Foamed concrete: properties, applications and potential', University of Dundee, Scotland, pp. 26-32.

CHEN, I. A., HARGIS, C.W. and JUENGER M.C.G. (2012). "Understanding expansion in calcium sulfoaluminate–belite cements". Cement and Concrete Research Vol.42, pp. 51–60.

CONCRETE INDUSTRY SUSTAINABLE CONSTRUCTION FORUM (CICSF), (2008). "Sheet C1-Embodied CO2 of Concrete and Reinforced Concrete".

CONCRETE SOCIETY (2009). "Foamed concrete- application and specification". Good Concrete Guide 7. Concrete Society.

CROCKER, M.J. (1998). "Handbook of acoustics". John Wiley & Sons, Inc.

DEMIRBOĞA, R., GÜL, R. (2003). "The effects of expanded perlite aggregate, silica fume and fly ash on the thermal conductivity of lightweight concrete". Cement and Concrete Research, Vol.33, pp. 723-727.

DE ROSE, L., MORRIS, J. (1999). The influence of the mix design on the properties of micro-cellular concrete". In 'Specialist techniques and materials for concrete construction' from the proceedings of the International Conference 'Creating with concrete' (Ed R K Dhir and Henderson), University of Dundee, Scotland, 8 - 10 September 1999, Thomas Telford, pp. 185-197.

DONG, W., FALTENS, T., PANTELL, M., SIMON, D., THOMPSON, T., DONG, W. (2009). "Acoustic Properties of Organic/Inorganic Composite Aerogels". Materials Research Society, 2009 MRS Spring Meeting, Vol.1188.

DRANSFIELD, J.M. (2000). "Foamed Concrete: Introduction to the product and its properties". One day awareness seminar 'Foamed concrete: properties, applications and potential', University of Dundee, Scotland, pp.1-8.

DHIR, R.K., JONES, M.R. and NICOL, L.A. (1999). "Development of structural grade foamed concrete". Final Report, DETR Research Contract 39/3/385, pp.84.

EUROPEAN COMMISSION (EC)

EC (2002). "Directive 2002/49/EC of the European Parliament and of the Council of 25 June 2002 relating to the assessment and management of environmental noise". Official Journal of the European Union, 18 July 2002.

EC (2011a). "Construction Products Regulation (CPR)- Regulation (EU) No 305/2011 of The European Parliament and of the Council of 9 March 2011 laying down harmonised conditions for the marketing of construction products and repealing Council Directive 89/106/EEC". Official Journal of the European Union, 4 April 2011.

EC (2011b). "Report from the Commission to the European Parliament and the Council on the implementation of the Environmental Noise Directive in accordance with Article 11 of Directive 2002/49/EC". COM(2011) 321 final, Brussels, 1 June 2011.

GIANNAKOU, A. and JONES, M.R. (2002). "Potential of foamed concrete to enhance the thermal performance of low-rise dwellings". In 'Innovations and developments in concrete materials and construction' by Dhir,R.K, Hewlett, P.C. and Csetenyi, L.J., from proceedings of the International, Congress 'Challenges of construction' in the University of Dundee. Dundee, Scotland. Thomas Telford Ltd, pp.533-544.

GLASSER, F.P. and ZHANG, L. (2011). "High-performance cement matrices based on calcium sulfoaluminate-belite compositions". Cement and Concrete Research, Vol. 31, pp. 1881–1886.

HALL, C. (1989). "Water sorptivity of mortars and concretes: a review". Magazine of Concrete Research, Vol.41, No. 147, pp.51-61.

HALL, C. and KAM MING TSE, T. (1989). "Water movement in porous building materials, VII, The sorptivity of mortars". Building Environment,Vol.21,pp.113-118.

HAN, F., SEIFFERT, G., ZHAO, Y., GIBBS, B. (2003). "Acoustic absorption behaviour of an open-celled aluminium foam". Journal of Physics D: Applies Physics, Vol. 36, No.3, pp.294-302, INSTITUTE OF PHYSICS PUBLISHING.

HIGHWAY AUTHORITIES AND UTILITIES COMMITTEE (HAUC) (2010). "New Roads and Street Works Act 1991. Specification for the Reinstatement of Openings in Highways". Code of Practice 3rd Edition (England), April 2010.

INTERNATIONAL ORGANIZATION for STANDARDIZATION

ISO 8302:1991. Thermal insulation. Determination of steady-state thermal resistance and related properties. Guarded hot plate apparatus.

ISO 10534-1:1996. Acoustics. Determination of sound absorption coefficient and impedance in impedance tube. Method using standing wave ratio.

IOANNOU, S., REIG, L., PAINE, K., QUILLIN, K. (2014). "Properties of a ternary calcium sulfoaluminate–calcium sulfate–flyash cement". Cement and Concrete Research, Vol. 56, pp.75-83.

JIS A 1162:1973. "Testing methods for volume change of cellular concrete". Japanese Industrial Standard / Japanese Standards Association.

JONES, M.R. (2000). "Foamed concrete for structural use". One day awareness seminar on 'Foamed concrete: properties, applications and potential', University of Dundee, Scotland, 23 March 2000, pp.54-79.

JONES M.R., McCARTHY A. and McCARTHY M.J. (2003). "Moving fly-ash utilisation in concrete forward: a UK perspective", Proceedings of the '2003 International Ash Utilization Symposium', Center for Applied Energy Research, University of Kentucky.

JONES M.R., McCARTHY A. and DHIR R.K. (2004). "Development of foamed concrete insulating foundations for buildings and pilot demonstration project". DETR Contract 39/03/621 (CC 2046), Concrete Technology Unit, University of Dundee, February 2004, 329 pp.

JONES, M.R., McCARTHY, A. (2005a). "Preliminary views on the potential of foamed concrete as a structural material". Magazine of Concrete Research,Vol. 57, No.1, pp.21-31.

JONES, M.R., McCARTHY, A. (2005b). "Utilising unprocessed low-lime coal fly ash in foamed concrete". Journal of Fuel. No. 84. pp. 1398-1409.

JONES, M.R., McCARTHY, A. (2005c). "Behaviour and assessment of foamed concrete for construction applications". In "Use of foamed concrete in construction" by Dhir, R.K., Newlands, M.D. and McCarthy, A., from proceedings of the International Conference in the University of Dundee. Dundee, Scotland.

JONES, M.R., McCARTHY, A. (2006). "Heat of hydration in foamed concrete: Effect of mix constituents and plastic density". Cement and Concrete Research, Vol. 36(6), pp. 1032-1041.

JONES, M.R., ANSELL, T. and ALDRIDGE, D. (2009). "Foamed concrete for sustainable construction" in 'Concrete'. Global Magazine of the Concrete Society, June, 2009, pp. 16-18.

JONES, M.R., ZHENG, L., YERRAMALA, A., RAO, K.S. (2012). "Use of recycled and secondary aggregates in foamed concrete". Magazine of Concrete Research, Vol. 64(6), pp. 513-525.

JONES, M.R., ZHENG, L. (2013). "Energy absorption of foamed concrete from low–velocity impacts. Magazine of Concrete Research, Vol. 65(4), pp. 209-219.

JOSHI, R.C. and LOHTIA, R.P. (1997). "Fly ash in concrete. Production, properties and uses". Advances in concrete technology, Vol. 2. The University of Calgary, Alberta, Canada. Gordon and Breach Science Publishers.

JUENGER, M.C.G., WINNEFELD, F., PROVIS, J.L. and IDEKER, J.H. (2011). "Advances in alternative cementitious binders". Cement and Concrete Research, Vol. 41, pp. 1232-1243.

KEARSLEY, E.P. (1996). "The use of foamed concrete for affordable development in third world countries". Appropriate concrete technology, Proceedings from the

International Conference 'Concrete in the service of mankind' (Ed R.K. Dhir and M.J. McCarthy), E&FN Spon, London, 1996, pp. 233-243.

KEARSLEY E.P. (1999b). "Just foamed concrete – an overview". In 'Specialist techniques and materials for concrete construction' from the proceedings of the International Conference 'Creating with concrete' (Ed R K Dhir and Henderson), University of Dundee, Scotland, 8-10 September 1999, Thomas Telford, pp. 227-237.

KEARSLEY, E.P. and WAINWRIGHT, P.J. (2001a). "Porosity and permeability of foamed concrete". Cement and Concrete Research, Vol. 31(5), pp. 805-812.

KEARSLEY, E.P. and WAINWRIGHT, P.J. (2001b). "The effect of high fly ash content on the compressive strength of foamed concrete". Cement and Concrete Research, Vol. 31(1), pp. 105-112.

KEARSLEY E.P. and MOSTERT, H.F. (2005). "Designing mix composition of foamed concrete with high fly ash contents" in 'Use of foamed concrete in construction' by Dhir, R.K., Newlands, M.D. and McCarthy A. from the proceedings of the International Conference in the University of Dundee, Scotland, 5 July 2005, pp. 29-36.

KEARSLEY, E.P. and WAINWRIGHT, P.J. (2002a). "The effect of porosity on the strength of foamed concrete". Cement and Concrete Research, Vol. 32(2), pp. 233-239.

KEARSLEY, E.P. and WAINWRIGHT, P.J. (2002b). "Ash content for optimum strength of foamed concrete". Cement and Concrete Research, Vol. 32, pp. 241-246.
KIM, K., JEON, S., KIM, J., YANG, S. (2003). "An experimental study on thermal conductivity of concrete". Cement and Concrete Research, Vol. 33, Issue 3, pp.363–371.

KIM, H.K., LEE, H.K. (2010). "Influence of cement flow and aggregate type on the mechanical and acoustic characteristics of porous concrete". Applied Acoustics, Issue 71 pp.607–615.

KHAYAT, K.H. and ASSAAD, J. (2002). "Air-void stability in self-consolidating concrete". ACI Materials Journal, Vol. 99, Issue 4, pp. 408-416.

KREITH, F. and BOHN, M.S. (2001). "Principles of heat transfer". 6th edition. Brooks/Cole, USA, 2001.

KUTRUFF, H. (2000). "Room acoustics". 4th edition, London: Spon Press, pp.163-164.

LAUKAITIS, A., FIKS, B. (2006). "Acoustical properties of aerated autoclaved concrete". Applied Acoustics, Issue 67, pp.284–296.

LEE, M. Y., BRONOWSKI, D. R. and HARDY, R. D. (2004). "Laboratory Constitutive Characterization of Cellular Concrete". Albuquerque: Snadia National Laboratories.

LEE, J., KIM, G.H., HA, C.S. (2011). "Sound absorption properties of polyurethane/ nano- silica nanocomposite foams". Wiley Online Library (wileyonlinelibrary.com).

LYONS, A. (2010). "Materials for architects and builders". 4th edition. Oxford: Elsevier, pp. 342-343.

MALOU, Z. and CABRILLAC, R. (1999). "Configuration of pores on the mechanical and thermal characteristics of cellular concrete through a homogenization method". In 'Specialist techniques and materials for concrete construction' from the proceedings of the International Conference 'Creating with concrete' (Ed R K Dhir and Henderson), University of Dundee, Scotland, 8 - 10 September 1999, Thomas Telford, pp. 209-218.

McCARTHY, A. (2004). "Thermally insulating foundations and ground slabs for sustainable housing using foamed concrete". PhD Thesis. University of Dundee.
McGOVERN, G. (2000). "Manufacture and supply of ready-mix foamed concrete". One day awareness seminar 'Foamed concrete: properties, applications and potential', University of Dundee, Scotland, pp. 12-22.

MOHAMMAD, M. (2011). "Development of foamed concrete enabling and supporting design". PhD Thesis. University of Dundee.

MOSANENZADEH, S.G., NAGUIB, H.E., PARK, C.B., ATALLA, N. (2013). "Development, characterization, and modelling of environmentally friendly open-cell acoustic foams". Polymer engineering and science. Society of Plastics Engineers, 2013, Wiley Online Library, pp. 1979-1989.

Mineral Products Association (MPA)

MPA (2010). "Concrete industry sustainability performance report. 3rd report: 2009 performance data". MPA, The Concrete Centre. London, 2010.

MPA (2011a). "Specifying sustainable concrete". MPA, The Concrete Centre.

MPA (2011b). "Novel cements: low energy, low carbon cements". MPA Cement Fact Sheet No. 12. MPA Cement.

MPA (2012a). "The Concrete Industry Sustainable Construction Strategy". MPA, The Concrete Centre.

MPA (2012b). "Concrete industry sustainability performance report. 5th report: 2011 performance data". MPA, The Concrete Centre.

MPA (2013). "Concrete industry sustainability performance report. 6th report: 2012 performance data". MPA, The Concrete Centre. London, 2013.

MYERS, D. (1992). "Surfactant Science and Technology". 2nd Edition, VCH Publishers, Inc., USA.

NATIONAL RESEARCH COUNCIL CANADA (NRCC) (1990). "Sound transmission loss measurements through 190 mm and 140 mm blocks with added drywall and through cavity block walls" by Warnock A.C.C. Internal Report No. 586. NRCC, Institute for Research in Construction.

NAMBIAR, E.K.K., RAMAMURTHY, K. (2006). "Influence of filler type on the properties of foam concrete". Cement and concrete composites, Vol.28, pp. 475-480.
NAMBIAR, E.K.K., RAMAMURTHY, K. (2007a). "Air-void characterisation of foam concrete". Cement and Concrete Composites, Vol. 37, Issue 2, pp. 221-230.

NAMBIAR, E.K.K., RAMAMURTHY, K. (2007b). "Sorption characteristics of foam concrete". Cement and Concrete Composites, Vol. 37, Issue 9, pp. 1341-1347.

NAMBIAR E.K.K and RAMAMURTHY K. (2008). "Fresh state characteristics of foam concrete". Journal of Materials in Civil Engineering, Vol. 20, Issue 2, pp. 111–117.

NARAYANAN, N. and RAMAMURTHY, K. (2000). "Structure and properties of aerated concrete: a review". Cement and Concrete Composites, Vol. 22, pp.321-329.

NEVILLE, A.M. (2011). "Properties of concrete". 5th edition, Pearson Education Ltd.

OTHUMAN, M. A., WANG, Y.C. (2011). "Elevated-temperature thermal properties of lightweight foamed concrete". Construction and Building Materials, Vol. 25, pp.705-716.

QIAN, X. and ZHENG, L. (1990). "The study of thermal expansion coefficient about fly-ash aerated concrete". Silicate Building Products, Vol. 90, No. 2, pp. 1-3 (in Chinese).

RAO, K, S. (2008). "Development of concrete materials with no or minimal primary aggregate content". Ph.D. Thesis. University of Dundee.

RAMAMURTHY K., NAMBIAR, E.K.K., RANJANI, G.I S. (2009). "A classification of studies on foam concrete". Cement and concrete composites, Vol. 31, pp.388-396.

RILEM (1991). "Fly ash in concrete. Properties and performance." RILEM Report 7 edited by Wesche, W. Chapman & Hall, London.

SOMASUNDARAN, P. (2006). "Surface forces' role in the foaming behaviour of liquids" in 'Encyclopedia of Colloid and Surface Science, Vol. 8, 2nd edition'. Taylor&Francis Group.

STEVENSON, P. (2011). "Foam engineering: fundamentals and applications". 2nd edition, Somerset, NJ, USA, Wiley, 2011. Chapter 5, pp. 75-89.

TANAÇAN, L., ERSOY, H.Y., ARPACIOĞLU, Ü. (2009). "Effect of high temperature and cooling conditions on aerated concrete properties". Construction and Building Materials, Vol. 23, Issue 3, pp. 1240–1248.

TARASOV, A.S., KEARSLEY, E.P., KOLOMATSKIY, A.S., MOSTERT, H.F. (2010). "Heat evolution due to cement hydration in foamed concrete". Magazine of Concrete Research, Vol. 62, Issue 12, pp. 895-906.

UNIVERSITY OF DUNDEE (UoD) TECHNOLOGY BULLETIN (2007). "Foamed concrete", University of Dundee, Issue 13.

TAYLOR, R.P. (2011). "The art and science of foam bubbles". Nonlinear Dynamics, Psychology, and Life Sciences, Vol. 15, No.1, pp. 129-136.

TURNER, M. (2001). "Fast set foamed concrete for same day reinstatement of openings in highways" in Proceedings of the One Day Seminar on Foamed Concrete: Properties, Applications and Latest Technological Developments, Loughborough University, pp. 12–18.

UNITED KINGDOM QUALITY ASH ASSOCIATION (UKQAA) (2003). "Pulverised Fuel Ash in aerated concrete blocks". Technical Data Sheet 7.1.

UNITED KINGDOM WATER INDUSTRY RESEARCH (UKWIR) (1995). "Specification of foamed concrete". Report Ref. No. 95/WM/01/7, 24 pp.

VAISMAN, L., WAGNER, H. D., MAROM, G. (2006). "The role of surfactants in dispersion of carbon nanotubes". Advances in Colloid and Interface Science, Vol. 128–130, pp.37–46.

VALORE, R.C. (1961). "Foam and gas concretes" in 'Structural Foams' proceedings of a Conference presented as part of the 1960 Fall Conference of the Building Research Institute. Division of Engineering and Industrial Research. Publication 892, National Academy of Sciences-National Research Council, Washington, DC.

VISAGIE, M. and KEARSLEY, E.P. (1999a). "Micro-properties of foamed concrete". In 'Specialist techniques and materials for concrete construction' from the proceedings of the International Conference 'Creating with concrete' (Ed R K Dhir and Henderson), University of Dundee, Scotland, 8 - 10 September 1999, Thomas Telford, pp. 173-184.

WEAIRE, D. and HUTZLER, S. (1999). "The physics of foams". Clarendon Press, Oxford.

WEE, T., BABU, D.S., TAMILSELVAN, T. and LIM, H. (2006). "Air-void system of foamed concrete and its effect on mechanical properties". ACI Materials Journal, 103(1), pp. 45-52.

WEI, S., YIGIANG, C., YUNSHENG, Z., JONES, M.R. (2013). "Characterization and simulation of microstructure and thermal properties of foamed concrete". Construction and Building Materials, Vol.47, pp. 1278-1291.

WEI, S., YUNSHENG, Z., JONES, M.R. (2014). "Using the ultrasonic wave transmission method to study the setting behaviour of foamed concrete". Construction and Building Materials, Vol.5, pp. 62-74.

WINNEFELD, F., LOTHENBACH, B. (2010). "Hydration of calcium sulfoaluminate cements. Experimental findings and thermodynamic modelling". Cement and Concrete Research, Vol. 40, Issue 8, pp.1239-1247.

WIMPENNY, D.E. (1996). "Some aspects of the design and production of foamed concrete". Appropriate concrete technology, Proceedings from the International

Conference 'Concrete in the service of mankind' (Ed R.K. Dhir and M.J. McCarthy), E&FN Spon, London, 1996, pp.245-254.

Waste & Resources Action Programme (WRAP)

WRAP (2005). "Recycled and secondary aggregates in foamed concrete" by Jones M.R., McCarthy A. and Dhir R.K. DTI/WRAP Aggregates Research Programme STBF 13/13C. WRAP, January 2005, 67 pp.

WRAP (2007). "Specification and Quality Control of Foamed Concrete Incorporating RSA" by Jones M.R., Zheng, L., McCarthy A., Dhir R.K. and Yerramala, A. Aggregate Research Programme/Technical Guidance Document. WRAP, February 2007, 17 pp.

XU, Y., CHUNG, D. D. L. (2000). "Effect of sand addition on the specific heat and thermal conductivity of cement". Cement and Concrete Research, Vol. 30, No. 1, pp. 1175–1178.

YAKOVLEV, G., KERIENE, J., GAILUS, A., GIRNIENE, I. (2006). "Cement based foam concrete reinforced by carbon nanotubes". ISSN 1392-1320 Materials Science (MedŽiagotyra). Vol. 12, No.2.

YERRAMALA, A. (2008). "Development and characteristics of foamed concrete containing fine recycled and secondary aggregate. Ph.D. Thesis. University of Dundee.

ZHANG, X., WANG, S., and LI, H. (2011). "Sound Absorption Property of Multilayered Aluminum Foam Structure". Bioinformatics and Biomedical Engineering (iCBBE) 5th International Conference on 10-12 May 2011.

Websites

Arry (2014). "Industrial grade MWNTs".
Available at: www. arry-nano.com/ [accessed in April 2014]

Brüel & Kjær (1955). "Standing Wave Apparatus". Technical Review No.1.
Available at: http://www.bksv.co.uk/ [accessed in November, 2014]

Fordham, M. (2010). "Sustainability matrix-Green offices". Max Fordham.
Available at: http://www.maxfordham.com/ [accessed in January, 2012]

Freiberger, M. (2009). "Kelvin's bubble burst again". Plus Magazine.
Available at: https://plus.maths.org/content/kelvins-bubble-burst-again [accessed in February, 2014]

Hebel (2013). "Technical Hebel AAC properties".
Available at: http://www.hebel-usa.com/en/content/technical_features_2533.php [accessed in December 2014]

Nanotechnology Now (2014). "Nanotubes and Buckyballs".
Available at: www.nanotech-now.com/ [accessed in April 2014]

Propump Ltd (2014)
Available at: www.propump.co.uk [accessed in April, 2014]

UNITED KINGDOM GREEN BUILDING COUNCIL (UKGBC) (2012). "Key statistics".
Available at: http://www.ukgbc.org/ [accessed in December 2014]

PPENDIX A

PARTICLE SIZE DISTRIBUTION OF CEMENTS

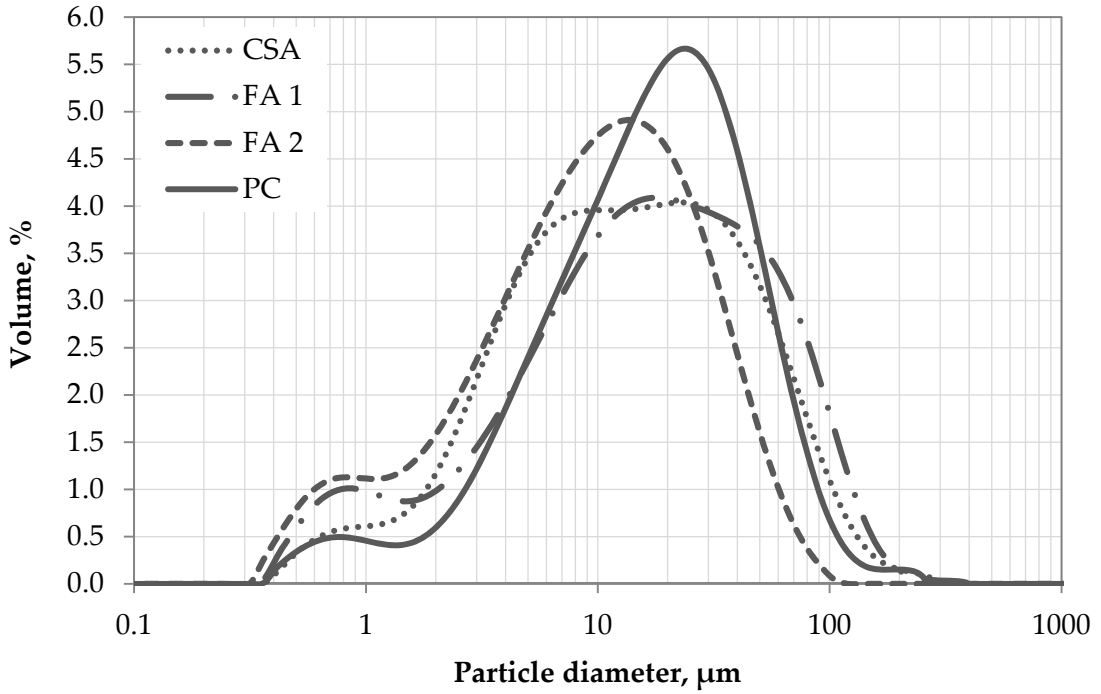

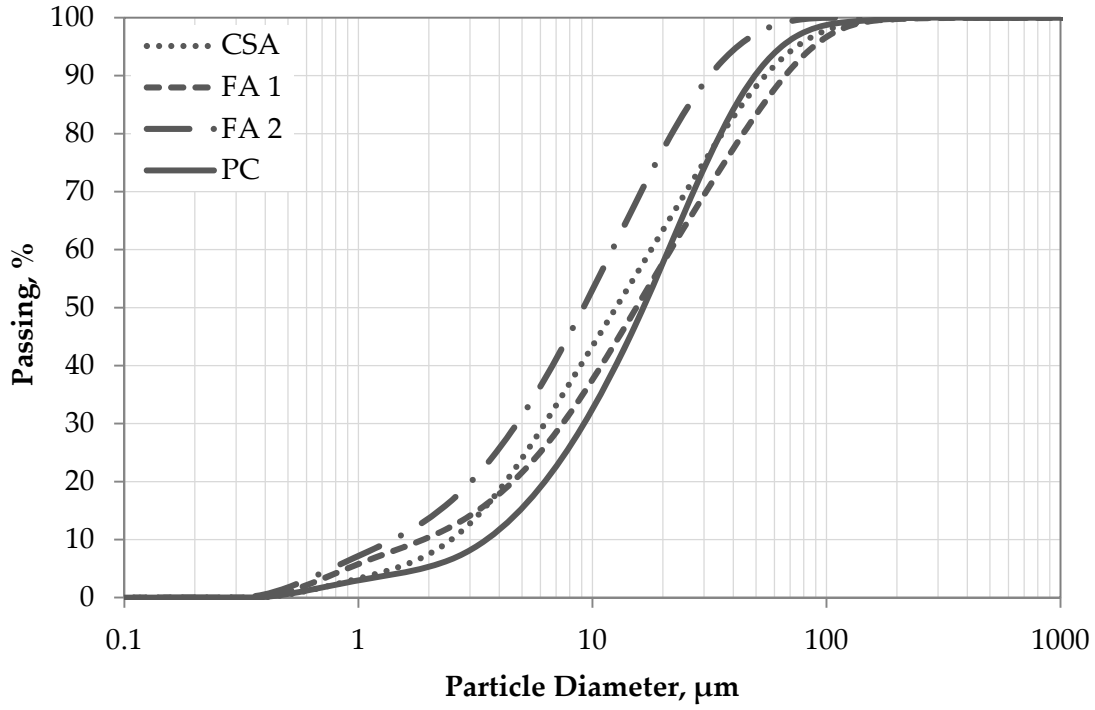

Figure A1. Particle size distribution of the cements used in the main study

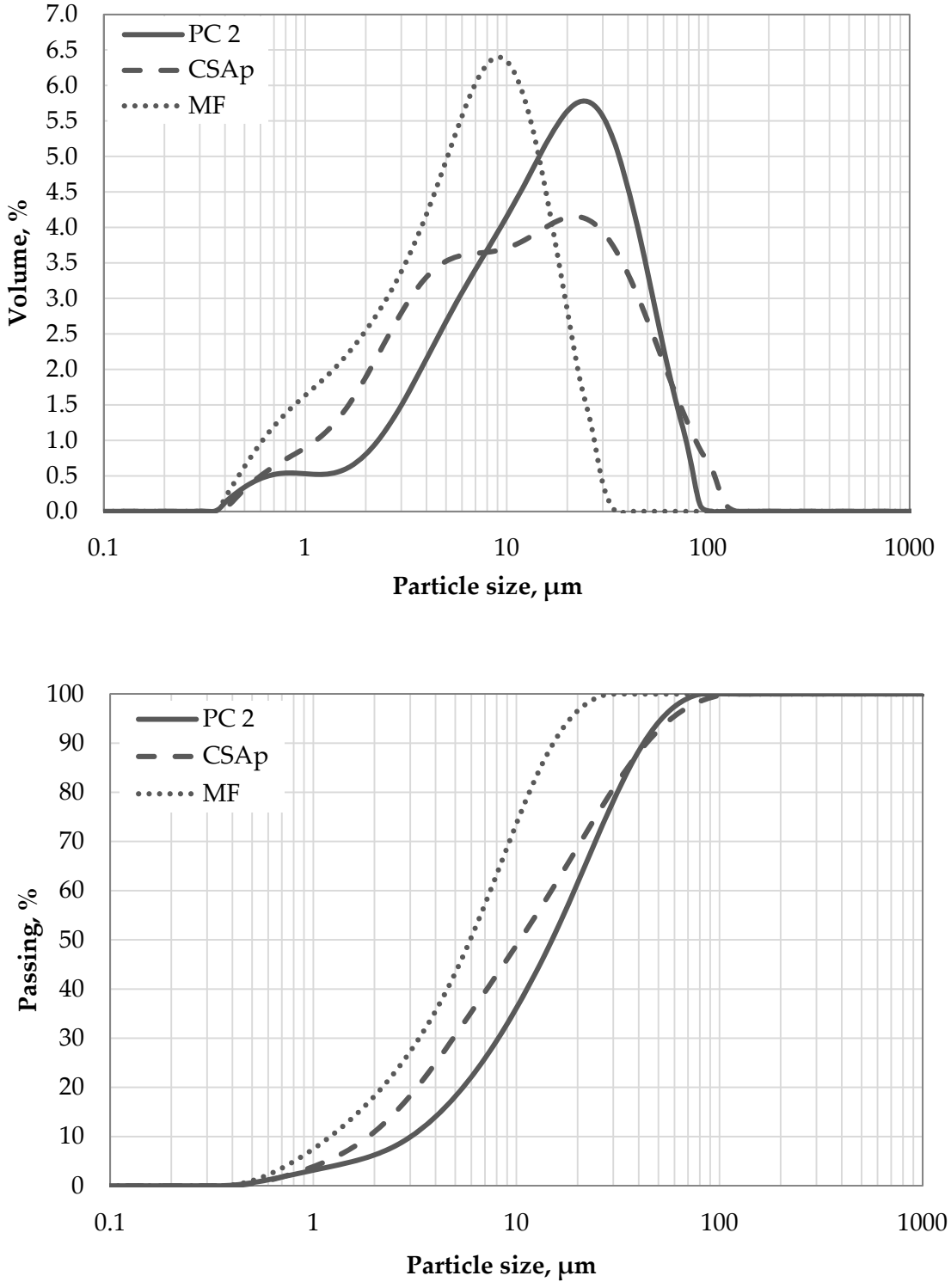

Figure A2. Particle size distribution of the alternative cements

APPENDIX B

SCANNING ELECTRON MICROSCOPY & CT SCANNING IMAGES

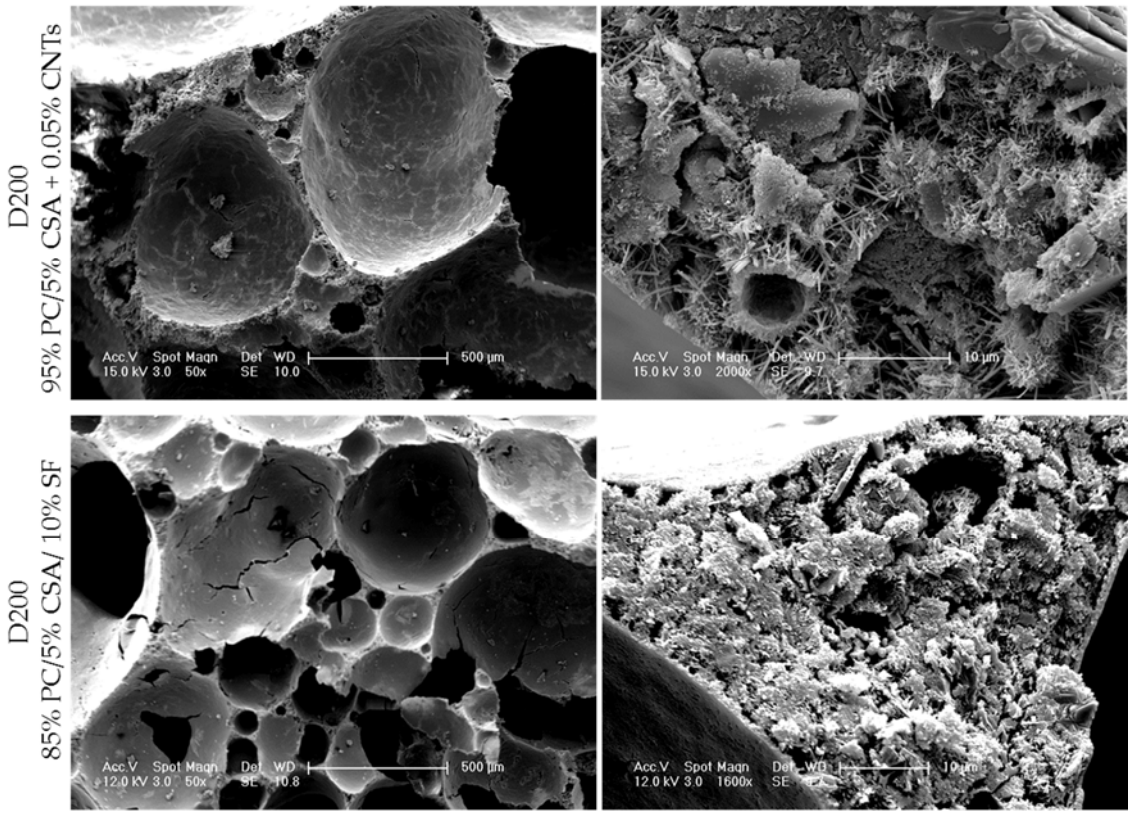

Figure B.1 Microstructure of D200 SF and CNT foamed concretes

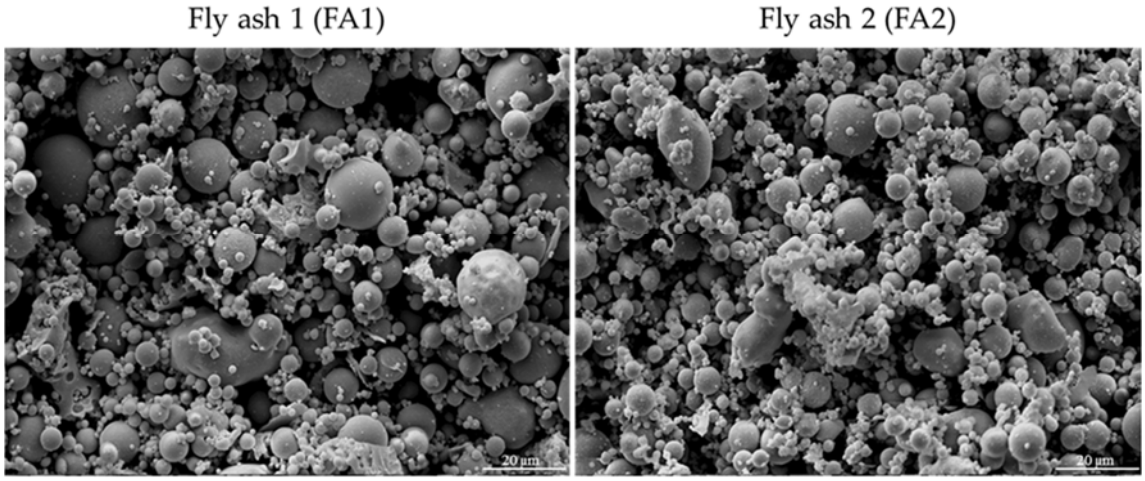

Figure B.2 Microstructure of FA1 and FA2

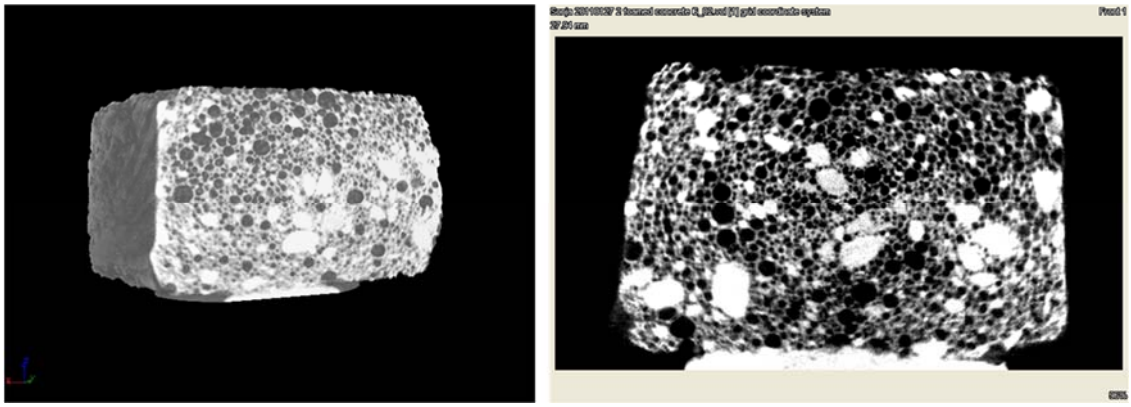

Figure B.3 CT Scanning images of D600 foamed concrete (3D volume view (left), 2D front view (right); resolution: 75μm)

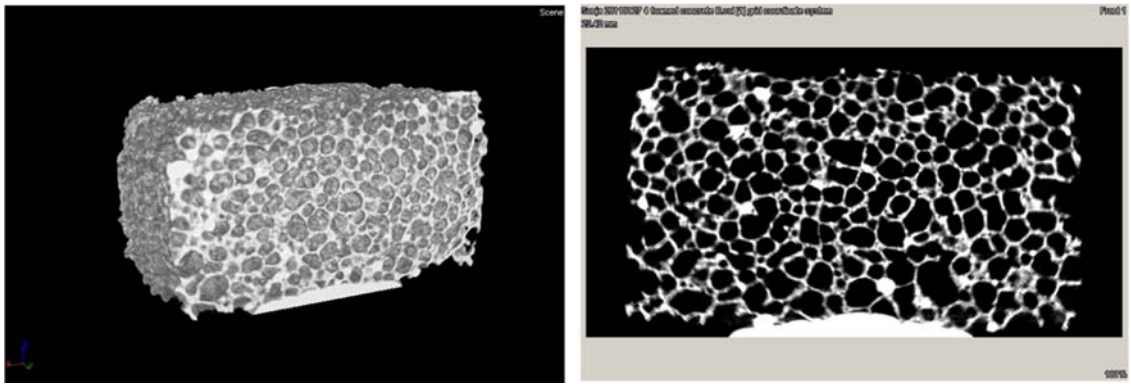

Figure B.3 CT Scanning images of D300 foamed concrete (3D volume view (left), 2D front view (right); resolution: 75μm)

APPENDIX C

AN EXAMPLE EMBODIED CARBON DIOXIDE (eCO_2) CALCULATION

Approach followed to calculate the amount of surfactant in a 1 m^3 foamed concrete mix

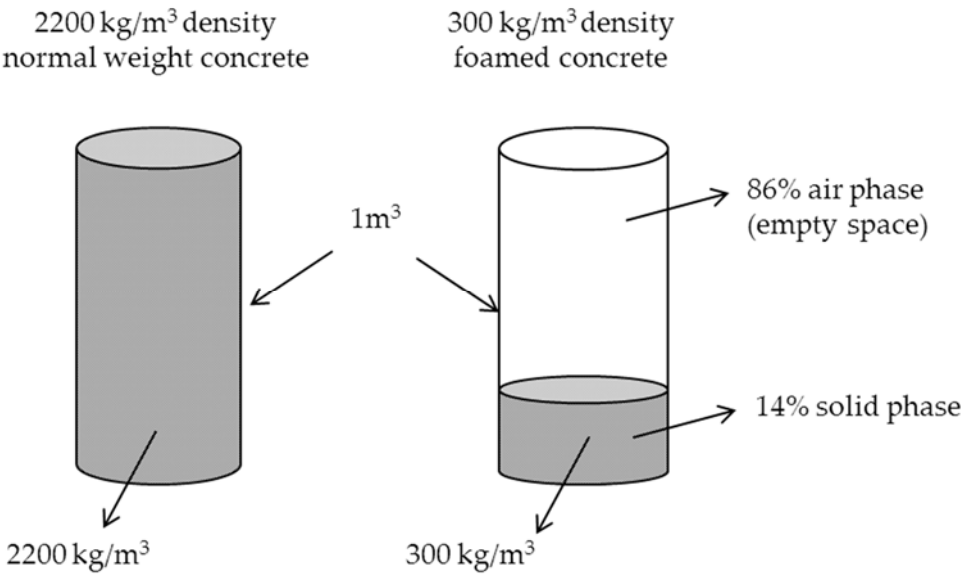

Figure C.1 Approach followed to calculate the amount of surfactant

Figure C.1 illustrates the approach followed to calculate the amount of surfactant used for 1 m^3 of foamed concrete at a given plastic density. Firstly, volume of air (foam) is calculated by comparing the solid phases of a normal weight concrete (with 2200 kg/m^3 density) and a 300 kg/m^3 foamed concrete in 1m^3 mix. Then the following calculation is carried out.

0.86 m^3 of foam present in 1 m^3 of 300 kg/m^3 foamed concrete mix;

Foam density = 50 kg/m^3 (average)

0.86 * 50 = 43 kg/m^3 => 43 litres of [water + surfactant]

60g of surfactant is added for per litre of water, therefore 5.6% of 1 litre [water + surfactant] solution is surfactant.

Therefore;

43 * 0.056 = 2.4 kg of surfactant is present in 1 m^3 of 300 kg/m^3 foamed concrete mix.

An example eCO_2 calculation for 90%PC/10%CSA/40%FA 300 kg/m³ density foamed concrete mix (according to the method described in CICSF, 2008)

Table C.1 ECO_2 of the constituents (MPA, 2011a)

eCO_2 of the constituents, kg CO_2 / tonne	
Portland cement	930
CSA cement	744*
Fly ash	4
Surfactant	0.22
Water	0.3

* Calculated as around 80% of eCO_2 of PC (MPA, 2011b)

Table C.2 Mix proportions for 300 kg/m³ mix

Mix constituent proportions, kg/m³	
Cement content	200
Water content	100
Surfactant content	2.4
No fine aggregates	0

Therefore, using the values provided in Table C.1 and C.2, eCO_2 is calculated as follows:

$eCO_2 = [(0.5 * 200 * 930) + (0.1 * 200 * 744) + (0.4 * 200 * 4) + (100 * 0.3) + (2.4 * 0.22)]/1000$

$= 108$

≈ 110 kg eCO_2 per 1 m³ of 300 kg/m³ foamed concrete mix

APPENDIX D

SOUND ABSORPTION COEFFICIENT VALUES

Table D.1 Sound absorption coefficients of D600 FC

600 kg/m³	Sound absorption coefficient (α)		
	Specimen thickness, mm		
Frequency, Hz	**25**	**50**	**70**
125	0.12	0.07	0.05
250	0.17	0.23	0.10
500	0.19	0.58	0.83
1000	0.65	0.80	0.59
2000	0.25	0.10	0.46
2500	0.31	0.19	0.31
3150	0.87	0.87	0.87
4000	0.64	0.59	0.54

Table D.2 Sound absorption coefficients of D500 FC

500 kg/m³	Sound absorption coefficient (α)		
	Specimen thickness, mm		
Frequency, Hz	**25**	**50**	**70**
125	0.01	0.06	0.06
250	0.08	0.19	0.17
500	0.20	0.39	0.66
1000	0.43	0.79	0.51
2000	0.12	0.10	0.11
2500	0.17	0.09	0.11
3150	0.93	0.93	0.93
4000	0.63	0.68	0.72

Table D.3 Sound absorption coefficients of D300 FC

300 kg/m³	Sound absorption coefficient (α)		
	Specimen thickness, mm		
Frequency, Hz	**25**	**50**	**70**
125	0.03	0.05	0.11
250	0.14	0.13	0.17
500	0.26	0.70	0.55
1000	0.82	0.59	0.60
2000	0.42	0.34	0.26
2500	0.45	0.26	0.28
3150	0.88	0.87	0.88
4000	0.75	0.75	0.72

Table D.4 Sound absorption coefficients of D300 fly ash FC

300 kg/m³ (FA)	Sound absorption coefficient (α)		
	Specimen thickness, mm		
Frequency, Hz	**25**	**50**	**70**
125	0.09	0.07	0.05
250	0.34	0.23	0.10
500	0.19	0.42	0.83
1000	0.88	0.80	0.73
2000	0.43	0.26	0.35
2500	0.53	0.27	0.40
3150	0.94	0.93	0.93
4000	0.82	0.77	0.77

Table D.5 Sound absorption coefficients of D200 FC

200 kg/m³	Sound absorption coefficient (α)		
	Specimen thickness, mm		
Frequency, Hz	**25**	**50**	**70**
125	0.10	0.06	0.16
250	0.20	0.13	0.16
500	0.28	0.79	0.88
1000	0.87	0.74	0.76
2000	0.36	0.34	0.42
2500	0.58	0.45	0.44
3150	0.96	0.95	0.95
4000	0.82	0.78	0.81

Table D.6 Sound absorption coefficients of D200 silica fume FC

200 kg/m³ (SF)	Sound absorption coefficient (α)		
	Specimen thickness, mm		
Frequency, Hz	**25**	**50**	**70**
125	0.15	0.07	0.08
250	0.26	0.14	0.13
500	0.22	0.65	0.75
1000	0.83	0.70	0.66
2000	0.39	0.56	0.52
2500	0.26	0.61	0.65
3150	0.92	0.93	0.95
4000	0.73	0.74	0.83

Table D.7 Sound absorption coefficients of D200 carbon nanotube FC

200 kg/m³ (CNT)	Sound absorption coefficient (α)		
	Specimen thickness, mm		
Frequency, Hz	**25**	**50**	**70**
125	0.01	0.03	0.18
250	0.18	0.15	0.14
500	0.23	0.85	0.82
1000	0.89	0.88	0.86
2000	0.29	0.57	0.61
2500	0.59	0.74	0.89
3150	0.93	0.95	0.97
4000	0.79	0.88	0.92